University of Salerno

Department of Chemistry and Biology "A. Zambelli"

Ph.D. in Chemical, Biological and Environmental Sciences

Curriculum in Chemical Sciences

XXXV Doctoral Cycle

Macrocycles: new properties and applications

Supervisor:

Prof. Irene Izzo

Ph.D. student:

Alicja Araszczuk

Matr. 8801800007

Coordinator:

Prof. Claudio Pellecchia

Academic Year 2021/2022

To Damian, Małgorzata and Adam

“Satisfaction of one's curiosity is one of the greatest sources of happiness in life.”

Linus Pauling

Index

Abbreviations

ACN: Acetonitrile

AcOEt: Ethyl acetate

AcOH: Acetic acid

Ar: Aryl

Bn: Benzyl

COSY: Correlation spectroscopy

CuAAC: Copper Catalyzed-Azide-Alkyne-Cycloaddition

DCM: Dichloromethane

DFT: Density functional theory

DIC: *N,N*-Diisopropylcarbodimide

DIPEA: *N,N*-Diisopropylethylamine

DMF: *N,N*-Dimethylformamide

DMSO: Dimethyl sulfoxide

EtOH: Ethanol

Fmoc: 9-Fluorenylmethoxycarbonyl

HATU: *O*-(7-azabenzotriazol-1-yl)-*N,N,N′,N′*-tetramethyluronium hexafluorophosphate

HFIP: 1,1,1,3,3,3-Hexafluoroisopropanol

HMBC: Heteronuclear multiple bond correlation

HMQC: Heteronuclear multiple quantum coherence

HPLC: High-performance liquid chromatography

HRMS: High resolution mass spectrometry

MeOH: Methanol

Nspe: *N*-((*S*)-1-Phenylethyl)glycine

Ph: Phenyl

RP-HPLC: Reverse-phase HPLC

Sar: Sarcosine

TCDE: Tetrachlorodideuteroethane

TFA: trifluoroacetic acid

TFPB: Tetrakis[3,5-bis(trifluoromethyl)phenyl]borate

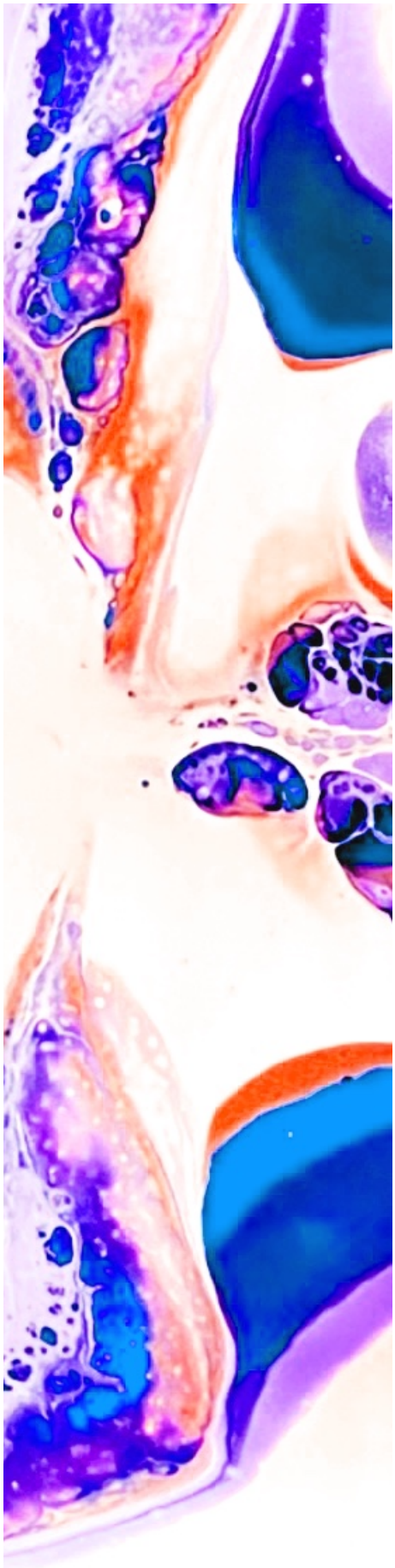

Chapter 1

INTRODUCTION

1. INTRODUCTION

1.1. The exploration of macrocyclic chemistry

In principle, macrocycles constitute a class of chemical compounds which exhibit molecular recognition and complexation properties. They are characterized by a cyclic skeleton comprising at least twelve atoms.[1] However, the dimension of naturally occurring macrorings can exceed even fifty atoms. Structural analysis of natural products revealed that 14-, 16-, and 18-member scaffolds constitute the most typical macrocyclic frameworks.[2] Over recent decades, a wide variety of macrocyclic molecules has been designed and synthetized or isolated from natural sources.[3]

In the rich history of macrocyclic chemistry, crown ethers possess the status of protoplasts. The first macrocyclic polyether, dibenzo[18]crown-6 (**Figure 1. 1**), was obtained accidentally in 1967 by Pedersen. To the very first synthetic macroring and its analogues were given the name "crown ethers" due to the crown-like appearance of their complexes with alkali and alkaline earth metal cations.[4,5] After pioneering research of Pedersen, in 1969, Lehn demonstrated that cations can be completely encapsulated by macrobicyclic polyethers called cryptands.[6] On the other hand, Cram developed new sophisticated cyclic macrosystems: cavitands and spherands, able to bind not only Group IA and IIA metal cations but even small organic molecules.[7] These extraordinary discoveries have led to the emergence of host-guest and supramolecular chemistry, and to the Nobel Prize in Chemistry in 1987 shared by Pedersen, Lehn and Cram "*for the development and use of molecules with structure-specific interactions of high selectivity*".[8]

[1] Yudin, A.K. *Chem. Sci*. **2015**, *6*, 30-49.
[2] Frank, A.T.; Farina, S.N.; Sawwan, N.; Wauchope, O.R.; Qi, M.; Brzostowska, E.M.; Chan, W.; Grasso, F.W.; Habereld, P.; Greer, A. *Mol. Diversity*, **2007**, *11,* 115–118.
[3] Wessjohann, L.A.; Ruijter, E.; Garcia-Rivera, D.; Brandt, W. *Mol. Diversity* **2005**, *9*, 171–186.
[4] Pedersen, C.J. *J. Am. Chem. Soc*. **1967**, *89*, 2495–2496.
[5] Pedersen, C. J. *J. Am. Chem. Soc*. **1967**, *89*, 7017–7036.
[6] Dietrich, B.; Lehn, J.M.; Sauvage, J.P. *Tetrahedron Lett*. **1969**, *10*, 2885–2888.
[7] Cram, D.J.; J. M. Cram, *Science*, **1974**, *183*, 803–809.
[8] Izatt, R.M. *Chem. Soc. Rev.* **2017**, *46*, 2380-2384.

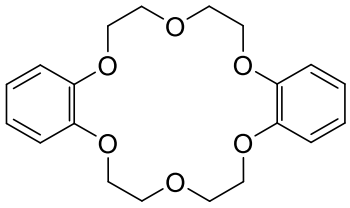

Figure 1. 1. Structure of dibenzo[18]crown-6

Since the unexpected discovery of macrocyclic polyethers, the chemistry of synthetic macrocycles has flourished. In the past decades, a wide variety of synthetic macrorings has been prepared and described (e.g., calixarenes, pillalarenes, cucurbiturils, **Figure 1. 2**), giving a significant contribution to macrocyclic chemistry, principally relative to self-assembly and molecular recognition processes.[9]

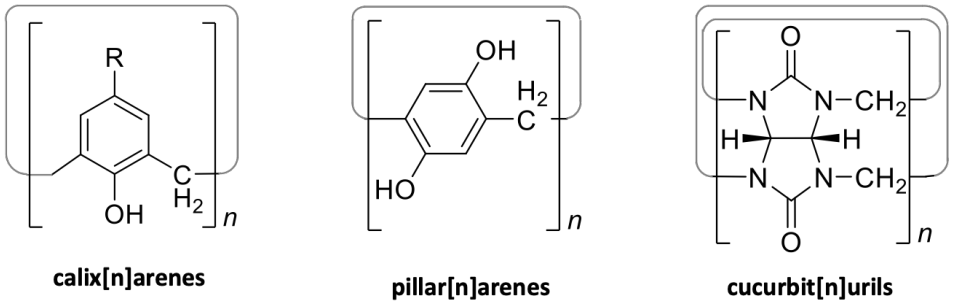

Figure 1. 2. Examples of macrocyclic hosts (calixarenes, pillalarenes, cucurbiturils)

1.2. Macrocyclic oligoamides: sequence-defined foldamers

Nature employs macrocyclic scaffolds for the recognition of ions, small molecules, as well as extended macromolecular surfaces.[10] Similarly, synthetic macrorings are being designed to bear specific molecular recognition abilities for applications in various disciplines, from medicinal chemistry to material sciences and catalysis.[11] Macrocyclic molecules differ in their complexing preferences due to the divergences in size, conformation, and chemical properties. Consequently, an accurate synthetic control on these features is crucial for obtaining scaffolds adequately tailored for their specific applications.

[9] Liu, Z.; Nalluri, S.K.M.; Stoddart, J.F. *Chem. Soc. Rev.* **2017**, *46,* 2459.
[10] Villar, E. A.; Beglov, D.; Chennamadhavuni, S.; Porco, J. A.; Kozakov, D.; Vajda, S.; Whitty, A. *Nat. Chem. Biol*. **2014**, *10*, 723−731.
[11] Pinalli, R.; Pedrini, A.; Dalcanale, E. *Chem. Soc. Rev*. **2018,** *47,* 7006−7026.

Macrocycles possessing a distinct cavity are defined as container molecules or cavitands. This group comprises previously mentioned calixarenes or cucurbiturils.[12,13] Even though all these macrocycles and their molecular recognition abilities have been widely studied, the synthesis of the heterofunctionalized derivatives still presents a challenge. Since cavitands are generally prepared *via* one-pot cyclooligomerization reaction, multiple cyclic and acyclic byproducts are generated during their synthesis. Moreover, the target macrocycles' functionalization sites are chemically equivalent, which significantly obstructs their heterofunctionalization.[14]

Bearing in mind these limitations, for example, Hamilton et al. decided to work on a new approach towards cavitands' heterofunctionalization.[15] The authors have focused their attention on peptidomimetic foldamers composed of 2,4-dialkoxy-*meta*-aminomethylbenzoic acid (MAMBA) monomers.[16] The chemical strategy towards heterofunctionalized cavitands provides for a sequential coupling with subsequent macrocyclization (**Scheme 1. 1**).

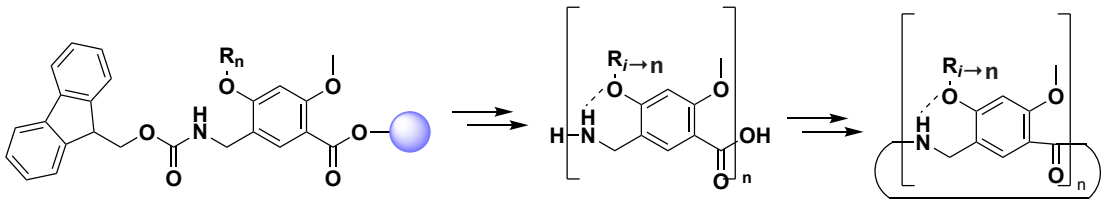

Scheme 1. 1. Synthetic route towards heterofunctionalized cavitands.

The use of the solid phase synthetic methods offers considerable benefits compared to the synthesis in solution, such as quick construction of target macromolecules, effortless purification, and high yields.[17] In order to assemble MAMBA oligomers on-resin, orthogonally protected monomers (with free carboxylic acid function) were prepared in solution by taking advantage of classical transformations.[16] In total, ten building blocks based on *β*-resorcyclic acid and decorated with different side chains have been prepared (**Figure 1. 3**).

[12] Lagona, J.; Mukhopadhyay, P.; Chakrabarti, S.; Isaacs, L. *Angew. Chem., Int. Ed*. **2005**, *44*, 4844− 4870.
[13] Ikeda, A.; Shinkai, S. *Chem. Rev*. **1997**, *97*, 1713−1734.
[14] Salorinne, K.; Nauha, E.; Nissinen, M.; Ropponen, J. *Eur. J. Org. Chem*. **2013**, 1591−1598.
[15] Meisel, J.W.; Hu, C.T.; Hamilton, A.D. *Org.Lett.* **2019**, *21,* 7763-7767.
[16] Meisel, J. W.; Hu, C. T.; Hamilton, A. D. *Org. Lett.* **2018,** *20*, 3879−3882.
[17] Merrifield, R. B. *J. Am. Chem. Soc.* **1963**, *85*, 2149−2154.

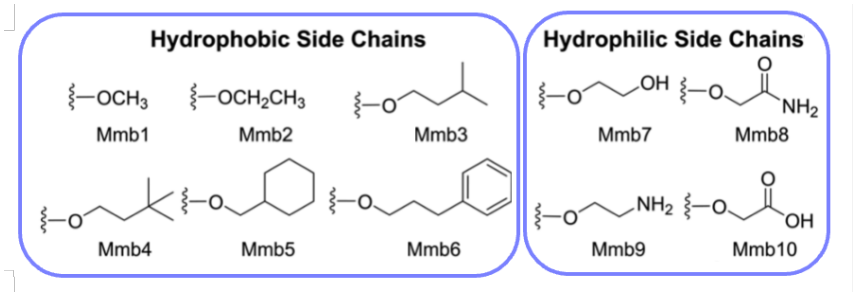

Figure 1. 3. Side chains used for decoration of oligoamides.

Then, MAMBA oligomers were elongated on chlorotrityl resin by starting with the loading of *C*-terminal residue and proceeding with iterative cycle of backbone amine Fmoc-deprotections and amide couplings. Finally, all the oligomers were cyclized in solution in the head-to-tail fashion, and then globally deprotected to yield a series of sequence-defined macrocyclic MAMBA tetramers and pentamers (**Figure 1. 4**).

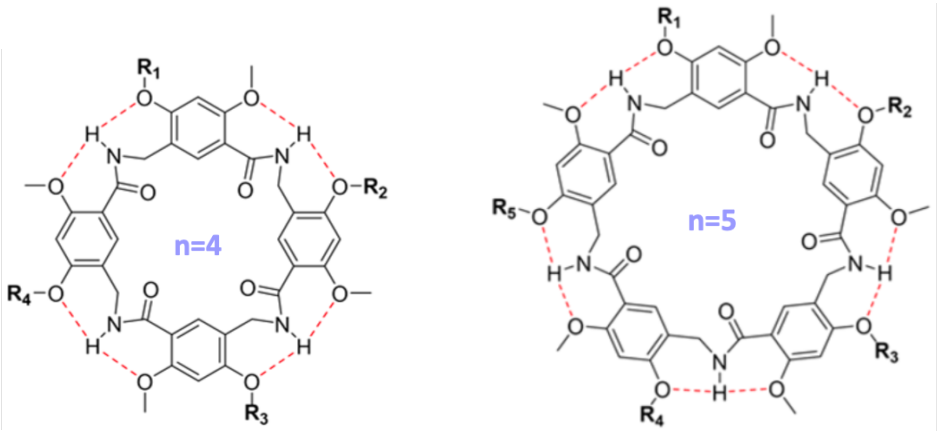

Sequence	Linear Yield[a]	Cyclization Yield[b]	Isolated Yield[c]
Cyclo(Mmb1)$_4$	89%	69%	61%
Cyclo(Mmb4-7-5-8)	94%	69%	65%
Cyclo(Mmb3-9-6-10)	89%	69%	61%
Cyclo(Mmb1)$_5$	91%	90%	62%
Cyclo(Mmb5-4-3-2-1)	96%	64%	82%
Cyclo(Mmb8-7-10-9-6)	98%	44%	43%

Figure 1. 4. Synthesis of heterofunctionalized MAMBA cavitands. [a]Yield for the side-chain-protected oligomer after cleavage from resin. [b]Yield for the cyclization step for the purified macrocycle after side-chain deprotection. [c]Overall yield for the isolated products

Macrocyclic oligoamides developed by Hamilton et al. are dynamic cavitands characterized by a tube conformation stabilized by the bifurcated hydrogen bonding[18] between adjacent units. Additionally, the presence of the benzylic methylene linkers assists in rendering the macrocyclic structure more flexible and thus enables the potential conformational alterations. The study of the Hamilton group has brought an important contribution to the chemistry of macrocycles as it paves the way towards previously unreachable heterofunctionalized cavitands. The proposed approach can be employed for the generation of diverse sequence-defined foldamers designed for wide range of applications, leading to a significant expansion of the chemical space of macrocyclic molecules.

1.3. Cyclic peptoids: polymers of *N*-substituted glycines

Peptoids (polymers of *N*-substituted glycines) constitute a fascinating class of biomimetic oligoamides, structurally associated with peptides but exhibiting distinct structural and biological features.

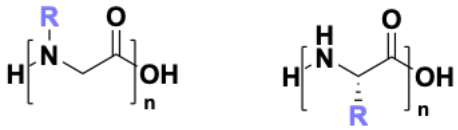

Peptoid Peptide

Figure 1. 5. Comparison of peptoid and peptide structures.

From a structural point of view, a key difference between peptides and peptoids lies in the shift of the side chains from the α-carbon to the amide nitrogen (**Figure 1. 5**). This relocation means that the peptoid backbone is missing stereogenic centers and amide protons. Therefore, peptoids result to be more resistant to enzymatic degradation and more flexible. The main source of the conformational heterogeneity is due to *cis-trans* isomerization around the amide bond (**Figure 1. 6**).[19]

[18] Rudkevich, D. *M. Chem. Eur. J.* **2000**, *6*, 2679.
[19] De Riccardis, F. *Eur. J. Org. Chem.* **2020**, *2020*, 2981−2994.

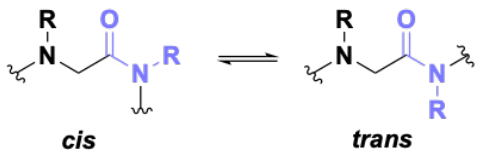

Figure 1. 6. Cis-trans isomerization of amide bond.

The peptoids' preparation relies on the "sub-monomeric" approach developed by Zuckermann and co-workers.[20] It is a solid-phase synthesis strategy comprising two key steps repeated iteratively until the desired sequence is obtained: acylation, typically with bromoacetic acid, followed by substitution with a primary amine. Once a target oligomer is constructed, it is cleaved from the 2-chlorotrityl resin in mild acidic conditions, yielding a linear peptoid with a free terminal carboxyl group and a secondary amine ready to be coupled in the presence of guanidinium/phosphonium salts or carbodiimides condensing agents (**Scheme 1. 2**). The head-to-tail cyclization of linear oligomers limits backbone movement, increases rigidity and reduces the number of possible conformations: briefly, leads to the formation of more stable scaffolds.[21] Additionally, it was demonstrated that linear peptoids can be cyclized by side-chain to side-chain coupling, *via* ruthenium alkylidene catalysed ring closing metathesis, thiol-ene reaction, or copper(I)-catalyzed azide-alkyne cycloaddition (CuAAC).[22]

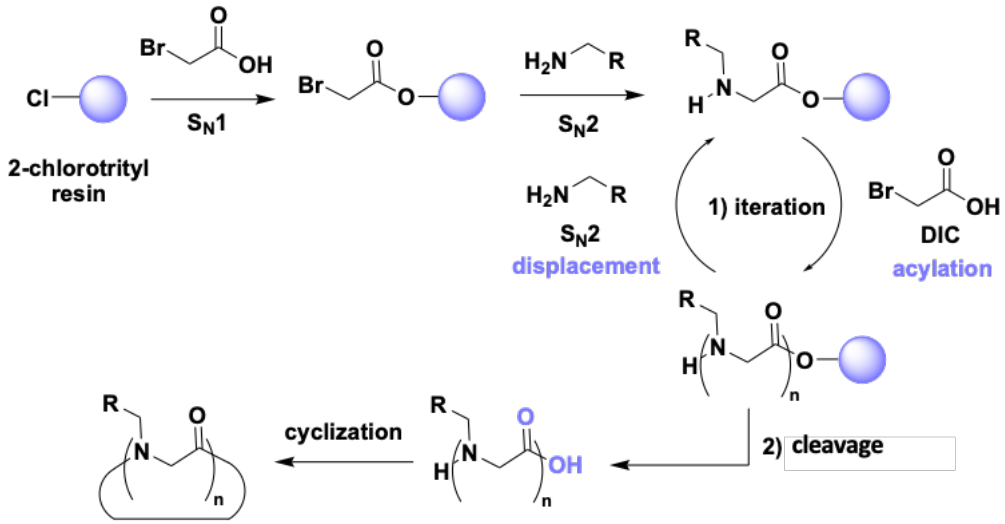

Scheme 1. 2. Synthetic route towards cyclic peptoids.

[20] Zuckermann, R.N.; Kerr, J.M.; Kent, S.B.H.; Moos, W.H. *J. Am. Chem. Soc.* **1992**, *114*, 10646–10647.
[21] Shin, S. B. Y.; Yoo, B.; Todaro, L. J.; Kirshenbaum, K. *J. Am. Chem. Soc.* **2007**, *129*, 3218–3225.
[22] D'Amato, A. *Eur. J. Org. Chem.* **2022**, No. e202200665.

Within last years, cyclic peptoids have been investigated as versatile scaffolds to perform numerous functions. In particular, macrocyclic *N*-substituted glycine oligomers have shown a significant potential in catalysis,[23] as bioactive agents,[24] in material science[25] and as precursors of peraza-macrocycles.[26] Moreover, the versatility of their preparation method enables wide structural flexibility and effortless introduction of diverse aromatic spacers into the peptoid oligoamide backbone, producing the valuable class of "extended peptoids"[27,28] with excellent conformational properties[29,30] (even without intramolecular H-bonding) and metal chelating abilities.[31]

[23] Schettini, R.; De Riccardis, F.; Della Sala, G.; Izzo, I. *J. Org. Chem.* **2016**, *81*, 2494−2505
[24] Huang, M. L.; Shin, S. B. Y.; Benson, M. A.; Torres, V. J.; Kirshenbaum, K. *Chem. Med. Chem.* **2012**, *7*, 114−122.
[25] Meli, A.; Macedi, E.; De Riccardis, F.; Smith, V. J.; Barbour, L. J.; Izzo, I.; Tedesco, C. *Angew. Chem., Int. Ed.* **2016**, *55*, 4679−4682.
[26] Schettini, R.; D'Amato, A.; Pierri, G.; Tedesco, C.; Della Sala, G.; Motta, O.; Izzo, I.; De Riccardis, F. *Org. Lett.* **2019,** *21*, 7365−7369.
[27] Combs, D. J.; Lokey, R. S. *Tetrahedron Lett.* **2007**, *48*, 2679−2682.
[28] Hjelmgaard, T.; Roy, O.; Nauton, L.; El-Ghozzi, M.; Avignant, D.; Didierjean, C.; Taillefumier, C.; Faure, S. *Chem. Commun.* **2014**, *50*, 3564− 3567.
[29] Hjelmgaard, T.; Nauton, L.; De Riccardis, F.; Jouffret, L.; Faure, S. *Org. Lett.* **2018**, *20*, 268−271.
[30] Hayakawa, M.; Ohsawa, A.; Takeda, K.; Torii, R.; Kitamura, Y.; Katagiri, H.; Ikeda, M. *Org. Biomol. Chem.* **2018**, *16*, 8505−8512.
[31] Meli, A.; Gambaro, S.; Costabile, C.; Talotta, C.; Della Sala, G.; Tecilla, P.; Milano, D.; Tosolini, M.; Izzo, I.; De Riccardis, F. *Org. Biomol. Chem.* **2016**, *14*, 9055−9062.

1.4. Aim of the project

This PhD thesis is focused on developing new sequence-defined macrocycles based on peptoidic scaffold.

Chapter 2 describes synthesis and characterization of new chiral peraza-macrocycles and their sodium complexes. The preparation of such macrocyclic ligands has been accomplished *via* backbone amides' reduction of corresponding cyclic peptoids.

Chapter 3 is devoted to attempts in the synthesis of cyclic thiopeptoids (possessing C=O backbone bonds replaced with C=S ones). The synthesis of two thioamide bond precursors in peptoids and on-resin thioacylation trials are described.

Chapter 4 can be considered as an interface between the versatility of the copper(I)-catalyzed alkyne-azide cycloaddition chemistry and peptoid synthesis. In the first place, preparation, and characterization of a new class of macrocyclic triazole-containing "extended" peptoids is described.

The next study is dedicated to expanding the concept of backbone amide reduction for these new oligoamide macrocycles (including chiral derivatives), which leads to a new class of macrocycles possessing complexation abilities.

Lastly, a preparation of new polar macrocyclic peptoids *via* CuAAC-mediated conjugation between propargyl-functionalized cyclopeptoidic platforms and suitably designed azides is described.

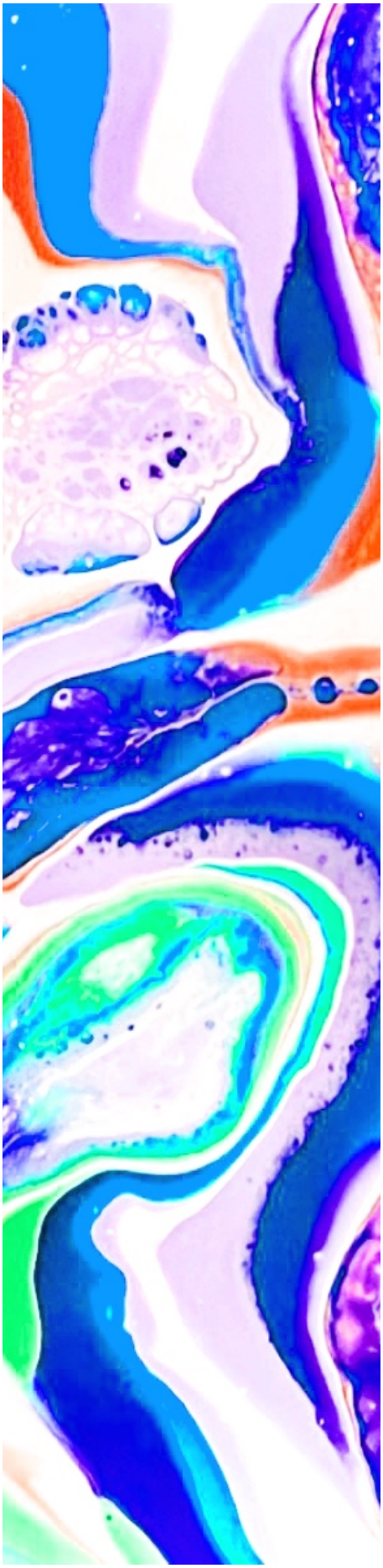

Chapter 2

CHIRAL PERAZA-MACROCYCLES

2. CHIRAL PERAZA-MACROCYCLES

2.1. Introduction

2.1.1. Cyclic *N*-substituted polyamines and their metal complexes

Peraza-macrocycles (*N*-substituted cyclic polyamines), such as cyclen[32] (1,4,7,10-tetraazacyclododecane) and hexacyclen (1,4,7,10,13,16-hexaazacyclooctadecane) (**Figure 2. 1**) derivatives, are known to form stable complexes with metal ions[33] and are commonly used as supramolecular[34] and biomedical[35] tools, sensors[43] and functional materials.[36] Whereas the area of research regarding hexacyclen ligands and their complexes is still restricted[37], the cyclen derivatives chemistry is flourishing due to their application as contrast agents for magnetic resonance imaging (MRI).[38]

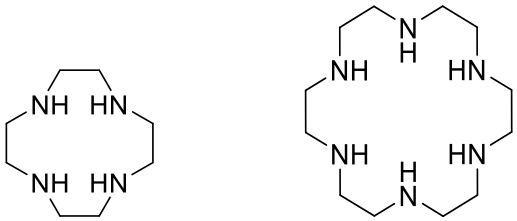

2.1 **2.2**

Figure 2. 1. Cyclen (**2.1**) and hexacyclen (**2.2**) structures.

To date, cyclen is widely employed as a macrocyclic ligand for complexation with diverse transition metal ions. The presence of coordinating pendant arms can considerably improve the stability of the complexes *via* macro ring-sidearm cooperativity. For instance, DOTA (1,4,7,10-Tetraazacyclododecane-1,4,7,10-tetraacetic acid), has been developed as a potent Ca^{2+} binder - stronger than classical metal chelates such as EDTA. Moreover, DOTA is also a perfect candidate for a ligand of trivalent lanthanide cations.[32] For example, the crystal

[32] Viola-Villegas, N.; Doyle, R. *Coord. Chem. Rev*. **2009**, *253*, 1906.
[33] Austin, C.; Rodgers, M. *J. Phys. Chem.* **2014**, *118*, 5488.
[34] Lejault, P.; Duskova, K.; Bernhard, C.; Valverde, I.; Romieu, A.; Monchaud, D. *Eur. J. Org. Chem*. **2019**, 6146.
[35] Wahsner, J., Gale, E.; Rodríguez A.; Caravan, *P. Chem. Rev*. **2019**, *119*, 957.
[36] Nielsen, l.; Junker, A.; Sørensen, T. *Dalton Trans.* **2018**, *47*, 10360.
[37] Dyke, J.; Levason, W.; Light, M.; Pugh, D.; Reid, G.; Bhakho, H.; Ramasamib, P.; Rhyman, L. *Dalton Trans*. **2015**, *44*, 13853.
[38] Rashid, H.; Martines, M.; Jorge, J.; Moraes, P.; Umar, M.; Khan, K.; Rehman, H. *Bioorg. Med. Chem*. **2016**, *24*, 5663.

structure of DOTA-Eu^{3+} is characterized by a nona-coordinated anionic complex with a capping water molecule at the ninth coordination site (**Figure 2. 2**).[39]

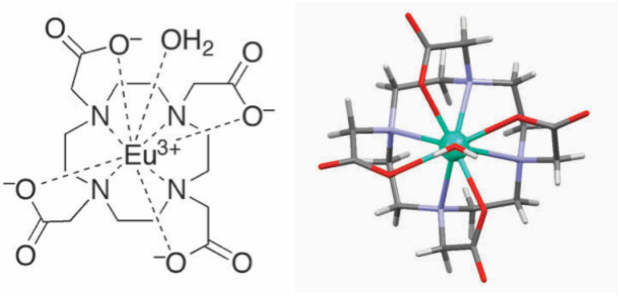

2.3

Figure 2. 2. DOTA-Eu^{3+} complex structure[43]

Moreover, its sidearm functionalization arranges the topology suitably for different metal complexations. The very first crystal structure of octadentate cyclen-metal complex was published in 1982 by Buoen and co-workers, involving tetrakis-(2-hydroxyethyl)-cyclen (**Figure 2. 3**).[40]

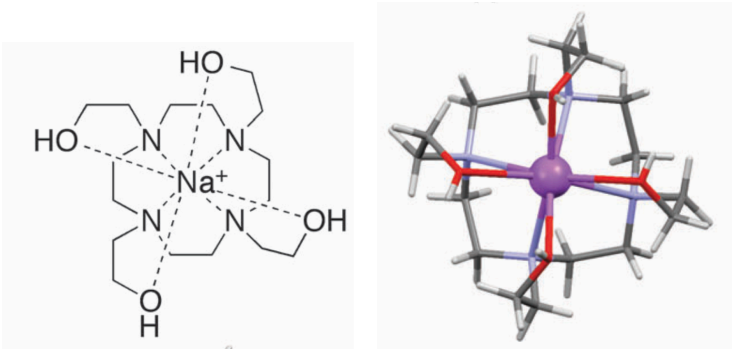

2.4

Figure 2. 3. Tetrakis-(2-hydroxyethyl)-cyclen-Na^{+} complex[43]

The 1,4,7,10-tetraazacyclododecane ring typically assumes a "square" conformation upon metal complexation in which the methylene groups are in the corners.[41] The 3D coordination structure models depend on the dimensions of the metal cations. Large cations including Na^{+}, K^{+}, Ca^{2+}, $Cd^{2+,}$ Hg^{2+} or Bi^{3+} are usually characterized by hepta- and octa-coordination, while

[39] Spirlet, M.; Rebizant, J.; Desreux, J.; Loncin, M. *Inorg. Chem.* **1984**, *23*, 359.
[40] Buoen, S.; Dale, J.; Groth, P.; Krane, J. *Chem. Commun.* **1982**, 1172.
[41] Dale*, J. Acta Chem. Scand.* **1973**, *27*, 1130.

trivalent lanthanide ions favor nona- and deca-coordination (including one coordinative solvent or anionic species). On the contrary, small Zn^{2+} and transition metal cations tend to adopt penta- or hexa-coordination. Large metal cations do not fit in the center of the 1,4,7,10-tetraazacyclododecane's cavity and consequently are placed above the macrocyclic structure. Four pendant arms are wrapped around the cations to form quasi-cryptate complexes.

Hexacyclen (1,4,7,10,13,16-hexaazacyclooctadecane) can be considered as the aza analogue of 18-crown-6 (1,4,7,10,13,16-hexaoxacyclooctadecane). There is significant interest in hexacyclen ligands due to their selectivity for various metal cations (i.e., alkali, alkaline earth, heavy metal, and transition) cations. When compared with cyclen, the cavity of the hexadentate 1,4,7,10,13,16-hexaazacyclooctadecane is characterized by greater flexibility. In consequence, hexacyclen derivatives can entirely encapsulate the metal cation.[42]

2.1.2. Structural dynamism of peraza-macrocycle complexes

Structural dynamism has an important role in synthetic and biological systems, as it governs functions and structures of numerous molecules and their assemblies.[43]

The metal complexes of cyclen ligands (e.g., tetrabenzylcyclen (**2.5**) sodium complex; **Figure 2. 4**) exhibit structural dynamism because of the intrinsic flexibility of the 1,2-diaminoethylene units (with clockwise, δ, or counterclockwise, λ, ordering; **Figure 2. 5**)[48] and sidearms (with clockwise, Δ, or counterclockwise, Λ, arrangement; **Figure 2. 6**).[44]

[42] Drew, M.; Santos, M. *Struct. Chem*. **1993**, *4*, 5-14.
[43] Shinoda, S. *Chem. Soc. Rev*. **2013**, *42*, 1825-1835.
[44] Herman, P.; Kotek, J.; Kubicek, V.; Lukes, I. *Dalton Trans*. **2008**, 3027.

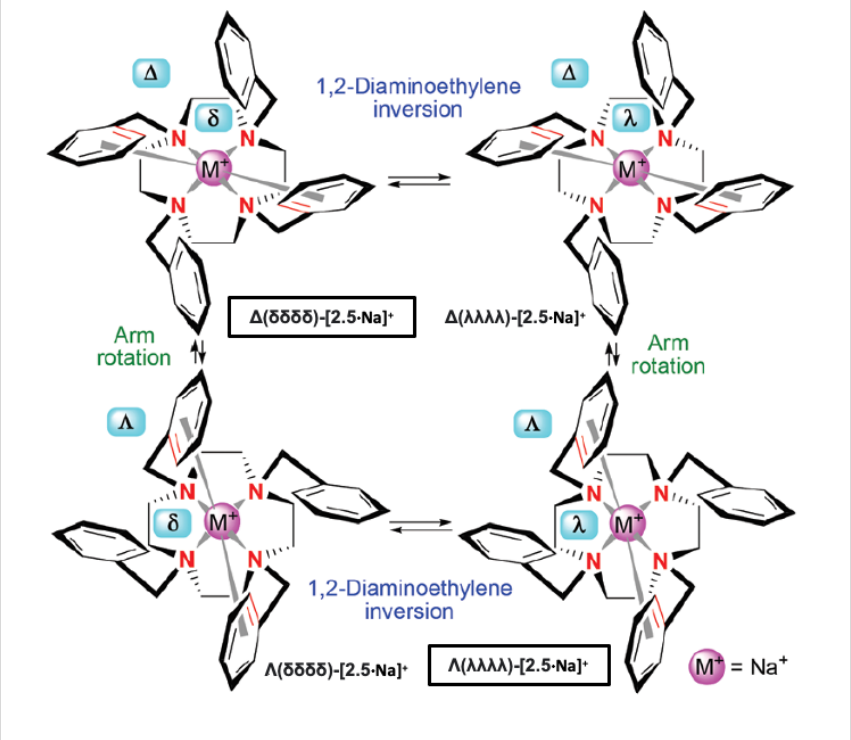

Figure 2. 4. Schematic structures of the four stereoisomers of tetrabenzylcyclen sodium complex in their stable "square" conformation (observed from the sidearm donors' square plane). [45]
(X-ray structure of [**2.5**·Na]⁺; CCDC 1941541)

Figure 2. 5. Equilibrium between the δ and λ gauche conformations of 1,2-diaminoethylene cyclen units[45]

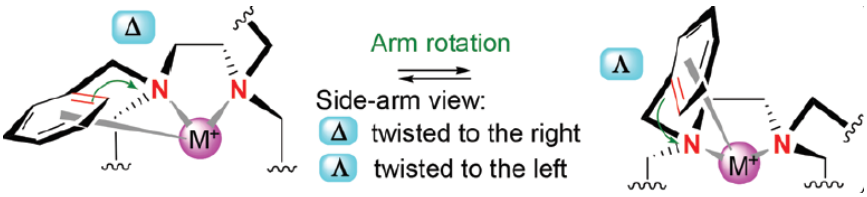

Figure 2. 6. Equilibrium between Δ/Λ side arm conformations[45]

Of the four potential equilibrating stereoisomers (i.e., two pairs of Δ(δδδδ)/Λ(λλλλ) and Λ(δδδδ)/Δ(λλλλ) enantiomers), the enantiomorphous Δ(δδδδ)/Λ(λλλλ) pair predominates

[45] Schettini, R.; D'Amato, A.; Araszczuk, A. M.; Della Sala, G.; Costabile, C.; D'Ursi, A. M.; Grimaldi, M.; Izzo, I.; De Riccardis, F. *Org. Biomol. Chem.* **2021**, *19*, 7420.

because of the larger conformational space above the 1,2-diaminoethylene unit with the torsion angle $\Phi_{(Ph)C-N-C-C}$ = −163° (**Figure 2. 7**).[48] A narrower space on the adjacent unit, with $\Phi'_{(Ph)C-N-C-C}$ = +76°, hampers the formation of the mismatched Λ(δδδδ)/Δ(λλλλ) stereoisomers.

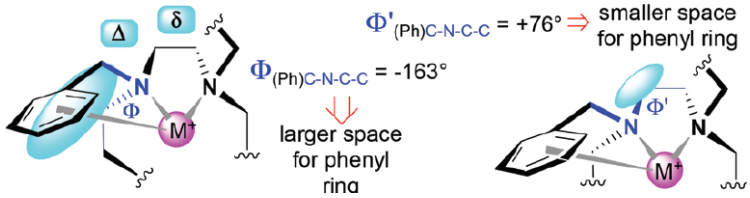

Figure 2. 7. $\Phi_{(Ph)C-N-C-C}$ bond torsion angles connecting the side chain and 1,2-diaminoethylene units – in blue; from the X-ray structure of tetrabenzylcyclen sodium complex[48,45]

Metal complexes of hexacyclen derivatives (e.g., [(Me_6hexacyclen)·M]$^+$) demonstrate different orderings depending on the dimension of the complexed metal cation.[37] Small cations (such as Li^+) favor C_2-symmetric (δδλδδλ)-puckered conformations. On the other hand, (δλδλδλ)-D_{3d}-symmetric species, with *N*–Me groups alternating "up-down" around the ring, are prevalent in the case of larger metal cations such as K^+ or Rb^+ (**Figure 2. 8**).

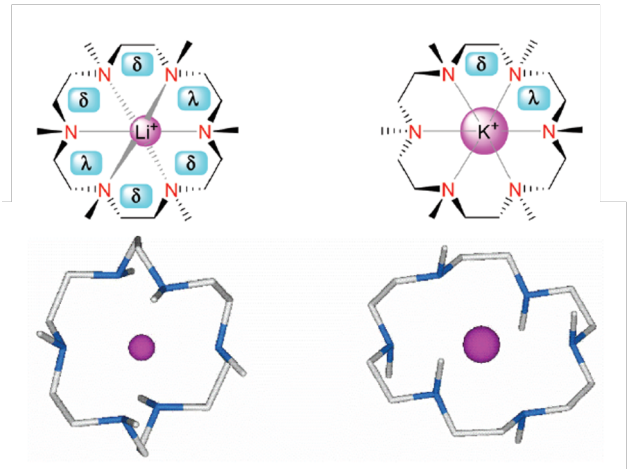

2.6a **2.6b**

Figure 2. 8. Schematic and X-ray structures of (δδλδδλ)-[(Me6hexacyclen)·Li]$^+$ and (δλδλδλ)-[(Me6hexacyclen)·K]$^+$ complexes.[37] Hydrogen atoms have been omitted for clarity. Atom type: C, light grey; N, blu.

2.1.3. From cyclic peptoids to peraza-macrocycles

N-Functionalization of cyclic polyamines with four identical pendant arms is straightforward. On the other hand, the preparation of hetero- or unsymmetrically substituted macrocycles is more synthetically challenging.[46] Their synthesis depends on high-priced cyclic precursors, arduous protecting group manipulations and finally low yield regioselective reactions.[47]

The demand for a versatile synthetic strategy towards efficient peraza-macrocyclic chelators prompted Izzo and De Riccardis group to develop an innovative approach based on the intra-annular amide reduction of cyclic peptoids.[48] This straightforward method makes it possible to avoid tedious post synthetic modifications, the installation of *N*-side chains occurs early in the synthetic process.

The preparation of polydentate aza-coronands (**Scheme 2. 1**) relies on "sub-monomer" solid-phase synthesis of linear precursors,[49] subsequent high dilution cyclization,[50] tertiary amide reduction, and when apposite, *N*-debenzylation.[51]

[46] Denat, F.; Brandes, S.; Guilard, R. *Synlett* **2000**, 561-574.
[47] Lattuda, l.; Barge, A.; Cravotto, G.; Giovenzana, G.B.; Tei, L. *Chem. Soc. Rev.* **2011,** *40,* 3019-3049.
[48] Schettini, R.; D'Amato, A.; Pierri, G.; Tedesco, C.; Della Sala, G.; Motta, O.; Izzo, I.; De Riccardis, F. *Org. Lett.* **2019**, *21*, 7365-7369.
[49] Zuckermann, R.; Kerr, J.; Kent, S.; Moos, W. J. *Am. Chem. Soc.* **1992,** *114*, 10646-10647.
[50] Shin, S.; Yoo, B.; Todaro, L.; Kirshenbaum, K. *J. Am. Chem. Soc.* **2007,** *129,* 3218-3225.
[51] Huang, Y.; Liu, Y.; Liu, S.; Wu, R.; Wu, Z. *Eur. J. Org. Chem*. **2018**, 2018, 1546-1551.

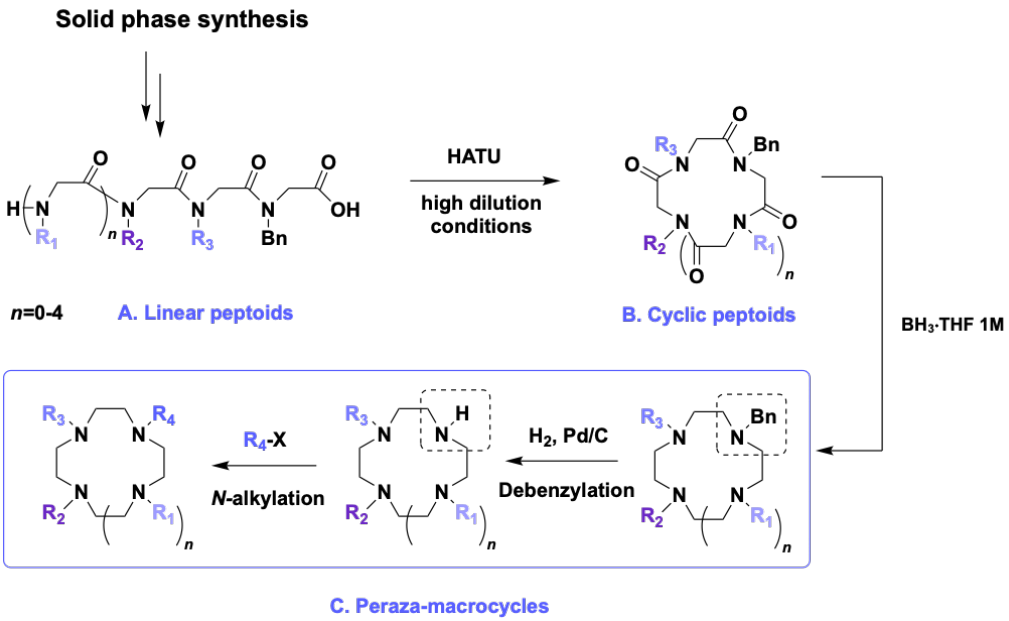

Scheme 2. 1. From peptoids to perazamacrocycles: new synthetic approach.

Moreover, it is worth emphasizing that comparing the new approach with the classic ones, the striking advantages of the new methodology emerge. Firstly, it allows the quick construction of different-sized peraza-macrocycles, following the same procedure. Secondly, the new approach expands the accessible chemical space, due to the wide variety of commercially available primary amines, potentially employed for the linear precursors' preparation.

2.1.4. Research targets

While there is exclusively a single example of a chiral, totally *N*-substituted hexa-aza macrocycle in the literature,[52] numerous chiral cyclen complexes have been reported (principally DOTA analogues).[43] In these molecular species, strategically positioned stereogenic centers provide the formation of sterically locked recognition agents,[53] MRI probes,[54] luminescent sensors, [55] and chiral argentivorous molecules.[56] Regrettably, the

[52] Izatt, R.M. *J. Heterocycl. Chem.* **1999**, *36*, 347.
[53] Misaki, H.; Miyake, H.; Shinoda, S.; Tsukube, H. *Inorg. Chem.* **2009**, *48*, 11921.
[54] Woods, M.; Botta, M.; Avedano, S.; Wang, J.; Sherry, A.D. *Dalton Trans.* **2005,** 3829.
[55] Dickins, R.S.; Howard, J. A. K.; Lehmann, C. W.; Moloney, J.; Parker, D.; Peacock, R. D. *Angew. Chem. Int. Ed. Engl.* **1997**, *36*, 521.
[56] Lee, E.; Okazaki, C.; Tenma, H.; Hosoi, Y.; Ju, H.; Ikeda, M.; Kuwahara, S.; Habata, Y. *Inorg. Chem*. **2020,** *59*, 13435.

synthesis of chiral macrocycles requires complex synthetic procedures,[53] arduous manipulation of protecting groups[47] and demanding stereospecific steps.[54]

The aim of this research was to prepare and study the previously inaccessible chiral peraza-macrocyclic ligands by taking advantage of synthetic strategy disclosed by our research group in 2019.[48] The study was focused on cyclen and hexacyclen derivatives containing chiral centers in the pendant arms or in the second variant inserted into the backbone. The impact of (*S*)-1-phenylethyl side chain and (*S*)-pyrrolidine rings on the structural dynamism of metalated peraza-macrocycles has been evaluated.

2.2. Structural dynamism of chiral sodium peraza-macrocycle complexes

2.2.1. Results and discussion

2.2.1.1 Synthesis of peraza-macrocycle ligands 2.7-2.13

The preparation of the model polydentate macrocycles **2.7-2.13** was achieved *via* borane reduction[48] of the corresponding known *cis–trans–cis–trans*–(*ctct*)-**2.14**, *ctct*-**2.15**, *cctcct*-**2.16**, *cctcct*-**2.17**,[57] all-*cis*-**2.19**,[58] conformationally heterogeneous **2.20**,[59] and new *ctct*-**2.18** chiral cyclic peptoids (**Scheme 2. 2**).

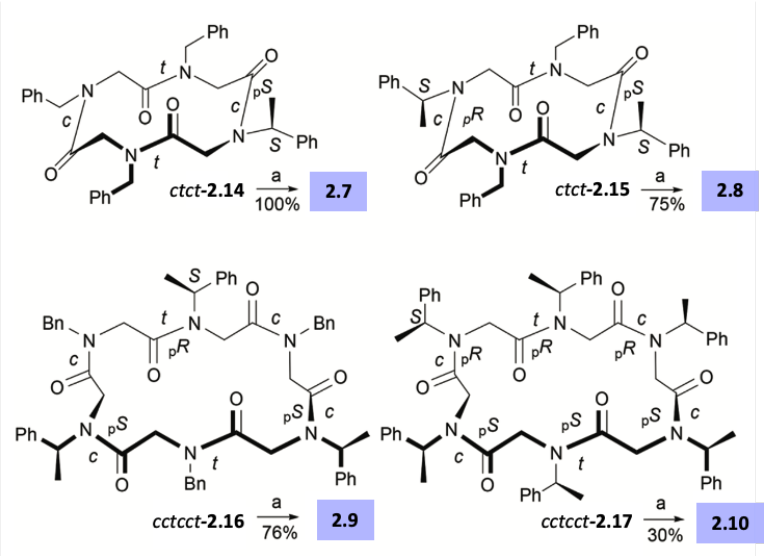

[57] D'Amato, A.; Pierri, G.; Tedesco, C.; Della Sala, G.; Izzo, I.; Costabile, C.; De Riccardis, F. *J. Org. Chem*. **2019**, *84*, 10911.
[58] Schettini, R.; De Riccardis, F.; Della Sala, G.; Izzo, I. *J. Org. Chem*. **2016,** *81*, 2494.
[59] Schettini, R.; Nardone, B.; De Riccardis, F.; Della Sala G.; Izzo, I. *Eur. J. Org. Chem*. **2014**, 7793.

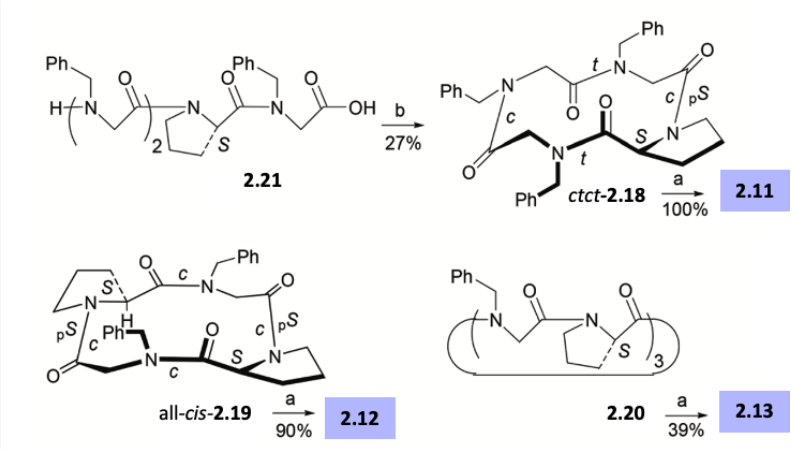

Scheme 2. 2. Schematic structures of cyclic peptoid precursors 2.14-2.20 (and linear peptoid 2.21) as their major conformational isomers and reaction conditions/yields for the crucial reductive step. (a) 1. BH_3·THF (5.0 equivalents for each amide group) in THF, 90° for 24 h; 2. H_2O; 3. 1 N HCl reflux, CsOH·H_2O; extraction in an organic solvent. (b) HATU, DIPEA in DMF, r.t. for 18 h. *c* and *t* define the *cis/trans* amide bond geometry; descriptors p*R*/p*S* report the amide bond planar chirality[60]

The monoprolinated cyclic compound **2.18**, valuable to conclude the (*S*)-pyrrolidine series, was obtained from the corresponding linear precursor H-(*N*pm)$_2$-L-Pro-Npm-OH (**2.21**) *via* mixed "sub-monomer"/monomer solid-phase approach[58,59] and head-to-tail macrocyclization.[57,58]

2.18 was isolated in good purity (>90%, HPLC analysis) as a prevalent *ctct*[61] conformational isomer. The *ctct* amide bond geometry was deduced by the NMR analysis and energetic considerations. Specifically, the ^{13}C NMR signal at δ 22.0 (C$^{\gamma}$ L-proline) was diagnostic of a *cis* X-Pro amide junction (C$^{\gamma}$ L-proline resonance at δ = 21.7 and δ = 24.0 for the *cis* and *trans* X-Pro units, respectively).[62,63] Another *cis* peptoid bond was confirmed by the high ^{1}H NMR Δδ value (1.78 ppm) observed for the Npm diastereotopic methylene benzyl protons (syn in relation to a deshielding carbonyl group,[64] δ 5.52 and 3.74). The two remaining *N*pm side

[60] De Riccardis, F. *Eur. J. Org. Chem*. **2020**, 2981.
[61] D'Amato, A.; Schettini, R.; Della Sala, G.; Costabile C.; Tedesco, C.; Izzo, I.; De Riccardis, F. *Org. Biomol. Chem*. **2017**, *15*, 9932.
[62] Ueno, K.; Shimizu, T. *Biopolymers*, **1983**, 22, 633.
[63] Izzo, I.; Ianniello, G.; De Cola, C.; Nardone, B.; Erra, L.; Vaughan, G.; Tedesco, C.; De Riccardis, F. *Org. Lett*. **2013**, *15*, 598.
[64] D'Amato, A.; Volpe, R.; Vaccaro, M.C.; Terracciano, S.; Bruno, I.; Tosolini, M.; Tedesco, C.; Pierri, G.; Tecilla, P.; Costabile, C.; Della Sala, G.; Izzo, I.; De Riccardis, F. *J. Org. Chem*. **2017**, *82*, 8848.

chains demonstrated low methylene benzyl Δδ values (0.35 and 0.08 ppm), suggesting *trans* amide geometries. Excluding the strained *cctt* isomers, three *ctct* conformers **2.18**, **2.18a** and **2.18b** were recognized as reliable candidates (i.e., cyclo-[(*cis*,pS)L-Pro-(*trans*,pS)Npm^1-(*cis*,pR)*N*pm^2 (*trans*,pR)*N*pm^3], cyclo-[(*cis*,pR)L-Pro-(*trans*,pR)*N*pm^1-(*cis*,pS)*N*pm^2-(*trans*,pS)*N*pm^3], and cyclo-[(*cis*,pR)L-Pro-(*trans*,pS)*N*pm^1-(*cis*,pR)*N*pm^2-(trans,pS)*N*pm^3], respectively, **Figure 2. 9**).

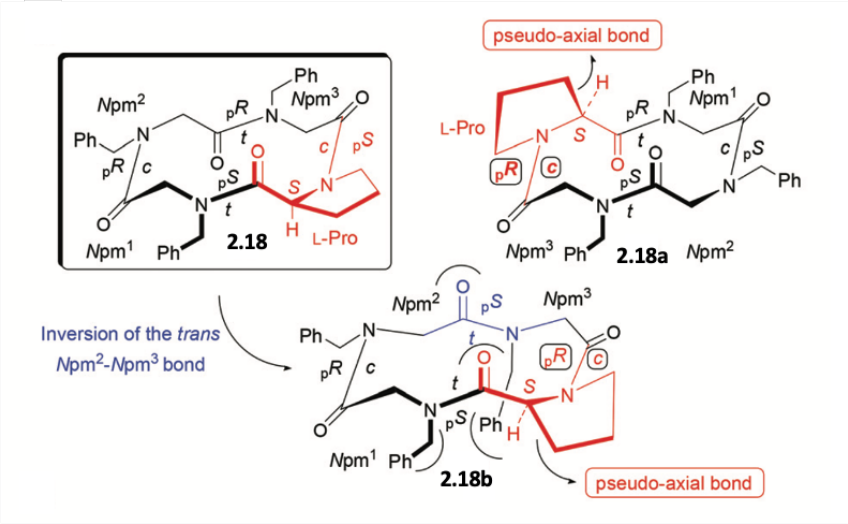

Figure 2. 9. Schematic structures of the three potential *ctct* conformational isomers of cyclo-(L-Pro-Npm$_3$): **2.18**, **2.18a**, and **2.18b**.

The DFT calculations at the BP86/ TZVP level[65] (**Figure 2. 10**), revealed that **2.18** (containing an *N*pm^3-(*cis*,pS)L-Pro bond) was the most stable species. On the other hand, theoretical analyses excluded **2.18a** (E = 20.9 kcal mol^{-1}) on account of a pseudo-axial CH$_{(S)}$-CH$_2$ pyrrolidine bond (connected to an energetically disfavored X-(*cis*,pR)L-Pro peptoid bond). The third *ctct*-macrocycle (**2.18b**, ΔE = 8.9 kcal mol^{-1}), with a flipped *N*pm^2–*N*pm^3 *trans* amide bond (depicted in blue color in **Figure 2. 9**), demonstrated unfavorable steric interactions between the facing *trans* *N*pm residues.

[65] DFT calculations were performed by prof. C. Costabile, Dpt. of Chemistry and Biology "A. Zambelli", Univ. of Salerno.

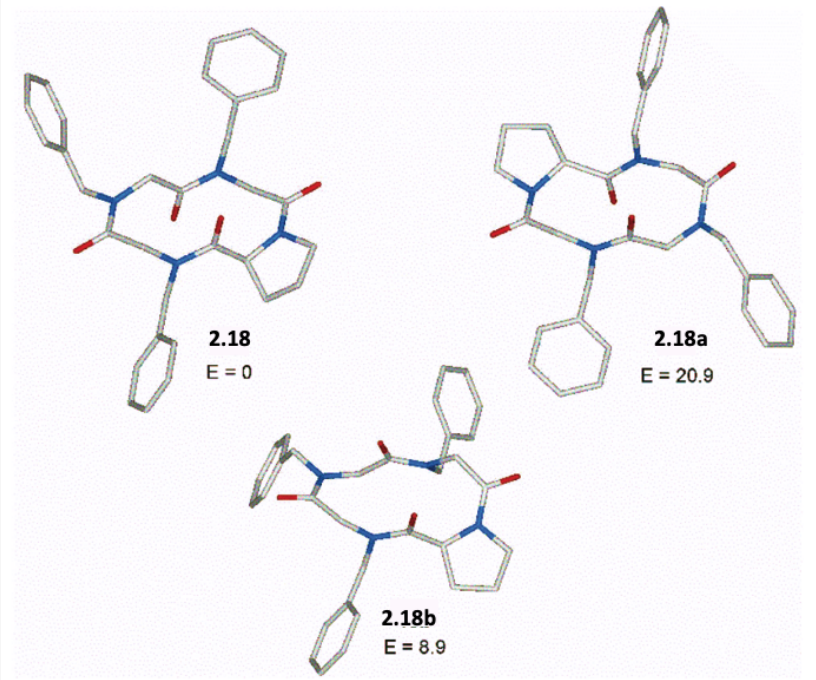

Figure 2. 10. Minimum energy structures of the three potential *ctct* conformational isomers of cyclo-(L-Pro-Npm_3): **2.18**, **2.18a**, and **2.18b,** and their internal energies in $CHCl_3$ expressed in kcal mol^{-1}. Hydrogen atoms have been omitted for clarity. Atom type: C, light grey; O, red; and N, blue.

The chiral macrocyclic peptoid precursors **2.15**-**2.21** were exposed to the key BH_3-mediated reduction (**Scheme 2. 2**), a rather soft reaction known to conserve the α-configuration of natural amino acids,[66] including prolines.[67] While good yields were obtained for cyclic tetrapeptoids **2.7**, **2.8**, **2.11**, and **2.12** (from 75% to 100%), the larger congeners **2.9**, **2.10**, and **2.13** were isolated with lower yields (from 30% to 76%; ^{1}H NMR analysis, **Figure 2. 11**).

2.2.1.2 Sodium binding studies on peraza-macrocycles 2.7-2.13

The coordination chemistry of the sodium ion with neutral ligands is dominated by oxygen-donor ligands, as crown ethers and cryptands.[68] However, Na^+, as well as Ag^+,[69] likewise coordinates to the less electronegative N-donor atoms due to the low energy of the Na[BAr^F] salts in poorly coordinating solvents. Addition of 1.0 equiv. of NaTFPB to 5.0 mM solutions of

[66] Alcaro, M.C.; Orfei, M.; Chelli, M.; Ginanneschi, M.; Papini, A.M. *Tetrahedron Lett.* **2003**, *44*, 5217.
[67] Bolm, C.; Meyer, N.; Raabe, G.; Weyhermüller, T.; Botheb, E. *Chem. Commun*. **2000**, 2435.
[68] Steed, J.W.; Atwood, J.L. Supramolecular Chemistry, Wiley & Sons, Ltd, Chichester, UK, **2009,** 2, 116.
[69] Lee, E.; Okazaki, C.; Tenma, H.; Hosoi, Y.; Ju, H.; Ikeda, M.; Kuwahara, S.; Habata, Y. Inorg. Chem. **2020**, 59, 13435.

2.7–**2.9**, **2.11**, and **2.13** in $CDCl_3$ or toluene-d_8 (**2.12**) induced discernible variation of their ^{1}H NMR spectra, demonstrating substantial conformational changes (^{1}H NMR analysis, **Figure 2. 11**).

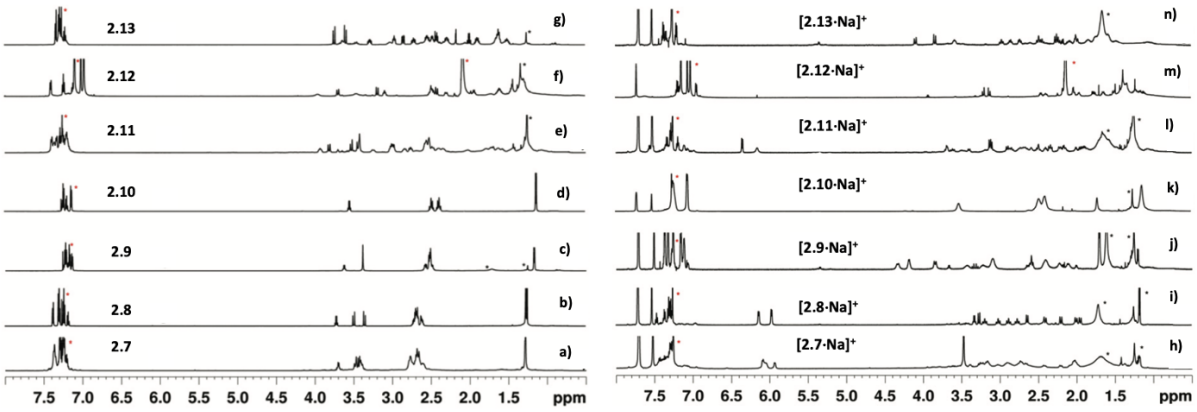

Figure 2. 11. ^{1}H NMR spectra of peraza-macrocycles **2.7**-**2.13** (a-g; 5.0 mM solutions in $CDCl_3$, or toluene-d_8, for **2.11**, 600 MHz) and ^{1}H NMR spectra of their sodium complexes (h-n; 5.0 mM solutions in $CDCl_3$, or toluene-d_8 in the presence of 1.0 eq of NaTFPB, 600 MHz). Residual solvent peaks are labelled with a red asterisk. Water/lipid impurities are labelled with a black asterisk..

While the complexes of peraza-coronands **2.8**, **2.9**, **2.12**, and **2.13** (**Figure 2. 11i**, **j**, **m** and **n**) provided spectroscopically homogeneous species, those concerning hosts **2.7** and **2.11** gave mixtures of multiple conformers and were not investigated further. Addition of NaTFPB to a $CDCl_3$ solution of **2.10** resulted in signal broadening and therefore was also not further examined.

2.2.1.3 Structure of cyclen complexes [2.8·Na]$^+$ and [2.12·Na]$^+$

The first complex to be studied was [**2.8**·Na]$^+$. The peraza-macrocyclic ligand, decorated with two (*S*)-(1-phenylethyl) side chains, belongs to the rare class of neutral chiral tetraaza-macrocycles.[70,71] Stepwise quantitative additions of NaTFPB to a 5.0 mM solution of **2.8** in $CDCl_3$ led to the formation of a two-fold symmetric metalated species, as confirmed by the simplification of the ^{1}H NMR (**Figure 2.11i**) and ^{13}C NMR spectra. A 1 : 1 host : guest stoichiometric ratio was determined from ^{1}H NMR peak integration and appeared to be

[70] Misaki, H.; Miyake, H.; Shinoda, S.; Tsukube, H. *Inorg. Chem*. **2009**, *48*, 11921.
[71] Glovenlock, L.J.; Howard, J.A.K.; Moloney, J.M.; Parker, D.; Peacock, R.D.; Siligardi, G. *J. Chem. Soc., Perkin Trans.* **1999**, *2*, 2415.

constant through gradual guest addition. The high resolution MALDI-MS spectrum of the complex additionally confirmed a species at m/z: 583.3946, [**2.8**·Na]$^+$. A marked upfield shift of the aromatic ortho-protons (δ = 6.14 and 5.97) suggested C_{Ar}–H···π interactions and Na^+-aryl η^2-hapticity. Analogous interrelationships have been already demonstrated for complexes of tetrabenzylcyclen[48] and its derivatives.[72]

The existence of three stereogenic components in complex [**2.8**·Na]$^+$ (i.e., the 1,2-diaminoethylene conformation (δ/λ), the helicity of the pendant arms (Δ/Λ), and the stereocenters of the side chains) results in the potential formation of four equilibrating C_2-symmetric diastereomers: (*S,S*)-Δ(δδδδ)-, (*S,S*)-Δ(λλλλ)-, (*S,S*)-Λ(δδδδ)-, and (*S,S*)-Λ(λλλλ)-[**2.8**·Na]$^+$ (**Figure 2. 12**).

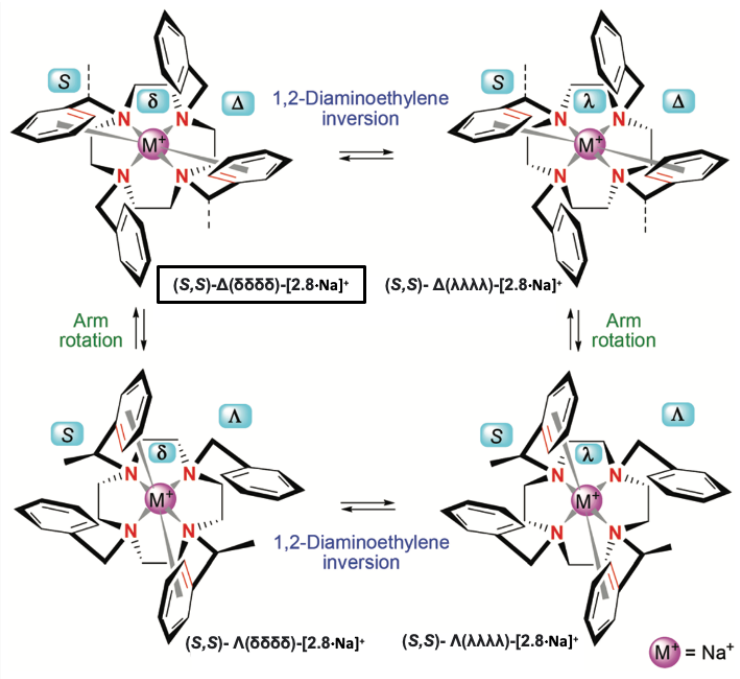

Figure 2. 12. Schematic structures of potential C_2-symmetric (*S,S*)-Δ(δδδδ)-, (*S,S*)-Δ(λλλλ)-, (*S,S*)-Λ(δδδδ)-, and (*S,S*)-Λ(λλλλ)-[**2.8**·Na]$^+$ conformers, observed from the side arms or Na^+ ion.

Molecular modelling studies of the four stereoisomers revealed significant internal energy divergences among the metalated species (**Figure 2. 13**). The lowest energy of the (*S,S*)-Δ(δδδδ)-[**2.8**·Na]$^+$ diastereoisomer was assigned to the stabilizing anti-relationship between

[72] Habata, Y.; Ikeda, M.; Yamada, S.; Takahashi, H.; Ueno, S.; Suzuki, T.; Kuwahara, S. *Org. Lett.* **2012**, *14*, 4576.

the metal ion and methyl group (evidently visible in the top view of the complex, **Figure 2. 13a**).[73,74] The higher energy of the (*S,S*)-Δ(λλλλ) and (*S,S*)-Λ(δδδδ) species (**Figure 2. 13b**, and **c**, 10.8 and 12.8 kcal mol^{-1}, respectively) was attributed to the unfavorable side chain/1,2-diaminoethylene unit interactions (with the $\Phi_{(Ph)C-N-C-C}$ torsion angle ~−80°). On the other hand, disadvantageous placement of the methyl substituents in relation to the metal ion increased the energies of the (*S,S*)-Λ(λλλλ) stereoisomer to 5.4 kcal mol^{-1} (**Figure 2. 13d**).

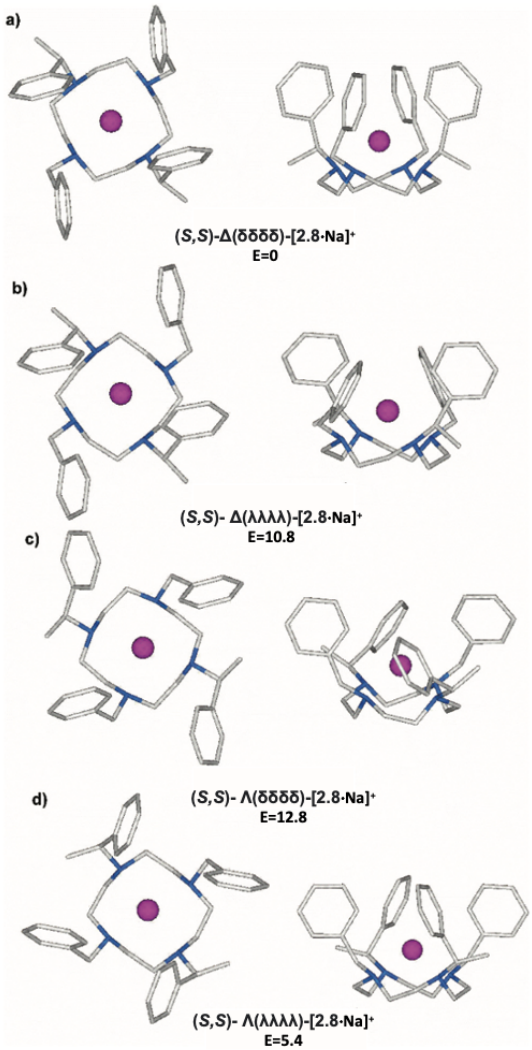

Figure 2. 13. Minimum energy structures of (a) (*S,S*)-Δ(δδδδ)-, (b) (*S,S*)- Δ(λλλλ)-, (c) (*S,S*)-Λ(δδδδ)-, and (d) (*S,S*)-Λ(λλλλ)-[**2.8**·Na]+ (observed from the top: left, and observed from the side, right) and their internal energies in $CHCl_3$ expressed in kcal mol^{-1}. Hydrogen atoms have been omitted for clarity.
Atom type: C, light grey; N, blue; and Na, magenta.

[73] Woods, M.; Aime, S.; Botta, M.; Howard, J.A.K.; Moloney, J.M.; Navet, M.; Parker, D.; Port, M.; Rousseaux, O. *J. Am. Chem. Soc*. **2000**, *122*, 9781.
[74] Di Bari, L.; Pescitelli, G.; Sherry, A.D.; Woods, M. *Inorg. Chem*. **2005**, *44*, 8391.

X-ray diffractometric studies performed on Na^+ cyclen complexes attested the formation of the Δ(δδδδ)/Λ(λλλλ)[48,72] and (*S,S,S,S*)-Δ(δδδδ)[71] species (i.e., "p-type"[75] or twisted square antiprismatic, TSAP, isomers).[76] Although, whereas most of the these species gave broad NMR macro ring signals (due to slow Δ(δδδδ) ⇄ Λ(λλλλ) interconversion),[48,72,77] in [**2.8**·Na]$^+$ the pattern of *trans*-diaxial (δ 3.20, 3.03, 2.89, 2.78; dd, J ~13 Hz) and pseudoequatorial (δ 2.41, 2.21, 2.01, 1.96; d, J ~13 Hz) 1,2-diaminoethylene protons, assigned *via* 2D NMR experiments (**Figure 2. 14**) confirmed the generation of a rigid metal complex.

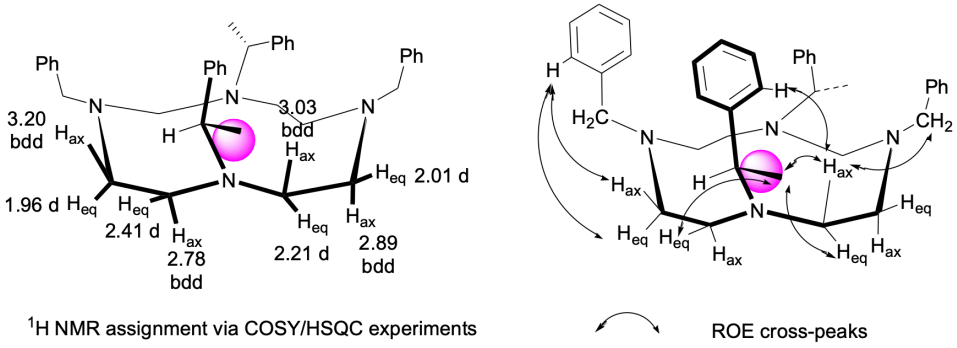

Figure 2. 14. ^{1}H NMR assignment for complex [2.8·Na]$^+$TFPB$^-$.

On the other hand, addition of NaTFPB to ligand **2.12** (**Figure 2.11m**, ^{1}H NMR analysis) resulted in the formation of a conformationally stable metalated species with distinguishable ^{1}H NMR macro ring (δ 2.46, 2.40, 2.17, 1.96, 1.76, 1.64, and 1.50), (*S*)-pyrrolidine (δ 2.04–2.01, 1.52–1.10), and methylene benzyl resonances (δ 3.20, 3.13, AB system with J ~13 Hz). Also in this case, a 1 : 1 host : guest stoichiometric ratio was determined from ^{1}H NMR peak integration and resulted to be constant through gradual guest addition. Once again, the formation of a monosodiated species was attested by the MALDI-MS spectrum showing a peak at *m/z*: 455.3272, [**2.12**·Na]$^+$.

[75] Di Bari, L.; Pintacuda, G.; Salvadori, P. *Eur. J. Org. Chem*. **2000**, 75.
[76] Nielsen, L.G.; Junker, A.K.R.; Sørensen, T.J. *Dalton Trans.* **2018**, *47*, 10360.
[77] Tsukube, H.; Mizutani, Y.; Shinoda, D.; Okazaki, T.; Tadokoro, M.; Hori, K. *Inorg. Chem*. **1999**, *38*, 3506.

In complex **[2.12**·Na]$^+$, the interconversion between (1*R*,2*S*,4*S*,7*R*,8*S*,10*S*)-(δδδδ)- and (1*S*,2*S*,4*R*,7*S*,8*S*,10*R*)-(δδδδ)-species (**Figure 2. 15**, left) and (1*R*,2*S*,4*S*,7*R*,8*S*,10*S*)-(λλλλ)- and (1*S*,2*S*,4*R*,7*S*,8*S*,10*R*)-(λλλλ)-species (**Figure 2. 15** , right) requires configurational inversion[78,79] of the nitrogen atoms[80] (the Na^+ ion relocation to the opposite side of the molecule is marked by the anti and syn relationship between the methyne (*S*)-pyrrolidine hydrogens and Na^+).

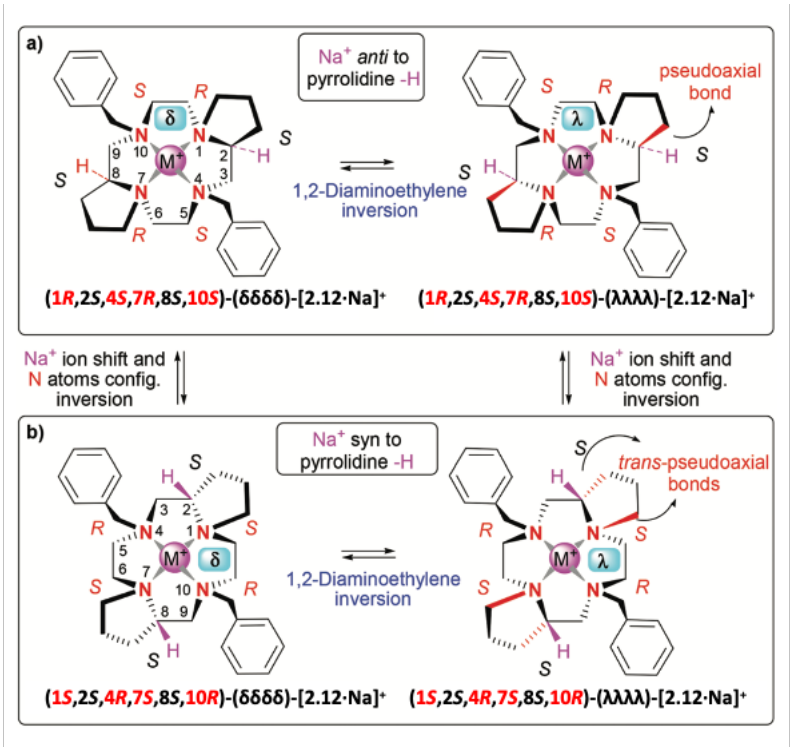

Figure 2. 15. Schematic structures of C_2-symmetric (a) (1*R*,2*S*,4*S*,7*R*,8*S*,10*S*)- (δδδδ)- and (1*R*,2*S*,4*S*,7*R*,8*S*,10*S*)-(λλλλ)-[**2.12**·Na]$^+$ conformers; (b) (1*S*,2*S*,4*R*,7*S*,8*S*,10*R*)-(δδδδ)- and (1*S*,2*S*,4*R*,7*S*,8*S*,10*R*)-(λλλλ)-[**2.12**·Na]$^+$ conformers, observed from the Na^+ ion. The absolute configurations of stereogenic carbon atoms are reported in black, and the absolute configurations of stereogenic nitrogen atoms are reported in red.

The DFT calculations excluded the geometrically unreachable (1*S*,2*S*,4*R*,7*S*,8*S*,10*R*)-(λλλλ)-[**2.12**·Na]$^+$ due to the *trans*-pseudodiaxial $CH_{(S)}$–CH_2/N_{pyrr}–CH_2 pyrrolidine bonds (depicted in red colour in **Figure 2. 15,** right, and **Figure 2. 16**).

[78] Gerus, A.; Slepokura, K.; Lisowski, J. *Polyhedron*, **2019**, *170*, 1151.
[79] Kuzmina, L.G.; Struchkov, Y.T.; Dunina, V.V.; Zalevskaya, O.A.; Potapov, V.M. *Russ. Chem. Bull*. **1986**, *35*, 1639.
[80] The absolute configuration of the nitrogen atoms was assigned following the CIP rules (the Na^+ ion has the highest priority)

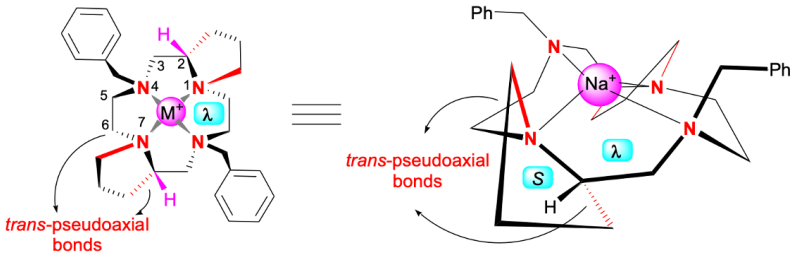

Figure 2. 16. Schematic structures of geometrically unreachable (1*S*,2*S*,4*R*,7*S*,8*S*,10*R*)-(λλλλ)-[**2.12**·Na]$^+$ model (top and side view).

The pseudoequatorial disposition of these two critical bonds in conformers (1*R*,2*S*,4*S*,7*R*,8*S*,10*S*)-(δδδδ)- and (1*S*,2*S*,4*R*,7*S*,8*S*,10*R*)-(δδδδ)-[**2.12**·Na]$^+$ (**Figure 2. 15**, left) drove their internal energies in toluene to values of 0 and 4.8 kcal mol^{-1}, respectivelly (**Figure 2. 17a**, and **b**). On the other hand, an underprivileged pseudoaxial orientation of the $CH_{(S)}$–CH_2 bond in conformer (1*R*,2*S*,4*S*,7*R*,8*S*,10*S*)-(λλλλ)-[**2.12**·Na]$^+$ (**Figure 2. 15**, right) increased its internal energy to 3.4 kcal mol^{-1} (**Figure 2. 17c**).

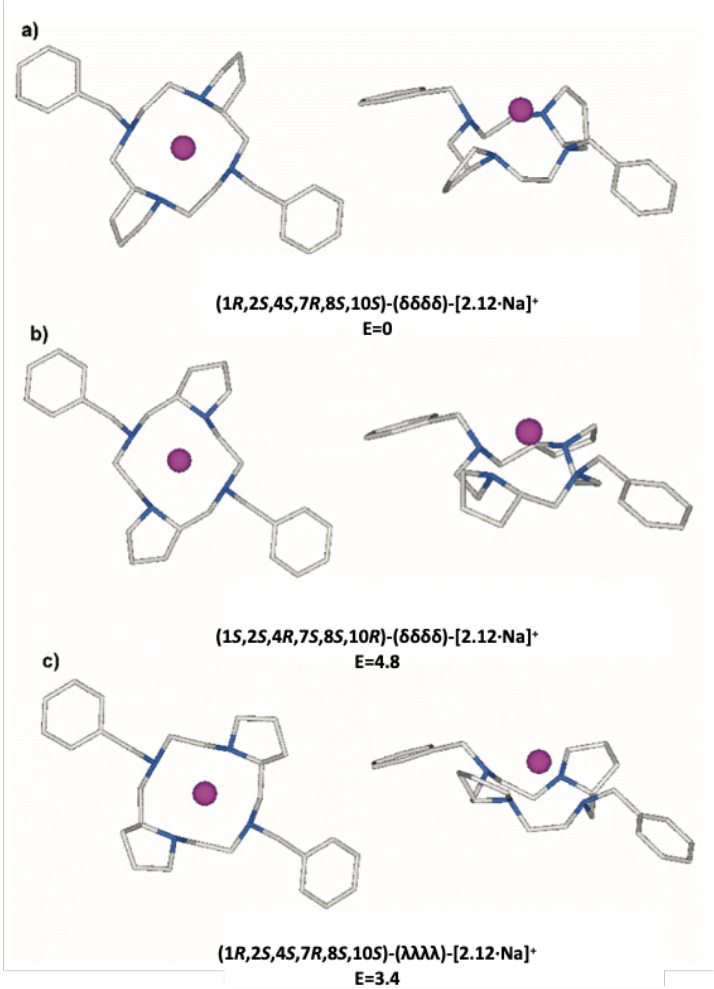

Figure 2. 17. Minimum energy structures of (a) (1*R*,2*S*,4*S*,7*R*,8*S*,10*S*)-(δδδδ)-, (b) (1*S*,2*S*,4*R*,7*S*,8*S*,10*R*)-(δδδδ)-, and (c) (1*R*,2*S*,4*S*,7*R*,8*S*,10*S*)-(λλλλ)- [**2.12**·Na]$^+$ (from the top, observed from the Na$^+$ ion, left, and side, right, view) and their respective internal energies in toluene expressed in kcal mol^{-1}. Hydrogen atoms have been omitted for clarity. Atom type: C, light grey; N, blue; and Na, magenta.

2.2.1.4 Structure of hexacyclen complexes [2.9·Na]$^+$ and [2.13·Na]$^+$

Polyaza-coronands characterized by an N6 donor set are known to be exceptional metal hosts.[78] Despite their promising potential, the only systematic research on hexacyclen ligands involving Group 1 cations has been performed by Reid et al.[37] (**Figure 2. 8**) on Me$_6$hexacyclen. The ^{1}H NMR spectra of these metal complexes demonstrated broad signals for the fluxional characteristics of the ligand.

Step-wise addition of NaTFPB to a 5.0 mM solution of **2.9** in $CDCl_3$ has led to the formation of a new species with a 1 : 1 host/guest ratio (**Figure 2.11j**, ^{1}H NMR analysis and MALDI-MS, m/z:

863.5832, [**2.9**·Na]$^{+}$). Broad ^{1}H NMR macro ring signals (between 3.4 and 2.0 ppm) showed a rather slow motion of the 1,2-diaminoethylene units with respect to the NMR timescale. The presence of definite side chain resonance patterns (at δ 4.19, 1.71, and 4.34, 3.85, respectively) indicated a time-averaged C_3-symmetric (δλδλδλ) arrangement similar to that exhibited by (δλδλδλ)-[(Me$_6$hexacyclen)·K]$^{+}$.[37] Curiously, due to the high symmetry of the complex, the (δλδλδλ) ⇄ (λδλδλδ) 1,2-diaminoethylene inversion leaves the structure of [**2.9**·Na]$^{+}$ intact (**Figure 2. 18**).

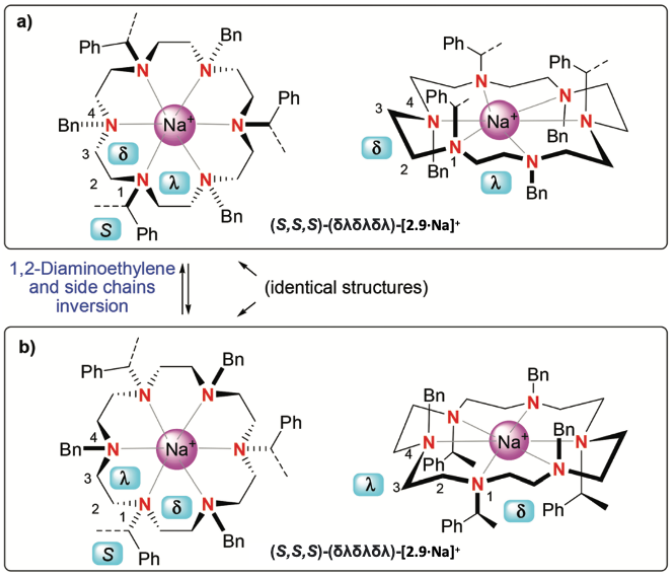

Figure 2. 18. (a) Schematic structures of the C_3-(δλδλδλ)-[**2.9**·Na]$^{+}$ conformational isomers after (b) identical after 1,2-diaminoethylene bond inversion (from the top view, left, and side view, right).

A theoretical model of (*S,S,S*)-(δλδλδλ)-[**2.9**·Na]$^{+}$ was realized through the assistance of DFT calculations and (**Figure 2. 19**) and it shows that the six nitrogen atoms participate in the coordination with the metal ions while the bulkier aromatic rings exhibit an anti-relationship in relation to the Na^{+} ion.

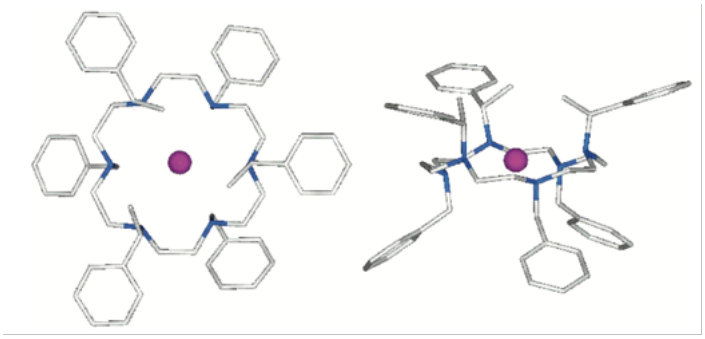

Figure 2. 19. Minimum energy structures of C_3-symmetric (*S,S,S*)-(δλδλδλ)-[**2.9**·Na]+ (view from the top, left, and side view, right). Hydrogen atoms have been omitted for clarity. Atom type: C, light grey; N, blue; and Na, magenta.

We wondered whether the slight conformational control induced by the chiral side chains in [**2.9**·Na]$^+$ might be enhanced by the (*S*)-pyrrolidine residues present in ligand **2.13**. Radical changes of the ^{1}H NMR spectra were observed after stepwise addition of NaTFPB to a 5.0 mM solution of the peraza-macrocycle **2.13** in $CDCl_3$. Signal integration attested a 1 : 1 metal-to-ligand ratio (^{1}H NMR analysis and MALDI-MS, m/z: 671.4959, [**2.13**·Na]$^+$, **Figure 2.11n**). In contrast to [**2.9**·Na]$^+$, complex [**2.13**·Na]$^+$ revealed an explicit ^{1}H NMR resonance pattern for 1,2-diaminoethylene (δ 3.58, 2.97, 2.86, and 2.73) and methylene benzyl (δ 4.09, 3.84 J ~13 Hz) protons congruent with a rigid C_3-symmetric complex (**Figure 2. 20**).

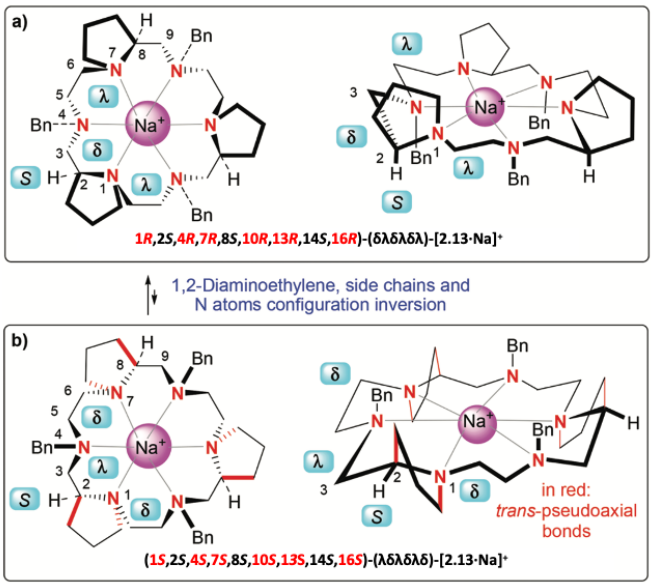

Figure 2. 20. (a) Schematic structures of the C_3-symmetric (1*R*,2*S*,4*R*,7*R*,8*S*,10*R*,13*R*,14*S*,16*R*)-(δλδλδλ)- and (b) (1*S*,2*S*,4*S*,7*S*,8*S*,10*S*,13*S*,14*S*,16*S*)-(λδλδλδ)- [**2.13**·Na]$^+$ conformational isomers (from the top, left, and side view, right,). The absolute configurations of stereogenic carbon atoms are reported in black, and the absolute configurations of stereogenic nitrogen atoms are reported in red.

Of the two potential inequivalent structures (i.e., (1*R*,2*S*,4*R*,7*R*,8*S*,10*R*,13*R*,14*S*,16*R*)-(δλδλδλ)-[**2.13**·Na]$^+$ and (1*S*,2*S*,4*S*,7*S*,8*S*,10*S*,13S,14*S*,16*S*)-(λδλδλδ)-[**2.13**·Na]$^+$, **Figure 2. 20a**, and **b**, respectively), the second one was rejected in the theoretical studies on account of the sterically unavailable *trans*-pseudodiaxial $CH_{(S)}$–CH_2/N_{pyrr}–CH_2 pyrrolidine bonds (**Figure 2. 20b**).

The minimum energy model (1*R*,2*S*,4*R*,7*R*,8*S*,10*R*,13*R*,14*S*,16*R*)-(δλδλδλ)-[**2.13**·Na]$^+$ was obtained by DFT studies and is shown in **Figure 2. 21**.

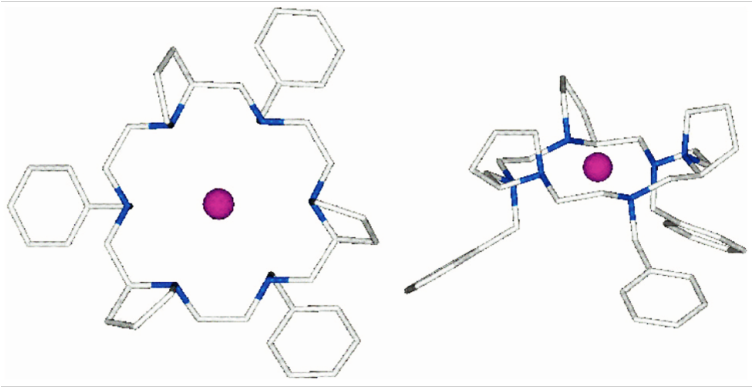

Figure 2. 21. Minimum energy structure of the C_3-symmetric (1*R*,2*S*,4*R*,7*R*,8*S*,10*R*,13*R*,14*S*,16*R*)-(δλδλδλ)-[**2.13**·Na]$^+$ conformational isomer (from the top view, left, and side view, right). Hydrogen atoms have been omitted for clarity. Atom type: C, light; N, blue; and Na, magenta.

2.2.2. Conclusions

The study performed on the new [**2.8**·Na]$^+$, [**2.12**·Na]$^+$, [**2.9**·Na]$^+$, and [**2.13**·Na]$^+$ species, characterized by various sizes and numbers of chiral *N*-(*S*)-1-phenylethyl side chains or (*S*)-pyrrolidine rings, illustrates how the structural features of the peraza-macrocycles influence structural dynamism.

Analogously to cyclic peptoids,[60] the incorporation of stereocenters into the peraza-macrocycle backbone or in the side chains brings significant consequences for the conformational properties of the metal complexes. Specifically, the use of the (*S*)-pyrrolidine units leads to the formation of unique, rigid peraza-macrocyclic species.

It is worth emphasizing that while in cyclic peptoids and their metal complexes, a single stereocenter can organize their structure,[81] in the case of peraza-macrocyles, alternated chiral/achiral submonomers are necessary to provide conformational stability.

The new synthetic method towards chiral peraza-macrocycles *via* cyclic peptoids paves new ways for simple preparation of neutral N_4 and N_6 donors. The sequence-controlled synthetic approach allows for strategic positioning of stereogenic centers and enables the generation of conformationally stable metal complexes.

2.2.3. Experimental section

2.2.3.1 General methods

Starting materials and reagents purchased from commercial suppliers were generally used without purification unless otherwise mentioned. Reaction temperatures were measured externally; reactions were monitored by analytical thin layer chromatography (TLC) on precoated silica gel plates (0.25 mm) and visualized using UV light. Flash chromatography was performed on silica gel 60 (particle size: 0.040–0.063 mm) and the solvents employed were of analytical grade. The purity grade of cyclic peptoids was controlled by HPLC analysis using a C18 reversed-phase analytical column (Bondapak, 10 µm, 125 Å, 3.9 mm × 300 mm) run with linear gradients of ACN (0.1% TFA) into H_2O (0.1% TFA) over 30 min, at a flow rate of 1.0 mL min^{-1}, using a Modular HPLC System JASCO LC-NET II/ADC equipped with a JASCO Model PU-2089 PlusPump and a JASCO MD-2010 Plus UV–vis multiple wavelength detector set at 220 nm. High resolution mass spectra (HRMS) were recorded on a Bruker Solarix XR Fourier transform ion cyclotron resonance mass spectrometer (FTICR-MS) equipped with a 7T magnet, using matrix-assisted laser desorption/ionization (MALDI). Model macrocycles and their metal complexes were dissolved in acetonitrile (1 mg mL^{-1} solution) and mixed with 2,5-dihydroxybenzoic acid (DHB, 1 mg mL^{-1} in methanol) (for the free hosts) or, for the formation of the sodium complexes, a 10 : 1 solution of trans-2-[3-(4-tert-butylphenyl)-2-methyl-2-propenylidene]malononitrile (DCTB, 1 mg mL^{-1} in chloroform) and sodium trifluoroacetate (10 mg mL^{-1} in ethanol) (for the sodium complexes) as the matrix in a 1 : 1 ratio, and then spotted

[81] D'Amato, A.; Pierri, G.; Costabile, C.; Della Sala, G.; Tedesco, C.; Izzo, I.; De Riccardis, F. *Org. Lett*. **2018**, *20*, 640.

on a Bruker Standard stainless steel target. Yields refer to chromatographically and/or spectroscopically (^{1}H and ^{13}C NMR) pure materials. ^{1}H NMR and ^{13}C spectra were recorded on Bruker DRX 600 MHz and Bruker DRX 400 instruments. Chemical shifts (δ) are reported in ppm relative to the residual solvent peak ($CHCl_3$, δ = 7.26; $^{13}CDCl_3$, δ = 77.0) and the multiplicity of each signal is designated by the following abbreviations: s, singlet; d, doublet; t, triplet; dt, double triplet; m, multiplet. Coupling constants (J) are quoted in hertz. Traces of HCl have been removed from $CDCl_3$ by filtering the deuterated solvent on activated basic alumina.

DFT calculations were performed by prof. C. Costabile, Dpt. of Chemistry and Biology "A. Zambelli", Univ. of Salerno.

2.2.3.2 Solid-phase synthesis of linear peptoid 2.21

2-Chlorotrityl chloride resin (2,α-dichlorobenzhydryl-polystyrene cross-linked with 1% DVB; 100–200 mesh; 1.47 mmol g^{-1}, 0.200 g, 0.290 mmol) was washed with DCM (3 × 2 mL) and DMF (3 × 2 mL) and then swelled in dry DCM (2 mL) for 45 min. Bromoacetic acid (0.066 g, 0.47 mmol) and DIPEA (255 µL, 1.47 mmol) in dry DCM (2 mL) were added to the resin and the vessel was stirred on a shaker platform for 60 min at room temperature. After the resin was washed with DMF (3 × 2 mL), DCM (3 × 2 mL) and then with DMF (3 × 2 mL), a solution of benzylamine (320 µL, 2.94 mmol) in dry DMF (2 mL) was added to the bromoacetylated resin. The mixture was left on the shaker platform for 40 min at room temperature, and then the resin was washed with DMF (3 × 2 mL), DCM (3 × 2 mL) and then with DMF (3 × 2 mL). A subsequent bromoacetylation reaction was accomplished by reacting the oligomer with a solution of bromoacetic acid (0.409 g, 2.94 mmol) and DIC (500 µL, 3.33 mmol) in dry DMF (2 mL), stirring on a shaker platform for 40 min at room temperature. Subsequently, the reaction with benzylamine was repeated as described previously. Once the resin has been washed, a solution of *N*-Fmoc-$_L$-proline (0.294 g, 0.87 mmol), HATU (0.320 g, 0.84 mmol) and DIPEA (202 µL, 1.16 mmol) in dry DMF (2 mL) was added and left on a shaker platform for 1 h and after washed with DMF (3 × 2 mL), DCM (3 × 2 mL) and DMF (3 × 2 mL). Fmoc group was deprotected by sequential additions of two aliquots of 20% piperidine/DMF (v/v, 3 mL), stirring on a shaker platform for 3 and 7 min respectively, followed by extensive washes with

DMF (3 × 2mL), DCM (3 × 2 mL) and DMF (3 × 2 mL). Subsequent bromoacetylation and substitution with benzylamine were performed in the previously described conditions to complete the tetraoligomeric sequence. The linear peptoid was cleaved from resin by treatment with three aliquots of a solution of 20% HFIP in dry DCM (v/v; 3 × 2 mL), with stirring each time on the shaker platform for 30 min at room temperature and filtering the resin away after each treatment. The combined filtrates were concentrated in vacuo. The final product was analysed by ESI mass spectrometry and RP-HPLC and used for the cyclization step without further purification.

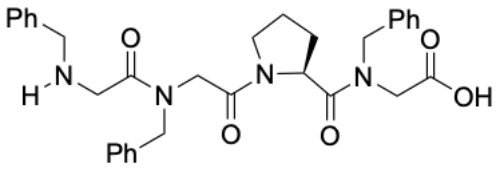

2.21

2.21: white amorphous solid, 0.164 g, 100% yield; Rt 8.2 min; HRMS (MALDI): *m/z* $[M+H]^+$ calcd for $C_{32}H_{37}N_4O_5^+$ 557.2758; found 557.2749.

2.2.3.3 High dilution cyclization: synthesis of cyclic peptoid 2.18

To a stirred solution of HATU (0.400 g, 1.05 mmol) and DIPEA (280 µL, 1.61 mmol) in dry DMF (80 mL) at room temperature, a solution of the linear precursor **2.21** (0.260 mmol) in dry DMF (7 mL) was added using a syringe pump in 3 h. After 18 h, the resulting mixture was concentrated in vacuo, diluted with DCM (100 mL) and washed with 1 M HCl (2 × 50 mL). The aqueous layer was extracted with DCM (2 × 100 mL) and the combined organic phases were washed with water (150 mL), dried over $MgSO_4$, and concentrated in vacuo. The crude cyclic peptoid **2.18** was purified by reversed-phase chromatography on C_{18} bonded silica.

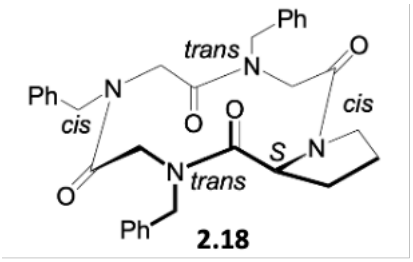

2.18

ctct-**2.18**: white amorphous solid, 0.038 g, 27% yield; Rt 10.9 min; HRMS (MALDI): *m/z* $[M+H]^+$ calcd for $C_{32}H_{35}N_4O_4^+$ 539.2653; found 539.2681.

^{1}H NMR (600 MHz, $CDCl_3$) δ: 7.41–7.38 (2H, m, Ar–*H*), 7.34–7.28 (4H, overlapping signals, Ar–*H*), 7.22–7.21 (5H, overlapping signals, Ar–*H*), 7.06 (4H, d, *J* 7.6 Hz, Ar–*H*), 5.52 (1H, d, *J* 14.4 Hz, $N_{trans}CHHPh$), 5.41 (1H, d, *J* 14.3 Hz, NC*H*HC=O), 5.36 (1H, d, *J* 15.1 Hz, NC*H*HC=O), 4.85 (1H, d, *J* 8.0 Hz, C*H*C=O), 4.78 (1H, d, *J* 17.2 Hz, $N_{cis}CHHPh$), 4.43 (1H, d, *J* 17.2 Hz, $N_{cis}CHHPh$), 4.40 (1H, d, *J* 18.3 Hz, $N_{cis'}CHHPh$), 4.32 (1H, d, *J* 18.3 Hz, $N_{cis'}CHHPh$), 4.31 (1H, d, *J* 17.1 Hz, NC*H*HC=O), 3.74 (2H, overlapping d, J 14.4 Hz, $N_{trans}CHHPh$ and $NCHHCH_2CH_2$), 3.66 (1H, m, $NCHHCH_2CH_2$), 3.50 (1H, d, *J* 15.1 Hz, NCH*H*C=O), 3.47 (1H, d, *J* 14.5 Hz, NC*H*HC=O), 3.46 (1H, d, J 14.5 Hz, NCH*H*C=O), 2.04–1.91 (4H, overlapping m, $NCH_2CH_2CH_2$).

^{13}C NMR (150 MHz, $CDCl_3$) δ: 170.6 (*C*=O), 168.7 (*C*=O), 168.2 (*C*=O), 167.8 (*C*=O), 135.9 (Ar–*C*), 135.4 (Ar–*C*), 134.9 (Ar–*C*), 129.1 × 3 (Ar–*C*H), 128.8 × 2 (Ar–*C*H), 128 × 2 (Ar–*C*H), 127.9 × 2 (Ar–*C*H), 127.8 × 2 (Ar–*C*H), 126.8 × 2 (Ar–*C*H), 126.6 × 2 (Ar–*C*H), 58.6 (C^{α} L-Pro-*C*H), 50.5 ($N_{trans}CH_2Ph$), 50.0 ($N_{cis}CH_2Ph$), 49.5 ($NCH_2C=O$), 49.2 ($N_{cis'}CH_2Ph$), 47.6 (*NC*HC=O), 47.5 (*NC*HC=O), 47.3 (L-Pro-*N*-*C*H), 31.2 (C^{β} L-Pro-CH_2), 22.0 (C^{γ} L-Pro-CH_2).

2.2.3.4 Reduction reaction: synthesis of peraza cycloalkanes 2.7 and 2.8

To a solution of the cyclic peptoid (0.20 mmol) in dry THF (2 mL), in a reactivial, a 1.0 M solution of the borane tetrahydrofuran complex in THF (5.0 equivalents for every amide group) was added dropwise and the mixture was heated at 90 °C for 24 h. It was then cooled to 0 °C and water (11mL) was slowly added to react with the excess of BH_3. The mixture was then concentrated under high vacuum. The residue was dissolved in 1 N HCl (68 mL) and the mixture was heated to reflux for 3 h. It was then cooled to room temperature and $CsOH{\cdot}H_2O$ was added until pH >11. The solution was extracted three times with DCM (3 × 160 mL). The combined organic layers were dried over $MgSO_4$ and concentrated in vacuo. The products were purified on basic aluminium oxide (100% dichloromethane to 90:10 dichloromethane:methanol), then precipitated from hot acetonitrile, and finally subjected to spectrometric and spectroscopic analysis.

2.2.3.5 Reduction reaction: synthesis of peraza cycloalkanes 2.9-2.13

To a solution of the cyclic peptoid (0.025 mmol) in dry THF (300 µL), in a reacti-vial, a 1.0 M solution of the borane tetrahydrofuran complex in THF (5.0 equivalents for every amide group) was added dropwise and the mixture was heated at 90 °C for 24 h. It was then cooled to 0 °C and water (1.0 mL) was slowly added to react with the excess of BH_3. The mixture was then concentrated under high vacuum. The residue was dissolved in 1 N HCl (6 mL) and the mixture was heated to reflux for 3 h. It was then cooled to room temperature and refluxed for 3 h. It was then cooled to room temperature and $CsOH{\cdot}H_2O$ was added until pH >11. The solution was extracted three times with DCM (3 × 10 mL). The combined organic layers were dried over $MgSO_4$ and concentrated in vacuo. The products were purified on basic aluminium oxide (100% dichloromethane to 90:10 dichloromethane:methanol), and then subjected to spectrometric and spectroscopic analysis.

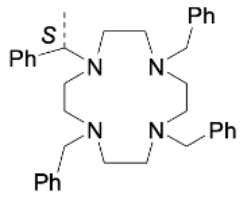

2.7

2.7:[56] white solid, 0.10 g, 100% yield; HRMS (MALDI): *m/z* $[M+H]^+$ calcd for $C_{37}H_{47}N_4^+$ 547.3795; found 547.3823. $[\alpha]_D^{25}$=−14.1 (c = 0.53, $CHCl_3/CH_3OH$ = 1:19).

$[C_{37}H_{46}N_4]$: C, 81.27; H, 8.48; N, 10.25. Found: C, 81.32; H, 8.55; N, 10.11%. Mp: 83.8–88.0 °C.

^{1}H NMR (600 MHz, $CDCl_3$) δ: 7.36–7.20 (20H, overlapping signals, Ar*H*), 3.70 (1H, q, *J* 6.7 Hz, NC*H*(CH_3)Ph), 3.49–3.39 (6H, overlapping, CH_2Ph), 2.77–2.61 (16H, overlapping, NCH_2CH_2), 1.28 (3H, d, *J* 6.7 Hz, CH_3, overlapped with lipid signal).

^{13}C NMR (100 MHz, $CDCl_3$) δ: 144.4 (Ar–*C*), 139.9 × 3 (Ar– *C*), 129.1 × 6 (Ar–*C*H), 128.0 × 6 (Ar–*C*H), 127.9 × 6 (Ar–*C*H), 126.6 (Ar–*C*H), 126.4 (Ar–*C*H), 59.8 × 4 (Ph–*C*H and Ph–*C*H_2), 53.2 × 2 (–*C*H_2–*C*H_2–), 52.5 × 4 (–*C*H_2–*C*H_2–), 49.0 × 2 (–*C*H_2– *C*H_2–), 16.5 (*C*H_3).

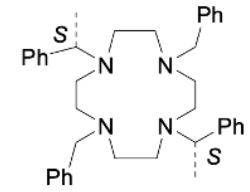

2.8

2.8: colorless oil, 0.084 g, 75% yield; HRMS (MALDI): *m/z* $[M+H]^+$ calcd for $C_{38}H_{49}N_4^+$ 561.3952; found 561.3978. Anal. calcd for $[C_{38}H_{49}N_4]$: C, 81.38; H, 8.63; N, 9.99. Found: C, 81.42; H, 8.65; N, 9.92% $[\alpha]_D^{25}$= −19.1 (c = 0.53, $CHCl_3/CH_3OH$ = 1:19)

^{1}H NMR (600 MHz, CDCl3) δ: 7.38 (4H, d, *J* 7.2 Hz, Ar*H*), 7.31–7.28 (8H, overlapping, Ar*H*), 7.25–7.22 (6H, m, Ar*H*), 7.18 (2H, m, Ar*H*), 3.72 (2H, q, J 6.7 Hz, NC*H*(CH_3)Ph), 3.49 (2H, d, J 13.7 Hz, NC*H*HPh), 3.36 (2H, d, *J* 13.7 Hz, NCH*H*Ph), 2.73–2.66 (12H, m, NCH_2CH_2), 2.63–2.60 (4H, m, NCH_2CH_2), 1.26 (6H, d, *J* 6.7 Hz, CH_3).

^{13}C NMR (150 MHz, $CDCl_3$) δ: 145.0 × 2 (Ar–*C*–CH(CH_3)N), 140.8 × 2 (Ar–*C*–CH_2N), 129.8 × 4 (Ar–*C*H), 128.7 × 4 (Ar–*C*H), 128.6 × 4 (Ar–*C*H), 128.5 × 4 (Ar–*C*H), 127.3 × 2 (Ar–*C*H), 127.1 × 2 (Ar–*C*H), 60.5 × 2 (Ph–*C*H), 59.7 × 2 (Ph–*C*H_2), 53.8 × 4 (–CH_2–*C*H_2–NCH_2Ph), 49.3 × 4 (–CH_2–*C*H_2–NCH(CH_3)Ph), 16.5 × 2 (*C*H_3).

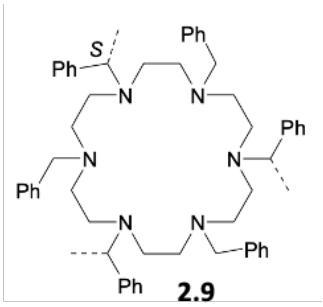

2.9

2.9: colorless oil, 0.016 g, 76% yield; HRMS (MALDI): *m/z* $[M+H]^+$ calcd for $C_{57}H_{73}N_6^+$ 841.5891; found 841.5980. Anal. calcd for $[C_{57}H_{72}N_6]$: C, 81.38; H, 8.63; N, 9.99. Found: C, 81.40; H, 8.66; N, 9.98% $[\alpha]_D^{25}$= −2.3 (c = 0.53, CHCl /CH_3OH = 1:19).

^{1}H NMR (600 MHz, $CDCl_3$) δ: 7.25–7.13 (30H, m, Ar*H*), 3.63 (3H, q, *J* 6.8 Hz, NC*H*(CH_3)Ph), 3.39 (6H, s, CH_2Ph), 2.59–2.48 (24H, m, NCH_2CH_2), 1.17 (9H, d, *J* 6.8 Hz, CH_3).

^{13}C NMR (150 MHz, $CDCl_3$, mixture of conformers) δ: 144.2 × 3 (Ar–*C*–CH(CH_3)N), 139.8 × 3 (Ar–*C*–CH_2N), 128.8 × 6 (Ar–*C*H), 128.1 × 6 (Ar–*C*H), 127.9 × 6 (Ar–*C*H), 127.6 × 6 (Ar– *C*H), 127.6

× 3 (Ar–*C*H), 127.5 × 3 (Ar–*C*H), 60.6 × 3 (Ph–*C*H), 59.3 × 3 (Ph–*C*H_2), 53.9 × 6 (–CH_2–*C*H_2–NCH_2Ph), 49.4 × 6 (–CH_2–*C*H_2–NCH(CH_3)Ph), 16.8 × 3 (*C*H_3).

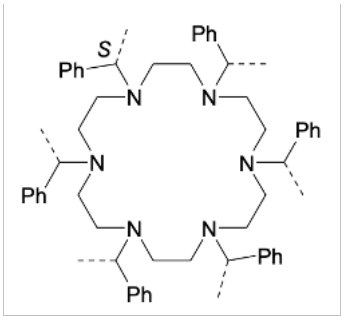

2.10

2.10: colorless oil, 0.0066 g, 30% yield; HRMS (MALDI): *m/z* $[M+H]^+$ calcd for $C_{60}H_{79}N_6^+$ 883.6361; found 883.6365. Anal. calcd for [$C_{60}H_{78}N_6$]: C, 81.59; H, 8.90; N, 9.51. Found: C, 81.63; H, 8.92; N, 9.47% $[\alpha]_D^{25}$= −29.3 (c = 0.53, CHCl /CH_3OH = 1:19)

^{1}H NMR (600 MHz, $CDCl_3$) δ: 7.26–7.22 (12*H*, overlapping, Ar*H*), 7.20–7.18 (6*H*, overlapping, Ar*H*), 7.13 (12H, Ar*H*), 3.54 (6H, q, *J* 6.8 Hz, NC*H*(CH_3)Ph), 2.48 and 2.39 (24H, m, NCH_2CH_2), 1.13 (18H, d, *J* 6.8 Hz, CH_3).

^{13}C NMR (150 MHz, $CDCl_3$) δ: 145.0 × 6 (Ar–*C*), 128.6 × 12 (Ar–*C*H), 128.4 × 12 (Ar–*C*H), 127.2 × 6 (Ar–*C*H), 60.6 × 6 (Ph–*C*H), 51.5 × 12 (–*C*H_2–*C*H_2–), 17.7 × 6 (*C*H_3).

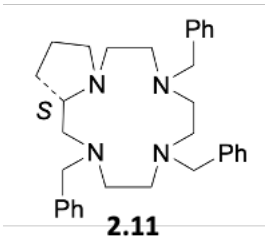

2.11

2.11: colorless oil, 0.012 g, 100% yield; HRMS (MALDI): *m/z* $[M+H]^+$ calcd for $C_{32}H_{43}N_4^+$ 483.3482; found 483.3479. Anal. calcd for [$C_{32}H_{42}N_4$]: C, 79.62; H, 8.77; N, 11.61. Found: C, 79.65; H, 8.80; N, 11.53% $[\alpha]_D^{25}$ = −11.2 (c = 0.53, $CHCl_3$/CH_3OH = 1:19).

^{1}H NMR (600 MHz, $CDCl_3$, mixture of conformers. Signals of the major species are reported) δ: 7.40–7.19 (15H, overlapping signals, Ar–*H*), 3.93 (1H, m, N–C*H*), 3.81 (1H, m, *J* 13.8 Hz, C*H*H–Ph), 3.53 (1H, m, *J* 13.9 Hz, C*H*H–Ph), 3.44 (1H, d, *J* 13.9 Hz, CH*H*–Ph), 3.43 (2H, overlapping, C*H*2–Ph), 3.24 (1H, bd, *J* 13.8 Hz, CH*H*–Ph), 3.03–2.97 (3H, overlapping, N–CH_2–CH_2), 2.84 (1H,

br m, N–CH*H* (Pro)), 2.76 (1H, m, N–CH_2– CH_2), 2.58–2.52 (7H, overlapping signals, N–CH_2–CH_2), 2.47 (1H, br m, N–CH*H* (Pro)), 2.41–2.35 (3H, overlapping signals, N–CH_2–CH_2), 1.78–1.55 (4H, overlapping signals, CH_2 (Pro)).

^{13}C NMR (150 MHz, CDCl3, mixture of conformers) δ: 140.0, 129.0, 128.1, 128.0, 126.5, 60.7, 60.3, 59.9, 55.1, 54.4, 53.0, 52.8, 52.3, 22.7.

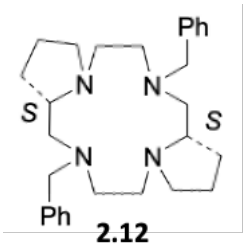

2.12

2.12: colorless oil, 0.010 g, 90% yield; HRMS (MALDI): *m/z* $[M+H]^+$ calcd for $C_{28}H_{41}N_4^+$ 433.3318; found 433.3327. Anal. calcd for [$C_{28}H_{40}N_4$]: C, 77.73; H, 9.32; N, 12.95. Found: C, 77.78; H, 9.34; N, 12.89% $[\alpha]_D^{25}$ = −17.6 (c = 0.53, CHCl /CH_3OH = 1:19).

^{1}H NMR (600 MHz, $C_6D_5CD_3$, mixture of conformers. Signals of the major species are reported) δ: 7.41 (4H, d*, J* 7.5, Ar*H*), 7.24 (4H, t, *J* 7.5, Ar*H*), 7.12 (2H, t*, J* 7.5, Ar*H*), 3.70 (2H, d, *J* 13.7, NC*H*HAr), 3.18 (2H, d, *J* 13.7, NCH*H*Ar), 3.09 (2H, t, *J* 8.1, CH_2CHN), 2.52–2.46 (10H, m, NCH_2CH_2), 2.42 (2H, m, NCH_2CH_2), 2.29–2.27 (2H, m, NCH_2CH_2), 1.94–1.91 (2H, m, NCH_2CH_2), 1.63–1.59 (4H, m, CH_2CH_2 (Pro)), 1.45–1.44 (4H, m, CH_2CH_2 (Pro)).

^{13}C NMR (150 MHz, $C_6D_5CD_3$, mixture of conformers. Signals of the major species are reported) δ: 141.0, 127.0, 63.2 (broad), 62.0, 55.7, 55.2, 53.0, 30.3, 23.2.

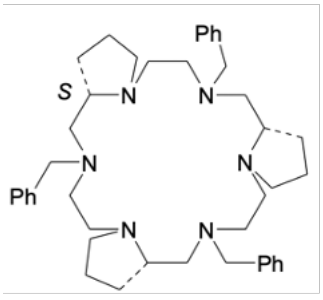

2.13

2.13: colorless oil, 0.0063 g, 39% yield; HRMS (MALDI): *m/z* $[M+H]^+$ calcd for $C_{42}H_{61}N_6^+$ 649.4952; found 649.4986. Anal. calcd for $[C_{42}H_{60}N_6]$: C, 77.73; H, 9.32; N, 12.95. Found: C, 77.77; H, 9.36; N, 12.88% $[\alpha]_D^{25}$ = −47.2 (c = 0.53, CHCl/CH_3OH = :19).

^{1}H NMR (600 MHz, $CDCl_3$, mixture of conformers. Signals of the major species are reported) δ: 7.34–7.20 (15H, overlapping signals, Ar–*H*), 3.74 (3H, d, *J* 13.7 Hz, N–C*H*H–Ph), 3.60 (3H, d, *J* 13.7 Hz, N–CH*H*–Ph), 3.28 (3H, m, N–C*H*H), 2.96 (3H, m), 2.85 (3H, dd), 2.72 (3H, m, N–C*H*H), 2.54 (3H, m, N–C*H*H), 2.47 (3H, m, N–CH*H*), 2.42 (3H, m), 2.29 (3H, m, N–CH*H*), 1.89 (3H, m, N–CH*H*), 1.63 (6H, m, N–CH_2–C*H*$_2$–CH_2), 1.51 (6H, m, N–CH_2–CH_2–C*H*$_2$).

^{13}C NMR (150 MHz, CDCl3, mixture of conformers) δ: 140.1, 129.0, 128.7, 128.3, 128.0, 126.9, 126.6, 64.1, 63.9, 63.4, 60.6, 60.4, 60.3, 60.1, 59.9, 55.1, 54.9, 54.6, 54.4, 54.1, 53.8, 53.6, 53.4, 30.4, 30.3, 30.1, 30.0, 22.5.

2.2.3.6 Formation of the Na^+ complexes

To a 5.0–10.0 mM solution of peraza-macrocycles in $CDCl_3$ (0.5 mL), increasing amounts of NaTFPB were added, up to 1.0 equiv. for cyclen derivatives, and up to 2.0 equiv. for hexacyclen derivatives. After every addition, the mixture was sonicated for 5 min at rt, and the ^{1}H NMR spectrum was recorded. Partial precipitation of insoluble complexes and the presence of broad signals (due to slow conformational motions) precluded the acquisition or full assignment of ^{13}C NMR spectra for [**2.7**·Na]$^+$TFPB$^-$ and [**2.11**·Na]$^+$TFPB$^-$.

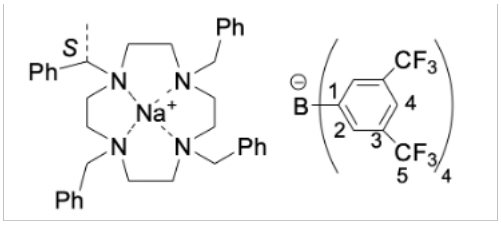

[**2.7**·Na]$^+$TFPB$^-$

[**2.7**·Na]$^+$TFPB$^-$. HRMS (MALDI): *m/z* $[M+Na]^+$ calcd for $C_{37}H_{46}N_4Na^+$ 569.3615; found 569.3782.

^{1}H NMR (600 MHz, CDCl3, mixture of conformers) δ: 7.71 (8H, s, TFPB-*o*-*H*), 7.52 (4H, s, TFPB-*p*-*H*), 7.45–7.28 (18H, overlapping signals, Ar–*H*), 6.10–5.93 (2H, br signals, Ar–*H*), 3.64–1.19 (26H, br signals, overlapping, NCH_2CH_2, NCH_2Ar, NC*H*CH_3).

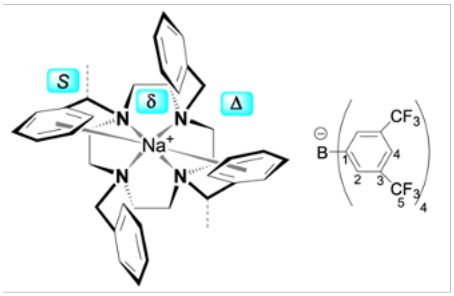

(*S*,*S*)-Δ(δδδδ)-[**2.8**·Na]$^{+}$[TFBP]$^{-}$

[**2.8**·Na]$^{+}$TFPB^{-}. HRMS (MALDI): *m/z* [M+Na]$^{+}$ calcd for $C_{38}H_{48}N_4Na^{+}$ 583.3771; found 583.3946.

^{1}H NMR (600 MHz, $CDCl_3$) δ: 7.71 (8H, s, TFPB-*o*-*H*), 7.53 (4H, s, TFPB-*p*-*H*), 7.47 (2H, t, *J* 7.4 Hz, *p*-Ar*H*), 7.37 (2H, t, *J* 7.1 Hz, *p*-Ar*H*), 7.32–7.27 (8H, m, Ar*H*), 6.14 (4H, d, J 7.2 Hz, *o*-Ar*H*), 5.97 (4H, d, *J* 7.2 Hz, *o*-Ar*H*), 3.33 (2H, q, *J* 6.9 Hz, NC*H*CH_3Ph), 3.27 (2H, d, *J* 12.1 Hz, NC*H*HPh), 3.20 (2H, bdd, *J* 13.2 Hz, NCH_2CH_2), 3.03 (2H, bdd, *J* 13.2 Hz, NCH_2CH_2), 2.89, (2H, bdd, *J* 13.2 Hz, NCH_2CH_2), 2.78 (2H, bdd, *J* 13.2 Hz, NCH_2CH_2), 2.64 (2H, d, *J* 12.1 Hz, NCH*H*Ph), 2.41 (2H, bd, *J* 13.2 Hz, NCH_2CH_2), 2.21 (2H, bd, *J* 13.2 Hz, NCH_2CH_2), 2.01 (2H, bd, *J* 13.2 Hz, NCH_2CH_2), 1.96 (2H, bd, *J* 13.2 Hz, NCH_2CH_2), 1.18 (6H, d, *J* 6.9 Hz, NCHCH_3Ph).

^{13}C NMR (150 MHz, $CDCl_3$) δ: 161.7 (q, J 50 Hz, *C*-1), 142.5 × 2 (Ar–*C*), 136.6 × 2 (Ar–*C*), 134.8 (*C*-2), 130.7 × 2 (Ar– *C*H), 130.2 × 2 (Ar–*C*H), 129.8 × 2 (Ar–*C*H), 129.6 × 2 (Ar–*C*H), 129.4 × 2 (Ar–*C*H), 128.9 (q, J 30 Hz, *C*-3), 128.6 × 2 (Ar–*C*H), 128.5 × 2 (Ar–*C*H), 128.3 × 2 (Ar–*C*H), 127.4 × 2 (Ar–*C*H), 126.2 × 2 (Ar–*C*H), 124.6 (q, J 270 Hz, *C*-5), 117.5 (*C*-4), 59.4 × 2 (N*C*H_2Ph), 56.8 × 2 (N*C*HCH_3Ph), 50.0 × 2 (NCH_2*C*H_2), 49.4 × 2 (NCH_2*C*H_2), 45.0 × 2 (N*C*H_2CH_2), 43.2 × 2 (N*C*H_2CH_2), 7.5 × 2 (NCH*C*H_3Ph).

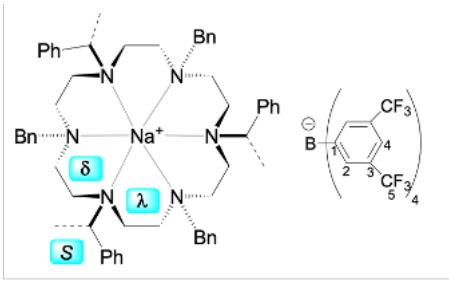

(*S*,*S*,*S*)-(δλδλδλ)-[**2.9**·Na]$^+$

[**2.9**·Na]$^+$TFPB$^-$. HRMS (MALDI): *m/z* [M+Na]$^+$ calcd for $C_{57}H_{72}N_6Na^+$ 863.5711; found 863.5832.

^{1}H NMR (600 MHz, $CDCl_3$, mixture of conformational isomers; only the signals of the major conformational species were reported) δ: 7.71 (8H, s, TFPB-*o*-*H*), 7.53 (4H, s, TFPB-*p*- *H*), 7.38–7.36 (8H, overlapping signals, Ar–*H*), 7.33–7.32 (8H, overlapping signals, Ar–*H*), 7.17–7.06 (14H, overlapping signals, Ar–*H)*, 4.34 (3H, bd, *J* 12.8 Hz, C*H*HPh), 4.19 (3H, q, *J* 6.6 Hz, C*H*CH$_3$Ph), 3.85 (3H, bd, *J* 12.8 Hz, CH*H*Ph), 3.43 (3H, br m, NC*H*$_2$), 3.22 (3H, br m, NC*H*$_2$), 3.10 (6H, broad signals, overlapping, NC*H*$_2$), 2.41 (6H, broad signals, overlapping, NC*H*$_2$), 2.23 (3H, br m, NC*H*$_2$), 2.12 (3H, br m, NC*H*$_2$), 1.71 (9H, d, J 6.6 Hz, CHC*H*$_3$Ph).

^{13}C NMR (150 MHz, $CDCl_3$) δ: 161.7 (q, J 50 Hz, *C*-1), 134.8 × 4 (*C*-2), 130.7 × 6 (Ar–*C*), 129.4 × 10 (Ar–*C*H), 129.0 (q, J 30 Hz, *C*-3), 128.5 × 10 (Ar–*C*H), 127.9 × 10 (Ar–*C*H), 124.6 (q, J 270 Hz, *C*-5), 117.5 (C-4), 59.0 × 3 (N*C*HCH$_3$Ph), 57.8 × 3 (N*C*H$_2$Ph), 51.2 × 6 (N*C*H$_2$), 47.2 × 6 (N*C*H$_2$), 20.8 × 3 (NCH*C*H$_3$Ph).

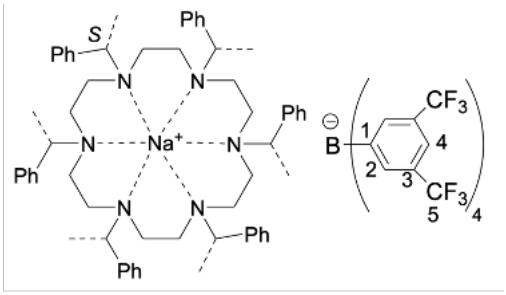

[**2.10**·Na]$^+$TFPB$^-$

[**2.10**·Na]$^+$TFPB$^-$. HRMS (MALDI): *m/z* [M+Na]$^+$ calcd for $C_{60}H_{78}N_6Na^+$ 905.6180; found 905.7970.

^{1}H NMR (600 MHz, $CDCl_3$) δ: 7.72 (8H, s, TFPB-*o*-*H*), 7.52 (4H, s, TFPB-*p*-*H*), 7.37–7.31 (18H, broad overlapping signals, Ar–*H*), 7.06 (12H, br d, *o*-Ar–*H*), 3.52 (6H, br s, $NCHCH_3$), 2.48–2.40 (24H, broad overlapping signals, NCH_2CH_2), 1.14 (18H, br s, $NCHCH_3$).

^{13}C NMR (150 MHz, $CDCl_3$) δ: 162.4 (q, J 50 Hz, *C*-1), 144.6 × 6 (Ar–*C*), 135.5 × 4 (*C*-2), 125.5 (q, J 30 Hz, *C*-3), 129.7 × 10 (Ar–*C*H), 128.4 × 10 (Ar–*C*H), 127.6 × 10 (Ar–*C*H), 124.7 (q, J 270 Hz, *C*-5), 118.2 (*C*-4), 60.3 × 6 (Ph–*C*H), 50.8 × 12 (–CH_2– CH_2–), 17.0 × 6 (CH_3).

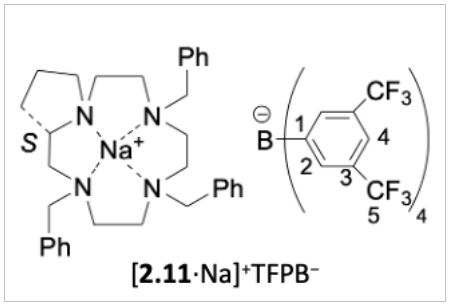

[**2.11**·Na]$^{+}$TFPB^{-}

[**2.11**]$^{+}$TFPB^{-}. HRMS (MALDI): *m/z* [M+Na]$^{+}$ calcd for $C_{32}H_{42}N_4Na^{+}$ 505.3302; found 505.3305.

^{1}H NMR (600 MHz, $CDCl_3$, mixture of conformers) δ: 7.71 (8H, s, TFPB-*o*-*H*), 7.53 (4H, s, TFPB-*p*-*H*), 7.35–7.29 (9H, overlapping signals, Ar–*H*), 7.19 (4H, t, *J* 7.8 Hz, Ar–*H*), 6.35 (2H, d, *J* 6.4 Hz, Ar–*H*), 3.69–1.89 (23H, broad overlapping signals, NCH_2CH_2, NCH_2Ph, NCH_2, CH), 1.79–1.59 (4H, overlapping with water signal, $NCH_2CH_2CH_2CH$).

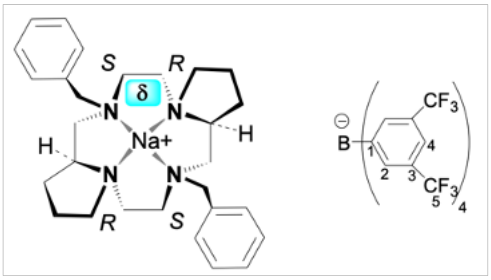

(1*R*,2*S*,4*S*,7*R*,8*S*,10*S*)-(δδδδ)-[**2.12**·Na]$^{+}$

[**2.12**·Na]$^{+}$TFPB^{-}. HRMS (MALDI): *m/z* [M+Na]$^{+}$ calcd for $C_{28}H_{40}N_4Na^{+}$ 455.3145; found 455.3272.

^{1}H NMR (600 MHz, $C_6D_5CD_3$) δ: 8.32 (8H, s, TFPB-*o*-*H*), 7.72 (4H, s, TFPB-*p*-*H*), 7.19–7.16 (8H, overlapping signals, Ar–*H*), 6.94 (2H, d, *J* 7.0 Hz, *o*-Ar–*H*), 3.20 (2H, d, *J* 13.3 Hz, C*H*HPh), 3.13 (2H, d, *J* 13.3 Hz, CH*H*Ph), 2.46 (2H, m, NC*H*HCH), 2.40 (2H, m, NCH_2CHHN(Pro)), 2.17 (2H, m,

CH*H*NBn), 2.04–2.01 (4H, overlapping signals, NCH_2(Pro)), 1.96 (2H, br m, NC*H*), 1.76 (2H, dd, *J* 15.4, 8.1 Hz, C*H*HNBn), 1.64 (2H, m, NCH*H*CH), 1.50 (2H, m, NCH$_2$CH*H*N(Pro)), 1.52–1.10 (8H, overlapping signals, NCH$_2$CH_2CH_2 (Pro)).

^{13}C NMR (150 MHz, $C_6D_5CD_3$) δ: 162.2 (q, J 50 Hz, *C*-1), 136.6 × 2 (Ar–*C*), 135.1 × 4 (*C*-2), 129.0 (q, J 30 Hz, *C*-3) and ×4 (Ar–*C*H), 128.8 × 4 (Ar–*C*H), 124.6 (q, J 270 Hz, *C*-5), 122.2 × 2 (Ar–*C*H), 117.6 (*C*-4), 67.9 × 2 (N*C*H), 61.8 × 2 (*C*H$_2$Ph), 57.3 × 2 (NCH$_2$*C*H$_2$N(Pro)), 55.7 × 2 (*C*H$_2$NBn), 52.3 × 2 (N*C*H$_2$CH), 50.7 × 2 (N*C*H$_2$(Pro)), 26.5 × 2 (NCH$_2$*C*H$_2$CH$_2$(Pro)), 22.8 × 2 (NCH$_2$CH$_2$*C*H$_2$(Pro)).

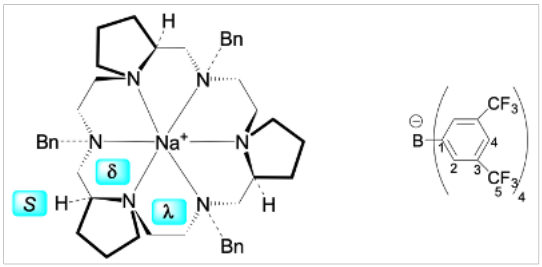

(1*R*,2*S*,4*R*,7*R*,8*S*,10*R*,13*R*,14*S*,16*R*)-(δλδλδλ)-[**2.13**·Na]$^+$

[**2.13**·Na]$^+$TFPB$^-$. HRMS (MALDI): *m/z* [M+Na]$^+$ calcd for $C_{42}H_{60}N_6Na^+$ 671.4772; found 671.4959.

^{1}H NMR (600 MHz, $CDCl_3$) δ: 7.70 (8H, s, TFPB-o-H), 7.52 (4H, s, TFPB-*p*-*H*), 7.39–7.32 (11H, overlapping signals, Ar–*H*), 7.21–7.19 (4H, overlapping signals, Ar–*H*), 4.09 (3H, d, *J* 13.4 Hz, C*H*HPh), 3.84 (3H, d, *J* 13.4 Hz, CH*H*Ph), 3.58 (3H, m, NC*H*CH$_2$), 2.97 (3H, m, NCHC*H*HN), 2.86 (3H, m, CH*H*NCH), 2.73 (3H, m, CH*H*NCH), 2.50–2.41 (6H, overlapping m, NCH_2CH$_2$NCH), 2.27–2.16 (6H, overlapping signals, NCHCH*H*N and NC*H*H(Pro)), 2.08 (3H, m, NCH*H*(Pro)), 2.01–1.98 (6H, broad overlapping signals, NCH$_2$CH_2CH_2(Pro)), 1.86–1.72 (6H, broad overlapping signals, NCH$_2$CH_2CH_2(Pro)).

^{13}C NMR (150 MHz, $CDCl_3$) δ: 161.7 (q, J 50 Hz, *C*-1), 134.8 × 4 (C-*2*), 131.7 × 3 (Ar–*C*), 130.3 × 6 (Ar–*C*H), 129.0 (q, J 30 Hz, *C*-3), 128.8 × 6 (Ar–*C*H), 128.5 × 3 (Ar–*C*H), 124.7 (q, J 270 Hz, *C*-5), 117.5 (*C*-4), 59.4 × 3 (N*C*HCH$_2$), 57.9 × 3 (*C*H$_2$Ph), 53.9 × 3 (*C*H$_2$NCH), 53.6 × 6 (NCH*C*H$_2$N and N*C*H$_2$CH$_2$NCH), 50.2 × 3 (N*C*H$_2$(Pro)), 24.6 × 3 (NCH$_2$*C*H$_2$CH$_2$(Pro)), 22.0 × 3 (NCH$_2$CH$_2$*C*H$_2$(Pro)).

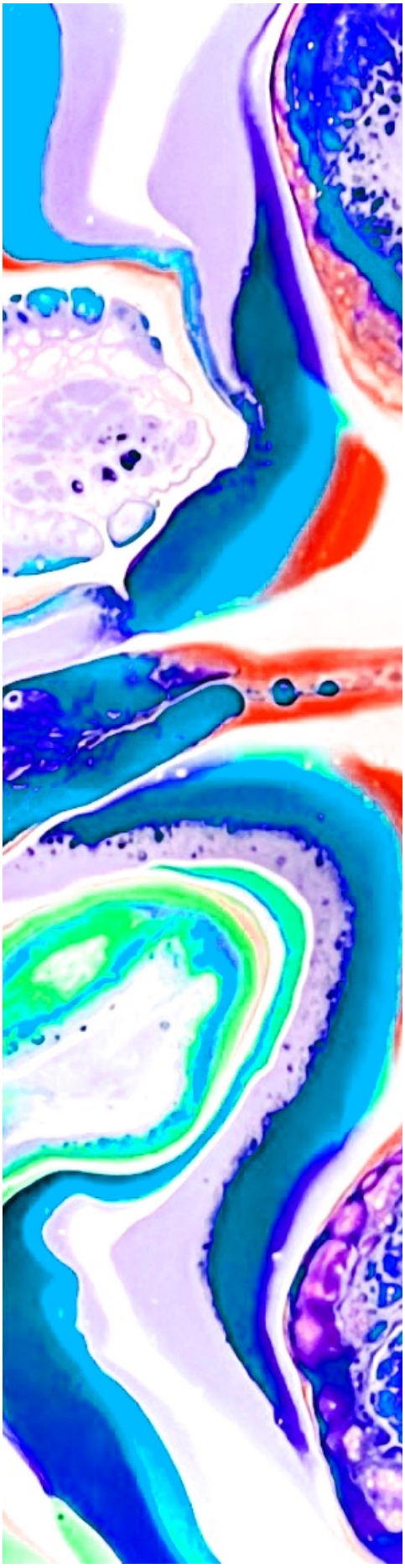

Chapter 3

THIOPEPTOIDS

3. THIOPEPTOIDS

3.1. Introduction

3.1.1. The nature of thioamides

Before the recognition of their presence in natural compounds, thioamides were seen as synthetic amide isosteres in peptides[82] and have been studied to improve properties of amide-containing compounds.[83] The potential advantages of introduction of thioamides into natural and synthetic molecules result from simultaneously discreet and drastic alterations of amide interactions caused by this single-atom replacement. First of all, thioamides are characterized by greater reactivity towards both nucleophiles, and electrophiles compared to amides.[84] Next, the C=S bond is weaker than C=O (130 vs 170 kcal/mol)[85] and thus they are commonly used as chemical synthesis intermediates. In addition, thioamides have stronger affinity for different metals with respect to amides. For example, the natural product methanobactin demonstrates unusually high affinity towards copper.[86]

The inequivalences in thioamide and amide geometries are responsible of many noncovalent interactions in thiopeptides. Despite a near-isosteric variation, sulfur is characterized by a larger van der Waals radius (1.85 Å)[87] and lower electronegativity (2.58) compared with oxygen (1.40 Å, 3.44). Peptide conformational alterations can be induced by the elongated C=S bond (1.71 Å vs 1.23 Å of the corresponding C=O bond),[88] and the higher rotational barrier for the C-N bond (~5 kcal/mol),[89] which significantly decreases conformational flexibility. In addition, thioamide N-H groups are more acidic (ΔpK_a=-6) compared with amide [90] and result to be better hydrogen bond donors.[91] On the other hand, the sulfur electron lone pairs of thioamides are weaker hydrogen bond acceptors with respect to oxygen electron lone pairs

[82] Patani, G. A.; La Voie, E.J. *Chem. Rev.* **1996**, *96*, 3147-3176.
[83] Reiner, A.; Wildemann, D.; Fischer, G.; Keifhaber, T. *J. Am. Chem. Soc.* **2008**, *130,* 8079-8084.
[84] Jagodzinski, T.S. *Chem. Rev*. **2003**, *103,* 197-228.
[85] Sifferlen, T.; Rueping, M.; Gademann, K.; Jaun, B.; Seebach, D. *Helv. Chim. Acta* **1999**, *82,* 2067-2093.
[86] Kim, H. J.; Graham, D.; DiSpirito, A. A.; Alterman, M. A.; Galeva, N.; Larive, C. K.; Asunskins, D.; Sherwood, P. M. A. *Science* **2004**, *305,* 1612-1615.
[87] Lee, H. J.; Choi, Y. S.; Lee, K. B.; Park, J.; Yoon, C. J. *J. Phys. Chem. A*. **2002**, *106,* 7010-7017.
[88] Truter, M. R. *J. Am. Chem. Soc.* **1996**, 997-1007.
[89] Wiberg, K. B.; Rush, D. J. *J. Am. Chem. Soc*. **2001,** *123*, 2038-8793.
[90] Bordwell, F.G. *Acc. Chem. Res.* **1998**, *21*, 456-463.
[91] Dudek, E. P.; Dudek, G. O. *J. Org. Chem.* **1967**, *32*, 823-824.

in amides.[92] Due to these characteristics, thioamides are an excellent tool for the assessment of the impact of a single hydrogen bond on protein folding and stability.

The sulfur substitution brings consequences also in terms of spectroscopic and electrochemical properties. The C=S bond is characterized by an ultraviolet absorption maximum at 265 ± 5 nm (vs 220 ± 5 nm for C=O) and an infrared stretch at 1120 ± 20 cm^{-1} (vs 1660 ± 20cm^{-1} for C=O).[93] In addition, the ^{13}C NMR chemical shift of C=S is found 30 ppm downfield (200-210 ppm) in comparison to C=O resonance.[94] The oxidation potential of a model thioamide is substantially lower with respect to the amide analogue (1.21 vs 3.29 eV).[95] All the characteristics of thioamides mentioned above are listed in the **Table 3. 1.**

Property	Amide	Thioamide
Van der Waals radius (Å)	1.40	1.85
C=X bond dissociation energy	170	130
C=X length (Å)	1.23	1.71
C-N rotational barier (kcal/mol)	17	22
Electronegativity of the heteroatom	3.44	2.58
C=X···H-N hydrogen bond (kcal/mol)	6.1	4.8
N-H pK_a	17	12
π- π* absorption (nm)	200	270

Table 3. 1. Physical properties of amides and thioamides.

[92] Hollosi, M.; Zewdu, M.; Kollat, E.; Majer, Z.; Kajtar, M.; Batta, G.; Kover, K.; Sandor, P. *Int. J. Pept. Protein Res.* **1990**, *36,* 173-181.
[93] Helbing, J.; Bregy, H.; Bredenbeck, J.; Pfister, R.; Hamm, P.; Huber, R.; Wachtveitl, J.; De Vico, L.; Olivucci, M. *J. Am. Chem. Soc.* **2004**, *126*, 8823-8834.
[94] Banala, S.; Sussmuth, R. D. *Chem. Bio. Chem*. **2010**, *11*, 1335-1337.
[95] Bordwell, F. G.; Algrim, D. J.; Harrelson, J. A. *J. Am. Chem. Soc*. **1988**, *110*, 5903-5904.

3.1.2. Thioamidated peptides

The benefits from application of thioamides as amide isosteres to strategically alter the peptides' properties, have attracted the interest of many scientists. Summarizing the previous paragraph, the oxygen-to-sulfur substitution has four crucial consequences:

- greater reactivity towards electrophiles, nucleophiles, and soft metals,
- different conformational properties,
- diverse hydrogen bonding tendencies,
- different photophysical and electrochemical properties.

The history of synthetic thioamidated peptides has begun with Vincent du Vigneaud's study on oxytocine (**Figure 3. 1**), which led him to the Nobel Prize.[96] His research was focused on the *C*-terminal amide of the cyclic nonapeptide hormon, known to be responsible for its activity. Du Vigneaud implemented the oxygen-to-sulfur substitution of the amide moiety which caused the oxytocine's biological activity reduction to ≤6%. The study outcome proved that despite the almost-isosteric character of thioamides and despite the presence of carbonyl groups able to participate in hydrogen bonds, this single atom substitution can induce crucial alterations in biological signaling.

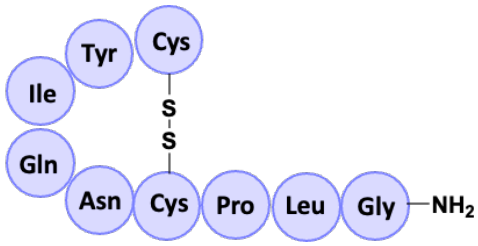

Figure 3. 1. Schematic representation of oxytocine structure.

Du Vigneaud's brilliant research unlocked new possibilities for peptide and peptidomimetic chemistry and inspired many scientists. For instance, Boger and co-workers employed thioamides as synthetic tools and probes of hydrogen bonding interactions with a backbone

[96] Jones, W. C.; Nestor, J. J.; Du Vigneaud, V. *J. Am. Chem. Soc*. **1973**, *95*, 5677-5679.

carbonyl in a glycopeptide antibiotic: vancomycin.[97] Due to the introduction of thioamides as valuable intermediates, different derivatives have been synthetized to evaluate their hydrogen bonding patterns. Then, they were tested with model target substrates to verify an established mechanism of action[97] and finally to develop more efficient analogues of vancomycin.[98]

As well, the photophysical properties of thioamides are meaningful for their applications. It was demonstrated that excitation of thioamides at 270 or 340 nm ($\pi \rightarrow \pi^*$ or $n \rightarrow \pi^*$ transition, accordingly),[93] enables the selective photo switching between the *cis* and *trans* geometry of the thioamide bond. This phenomenon was explored by Kiefhaber and Fischer in the context of studies on the activity of the enzyme ribonuclease S.[99] The cleaved enzyme necessitates the S-protein and complementary S-peptide for its proper activity. Insertion of a thioamide into the peptide sequence, at central position, had neglectable impact on enzyme activity (as deduced by hydrolysis of cytidine 2',3'-cyclic monophosphate). Notwithstanding, upon UV irradiation, the 30% *cis* isomerization of the thioamide bond was induced, leading to a 30% reduction in the enzyme activity without dissociation of the protein-peptide complex. This result showed that switching the thioamide geometry into *cis* form, leads to a conformation alteration that suppresses the enzymatic activity.

Other attributes of thioamides have been explored in protease research. The majority of studies focuses on the thioamides' effects on short peptide substrates of various proteases, with the goal of designing inhibitors and investigating the protease mechanism.[100]
In a recent study, the "O" to "S" replacement was implemented to glucagon like peptide 1 (GLP-1)[101] which stimulates insulin secretion and regulates glucose concentrations.[102] The application of GLP-1 for therapeutic purposes brings along the problem of its rapid

[97] Okano, A.; James, R. C.; Pierce, J. G.; Xie, J.; Boger, D. L. *J. Am. Chem. Soc*. **2012**, *134,* 8790-8793.
[98] Okano, A.; Nakayama, A.; Wu, K.; Lindsey, E. A.; Schammel, A. W.; Feng, Y.; Collins, K. C.; Boger, D. L. *J.Am. Chem. Soc.* **2015**, *137*, 3693-3704.
[99] Wildemann, D.; Schiene-Fsicher, C.; Aumuller, T.; Bachmann, A.; Kiefhaber, T.; Lucke, C.; Fischer, G. *J. Am. Chem. Soc.* **2007**, *129,* 4910-4918.
[100] Bond, M. D.; Holmquist, B.; Valle, B. L. J. *Inorg. Biochem*. **1986**, *28*, 97-105.
[101] Chen, X.; Mietlicki-Baase, G.; Barrett, T. M.; McGrath, L. E.; Koch-Laskowski, K.; Ferrie, J. J.; Hayes, M. R.; Petersson, E. J. *J. Am. Chem. Soc*. **2017**, *139*, 16688−16695.
[102] Komatsu, R.; Matsuyama, T.; Namba, M.; Watanabe, N.; Itoh, H.; Kono, N.; Tarui, S. *Diabets* **1989**, *38*, 902-905.

degradation by the enzyme dipeptidase 4 (DPP-4). By examining the crystal structure of DPP-4 with a peptide substrate (**Figure 3. 2**),[103] the presence of bifurcated hydrogen bonds with the carbonyls of the two *N*-terminal amino acid residues was observed. It was demonstrated that the insertion of thioamides at both sites (**Scheme 3. 1**) increases the DPP-4 resistence due to attenuated hydrogen bond acceptance by the thioamide unit. The study showed that the single-atom substitution at both terminal positions increased the half-life of the peptide from 2 minutes to 12 hours.[104]

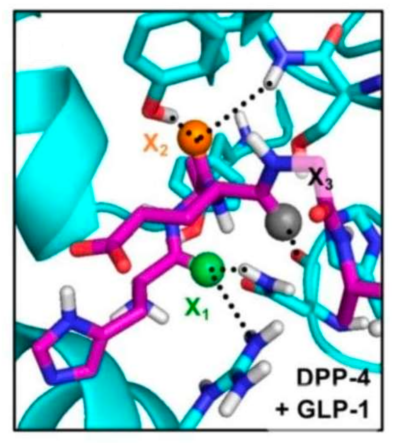

Figure 3. 2. Dipeptidase 4 (DPP-4, cyan) active site with a glucagon like peptide 1 (GLP-1, purple) *N*-terminal fragment bound. [103]

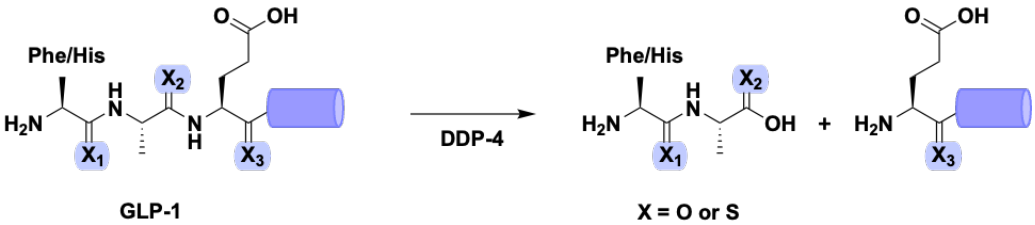

Scheme 3. 1. Incorporation of S into GLP-1 at the X_1 or X_2 position precludes dipeptidyl peptidase 4 (DPP-4) degradation of GLP-1.

Thioamides are present in the chemistry of cyclic peptides as well. Due to the large surface area in relation to molecular weight and improved bioavailability in comparison with linear congeners, macrocyclic peptides are suitable candidates for protein-protein interaction

[103] Aertgeerts, K.; Ye, S.; Tennant, M. G.; Kraus, M. L.; Rogers, J.; Sang, B. C.; Skene, R. J.; Webb, D. R.; Prasad, G. S. *Protein. Sci*. **2004,** *13*, 412-421.
[104] Chen, X.; Mietlicki-Baase, E. G.; Barrett, T. M.; McGrath, L. M.; Koch-Laskowski, K.; Ferrie, J.; Hayes, M. R.; Petersson E. J. *J. Am. Chem. Soc.* **2017**, *139*, 16688–16695.

inhibitors.[105] Unfortunately, despite their cyclic restraint, macrocycles may display notable conformational flexibility, which frequently renders them unspecific or low-affinity binders *in vivo*. A recent study of Chatterjee's research group demonstrated that insertion of a thioamide into a macrocyclic peptide scaffold induced the formation of a single conformer.[106] This result prompted the authors to investigate bioactive RGD peptides – antagonists of proangiogenic integrins, which constitute an important drug target.[105] The study showed that thioamide incorporation increases the activity of integrins agonist RGD peptides (**Table 3. 2**). Importantly, cyclic thiopeptide **3.1e,** prepared by Chatterjee and co-workers, resulted to be more stable and active than cilengitide (*N*-methylated cyclic peptide being in the Phase III of the clinical trials against glioblastoma, used as a reference for binding studies, **3.1a**).[107]

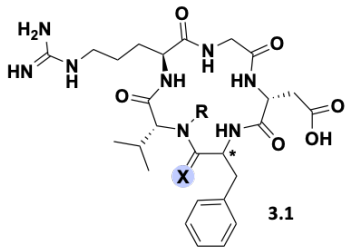

RGD Peptide	$t_{1/2}$	Breast Cancer	Glioblastoma
3.1a Cilengitide X=O, R=Me, *D-Phe	12 h	1.2 nM	3.0 nM
3.1b RGD-f X=O, R=H, *D-Phe	8 h	>10^5 nM	>10^5 nM
3.1c ThioRGD-f X=S, R=H, *D-Phe	9 h	4.0 nM	326 nM
3.1d RGD-F X=O, R=H, *L-Phe	7 h	>10^5 nM	>10^5 nM
3.1e ThioRGD-F X=S, R=H, *L-Phe	36 h	1.0 nM	1.6 nM

Table 3. 2. Summary of peptide serum stability ($t_{1/2}$) and activity (IC_{50} for binding to breast cancer cells and glioblastoma cells). Macrocycles **3.1c** and **3.1e** demonstrate higher levels of stability and activity compared to the corresponding amide peptides (**3.1b** and **3.1d**). **3.1e** is superior to cilengitide (**3.1a**) in all assays.

Described studies and their results demonstrate that thioamides are valuable tools for peptide chemistry. They can modulate the biological activity of biopolymers and due to the amide mimicry (with different physical properties) they enable the protein interactions' tuning to manipulate biological systems.

[105] Bock, J. E.; Gavenosis, J.; Kritzer, J. A. *ACS Chem. Biol*. **2013,** *8*, 488-499.
[106] Verma, H.; Khatri, B.; Chakraborti, S.; Chatterjee, *J. Chem. Sci.* **2018**, *9*, 2443-2451.
[107] Mas-Moruno, C.; Rechenmacher, F.; Kessler, H. *Anti-Cancer Agents Med. Chem.* **2010**, *10*, 753-768.

3.1.3. Synthesis of thiopeptides

One of the gravest limitations associated with studying thionated peptides has been the insertion of the thioamide moiety into the peptide sequence in a controlled and site-specific fashion. Different synthetic routes towards thiopeptides have been examined. The conceptually simplest one provides for a direct thionation in the presence of Lawesson's Reagent.[108] However, the use of thionating agents is often connected with a constraint of working in the excess of reagents under lengthy refluxing conditions in anhydrous solvents. Moreover, this methodology typically leads to an inseparable mixture of products.[109]

On the other hand, the site-specific insertion of a thioamide into the peptidic sequence of interest *via* thioamide precursor (during biooligomer's construction), constitutes a preferable alternative to attempt a selective transformation of a certain amide bond. There are various examples of such a methodology in the literature, for instance, activation of thioacids with phosphonium-based agents like tripyrrolidinophosphonium hexafluorophosphate (PyBOP)[110] or the preparation of thioacyl-benzimidazolinones.[111] Unfortunately, these strategies have in common two substantial drawbacks: low yields and racemization of the thioamide moiety.[112]

An improved alternative for a directed insertion of the thioamide moiety is based on the use of thioacyl-benzotriazoles, which are reactive enough to thioacetylate amines in the presence of a base and without the need of any additional activating agent.[113] The preparation of thioacyl-benzotriazole monomers provides for three synthetic steps. The thioamide precursors are usually obtained from orthogonally protected Fmoc amino acids, employing Lawesson's Reagent or P_4O_{10} for the thionation step. Then, they can be used for introducing the thioamide directly during solid phase peptide synthesis (SPPS) (**Scheme 3. 2**).

---

[108] Kessler, H.; Matter, H.; Geyer, A.; Diehl, H. J.; Kock, M.; Kurz, G.; Opperdoes, F. R.; Callens, M.; Wierenga, R. K. *Angew. Chem. Int. Ed*. **1992**, *31*, 328-330.
[109] Morita, H.; Nagashima, S.; Takeya, K.; Itokawa, H*. J. Chem. Soc., Perkin. Trans*. **1995**, *1*, 2327-2331.
[110] Kloss, F.; Chiriac, A. I.; Hertweck, C. *Chem. Eur. J.* **2014**, *20*, 15451-15458.
[111] Zacharie, B.; Sauve, G.; Penney, C*. Tetrahedron* **1993**, *49*, 10489-10500.
[112] Mahanta, N.; Miklos Szantai-Kis, D.; Petersson, E. J.; Mitchell D. A. *ACS Chem Biol* **2019**, *14*, 142-163.
[113] Shalaby, M. A.; Grote, C. W.; Rapoport, H*. J. Org. Chem.* **1996**, *61*, 9045, 9048.

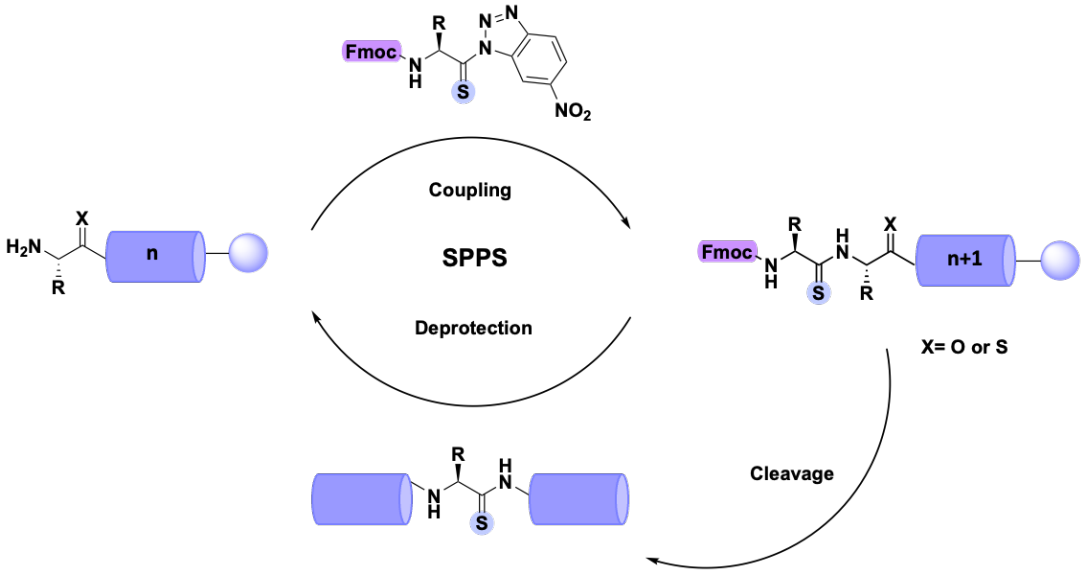

Scheme 3. 2. Site-specific installation of thioamides in solid phase peptide synthesis (SPPS).

3.1.4. Research targets

The goal of this project was to find a strategy to install thioamide bonds in the peptoid scaffold (**Figure 3. 3**). Why would this modification be beneficial? Firstly, thioamides, due to the "softer" character of sulfur, have a higher affinity for different metal cations compared to the oxygen in amides, which may lead to interesting complexation studies and new applications of cyclic peptoids. Additionally, the sulfur atom, which is larger in comparison to the oxygen, and the elongated C=S bond could potentially induce conformational changes, and finally, the higher rotational barrier around the C-N bond of thioamides may furnish the desirable conformational stability to these new peptoidic scaffolds.

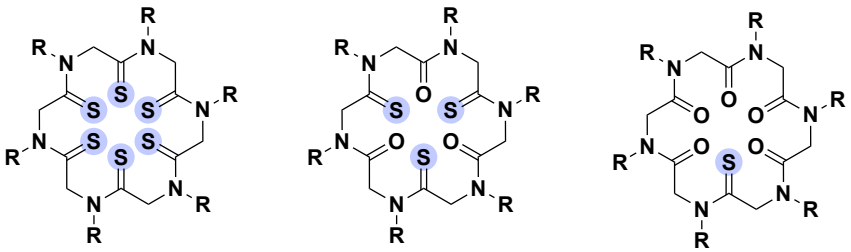

Figure 3. 3. Schematic structures of potential target cyclic thiopeptoids.

The initially projected phases for the preparation of cyclic thiopeptoids consisted of: 1) solution synthesis of a thioacylating reagent; 2) oligomerization on solid phase, *via* coupling of previously prepared building blocks; 3) Cyclization of linear precursors under high dilution conditions. Inspiration came from the synthesis of peptides containing thioamide bonds, *via* thioacyl-benzotriazoles, which are sufficiently reactive to thioacetylate amines in the presence of a base, and without other activating reagents. The approach considers a three-step synthesis of thioacyl-benzotriazole-containing monomers. Subsequently, these building blocks, due to the presence of thioacyl-benzotriazoles, can be anchored to the resin and exploited in solid-phase synthesis following standard protocols.

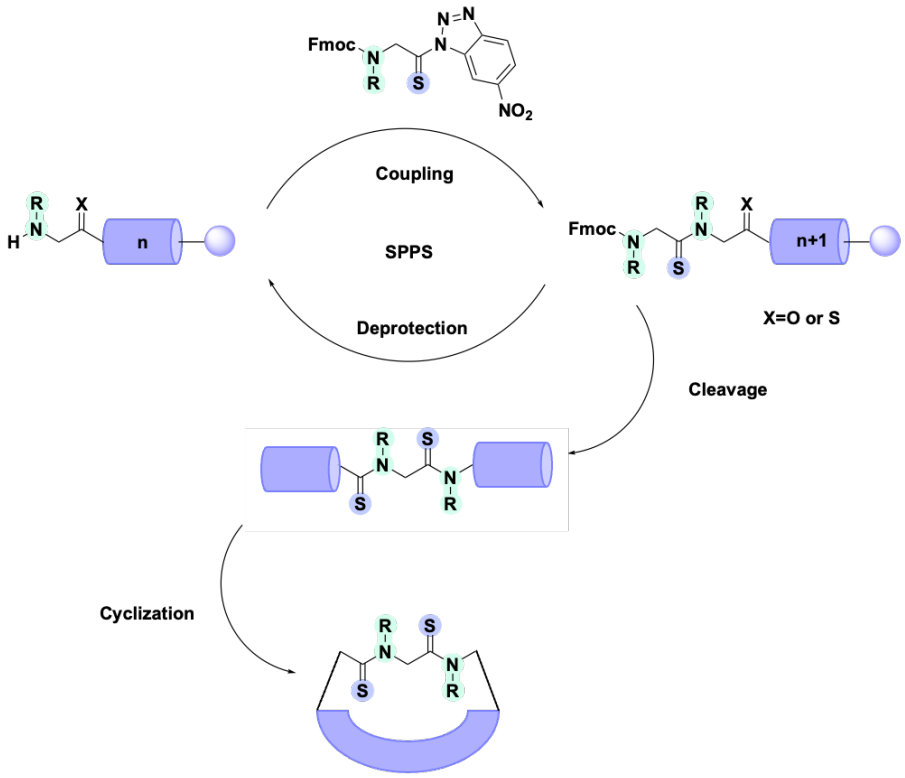

Scheme 3. 3. Shematic representation of the synthetic route towards cyclic thiopeptoids.

3.2. Development of a strategy toward cyclic thiopeptoids

3.2.1. Results and discussion

3.2.1.1 Synthesis of thioacylating agent with *N*-methyl group

To obtain the first precursor of the thioamide bond in peptoids, we decided to start as straightforwardly as possible, hence we opted for an *N*-methyl substituent. As a starting material, we used commercially available Fmoc-protected sarcosine, compatible with monomeric solid-phase synthesis on chlorotrityl resin. The synthesis of thioacylating agent with *N*-methyl group provides for three key steps: 1) Synthesis of *N*-Fmoc-sarcosine-2-amino-5-nitroanilide; 2) Thionation of *N*-Fmoc-sarcosine-2-amino-5-nitroanilide; 3) Synthesis of *N*-Fmoc-thionosarcosinyl-6-nitrobenzotriazole (**Figure 3. 4**).

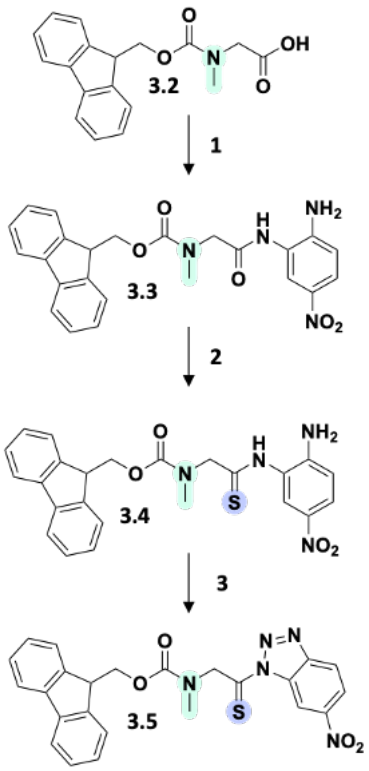

Figure 3. 4. Key intermediates of *N*-methyl containing thioacylating agent's synthesis.

The first stage comprises a coupling reaction between the free carboxyl group of *N*-protected sarcosine and 4-nitro-1,2-phenylenediamine (**Scheme 3. 4**), which allows subsequent conversion to benzotriazole. The most suitable coupling reagent for this step, as attested by our preliminary investigations, turned out to be 1-[Bis(dimethylamino)methylene]-1H-1,2,3-

triazolo[4,5-b] pyridinium 3-oxide hexafluorophosphate (HATU). Although HATU-mediated coupling reactions are widely described in the literature, it was quite challenging to optimize the reaction conditions. From our experimental work it was found that a stringent condition for the successful chemical transformation was a temperature of 25°C. Although at lower temperatures, the coupling reaction was not complete and unreacted sarcosine was still observed, at 25°C, we managed to obtain a target *N*-Fmoc-sarcosine-2-amino-5-nitroanilide (**3.3**).

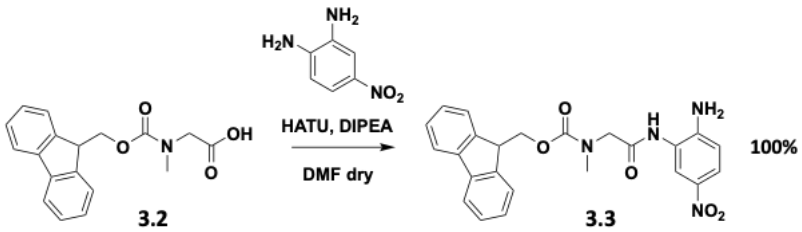

Scheme 3. 4. Synthesis of *N*-Fmoc-sarcosine-2-amino-5-nitroanilide.

The objective of the second synthetic step consisted in an oxygen-to-sulfur replacement. To that end, we employed a commonly used phosphorus pentasulfide (P_2S_5) as a sulfur donor. The synthetic methodology requires the use of thionation reagent in the presence of anhydrous sodium carbonate (Na_2CO_3) and THF dry as a solvent. (**Scheme 3. 5**). Importantly, even though this was not always emphasized in the literature, it was essential to work in anhydrous environment and in the absence of air. Otherwise, the reaction led to an inseparable mixture of thionated product and its oxygen-containing analog. Moreover, in this case as well, another key parameter turned out to be the temperature of 25 °C. The optimization of the synthetic procedure led to the isolation of the target compound **3.4**.

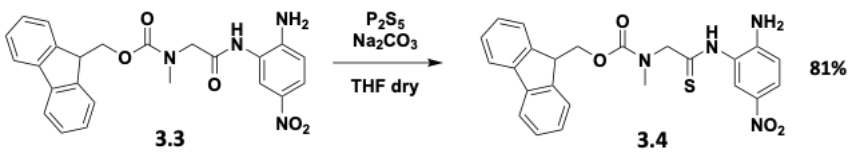

Scheme 3. 5. Thionation of *N*-Fmoc-sarcosine-2-amino-5-nitroanilide.

The final step involves the formation of a benzotriazole from previously obtained thioamide-containing precursor (**Scheme 3. 6**). The reaction begins by reacting, at a temperature of 40°C, the compound **3.3** with 95% acetic acid. At 0°C, sodium nitrite ($NaNO_2$) is added, and addition of cold distilled water affords the target product precipitation.

Although in the case of standard amino acids this step is rather straightforward, in the case of sarcosine we faced a significant reproducibility problem. Even though we succeeded to obtain and characterize the target molecule, each of subsequent synthetic attempts led to the mixture of unreacted thioamide precursor and thioacylating agent.

Despite our efforts and numerous experiments, we could not ensure the reproducibility of the synthesis of the *N*-methyl containing thioacylating agent. These results prompted us to investigate more sterically hindered *N*-benzyl substituent, which appeared to guarantee the reproducibility for the synthesis of the corresponding thioacylating agent (**3.11**).

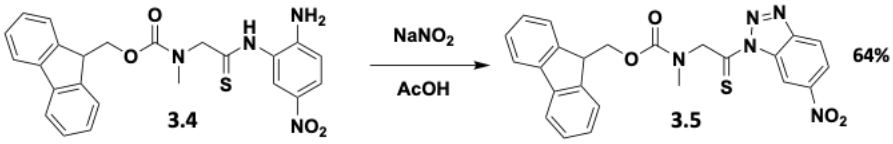

Scheme 3. 6. Synthesis of *N*-Fmoc-thionosarcosinyl-6-nitrobenzotriazole.

3.2.1.2 Synthesis of thioacylating agent with *N*-benzyl group

Preparation of the second thioacylating agent required two additional steps to obtain the starting Fmoc-*N*-benzylglycine. In particular, the stages consisted in reductive amination reaction (leading to *N*-benzyl glycine) and its subsequent Fmoc-protection according to procedures available in the literature (**Scheme 3. 7**).[114]

[114] Lake, F.; Linde, C. *Tetrahedron Letters* **2012**, *53*, 3927–3929.

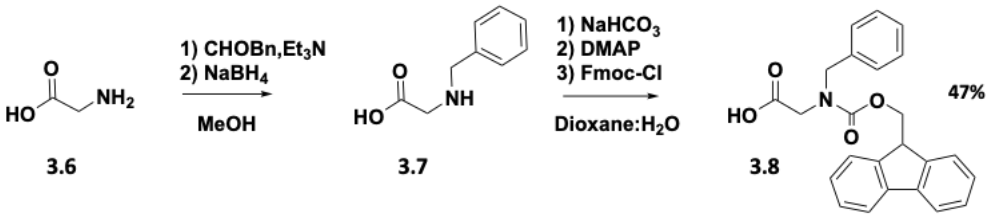

Scheme 3. 7. Synthesis of Fmoc-*N*-benzylglycine.

The remaining synthetic part, towards thioacylating agent, was performed in similar manner (respect to the synthesis of **3.5**). The stages were following: 1) Synthesis of Fmoc-*N*-benzyl-glycine-2-amino-5-nitroanilide; 2) Thionation of Fmoc-*N*-benzyl-glycine-2-amino-5-nitroanilide, 3) Synthesis of Fmoc-*N*-benzyl-thioglycinyl-6-nitrobenzotriazole (**Figure 3. 5**).

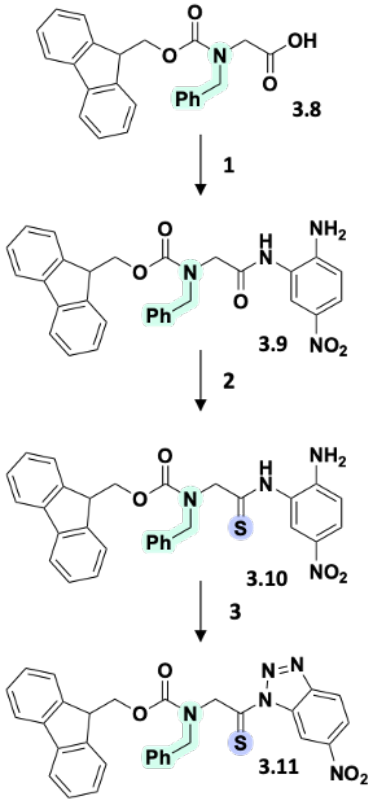

Figure 3. 5. Key intermediates of *N*-benzyl containing thioacylating agent's synthesis.

The compound **3.9** was obtained *via* HATU-mediated coupling reaction of Fmoc-*N*-benzyl glycine and 4-nitro-1,2-phenylenediamine in anhydrous DMF (according to **Scheme 3. 8**).

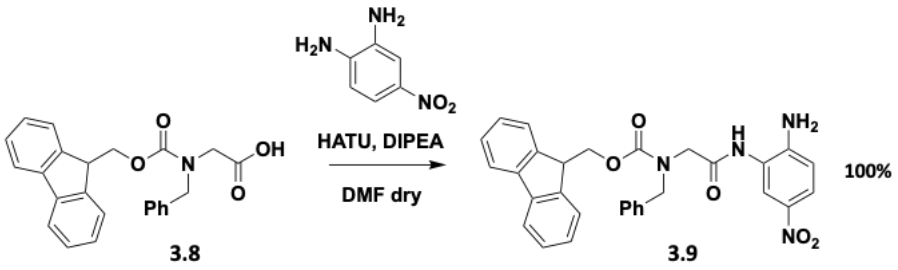

Scheme 3. 8. Synthesis of Fmoc-*N*-benzyl-glycine-2-amino-5-nitroanilide.

Subsequent thionation reaction (**Scheme 3. 9**) was performed, as in the previous case, in the presence of phosphorus pentasulfide, leading to a formation of desired compound **3.10**.

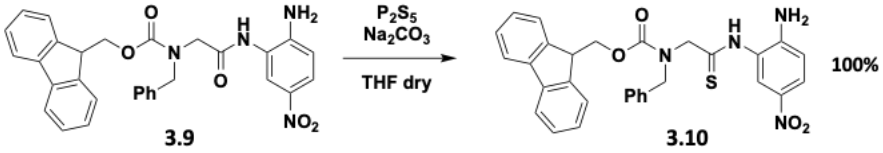

Scheme 3. 9. Thionation of Fmoc-N-benzyl-glycine-2-amino-5-nitroanilide.

The target **3.11** was obtained with the yield of 44% in the last synthetic step providing for a benzotriazole formation (**Scheme 3. 10**). In contrast to the synthesis of the analogous thioacylating agent with *N*-methyl, in this case no difficulty was encountered during the synthetic process and the synthesis proved to be highly reproducible.

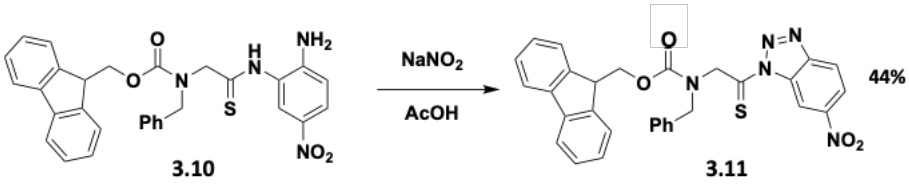

Scheme 3. 10. Synthesis of Fmoc-Tiocarbonyl-*N*-benzyl-Gly-nitrobenzotriazole.

3.2.1.3 On-resin thioacylation trials

To evaluate the reactivity of obtained thioacylating agent, and the ability to introduce the thioamide group into a peptoid sequence, it was decided to synthesize a peptoid trimer composed of *N*-benzyl glycine units for subsequent thioacylation tests. The linear oligomer

was synthetized by following standard sub-monomer approach procedures. Once the trimer **3.16** has been constructed, solid-phase acylation attempts were performed (Scheme 3. 11).

From preliminary studies performed in our laboratory, it was deduced that it is preferable to use three equivalents of thioamide-containing monomer to perform an on-resin thioacylation reaction. In the first attempt the equivalents were added in a single aliquot, while in the second trial (which turned out to be more successful, as the chloranil test confirmed the monomer coupling, in contrast to the first attempt), the three equivalents were divided into two aliquots (1.5 equivalent each). The reaction was performed on solid phase, adding the thioacylating agent into the reactor containing the previously prepared trimer in the presence of DCM as solvent. Piperidine 20% solution in DMF was used to deprotect the amine function. Subsequently, the oligomer was detached from the resin, using 20% solution of hexafluoro-2-propanol in dichloromethane.

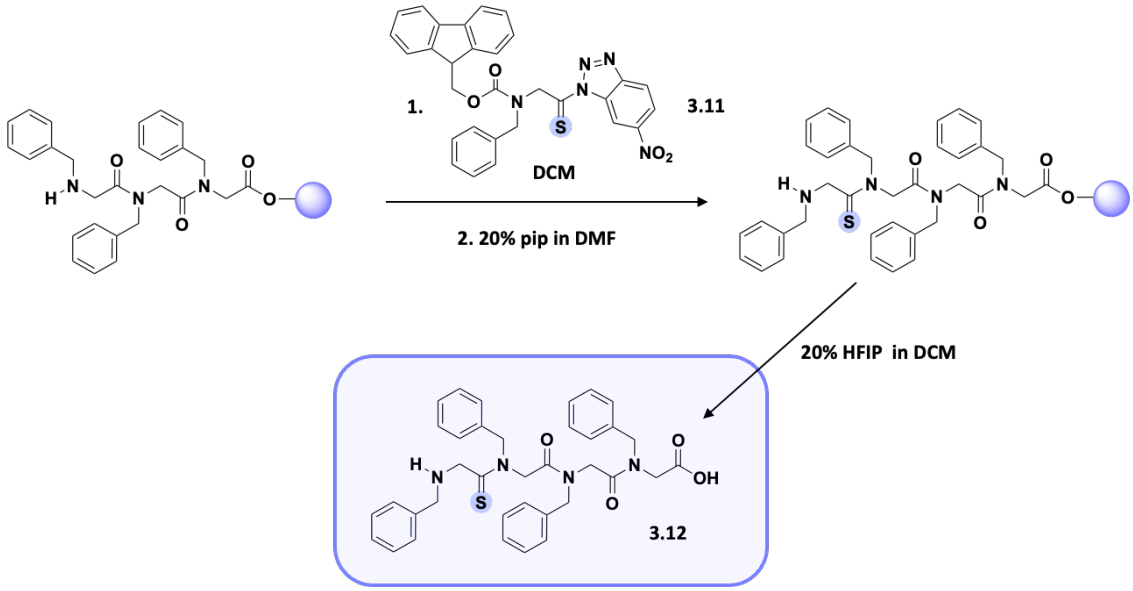

Scheme 3. 11. On-resin thioacylation.

The HR-MS analysis of the reaction crude confirmed a formation of expected linear thiopeptoid **3.12** (*m/z*=623.2718, $[M+H]^+$), and thus, we decided to proceed with its cyclization. Unfortunately, the ^1H NMR analysis of a crude mixture resulting from the cyclization revealed a formation of an already known cyclic trimer **3.13** decorated with

N-benzyl side chains[115] instead of the desired **3.14**. This result suggested that in reality, the *N*-benzyl-containing trimer was the main product resulting from the solid-phase synthesis (the cyclization of which furnished the macrocycle **3.13**), and the linear thiopeptoid **3.12**, presumably, was present in the mixture only in trace amounts. As the thioacylation reaction resulted to be not completely efficient, it requires further optimization, as well as the macrocyclization step.

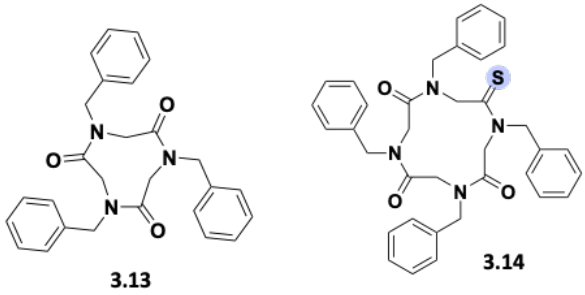

Figure 3. 6. Schematic structure of obtained product **3.13** (vs structure of the target macrocycle **3.14**).

3.2.2. Conclusions

In this work, the synthesis of new thioacylating agents with *N*-methyl and with *N*-benzyl groups was studied. Even though both compounds have been obtained and characterized, due to the major stability of **3.11** (compared to **3.5**) the on-resin thioacylation trials were performed only with *N*-benzyl containing thioamide precursor, finally leading to the formation of the first linear thiopeptoid **3.12**.

However, preliminary attempts to introduce a thioamide bond into peptoid sequence unfortunately did not result in obtaining the expected cyclic product **3.14**. This evidence, as well as the hardly achievable reproducibility of various experiments, highlights the complexity of this purpose, and explains the absence of cyclopeptoid systems containing *N*-alkylated thioamides in the literature.

[115] D'Amato, A.; Schettini, R.; Della Sala, G.; Costabile, C.; Tedesco, C.; Izzo, I.; De Riccardis, F. *Org. Biomol. Chem*. **2017**, *15*, 9932-9942.

3.2.3. Experimental section

3.2.3.1 General methods

Reagents and solvents were purchased from Sigma-Aldrich, TCI Chemicals, and Fluka. In reactions conducted under an inert atmosphere of nitrogen, the glassware was kept in an oven before each use, and commercially available anhydrous solvents or distillants were used for this type of reaction where necessary. An inert atmosphere was obtained by performing vacuum-nitrogen cycles. Each reaction was monitored by thin-layer chromatography (TLC), on Macherey-Nagel silica gel plates (0.25 mm), spots were detected with UV/Vis lamp at 254 nm wavelength, with ninhydrin or with iodine vapor. In some cases, the products were purified by flash chromatography on a Merck silica gel column (60 Mesh, particle size 0.040-0.063 mm). Qualitative analyses on peptoids were performed by HPLC with a reverse-phase C_{18} analytical column (Waters, Bondapak, 10 µm, 125 Å, 3.9 x 300 mm), eluent from 5% acetonitrile in water (+0.1% TFA) to 100% acetonitrile (+0. 1% TFA), with linear gradient in 30 min, flow rate 1 mL min^{-1}, using a Jasco BS 997-01 series liquid chromatography HPLC, equipped with a Jasco PU- 2089 Plus quaternary pump, a rheodyne 7725i injector and a Jasco MD-2010 Plus detector, variable wavelength and wavelength programmed at 220 nm or 260 nm. The products were dissolved in deuterated chloroform ($CDCl_3$) and subjected to ^{1}H NMR and ^{13}C NMR characterization, calibrating the signal to 7.26 ppm for proton and 77.0 ppm for carbon, recording spectra with 400 MHz or 300 MHz instruments. Chemical shifts are given in ppm, and signal assignments were performed thanks to the support of COSY and DEPT NMR spectra. *J* coupling constants are given in Hertz and multiplicities as: s (singlet), d (doublet), t (triplet), dd (doublet), m (multiplet), br s and br d for a broad singlet and doublet signal, respectively. HR-MS analysis of the thioacylating agents and acylation test products were performed with a high-resolution Fourier transform cyclotron ion resonance mass spectrometer using MALDI ionization.

3.2.3.2 Synthesis of thioacylating agent with *N*-methyl group

Synthesis of *N*-Fmoc-sarcosine-2-amino-5-nitroanilide

In a flask containing Fmoc-Sar-OH (1.00 g, 3.20 mmol, dissolved in dry DMF (9.7 mL) at a temperature of 25°C, HATU (1.22 g, 3.20 mmol) and DIPEA (1.1 mL, 6.4 mmol) were added. After a few minutes, 4-nitro-1,2-phenylenediamine (0.49 g, 3.2 mmol) was added. The reaction was left to stir for about 20 hours, and at the end a control TLC was performed, using 9:1 DCM/MeOH eluent chamber, UV detector and ninhydrin as a detection reagent.

Work-up was performed by adding a saturated solution of KCl (80 mL) to the flask; the formation of a precipitate was observed, and then an extraction with AcOEt (2 x 160 mL) was performed. The organic phase was washed with a saturated NaCl solution four times (4 x 160 mL). The organic phase was then anhydrified with Na_2SO_4 and solvents were removed. The reaction crude was subjected to ^{1}H NMR analysis and used in the next reaction without further purification.

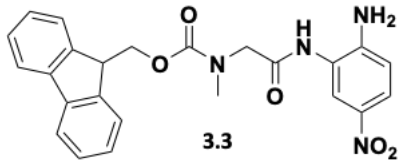

3.3

3.3: Orange amorphous solid, 1.43 g, 100% yield.

^{1}H NMR (400 MHz, $CDCl_3$, main conformer) δ: 8.13 (s, 1H, N*H*), 8.00 (br d, 1H, *J* 8.0 Hz, Ar-*H*), 7.77-7.69 (m, 3H, Ar-*H* and Fmoc-Ar-*H* overlapping), 7.57 (d, 2H, *J* 7.5 Hz, Fmoc-Ar-*H*), 7. 36 (m, 2H, Fmoc-Ar-*H*), 7.26 (m. 2H, Fmoc-Ar-*H*), 6.69 (d, 1H, *J* 8.0 Hz, Ar-*H*), 4.57 (br s, 2H, CH_2-Fmoc), 4.26 (t, 1H, *J* 5.4 Hz, C*H*-Fmoc), 3.99 (br s, 2H, NCH_2C=O), 3.03 (s, 3H, CH_3).

Thionation of *N*-Fmoc-sarcosine-2-amino-5-nitroanilide

P_2S_5 (1.69 g, 3.80 mmol) and anhydrous Na_2CO_3 (0.40 mg, 3.80 mmol) were placed in a flask, under nitrogen. Each solid was previously weighed into an anhydrous vial. To the flask containing both solids, distilled THF (24 ml) was added. Once the solution was clear, it was brought to 0°C, and after ten minutes, in a nitrogen atmosphere, **3.3** (1.43 g, 3.2 mmol) was dissolved in distilled THF (36.8 mL) and added to the mixture. After thirty minutes (at 0°C), the

reacting mixture was left stirring for 2 hours at 25°C. The reaction was monitored by TLC (DCM/MeOH eluent (9:1), UV/Vis detector and ninhydrin). Once the reaction was completed, the THF was removed. Then the resulting solid was solubilized in AcOEt (100 mL) and washed with a saturated solution of $NaHCO_3$ (3 x 50 mL). Finally, it was anhydrified with Na_2SO_4 and ethyl acetate was removed. The reaction crude was analyzed by ^1H NMR and used in the next step without further purification.

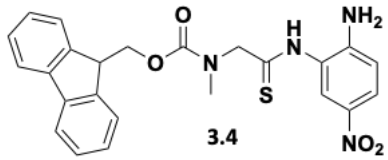

3.4

3.4: Yellow amorphous solid, 1.22 g, 81% yield.

^1H NMR (400 MHz, $CDCl_3$, main conformer) δ: 8.20 (s, 1H, N*H*), 8.02 (br d, 1H, *J* 8.0 Hz, Ar-*H*), 7.82-7.62 (m, 3H, Ar-H, Fmoc-Ar-*H* overlapping), 7.55 (d, 2H, *J* 7.5 Hz, Fmoc-Ar-*H*), 7.35 (t like, 2H, *J* 7.4 Hz, Fmoc-Ar-*H*), 7.26 (t like, 2H, *J* 7.4 Hz, Fmoc-Ar-*H*), 6.70 (d, 1H, *J* 8.0 Hz, Ar-*H*), 4.52 (br s, 2H, CH_2-Fmoc), 4.36 (br s, 2H, NCH_2C=S), 4.23 (t, 1H, *J* 5.7 Hz, C*H*-Fmoc), 3.06 (s, 3H, CH_3).

Synthesis of *N*-Fmoc-thionosarcosinyl-6-nitrobenzotriazole

In a flask containing **3.4** (1.08 g, 2.3 mmol), 95% AcOH (20 mL) was added, and the mixture was left stirring at 40°C until the solution become clear. Then, the temperature was brought to 4°C, $NaNO_2$ (0.28 g, 4.14 mmol) was added in three aliquots, and the mixture was left to stir for 1 h. Subsequently, the reaction was stopped by adding cold distilled water (60 mL) into the flask. The formation of light-yellow precipitate was observed. A vacuum filtration was then performed, the precipitate was washed with distilled water (3 × 20mL) and dried.

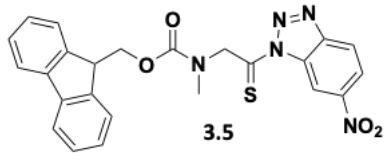

3.5

3.5: Light-yellow amorphous solid, 0.70 g, 64% yield (over three steps), HRMS (MALDI): *m/z* $[M+H]^+$ Calcd for $C_{24}H_{20}N_5O_4S^+$ 474.1236; Found 474.2264.

^{1}H NMR (400 MHz, $CDCl_3$, mixture of conformers) δ: 9.66 (d, 0.4H, *J* 1.8 Hz, Ar-*H*), 9.54 (d, 0.6H, *J* 1.8 Hz, Ar-*H*), 8.53 (dd, 0.6H, *J* 9.0, 1.8 Hz, Ar-*H*), 8.44 (dd, 0.4H, *J* 9.0, 1.8 Hz, Ar-*H*), 8.38 (dd, 0.6H, *J* 9.0 Hz, Ar-*H*), 8.31 (dd, 0.4H, *J* 9.0, Hz, Ar-*H*), 7.80 (dd, 0.8H, *J* 7.5 Hz, Fmoc-Ar-H), 7.68 (dd, 0.8H, *J* 7.5 Hz, Fmoc-Ar-*H*), 7.46-7.34 (dd, 0.4H, *J* 9.0, Hz, Ar-*H*), 7.46-7.34 (dd, 0.4H, *J* 9.0, Hz, Ar-*H*), 7.46-7.34 (dd, 0.5 H, *J*9.0, Hz, Ar-*H*, Ar-*H*, Ar-*H*) 16 (d, 1.2H, *J* 7.5 Hz, Fmoc-Ar-*H*), 7.11 (t like, 1.2H, *J* 7.4 Hz, Fmoc-Ar-*H*), 6.98 (t like, 1.2H, *J* 7.4 Hz, Fmoc-Ar-*H*), 5.29 (br s, 0.8H, Fmoc-Ar-*H*), 5.29 (br s, 0.8H, Fmoc-Ar-*H*, NCH_2C=S), 4.71 (br s, 1.2H, Fmoc-Ar-*H*), 4.71 (br s, 1.2H, Fmoc-Ar-*H*), 4.65 (d, 1.2H, *J* 4.2 Hz, CH_2-Fmoc), 4.50 (d, 0.8H, *J* 6.9 Hz, CH_2-Fmoc), 4.33 (t, 0.4H, *J* 6.9 Hz, C*H*-Fmoc), 4.07 (t, 0.6H, *J* 4.2 Hz, C*H*-Fmoc), 3.13 (s, 1.2H, CH_3), 2.97 (s, 1.8H, CH_3).

^{13}C NMR (100 MHz, $CDCl_3$, mixture of conformers) δ: 200.6, 199.7,156.7, 155.7, 149.6. 149.4, 148.7, 143.8, 143.7, 141.3, 141.0, 131. 8, 127.7, 127.1, 126.9, 125.1, 124.2, 122.1, 121.5, 121.3, 120.0, 119.3, 112.9, 112.5, 67.9, 66.2, 61.5, 60.6, 47.2, 47.1, 36.0, 35.7.

3.2.3.3 Synthesis of thioacylating agent with *N*-benzyl group

Synthesis of *N*-benzyl-glycine[114]

Before proceeding with the synthesis, a benzaldehyde purification procedure was performed: benzaldehyde (10 mL) was diluted with Et_2O (3 mL) and washed with a saturated solution of $NaHCO_3$ (3 x 5 mL). Next, the organic phase was washed with a saturated solution of NaCl (3 x 5 mL), anhydrified with $MgSO_4$, and then the solvent was removed. Glycine (1.00 g, 13.0 mmol), MeOH (16.2 mL), purified benzaldehyde (1.32 mL, 13.0 mmol) and Et_3N (3.70 mL, 2.6 mmol) were introduced into a flask. The resulting mixture was left to stir for 3 hours. Subsequently, the temperature was brought to 0°C and $NaBH_4$ (2.00 g, 53.2 mmol) was added in aliquots. After 20 hours, the reaction the solvent was removed, and the resulting crude was used in the following step without purification.

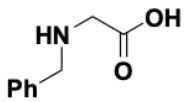

3.7

3.7: White amorphous solid, 4.39 g, 100% yield.

Synthesis of Fmoc-protected *N*-benzyl-glycine

In a flask, *N*-benzyl glycine, **3.7**, obtained in the previous step (4.39 g, 26.6 mmol), was dispersed in dioxane:H_2O 1:1 mixture (150mL). Under stirring, $NaHCO_3$ (5.36 g, 63.8 mmol), DMAP (0.16 g, 1.33 mmol) and Fmoc-Cl (8.94 g, 34.6 mmol) were introduced in three aliquots. After 20 hours of stirring, a work-up was performed. $KHSO_4$ (1M, 120 ml) was added until a pH of 3. The aqueous phase was extracted with AcOEt (3 x 100 ml) and anhydrified with anhydrous $MgSO_4$. Then the solvent was removed. The resulting crude was purified on flash silica gel; conditions: 90% - 70% A (A: petroleum ether; B: ethyl acetate + 0.1% AcOH).

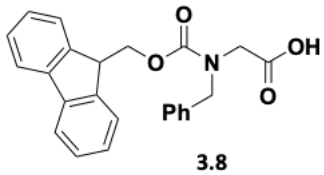

3.8

3.8: White amorphous solid, 4.83 g, 47% yield (over two steps).

^{1}H NMR (400 MHz, $CDCl_3$, conformer mixture) δ: 7.76 (m, 2H, Fmoc-Ar-*H*), 7.55 (d, 0.9H, *J* 7.5 Hz, Fmoc-Ar-*H*), 7. 49 (d, 1.1 H, Fmoc-Ar-*H*), 7.38 (t like, 1.8H, *J* 7.4 Hz, Fmoc-Ar-*H*), 7.30-7.23 (m, 5.2H, Fmoc-Ar-*H*, NCH_2Ar-*H* overlapping), 7. 19 (d, 0.9 H, *J* 6.9 Hz, NCH_2Ar-*H*), 7.07 (d, 1.1 H, *J* 6.9 Hz, N*C*H_2Ar-H),4.57 (m, 2.9H, CH_2-Fmoc and N*C*H_2Ar overlapping), 4. 48 (br s, 1.1H, N*C*H_2Ar) 4.26 (m, 1H, C*H*-Fmoc), 3.97 (br s, 1.1 H, N*C*H_2C=O), 3.75 (br s, 0.9H, N*C*H_2C=O).

Synthesis of Fmoc-*N*-benzyl-glycine-2-amino-5-nitroanilide

To solution of compound **3.8** (1.00 g, 2.58 mmol) in dry DMF (7.8 mL), HATU (0.98 g, 2.58 mmol) and DIPEA (0.9 mL) were added. After a few minutes, 4-nitro-1,2-phenylenediamine (408 mg, 2.58 mmol) was added and left stirring for 20 hours at a temperature of 25°C.

Work-up was performed by adding a saturated solution of KCl (65 mL); the formation of a precipitate was observed, and then an extraction with AcOEt (2 x 130 mL) was performed. The organic phase was washed with a saturated NaCl solution four times (4 x 130 mL). The organic phase was then anhydrified with Na_2SO_4 and solvents were removed. The reaction crude was subjected to ^{1}H NMR analysis and used it was used in the next reaction without further purification.

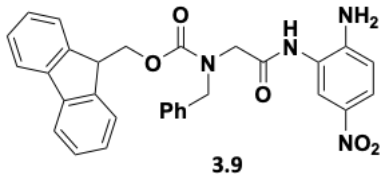

3.9

3.9: Orange amorphous solid, 1.11 g, 100% yield.

^{1}H NMR (300 MHz, CDCl3, main conformer) δ: 7.97 (br d, 1H, *J* 8.0 Hz, Ar-*H*), 7.75 (m, 3H, Ar-*H*, Fmoc-Ar-*H* overlapping), 7.55 (m, 2H, Fmoc-Ar- *H*), 7.37-7.22 (m, 7H, Fmoc-Ar-*H* and NCH_2-Ar-*H)*, 6. 99 (m, 2H, NCH_2-Ar-*H*), 6.66 (d, 1H, J 6.4 Hz, Ar-*H*), 4.57 (br s, 2H, C*H*$_2$-Fmoc), 4.54 (br s, 2H, NC*H*$_2$Ar), 4.26 (t, 1H, *J* 6.4 Hz, C*H*-Fmoc), 3.93 (br s, 2H, NC*H*$_2$C=O).

Thionation of Fmoc-*N*-benzyl-glycine-2-amino-5-nitroanilide

P_2S_5 (1.38 g, 3.10 mmol) and anhydrous Na_2CO_3 (0.33 mg, 3.10 mmol) were placed in a flask, under nitrogen. Each solid was previously weighed into an anhydrous vial. To the flask containing both solids, distilled THF (20.6 mL) was added. Once the solution was clear, it was brought to 0°C. After ten minutes, in a nitrogen atmosphere, **3.9** (1.34 g, 2.58 mmol) was dissolved in distilled THF (28 mL), and then added to the mixture. After thirty minutes (at 0°C), the reacting mixture was left stirring for 2 hours at 25°C. The reaction was monitored by TLC (DCM/MeOH eluent (9:1), UV/Vis detector and ninhydrin). Once the reaction was completed, the THF was removed. The resulting solid was solubilized in AcOEt (100 mL) and washed with a saturated solution of $NaHCO_3$ (3 x 50 mL). Finally, it was anhydrified with Na_2SO_4 and ethyl acetate was removed. The reaction crude was analyzed by ^{1}H NMR and used in the next step without further purification.

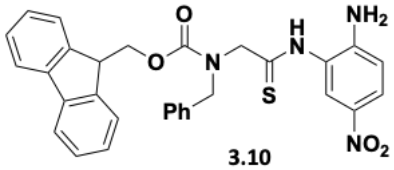

3.10

3.10: yellow amorphous solid, 0.739 g. 100% yield.

^{1}H NMR (400 MHz, $CDCl_3$, main conformer) δ: 7.98 (br d, 1H, *J* 8.0 Hz, Ar-*H*), 7.75 (m, 3H, Ar-H, Fmoc-Ar-*H* superimposed), 7.55 (m, 2H, Fmoc-Ar-*H*), 7.39-7.23 (m, 7H, Fmoc-Ar-*H* and NCH_2-Ar-*H*), 7. 00 (m, 2 H, NCH_2-Ar-*H*), 6.68 (d, 1H, *J* 6.4 Hz, Ar-*H*), 4.78 (d, 2H, *J* 5.2 Hz, C*H*$_2$-Fmoc), 4.54 (br s, 2H, NC*H*$_2$Ar), 4.36 (br s, 2H, NC*H*$_2$C=S), 4.28 (t, 1H, *J* 5.2 Hz, C*H*-Fmoc).

Synthesis of Fmoc-Thiocarbonyl-*N*-benzyl-Gly-nitrobenzotriazole (3.11)

In a flask containing **3.10** (0.739 g, 1.34 mmol) 95% AcOH (18 mL) was added and resulting mixture was left to stir at 40°C until the solution become clear. Then the temperature was brought to 4°C and $NaNO_2$ (0.16 g, 2.41 mmol) was added in three aliquots. It was then left to stir for one hour. Next, the reaction was stopped by pouring cold distilled water (106 mL) into the flask and it was allowed to precipitate by storing the flask in the refrigerator overnight. Then, a vacuum filtration was then performed, and the precipitate was washed with distilled water (3 x 20 mL) and the precipitate was dried.

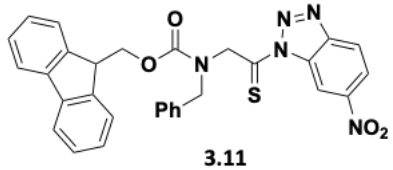

3.11

3.11: Light-orange amorphous solid, 0.32 g, 44% yield (over three steps), HRMS (MALDI): *m/z* $[M+Na]^+$ Calcd for $C_{30}H_{23}N_5NaO_4S^+$ 572.1363; Found 572.1867.

^{1}H NMR (400 MHz, $CDCl_3$, mixture of conformers) δ: 9.64 (d, 0.4 H, *J* 1.8 Hz, Ar-*H*), 9.52 (d, 0.6 H, *J* 1.8 Hz, Ar-*H*), 8.51 (dd, 0.6 H, *J* 9.0, 1.8 Hz, Ar-*H*), 8.43 (dd, 0.4 H, *J* 9.0, 1. 8 Hz, Ar-*H*), 8.35 (dd, 0.6 H, *J* 9.0 Hz, Ar-*H*), 8.28 (dd, 0.4 H, *J* 9.0, Hz, Ar-*H*), 7.76 (dd, 0.8 H, *J* 7.5 Hz, Fmoc-Ar-*H*), 7.56 (dd, 0.8 H, *J* 7.5 Hz, Fmoc-Ar-*H*), 7.43-7.40 (m, 2H, Fmoc-Ar-*H*), 7. 32-7.24 (m, 3.8H, Fmoc-Ar-*H*), 7.17-7.10 (m, 4.4H, Fmoc-Ar-*H*), 7.00 (t like, 1.2H, *J* 7.4 Hz, Fmoc-Ar-*H*), 5.22 (br s, 0.8H, Fmoc-Ar-*H*), 4.75 (d, 1.2H, *J* 2.7 Hz, C*H*$_2$-Fmoc), 4.61 (t like, 1.2H, *J* 7.4 Hz, Fmoc-Ar-*H*), 5.61 (d, 0.8H, *J* 4.2 Hz, C*H*$_2$-Fmoc), 4.60 (br s, 1.2H, NC*H*$_2$Ar), 4.59 (br s, 0.8H, NC*H*$_2$Ar), 4.54 (br s, 1.2H, NC*H*$_2$C=S), 4.33 (d, 0.4H, *J* 4.2 Hz, C*H*-Fmoc), 4.07 (d, 0.6H, *J* 2.7 Hz, C*H*-Fmoc).

^{13}C NMR (100 MHz, CDCl3, mixture of conformers) δ: 200.7, 199.8, 156.5, 156.9, 149.5, 149.4, 148.7, 148.6, 143.7, 143.6, 141.4, 141.0, 136.5, 136.4, 131.9, 131. 8, 128.8, 128.7, 128.1, 127.8, 127.7,127.5, 127.1, 126.9, 124.9, 124.2, 122.1, 122.0, 121,2, 120.0, 119.3, 112.9, 112.5, 67.9, 66.2, 58.7, 57.4, 51.4, 47.2.

3.2.3.4 Solid-phase synthesis of linear thiopeptoids

Synthesis of linear peptoid 3.15

0.050 g of 2-chlorotrityl resin (Novabiochem; 2,α-dichlorobenzhylhydryl-polystyrene crosslinked with 1% DVB; 100-200 mesh; 0.918 mmol/g) was washed with DCM (3 x 1 mL), DMF (3 x 1 mL) and DCM (3 x 1 mL). Next, swelling of the resin was carried out by adding dry DCM (0.5 ml) and leaving to stir for 45 minutes on the shaking platform. Next, the solution was filtered off and three cycles of DCM, DMF, DCM washes were carried out. For loading step, a solution of Fmoc-Sar-OH (1.6 eq, 74 mmol, 0.023 g) in dry DCM (0.5 mL) with DIPEA (5 eq, 0.04 ml) was added to the reactor and it was left stirring for 1h. Then, again three cycles of washes with DMF (3 x 1 mL), DCM (3x 1 mL), DMF (3 x 1 mL) were performed. Fmoc deprotection was performed with a 20% sulution of piperidine in DMF (2 x 0.5 mL), leaving the reactor stirring for 30 min. After another cycle of washes, the coupling of the second monomer was performed: a solution of Fmoc-Sar-OH (2.5 eq, 0.037 g) and HATU (2.9 eq, 0.049 g) in dry DMF (0.5 mL) and DIPEA (4 eq, 0.3 mL) were added into the reactor. After 1.5 h of stirring, a chloranil test was performed to monitor the reaction. Once the coupling was attested, filtration and washes were performed. The same sequence of operations was repeated for the coupling of the third monomer. The resin-bound trimer was used for thioacylation tests. Its identity was confirmed by HR-MS analysis (after a mini-cleavage).

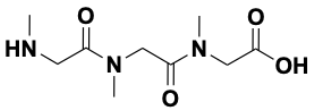

3.15

3.15: White amorphous solid, HRMS (MALDI): *m/z* $[M+H]^+$ Calcd for $C_9H_{18}N_3O_4^+$ 232.1292; Found 231.1462.

Synthesis of linear peptoid 3.16

To obtain this linear peptoid, solid-phase synthesis based on Zuckermann's sub-monomer method is used. 0.050 g of 2-chlorotrityl resin (Novabiochem; 2,α-dichlorobenzhylhydryl-polystyrene crosslinked with 1% DVB; 100-200 mesh; 0.918 mmol/g) were subjected to three cycles of washes with DCM (3 x 1 mL), DMF (3 x 1 mL), DCM (3 x 1 mL). Next, swelling in the

presence of dry DCM (0.5 mL) was performed by stirring for 45 min on the shaking platform. Next, three cycles of DCM, DMF, DCM washes were carried out. For loading, a solution of bromoacetic acid (1.6 eq, 93 mmol, 0.010 g) in dry DCM (0.5 mL) with DIPEA (5 eq, 0.04 mL) was added to the reactor and left stirring for 1h. Then, the reactor was emptied and washes with DMF (3 x 1 mL), DCM (3 x 1 mL), DMF (3 x 1 mL) were performed. Then, a solution of benzylamine (10 eq, 0.031 mL) in dry DMF (0.5 mL) was added to the reactor and left stirring for 40 minutes. For the construction of the second monomer, bromoacetic acid (10 eq, 0.064 g) was dissolved in dry DMF (0.5 mL) and with DIC (11 eq, 0.08 mL). After 40 min of stirring, a chloranil test was performed to monitor the reaction. The same procedure was repeated for in order to obtain the third monomer. The resin-bound trimer was used for thioacylation tests. Its identity was confirmed by HR-MS analysis after a mini-cleavage.

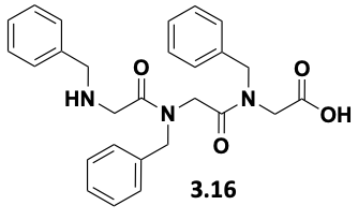

3.16

3.16: White amorphous solid, HRMS (MALDI): *m/z* $[M+H]^+$ Calcd for $C_{27}H_{29}N_3O_4^+$ 460.2231; Found 460.2227.

On-resin thioacylation

Thioacylating agent **3.11** (3 eq, 0.075 g) was dissolved in dry DCM (0.5 mL) and added into the reactor containing the peptoid trimer **3.16** bound to the resin in two (or single) aliquot(s), and left stirring for 30 min (or 30 min for each aliquot). Then a chloranil test was performed, followed by Fmoc deprotection (2 x 0.5 mL 20% piperidine solution in DMF: 2 x 7 min). After a cycle of DCM (3 x 1 mL), DMF (3 x 1 mL), and DCM (6 x 1 mL) washes, the linear thiopeptoid was detached from resin by a treatment with a 20% solution of HFIP in dry DCM, (3 x 1 mL; 3 x 30 min). Then the solvent was removed from collected filtrates. The mass spectrometry analysis attested formation of the linear thiopeptoid **3.12**, and it was used for cyclization step without purification.

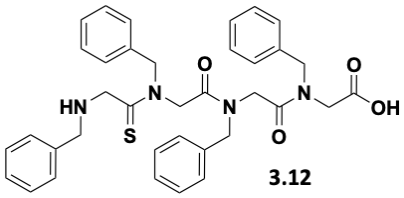

3.12

3.12: White amorphous solid, HRMS (MALDI): *m/z* $[M+H]^+$ Calcd for $C_{36}H_{39}N_4O_4S^+$ 623.2687; Found 623.2718.

3.2.3.5 Head-to-tail cyclization of linear thiopeptoid 3.12

A solution of the linear peptoid **3.12** (0.014 g, 0.14 mmol) in dry DMF (2.0 mL) was prepared under an inert atmosphere and added over 3h by syringe pump into a flask containing the solution of HATU (4 eq, 0.035g, 0.56 mmol) and DIPEA (6.2 eq, 0.025 mL, 0.87 mmol) in dry DMF (5.7 mL). A resulting mixture was allowed to stir overnight. Afterwards, DMF was removed. Next, the crude mixture was dissolved in DCM (30 mL) and washed with HCl (1.0 M, 2 x 15 mL). Then a final wash with distilled H_2O (15 mL) was perfomed. Then the resulting organic phase was anhydrified with $MgSO_4$ and the solvent was removed.

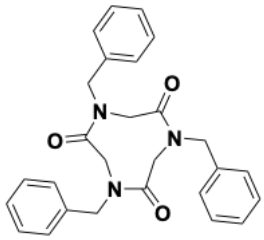

3.13

3.13:[115] white amorphous solid, 0.019 g, 19% yield, HRMS (MALDI): *m/z* $[M+H]^+$ Calcd for $C_{27}H_{28}N_3O_3^+$ 442.2125; Found 442.2121.

^{1}H NMR (400 MHz, $CDCl_3$) δ: 7.40-7.30 (15H, m), 5.54 (3H, d, *J* 14.4 Hz), 4.58 (3H, d, *J* 15.5 Hz), 4.21 (3H, d, *J* 14.4 Hz), 3.73 (3H, d, *J* 15.5 Hz).

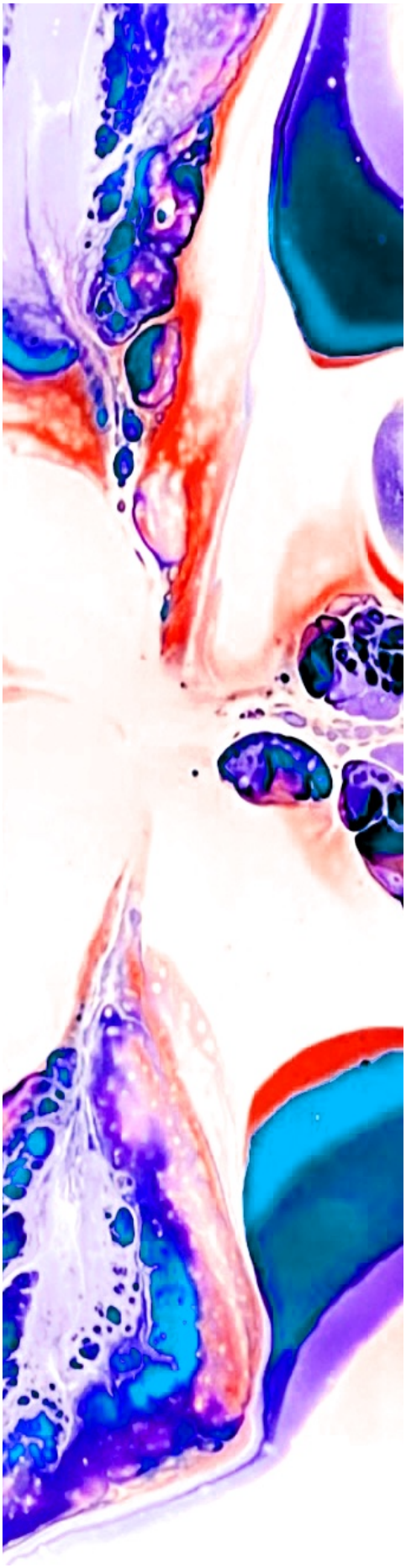

Chapter 4

TRIAZOLE-CONTAINING CYCLIC PEPTOIDS

4. TRIAZOLE-CONTAINING CYCLIC PEPTOIDS

4.1. Introduction

4.1.1. Disubstituted 1,2,3-triazoles

1,2,3-triazoles are heterocyclic compounds with relevant applications in various disciplines: from materials science, through nanotechnology,[116,117,118] to medicinal chemistry.[119,120,121,122] Their physicochemical properties render them an attractive tool for regulating conformational properties,[123,124,125] and enforcing non-covalent interactions or bio-conjugation processes, important for drug discovery.[126,127,128,129]

One of the most prominent features of these heterocyclic compounds is that they can mimic the amide bond.[130] The geometry and electronic attributes of 1,2,3-triazoles imply that they are excellent isosteres for the amide bond in both *trans* and *cis* configuration (depending on the substituents' position). The 1,4-disubstituted triazole can be considered as a *trans*-amide surrogate. The nitrogen's lone pair mimic the carbonyl oxygen of the amide, and the C-4 carbon atom electronically corresponds to the amide carbonyl carbon. Furthermore, as the dipole moment of triazole ring is somewhat higher compared to that of amides (~4.5 Debye vs. ~3.5 Debye), the proton bound to the C-5 carbon undergoes polarization and therefore it

[116] Finn, M. G.; Fokin, V. V. *Chem. Soc. Rev*., **2010**, *39*, 1231– 1232.
[117] Li, N.; Binder, W.H. *J. Mater. Chem*. **2011**, *21*, 16717-16734
[118] Dolci, M.; Toulemon, D.; Chaffar, Z.; Bubendorff, J-L.; Tielens, F.; Calatayud, M.; Zafeiratos, S.; Begin-Colin, S.; Pichon, B.P. *ACS Appl. Nano Mater*. **2019**, *2*, 554–565.
[119] Tahoori, F., Balalaie, S., Sheikhnejad, R., Sadjadi, M., and Boloori, P. *Amino Acids* **2014**, *46*, 1033–1046.
[120] Sun, H.; Liu, L.; Lu, J.; Qiu, S.; Yang, C.-Y.; Yi, H.; Wang, S. *Bioorg. Med. Chem. Lett.* **2010**, *20,* 3043–3046.
[121] Tassone, G.; Mazzorana, M.; Mangani, S.; Petricci, E.; Cini, E.; Giannini, G.; Pozzi, C.; MaramaiInt, S. *J. Mol. Sci*. **2022**, *23*, 9458.
[122] Liu, B.; Zhang, W.; Gou, S.; Huang, H.; Yao, J.; Yang, Z.; Liu, H.; Zhong, C.; Liu, B.; Ni, J.; Wang, R. *J. Pept. Sci.* **2017**, *23*, 824–832.
[123] Scrima, M.; Le Chevalier-Isaad, A.; Rovero, P.; Papini, A.M.; Chorev, M.; D'Ursi, A.M. *Eur. J. Org. Chem.* **2010**, 446–457.
[124] Horne, W. S.; Yadav, M. K.; Stout, C. D.; Ghadiri, M. R. J. *Am. Chem. Soc.* **2004**, *126*, 15366–15367.
[125] Oh, K.; Guan, Z. *Chem. Commun*. **2006**, 3069–3071.
[126] Kaur, J.; Saxena, M.; Rishi, N. *Bioconjugate Chem.* **2021**, *32*, 1455−147.
[127] Testa, C.; Papini, A.M.; Zeidler, R.; Vullo, D.; Carta, F.; Supuran, C.T.; Rovero, P. *Journal of Enzyme Inhibition and Medicinal Chemistry* **2022**, *37*, 592-596.
[128] Wan, Q.; Chen, J.; Chen, G.; Danishefsky, S.J. *J. Org. Chem*. **2006**, *71*, 8244–8249.
[129] Parrish, B.; Breitenkamp, R.B.; Emrick, T. *J. Am. Chem. Soc*. **2005**, *127*, 7404–7410.
[130] Recnik, L.M.; Kandioller, W.; Mindt, T.L. *Molecules* **2020**, *25*, 3576.

can act as H-bond donor similarly to NH in amides.[131] However, the only difference between 1,4-disubstituted triazole and *trans*-amide bond is the distance between substituents, R_1 and R_2. On the other hand, the 1,5-disubstituted triazole shares some substantial similarities with the *cis*-amide.[132] All the aforementioned relationships are depicted in **Figure 4. 1**.

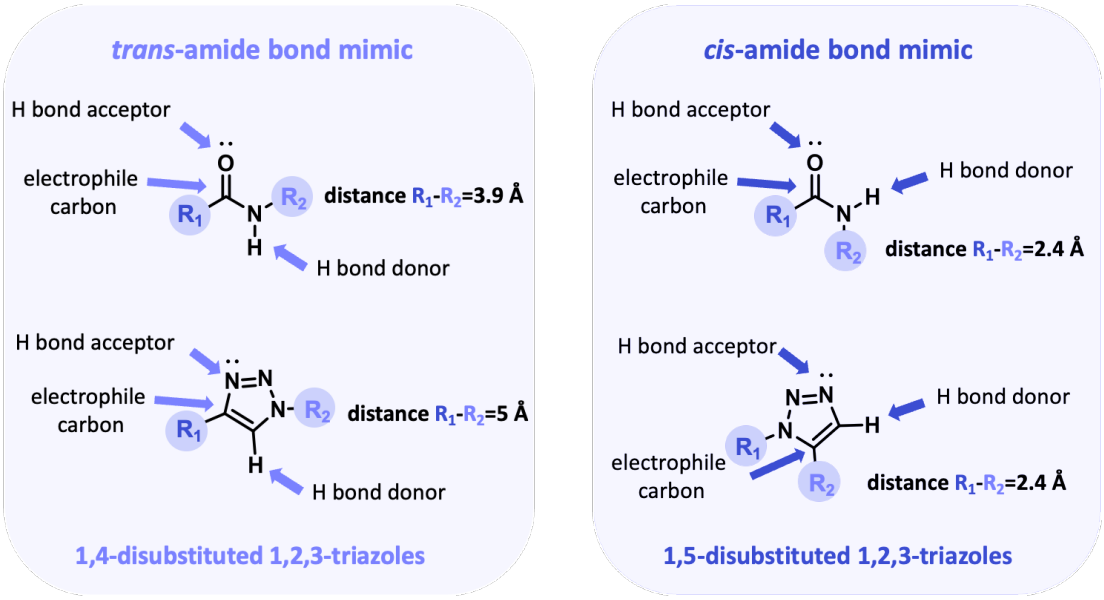

Figure 4. 1. Disubstituted 1,2,3-triazoles as amide bond mimics.

The Huisgen 1,3-dipolar cycloaddition between organic azides and alkynes is the most intuitive method of obtaining 1,2,3-triazoles.[133] However, this reaction is characterized by two essential drawbacks: slow rate and lack of regioselectivity.[134] These limitations have been overcome with the revelation that metal ions are able to catalyze the process. Sharpless[135] and Meldal[136] discovered that Cu(I) salts can catalyze the selective formation of 1,4-disubstituted-1,2,3-triazoles very efficiently and under mild conditions. Importantly, the unstable Cu(I) species can be obtained *in situ* from Cu(II) salts and the reaction can be performed in both organic and aqueous environments. These features have established the copper-catalyzed alkyne-azide cycloaddition (CuAAC) as a model example of so-called "click chemistry". Remarkably, K. Barry

[131] Palmer, M.H.; Findlay, R.H.; Gaskell, A.J. *J. Chem. Soc. Perkin Trans.* **1974**, *2*, 420–428.
[132] Tam, A.; Arnold, U.; Soellner, M.B.; Raines, R.T. *J. Am. Chem. Soc.* **2007**, *129*, 12670–12671.
[133] Huisgen, R. *Angew. Chem., Int. Ed. Engl*. **1963**, *2*, 633–645.
[134] Damodiran, M.; Muralidharan, D.; Permula, P. T. *Bioorg. Med. Chem. Lett,* **2009**, *19*, 3611–3614.
[135] Kolb, H. C.; Finn, M. G.; Sharpless, K. B. *Angew. Chem., Int. Ed.* **2001**, *40*, 2004–2021.
[136] Tornoe, C. W.; Christensen, C.; Meldal, M. *J. Org. Chem*. **2002**, *67,* 3057–3064.

Sharpless and Morten Meldal, along with Carolyn R. Bertozzi, were recently awarded with the Nobel Prize in Chemistry *for the development of click chemistry and bioorthogonal chemistry*. On the other hand, Fokin's group[137] found that the 1,5-disubstituted isomers can be obtained *via* Ru(II) catalysis (RuAAC). However, the regioselectivity and the efficiency of the transformation are slightly lower compared to CuAAC. The advances in these two catalytic methodologies enabled the individual synthesis of both compounds (**Scheme 4. 1**), starting from the same substrates, and allowed for structural as well as biomedical studies.

Scheme 4. 1. General synthetic strategies towards disubstituted 1,2,3-triazoles.

Additionally, it is important to note that, 1,2,3-triazoles, possessing several donor sites, can act as versatile ligands for metal coordination.[138] Interestingly, these heterocycles can perform the role of sensors for both anions and cations following different binding mechanisms.[139,140] The N2 and N3 atoms are able to participate in the selective recognition of various metal cations, while the C5–H···anions electrostatic interaction enables the anions' sensing.[141]

4.1.2. Peptidomimetics *via* Copper Catalyzed-Azide-Alkyne-Cycloaddition

Able to mimic the amide bond triazoles have an important role in peptidomimetic chemistry.[142] Due to the high dipole moment, the triazole moiety can align with that of other amide bonds and therefore stabilize the secondary structure of peptides.[143] Moreover, the aromatic heterocycle can participate in intra- and intermolecular π-interactions.[144] Compared with the amide bond, it is characterized by increased rigidity owing to its aromatic ring

[137] Boren, B. C.; Narayan, S.; Rasmussen, L. K.; Zhao, H.; Lin, Z.; Jia, G.; Fokin, V. V. *J. Am. Chem. Soc.,* **2008**, *130,* 8923– 8930.
[138] Moore, D.S.; Robinson, S.D. *Adv. Inorg. Chem*. **1988**, *32*, 171–239.
[139] Peng, R.; Xu, Y.; Cao, Q. *Chin. Chem. Lett.* **2018,** *29,* 1465–1474.
[140] Hua, Y.; Flood, A. H. *Chem. Soc. Rev.* **2010,** *39,* 1262–1271.
[141] Shad, M.S.; Santhini, P.V.; Dehaen, W. *Beilstein J. Org. Chem.* **2019,** *15,* 2142–2155.
[142] Staskiewicz, A.; Ledwon, P.; Rovero, P.; Papini, A.M.; Latajka, R. *Front. Chem*. **2021**, *9*, 674705.
[143] Massarotti, A.; Aprile, S.; Mercalli, V.; DelGrosso, E.; Grosa, G.; Sorba, G.; Tron, G.C. *Chem. Med. Chem.* **2014**, *9*, 2497–2508.
[144] Schulze, B.; Schubert, U.S. *Chem. Soc. Rev.* **2014**, *43*, 2522–2571.

structure. All these properties combined with stability to enzymatic cleavage, acid/base hydrolysis, and reductive or oxidative conditions, make disubstituted 1,2,3-triazoles the ideal mimetics of peptide bond.[145]

Over the past years, the CuAAC reaction has gained a considerable interest in the field of peptidomimetic chemistry since it can be applied in the design and synthesis of biomimetic oligomers in several different ways. It is a valuable tool for cyclisation reactions (head-to-tail, head/tail-to-sidechain, or sidechain-to-sidechain),[146,147,148] disulfide bridge substitution,[149] ligation of peptide fragments, and finally, for bioconjugation to other molecules.[150] The insertion of the triazole moiety into the peptide chain can be readily accomplished in both solution and on solid phase as illustrated in **Scheme 4. 2**.[151]

In particular, the CuAAC reaction can be carried out in solution between an *N*-protected α-amino alkyne and an α-azido carboxylic acid resulting in a triazole-containing dipeptide building block, ready to be used in solid-phase synthesis (**Scheme 4. 2a**). As an alternative, the reaction can be performed directly on solid phase, by the on-resin transformation of protected *N*-terminal amine into an azide, followed by a cycloaddition reaction with a protected α-amino alkyne in the presence of Cu(I) salt (**Scheme 4. 2b**). As mentioned before, CuAAC can be applied as well to ligate two longer peptide chains with an azide- and an alkyne-terminus, respectively (**Scheme 4. 2c**). Finally, the click reaction can be employed for the cyclisation step, leading to the formation of triazole-containing macrocyclic or polycyclic peptides (**Scheme 4. 2d**).

[145] Prasher, P.; Sharma, M. *Med. Chem. Comm.* **2019**, *10*, 1302–1328.
[146] Testa, C.; Papini, A.M.; Chorev, M.; Rovero, P. *Curr Top Med Chem*. **2018**, *18*, 591-610.
[147] Le Chevalier Isaad, A.; Papini, A.M.; Chorevc, M.; Rovero, P. *J. Pept. Sci*. **2009**, *15*, 451 – 454.
[148] D'Ercole, A.; Sabatino, G.; Paci, L.; Impresari, E.; Capecchi, I.; Papini, A.M.; Rovero, P. *Pept Sci*. **2020**, e24159.
[149] Testa, C.; D'Ursi, A.M.; Bernhard, C.; Denat, F.; Bello, C.; D'Addona, D.; Scrima, M.; Tedeschi, A.M.; Rovero, P.; Chorev, M.; Papini, A.M. *Peptide Science*. **2018**, e24071.
[150] Li, H.; Aneja, R.; Chaiken, I. *Molecules* **2013**, *18*, 9797–9817.
[151] Recnik, L.M.; Kandioller, W.; Mindt, T.L**.** *Molecules* **2020**, *25*, 3576.

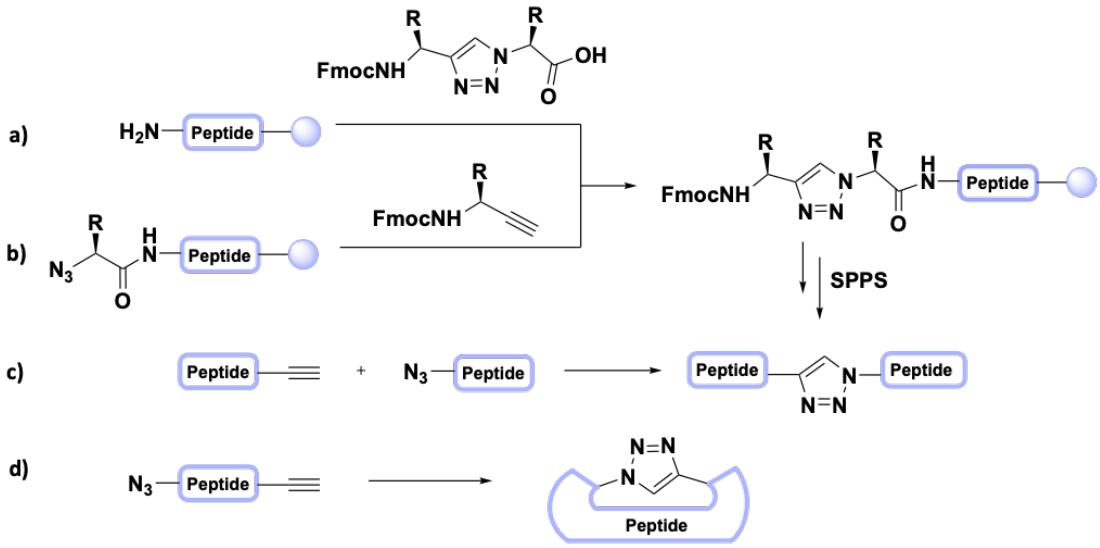

Scheme 4. 2. Different synthetic routes towards triazolo-peptidomimetics.

The importance of CuAAC in chemical ligation is also relevant for biologically active amide-containing small molecules, which are prone to hydrolysis and often characterized by a non-specific recognition. The amide-to-triazole replacement is usually studied in the context of compounds with amide bonds known to be responsible for biological activity. For instance, this methodology has been applied in the connection of two small molecules which led to the formation of molecules mimicking the HIV-1 protease inhibitor amprenavir (**Figure 4. 2a**).[152] Diverse lead compounds resulted from this research, among them AB2 (**Figure 4. 2b**) demonstrating biological activity against HIV-1 protease. The study showed that the triazole ring of AB2 is positioned in the site normally occupied by the amide residue of amprenavir, bound to the enzyme active site. Moreover, the crystallographic analysis revealed that the triazole's central nitrogen atom was located appropriately to participate in hydrogen bonding with the water molecule found in the active site of the enzyme. The outcome of this work demonstrated that the CuAAC reaction can be applied to create efficient biologically active compound *via* a simple ligation, and that disubstituted 1,2,3-traizoles can be employed successfully as isosteres for biochemically relevant amide bonds.

[152] Brik, A.; Alexandratos, J.; Lin, Y. C.; Elder, J. H.; Olson, A. J.; Wlodawer, A.; Goodsell, D. S.; Wong, C. H. *Chem. Bio. Chem*. **2005**, *6*, 1167–1169.

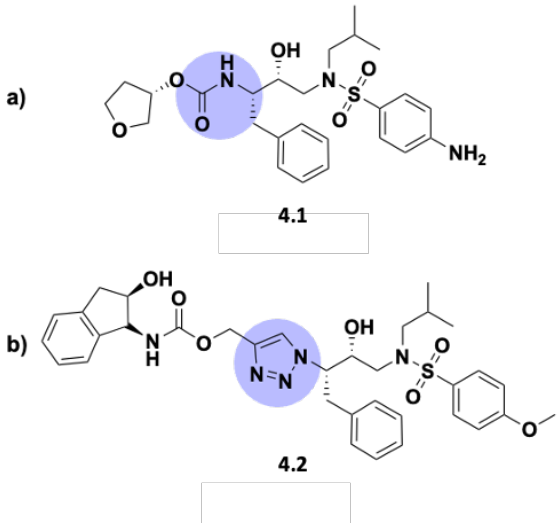

Figure 4. 2. Comparison of HIV protease inhibitor amprenavir **4.1** (containing hydrolytically labile amide bond) with lead compound AB2 **4.2** (containing stable triazole linkage) structures.

Recent studies show that the 1,2,3-triazole linkage can play an important role also in the formation of peptidomimetic foldamers (oligomers able to adopt stable secondary structures reinforced by non-covalent interactions).[153] For instance, the Ghadiri group has proved that triazole moiety can be employed to supersede dimeric peptide sequences in well-defined α-helical oligomers with marginal effect on the global secondary structure.[124] In particular, the authors substituted dipeptide sequences of GCN4 (a known α-helical peptide known for forming coiled-coil bundles) with triazole-isobutyl amino acids and demonstrated conservation of helical bundle organization (**Figure 4. 3**).

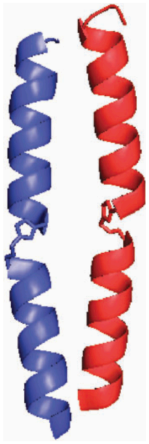

Figure 4. 3. Representation of triazole-containing peptide helices. Triazole linkages occur as elements of the main chain sequence about halfway through the helical structure. (For clarity, only two strands of the four-helix bundle are shown)[124]

[153] Holub, J.M.; Kirshenbaum, K. *Chem. Soc. Rev*. **2010**, *39*, 1325–1337

Another example worth quoting are the "triazolamers" (triazole-based oligomers in which up to four monomers are interconnected through a series of heterocyclic rings) developed by the Arora group.[154] These foldamers constitute a peculiar type of peptidomimetics as they do not possess any traditional peptide bond. Structural analysis of these compounds demonstrated that they tend to fold into "zig-zag" conformations with neighboring triazole dipoles pointing in opposite orientations. Moreover, the overall chirality of the peptidomimetic skeleton is retained when compared with similar α-peptide sequences (**Figure 4. 4**).

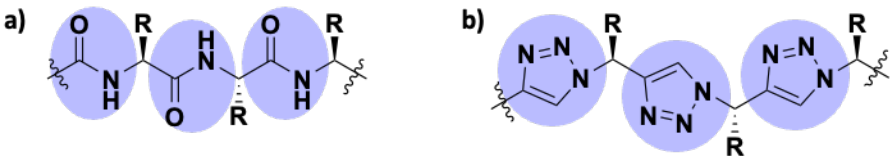

Figure 4. 4. Comparison of (a) *α*-peptide and (b) triazolamer structures.

Triazoles have been applied also in the development of β-turn mimetics (short peptide sequences, typically containing -Gly-Pro- units, able to invert the direction of a peptide backbone). The β-turns constitute frequent structural element of various protein-protein interfaces, rendering them an attractive synthetic target for therapeutics. The geometric features of triazole rings make them potentially compatible with structural characteristics of the -Gly-Pro- motif in some β-turns. In fact, the CuAAC reaction has been used to conjugate two peptide chains containing terminal azides and alkynes in order to obtain β-turn mimics.[125] The study showed that the presence of three-carbon aliphatic linkers on both sides of the heterocycle (**Figure 4. 5b**) is optimal to guarantee the appropriate folding.

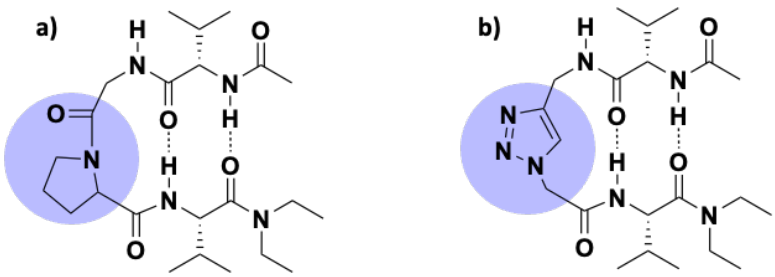

Figure 4. 5. Comparison of a) peptide β-turn and b) triazole β-turn structures[125]

[154] Angelo, N. G.; Arora, P. S. *J. Am. Chem. Soc*. **2005**, *127*, 17134–17135.

Macrocyclization of bioactive oligomers helps to pre-organize their structure, furnishing higher conformational stability, and enhanced proteolytic resistance. There are numerous synthetic ways to afford macrocyclic peptides and their mimics. Lately, the CuAAC reaction is gaining attention as a powerful cyclization method. For instance, cyclic peptide-based tyrosinase inhibitors involving Tyr-Pro-Val-Pro sequences are highly challenging to obtain due to a troublesome ring formation step. To overcome this problem, the Maarseveen's group synthesized a linear tetrapeptide with an analogous sequence, containing a *N*-terminus azide and alkyne-functionalized *C*-terminus.[155] Interestingly, the CuAAC-derived macrocycle (**Figure 4. 6b**) showed three times higher tyrosinase inhibitory activity, compared to the natural peptide (**Figure 4. 6a**).

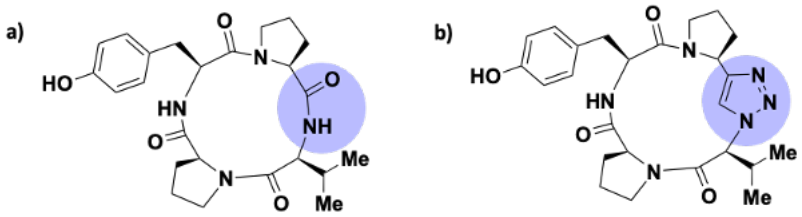

4.3 4.4

Figure 4. 6. Macrocyclic Tyr-Pro-Val-Pro tyrosinase inhibitors with (a) amide and (b) triazole.

The benefits of CuAAC chemistry have been explored also in the peptoid chemistry. For example, Izzo and Compain groups, employed cyclic *N*-propargyl α-peptoids of different sizes as molecular platforms to obtain a series of iminosugar clusters with different valency and alkyl spacer lengths *via* CuAAC reactions (**Figure 4. 7**).[156] Investigation of these molecules as *α*-mannosidase inhibitors led to notable multivalent effects and revealed the crucial importance of scaffold for binding affinity improvements.

[155] Bock, V.D.; Speijer, D.; Hiemstra, H.; Van Maarseveen, J.H. *Org. Biomol. Chem*. **2007,** *5*, 971–975.
[156] Lepage, M. L.; Meli, A.; Bodlenne, A.; Tarnus, C.; De Riccardis, F.; Izzo, I.; Compain, P. *Beilstein J. Org. Chem.* **2014**, *10*, 1406-1412.

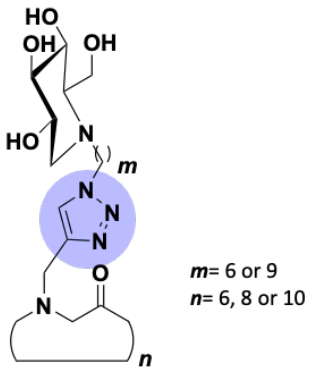

Figure 4. 7. Schematic representation of cyclopeptoid-based glycosidase inhibitors.

4.1.3. *Extended* cyclic peptoids

Within the last few years peptoids have emerged as a significant class of synthetically accessible hetero-oligomers and "foldamers". The sub-monomer method developed by Zuckermann, allows an access to a nearly unlimited variety of functionalized oligoamides due to the commercially available amines.[157] This approach has been successfully adopted for the creation of peptoid libraries,[158] thus demonstrating remarkable versatility in the introduction of a diverse range of amines. Accordingly, most of the research has been centered on modifications of the nucleophilic displacement step, while the haloacetic part was rather under-explored. However, the potential tunability of this component prompted scientists to explore the field, consequently leading to the emergence of a novel class of macromolecules called "extended peptoids" (oligomers based on aromatic building blocks).[159] The skeletons of new peptoid oligomers are "stretched" by aromatic spacers, providing generally higher rigidity of the backbone in relation to regular peptoids, which can be further increased by the macrocyclization.

The first macrocyclic representatives of extended peptoids family were introduced by Hjelmgaard, Faure *et al.* as macrocyclic arylopeptoids (cyclic *N*-alkylated aminomethyl

[157] Uno, T.; Beausoleil, E.; Goldsmith, R. A.; Levine, B. H.; Zuckermann, R. N. *Tetrahedron Lett.* **1999**, *40,* 1475–1478.
[158] Alluri, P. G.; Reddy, M. M.; Bachhawat-Sikder, K.; Olivos, H. J.; Kodadek, T. *J. Am. Chem. Soc*. **2003**, 125, 13995–14004.
[159] Combs, D. J.; Lokey, R. S. *Tetrahedron Lett.* **2007**, *48*, 2679–2682.

benzamides, **Figure 4. 8a**) in 2014.[160] The backbone of these peptoid-like oligomers is extended by the presence of a phenyl ring. The authors reported the efficient synthetic methodology towards *ortho*-, *meta*-, and *para*-arylopeptoids relied on sub-monomer approach and demonstrated the potential of the new class of macrocycles. Their subsequent studies expanded the arylopeptoid space with some cyclic oligomers composed of mixed *ortho*-, *para*-, and *meta*-arylopeptoid residues.[161] The study confirmed the efficacy of this modular design leading to topologically defined macrocycles, able to adopt sequence-dependent shapes (even with the lack of intramolecular H-bonding).[162]

Even though macrocyclic arylopeptoids are characterized by the excellent conformational properties, their preliminary cation binding studies revealed poor complexing capacities.[161] However, De Riccardis group demonstrated that the extension of the peptoid backbone by another methylene unit can improve the chelating abilities.[163] Due to this structural modification, a new class of extended macrocyclic peptoids has emerged: cyclic benzylopeptoids (**Figure 4. 8b**). The preparation of these novel macrocycles consists in monomer synthesis, solid-phase oligomerization, and cyclization. The authors described an efficient synthetic protocol towards different-sized macrocyles and evaluated their complexing capacities in the presence of sodium cations. The study revealed that macrocyclic benzylopeptoids composed of rigid units can form stable metal complexes of distinguished symmetry. These results have put the light on the potential application of macrocyclic extended peptoids in ion recognition, transmembrane transport, or catalysis.

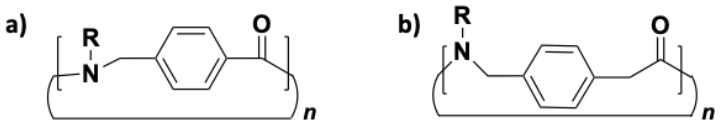

Figure 4. 8. Schematic structures of (a) cyclic arylopeptoids and (b) cyclic benzylopeptoids.

[160] Hjelmgaard, T.; Roy, O.; Nauton, L.; El-Ghozzi, M.; Avignant, D.; Didierjean, C.; Taillefumier, C.; Faure, S. *Chem. Commun.* **2014**, *50*, 3564− 3567.
[161] Hjelmgaard, T.; Nauton, L.; De Riccardis, F.; Jouffret, L.; Faure, S. *Org. Lett.* **2018**, *20*, 268−271.
[162] Hayakawa, M.; Ohsawa, A.; Takeda, K.; Torii, R.; Kitamura, Y.; Katagiri, H.; Ikeda, M. *Org. Biomol. Chem.* **2018**, *16*, 8505−8512.
[163] Meli, A.; Macedi, E.; De Riccardis, F.; Smith, V. J.; Barbour, L. J.; Izzo, I.; Tedesco, C. *Angew. Chem., Int. Ed.* **2016**, *55*, 4679−4682.

4.1.4. Research targets

Considering the versatility and broad synthetic potential of the "sub-monomeric" solid-phase approach and CuAAC chemistry, we decided to join their forces in developing new oligoamide-based macrocycles and further exploring the cyclopeptoid space.

Firstly, we focused our attention on the development of a new family of macrocyclic “extended peptoids”. The broad structural adaptability of peptoids’ synthesis enables introduction of aromatic spacers into their oligomeric sequence which potentially broadens the chemical space of the emerging “extended peptoids”. Among potential structural motives, that can be introduced into the peptoid backbone, heterocyclic triazoles wade into primacy due to their amide bond mimicry and coordination abilities, which can further enrich the well-known complexation capacities of cyclic peptoids. Implementation of these considerations led us to the elaboration of cyclic triazolopeptoids (**Figure 4. 9**).

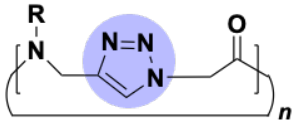

Figure 4. 9. Schematic structure of macrocyclic triazolopeptoids.

Subsequently, we broadened our studies on these novel macrocyclic systems by synthesizing derivatives with chiral side chains. Moreover, we investigated the reduction of backbone tertiary amides of cyclic triazolopeptoids,[164] which led us to obtain triazole-containing peraza-macrocycles demonstrating complexing capabilities.

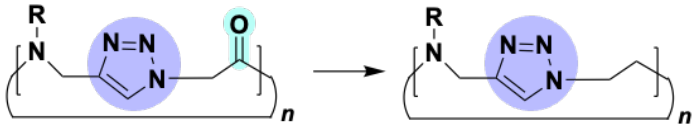

Scheme 4. 3. Schematic representation of backbone amide reduction in macrocyclic triazolopeptoids.

[164] Schettini, R.; D’Amato, A.; Pierri, G.; Tedesco, C.; Della Sala, G.; Motta, O.; Izzo, I.; De Riccardis, F. *Org. Lett.* **2019**, *21*, 7365-7369.

Another objective consisted in the CuAAC-mediated synthesis of tetrameric and hexameric cyclopeptoid systems containing polar side chains. The project sees as a key reaction a Huisgen 1,3-dipolar cycloaddition between cyclopeptoid derivatives containing *N*-propargyl side chains and suitably synthesized polar azides (**Scheme 4. 4**). The introduction of polar functionalities, in principle, can expand complexing potential of cyclic peptiods. Moreover, the versatile approach based on triazole-mediated pendant-arm conjugation, opens new perspectives in the context of the straightforward functionalization of peptoid macrocycles.

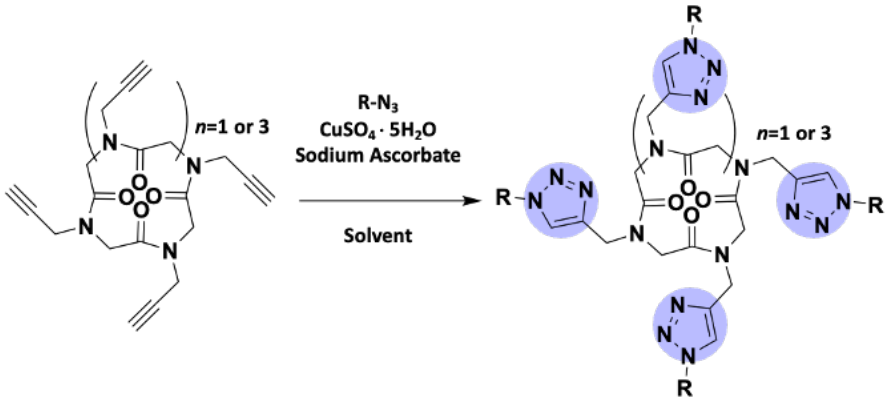

Scheme 4. 4. Schematic representation of CuAAC-mediated synthesis of new polar cyclic peptoids.

4.2. Cyclic triazolopeptoids

4.2.1. Results and discussion

4.2.1.1 Synthesis of new "extended" macrocyclic peptoids

The synthesis of linear triazolopeptoids was accomplished by taking advantage of the submonomer-based approach[165] on the solid phase. The submonomers, azidoacetic acid **4.5**[166] and *N*-benzylpropargyl amine **4.6**,[167] were prepared in solution in high yields. Importantly, the reductive amination,[167] yielding propargyl-armed **4.6**, demonstrates the potential of this synthetic method, which generally can produce diversely decorated macrocyles. **Scheme 4. 5** illustrates the synthetic pathway towards triazolopeptoids **4.9**-**4.11**.

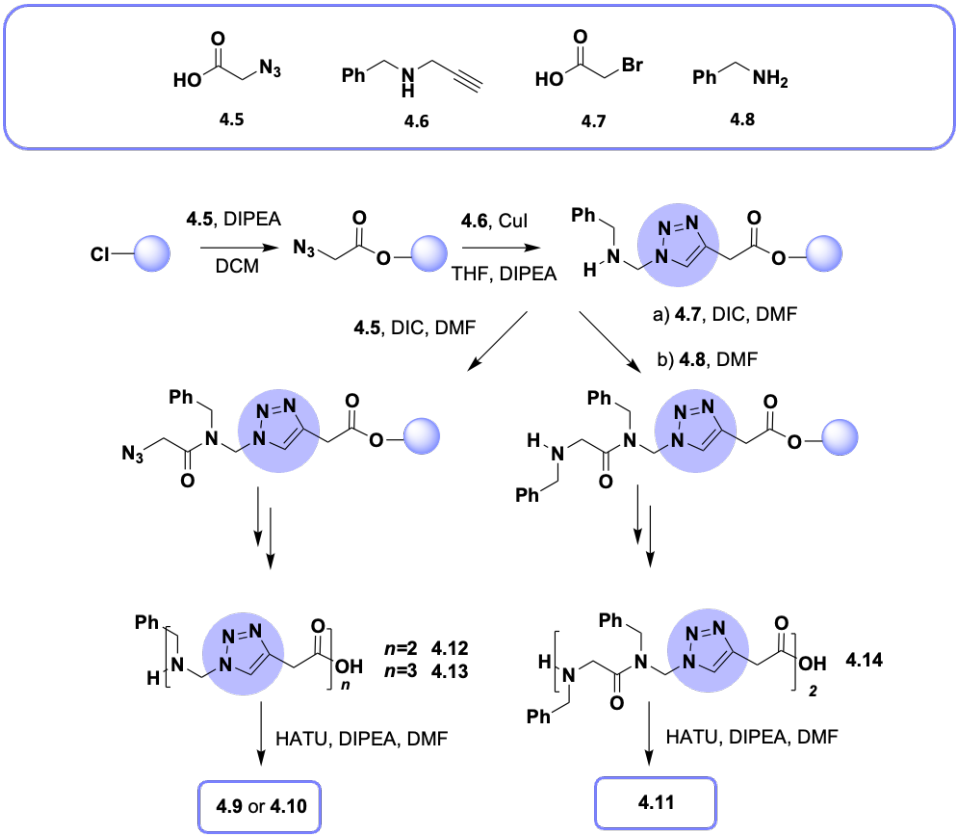

Scheme 4. 5. Synthetic route towards macrocyclic triazolopeptoids.

[165] Zuckermann, R.N.; Kerr, J.M.; Kent, S.B.H.; Moos, W.H. *J. Am. Chem. Soc.* **1992**, *114*, 10646–10647.
[166] Althuon, D.; Rönicke, F.; Fürniss, D.; Quan, J.; Wellhöfer, I.; Jung, N.; Schepers, U.; Bräse, S. *Org. Biomol. Chem.* **2015**, *13*, 4226–4230.
[167] Chang, Z.; Jing, X.; He, C.; Liu, X.; Duan, C. *ACS Catal.* **2018**, *8*, 1384–1391.

Specifically, after the first sub-monomer **4.5** had been loaded, the (3+2) Cu(I)-catalyzed cycloaddition reaction smoothly provided the first "extended" monomer on resin. This was subjected to acylation with azidoacetic acid **4.5** or bromoacetic acid **4.7**, depending on the target sequence. Iteration of cycloaddition/acylation steps provided in the first case (after the cleavage from the resin with HFIP 20% in DCM) the desired linear precursors **4.12** and **4.13** in quantitative yield. On the other hand, the addition of *N*-benzyl glycine and iteration of the synthetic steps produced linear precursor **4.14** also in quantitative yield. Subsequent HATU-induced macrocyclization under high-dilution conditions afforded target marcocyles **4.9**-**4.11** in 34%, 28%, and 24% yields, respectively.

4.2.1.2 Structural analysis of cyclic triazolopeptoids

The spectral analysis (^{1}H and ^{13}C NMR) of cyclodimer **4.9** revealed the presence of a conformationally stable symmetric compound[168] (**Figure 4. 10**). The presence of tertiary amides in cyclic oligomers is known to trigger the coexistence of multiple conformations in slow equilibrium on the NMR time scale. Whilst smaller cyclic trimeric and tetrameric peptoids show up as single conformers (on the NMR time scale), larger macrocycles (e.g., hexamers) display multiple conformations due to the limited n → π* orbital contacts[168] and weaker geometric constraints.

[168] For the definition of "conformationally stable": D'Amato, A.; Schettini, R.; Della Sala, G.; Costabile, C.; Tedesco, C.; Izzo, I.; De Riccardis, F. *Org. Biomol. Chem.* **2017**, *15*, 9932−9942.

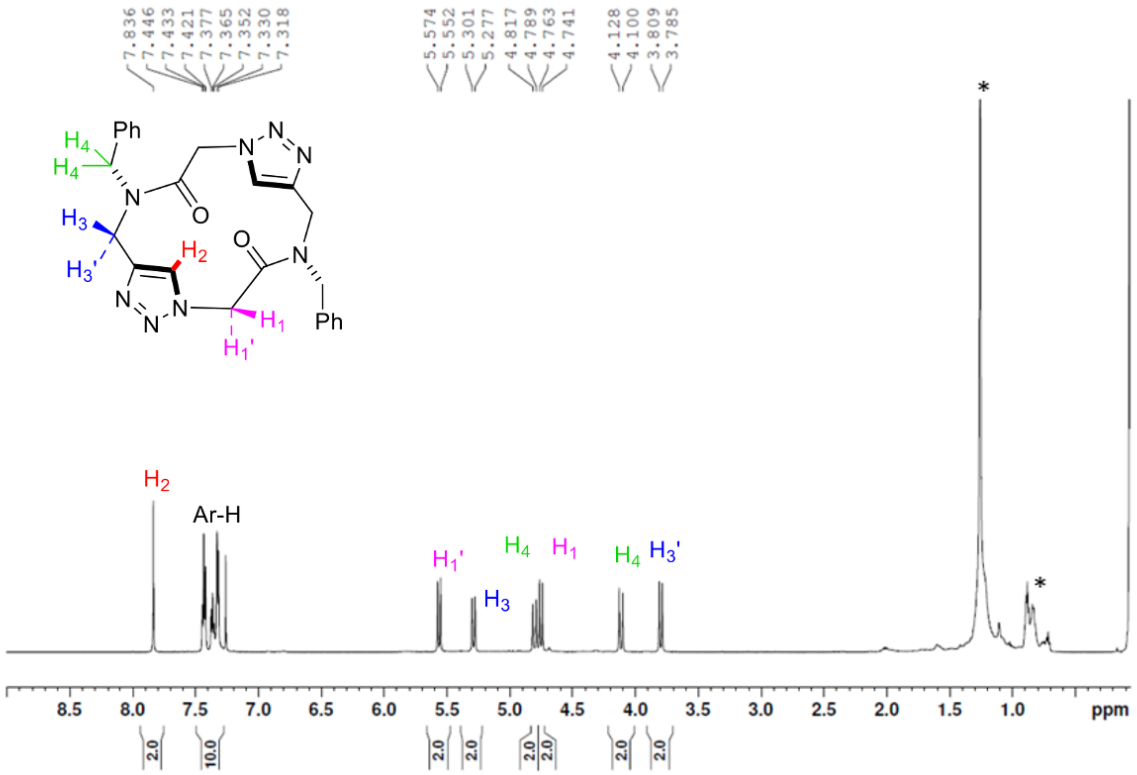

Figure 4. 10. ^{1}H NMR spectra (600 MHz, $CDCl_3$) of cyclic dimer **4.9**. Water and lipid impurities are labelled with asterisks.

To comprehend the structure of the compound **4.9** as well as the interactions stabilizing its backbone, computational studies were performed.[169] In accordance with the 2-fold symmetry disclosed through the NMR spectra, cyclodimer **4.9** could potentially adopt a C_2- or S_2-symmetric all-*trans* or all-*cis* conformation (**Figure 4. 11**, **Table 4. 1**).

[169] DFT calculations were performed by prof. C. Costabile, Dpt. of Chemistry and Biology "A. Zambelli", Univ. of Salerno.

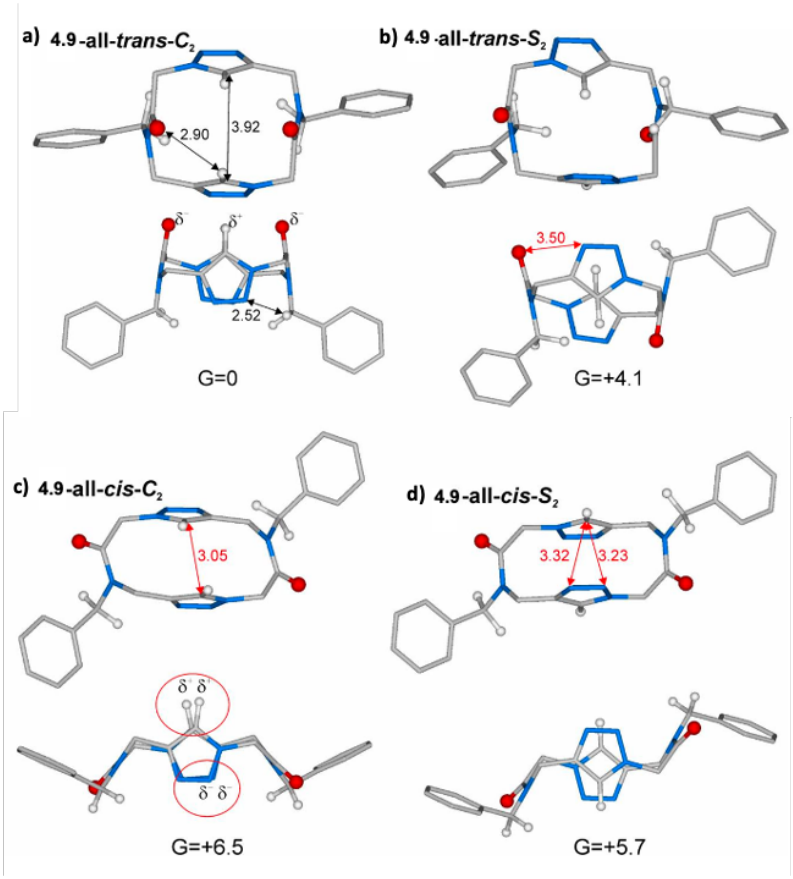

Figure 4. 11. Top and side view of minimum energies structures of all-*trans* S_2 or C_2 conformations and all-*cis* S_2 or C_2 conformations of cyclic dimer **4.9**. Free energies, calculated in $CHCl_3$ at the BP84/TZVP level, are in kcal/mol. Distances are in Å (in red distances of repulsive interactions and in black distances of attractive or non-repulsive interactions). Non-relevant hydrogens were omitted for clarity.

	E(gas)	G(gas)	E($CHCl_3$)	G($CHCl_3$)
4.9-all-*trans*-C_2	0	0	0	0
4.9-all-*trans*-S_2	7.4	6.2	5.2	4.1
4.9-all-*cis*-C_2	13.1	11.1	8.5	6.6
4.9-all-*cis*-S_2	10.8	8.7	7.8	5.7

Table 4. 1. Internal (E) and free energies (G) of minimum energy structures of **4.9** in gas phase and $CHCl_3$.

DFT calculations at the BP86/TZVP level revealed that the all-*trans* C_2-symmetric conformer (**Figure 4. 11a**) is the most stable structure (the S_2-symmetric all-*trans* and the C_2- and S_2-symmetric all-*cis* conformers demonstrated ΔG values that were 4.1, 6.5, and 5.7 kcal/mol higher, respectively, compared to that of the all-*trans* C_2-symmetric conformer).

Specifically, in the "square" all-*trans* C_2-symmetric conformation, the two triazoles act as H-bond acceptors of the CH_2 benzyl side chains and as carbonyl H-bond donors (**Figure 4. 11a**). This interaction explained the CH triazole ^{1}H NMR downfield shift (7.84 ppm).[170] The assignment was additionally confirmed by a ROESY experiment (**Figure 4. 12**) that revealed, on one hand, cross-peaks between triazole proton H_2 at 7.84 ppm and β protons H_3 and H_1 and, on the other hand, correlations between the *ortho* protons of aromatic rings and *α* protons $H_{1'}$ and $H_{3'}$ (**Figure 4. 12**).

Figure 4. 12. ROESY NMR (600 MHz, $CDCl_3$) of cyclic dimer **4.9**.

Moreover, the backbone conformation of the most stable conformer strictly reminds the analogous bis-triazole cyclic peptide observed previously by Ghadiri et al (**Figure 4. 13**).[171]

[170] Corredor, M.; Bujons, J.; Messeguer, A.; Alfonso, I. *Org. Biomol. Chem.* **2013**, *11*, 7318−7325.
[171] Beierle, J. M.; Horne, W. S.; van Maarseveen, J. H.; Waser, B.; Reubi, J. C.; Ghadiri, M. R. *Angew. Chem., Int. Ed.* **2009,** *48*, 4725−4729.

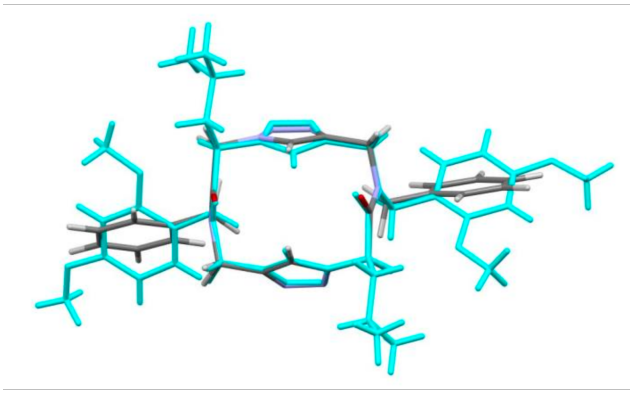

Figure 4. 13. Backbone atoms overlay between the most stable conformer of **4.9** and the analogous bis-triazole cyclic peptide obtained by Ghadiri and co-workers (cyan, CSD code SURWUY).[171] RMSD is 0.163 Å.

The C_2-symmetry suggested the presence of two enantiomorphous conformational isomers[168] (**Figure 4. 14**), which may be interconverted by contemporaneous inversion of the two amide bonds and triazole rings. As has been demonstrated for cyclic peptoids,[168] the coexistence of two conformational enantiomers can be revealed by ^{1}H NMR, using a chiral solvating agent in order to form diastereomeric supramolecular complexes.[168] Gradual addition of Pirkle's reagent [(*R*)-1-(9-anthryl)-2,2,2-trifluoroethanol] to a racemic solution of **4.9a** and **4.9b** in deuterated chloroform caused the splitting of most proton resonances (**Figure 4. 15b**, **c**).

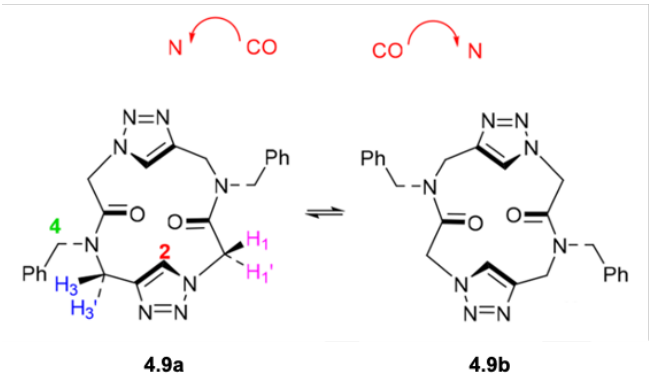

Figure 4. 14. Conformational enantiomers of cyclodimer **4.9**.

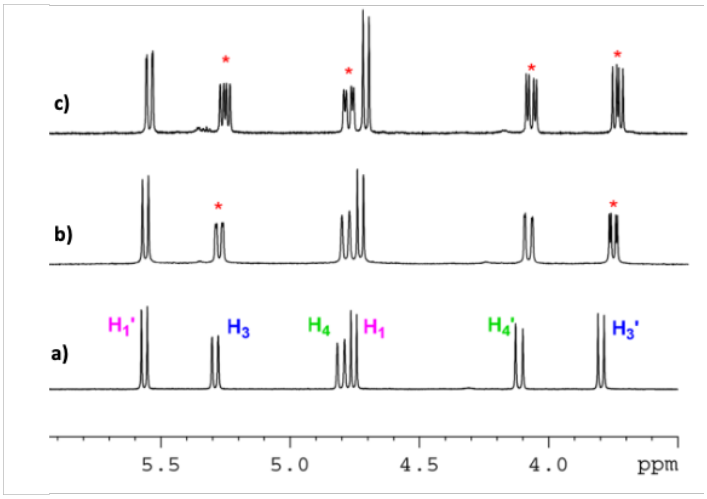

Figure 4. 15. (a) Expansion of **4.9** ^{1}H NMR spectrum (600 MHz, $CDCl_3$, 298 K, 8.0 mM solution). Quantitative stepwise addition of 1.0 (b) and 3.0 equivalents (c) of Pirkle's alcohol to conformational enantiomers **4.9a** and **4.9b**. Red asterisks denote split signals.

Variable temperature NMR (VT NMR) experiments in $C_2D_2Cl_4$ demonstrated the stability of the conformers up to 373 K (**Figure 4. 16**).

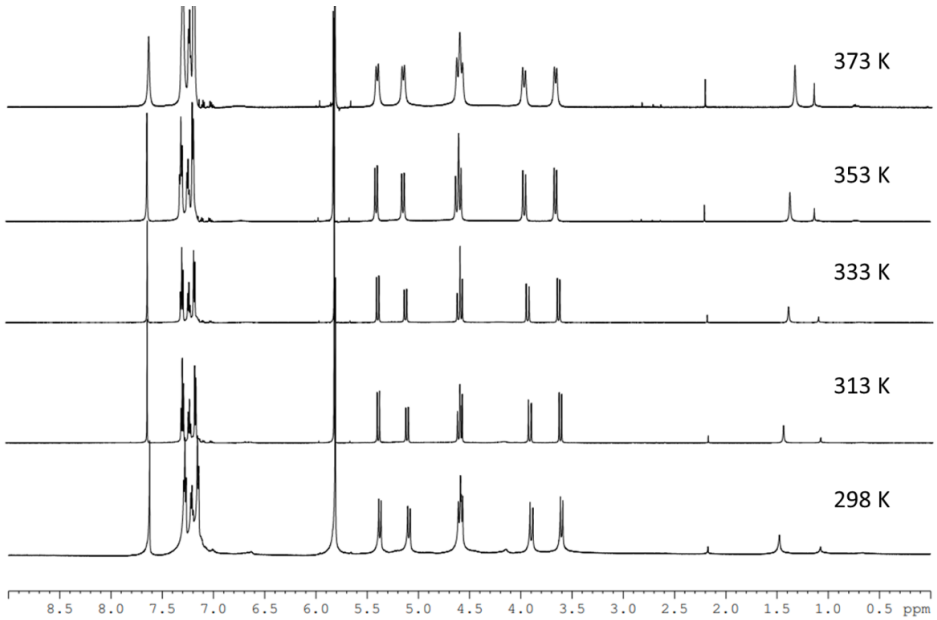

Figure 4. 16. Variable temperature 1H NMR spectra of compound **4.9** (600 MHz, $C_2D_2Cl_4$, 5.0 mM solution).

^{1}H and ^{13}C NMR analysis of cyclotrimer **4.10** and cyclic tetraamide **4.11** have suggested, analogously to hexameric cyclic peptoids, similar in size, the contemporaneous presence of diverse conformers in slow equilibrium on the NMR time scale. Their identity has been proven

by HR-MS and further confirmed by VT NMR in DMSO and $C_2D_2Cl_4$ solutions (**Figure 4. 17**, **Figure 4. 18**) with simplification of the NMR spectra into a set of broad singlets (*T* = 373 K).

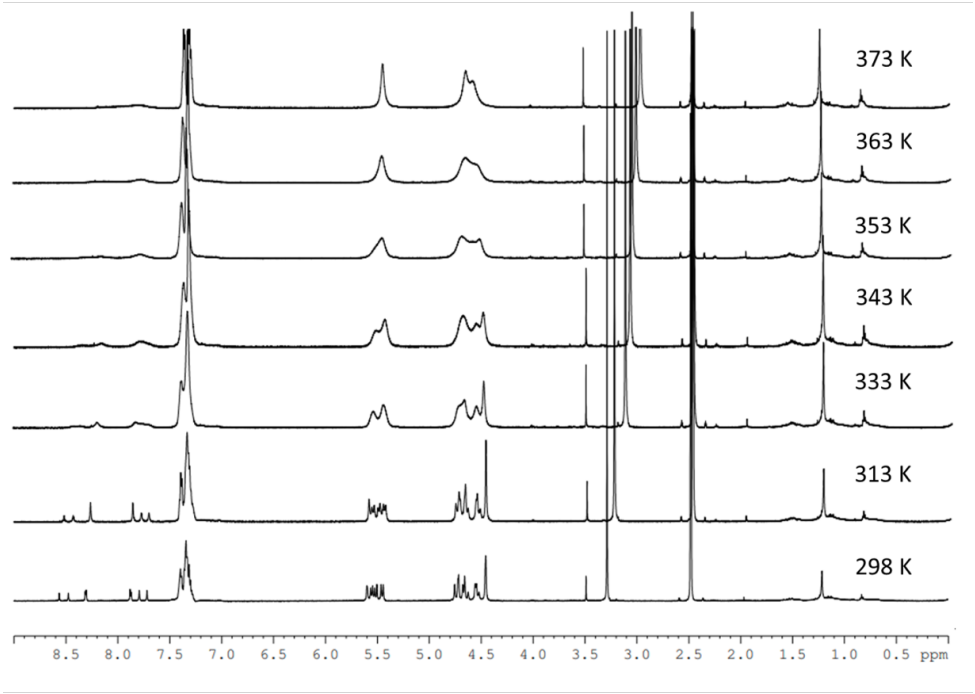

Figure 4. 17. Variable temperature ^{1}H NMR spectra of compound **4.10** (600 MHz, DMSO, 5.0 mM solution).

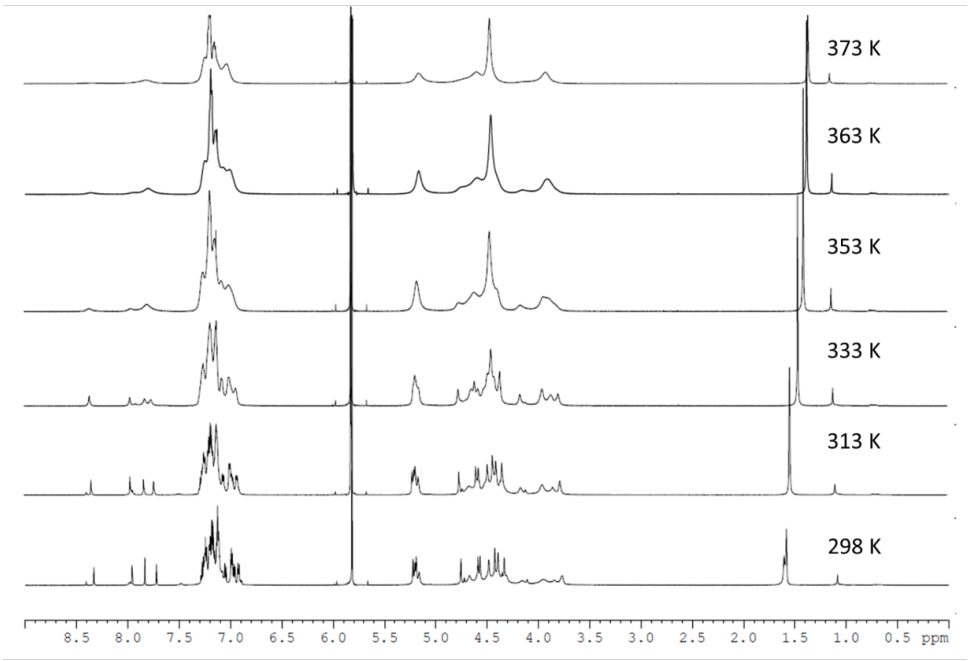

Figure 4. 18. Variable temperature ^{1}H NMR spectra of compound **4.11** (600 MHz, $C_2D_2Cl_4$, 5.0 mM solution).

Gratifyingly, the 20-membered triazolopeptoid **4.11** gave single crystals adequate for X-ray diffraction analysis (obtained by slow evaporation from an acetonitrile solution).[172] In the solid state, the macrocycle **4.11** displays crystallographic inversion symmetry with the tertiary amide bonds in the *trans* geometry (**Figure 4. 19**).

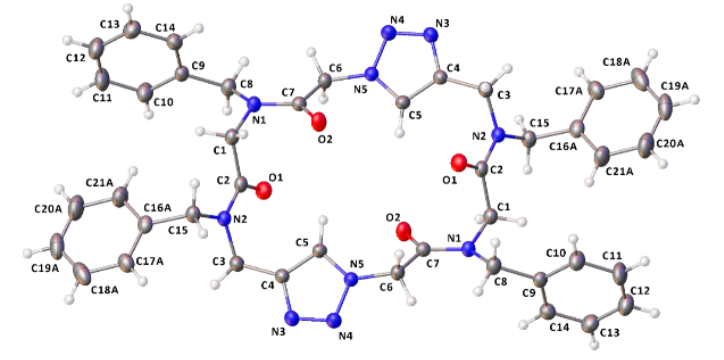

Figure 4. 19. ORTEP drawing for compound **4.11**. Atom types: C grey, O red, N blue, H white. For clarity, only the atoms with the highest occupancy factor are shown.

The structure of **4.11** is characterized by a flat shape, with the side chains positioned in a horizontal manner in relation to the macrocyclic plane. Reciprocal carbonyl-carbonyl interactions [173,174] (**Figure 4. 20**) are related with the short distances between the carbonyl groups (<3.22 Å) and O···C=O angles of 88.8(1)° and 81.5(1)° (**Table 4. 2**).

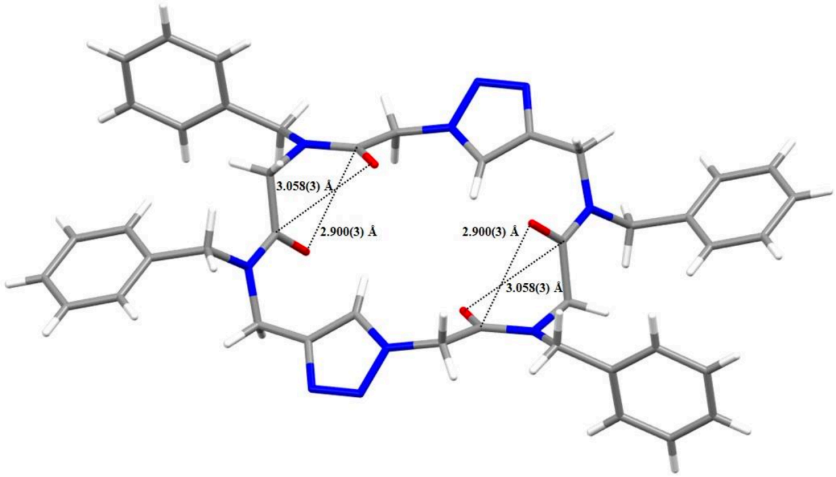

Figure 4. 20. Reciprocal CO···CO interactions in **4.11**, as shown by CO···CO distances below 3.22 Å. For clarity, only the atoms with the highest occupancy factor are shown.

[172] X-ray analyses were performed by dr. Giovanni Pierri and prof. Consiglia Tedesco, Dpt. of Chemistry and Biology "A. Zambelli", Univ. of Salerno.
[173] Newberry, R. W.; Raines, R. T. *Acc. Chem. Res.* **2017**, *50*, 1838−1846.
[174] Rahim, A.; Saha, P.; Jha, K. K.; Sukumar, N.; Sarma, B. K. *Nat. Commun.* **2017**, *8*, 78−90.

O1···C7 (d_1) (Å)	O2···C2 (d_2) (Å)	O1···C7-O2 (θ_1) (°)	O2···C2-O1 (θ_2) (°)
2.900(3)	3.058(3)	88.8(1)	81.5(1)

Table 4. 2. CO···CO distances and corresponding θ angles for macrocycle **4.11**.

In the solid state, molecules of **4.11** are aligned along the shortest *b* axis through hydrogen bonds which involves N4 of the triazole ring and the methylene hydrogen atom of the backbone (**Figure 4. 21**). This leads to an amphiphilic layered structure, where the backbone atoms establish the hydrophilic region and on the other hand, the benzyl side chains create the hydrophobic region. Lastly, the interlayer interactions are predominantly characterized by hydrophobic interactions and H−H contacts concerning the aromatic side chains. Interestingly, the peptide analogue of compound **4.11** (CSD code OKECUC), reported by Ghadiri et al.,[175] exhibited an entirely distinct macrocycle conformation with the triazole rings perpendicular to the plane of the macrocycle, exhibiting the tubular assembly of the macrocycles with ethanol molecules capped in the peptide nanotube.

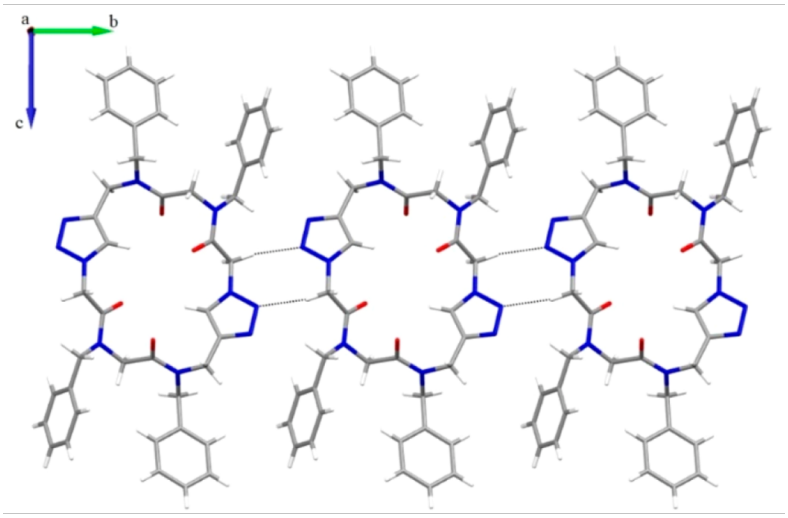

Figure 4. 21. H-Bonded ribbon of **4.11** along the shortest *b* axis (as viewed along the *a* axis). H-Bonds are depicted as black dotted lines.

[175] Horne, W. S.; Stout, C. D.; Ghadiri, M. R. A Heterocyclic Peptide Nanotube. *J. Am. Chem. Soc.* **2003**, *125*, 9372–9376.

4.2.2. Conclusions

In this work we reported a synthetic route towards first representatives of a new class of macrocyclic "extended peptoids". The characterization of backbone conformations of the cyclodimer **4.9** and macrocyclic tetraamide **4.11** were substantiated by computational investigations, NMR data and X-ray diffraction studies. The versatility of linear precursors' synthesis can potentially lead to a variety of sequence-defined oligomeric macrocycles of different sizes, containing 1,2,3-triazole spacers and decorated with diversified side chains. Importantly, the combination of the complexation capabilities of the cyclopeptoids with the unique coordination attitude of triazole rings has provided access to a new class of potential host macrocycles.

4.2.3. Experimental section

4.2.3.1 General procedures

Starting materials and reagents, purchased from commercial suppliers, were used without purification unless otherwise mentioned. HPLC analyses were performed on a JASCO LC-NET II/ADC equipped with a JASCO Model PU-2089 Plus Pump and a JASCO MD-2010 Plus UV-vis multiple wavelength detector set at 220 nm. The column used was a C_{18} reversed-phase analytical column (Waters, Bondapak, 10 µm, 125 Å, 3.9 mm × 300 mm) run with linear gradients of ACN (0.1% TFA) into H_2O (0.1% TFA) over 30 min, at a flow rate of 1.0 mL/min for the analytical runs. High resolution mass spectra (HRMS) were recorded on a Bruker Solarix XR (Bruker Daltonik GmbH, Bremen, Germany) Fourier transform ion cyclotron resonance mass spectrometer ((FTICR analyzer)) equipped with a 7T, using matrix-assisted laser desorption/ionization (MALDI) Yields refer to chromatographically and spectroscopically (^{1}H- and ^{13}C NMR) pure materials. NMR spectra were recorded on a Bruker DRX 600 (^{1}H at 600.13 MHz, ^{13}C at 150.90 MHz). Chemical shifts (δ) are reported in ppm relative to the residual solvent peak ($CHCl_3$, δ = 7.26; ^{13}CDCl3, δ = 77.00; C_2DHCl_4, TCDE, δ = 5.80; $(CH_3)_2SO$, DMSO, δ = 2.50; $(^{13}CH_3)_2SO$, DMSO, δ = 39.51) and the multiplicity of each signal is designated by the following abbreviations: s, singlet; d, doublet; t, triplet; m, multiplet; br, broad. 2D NMR

experiments such as COSY, HSQC and HMBC were performed for the full assignment of each signal. Coupling constants (*J*) are quoted in Hertz.

DFT calculations were performed by prof. C. Costabile, Dpt. of Chemistry and Biology "A. Zambelli", Univ. of Salerno.

X-ray analyses were performed by dr. Giovanni Pierri and prof. Consiglia Tedesco, Dpt. of Chemistry and Biology "A. Zambelli", Univ. of Salerno.

4.2.3.2 Procedure for solid-phase synthesis of 4.12, 4.13 and 4.14

Solid-phase synthesis of linear precursors 4.12 and 4.13

2-chlorotrityl chloride resin (2,α-dichlorobenzhydryl-polystyrene cross-linked with 1% DVB; 100– 200 mesh; 1.60 mmol g^{-1}, 0.100 g, 0.160 mmol) was washed with DCM (3 × 1 mL) and DMF (3 × 1 mL) and then swollen in dry DCM (1.0 mL) for 45 min. Azidoacetic acid, (handled carefully due to known explosive nature of azides), **4.5**, (0.026 g, 0.26 mmol) and DIPEA (139 µL, 0.80 mmol) in dry DCM (1.0 mL) were added to the resin and the vessel was stirred on a shaker platform for 60 min at room temperature. Then the resin was washed with DMF (3 × 1.0 mL), DCM (3 × 1.0 mL) and then with DMF (3 × 1.0 mL). Subsequent on-resin cycloaddition reaction was accomplished in the presence of copper iodide (0.046 g, 0.24 mmol), *N*-benzylprop-2-ynyl-1-amine, **4.6**, (0.046 g, 0.32 mmol), and DIPEA (1.4 mL, 8.00 mmol) in dry THF (1.5 mL). The resulting mixture was stirred overnight on the shaker platform at room temperature. Then the resin was washed with THF (5 x 1.0 mL), DMF (3 × 1.0 mL), DCM (3 × 1 mL) and with DMF (3 × 1.0 mL). Next, a solution of azidoacetic acid (0.162 g, 1.60 mmol) and DIC (273 µl, 1.76 mmol) in dry DMF (1.0 mL) was added to the resin and stirred on a shaker platform for 40 min at room temperature. Then the resin was washed again with DMF (3 × 1.0 mL), DCM (3 × 1.0 mL) and DMF (3 × 1.0 mL). After, the cycloaddition reaction was repeated following the procedure described above. The preparation of triazolopeptoid **4.13** needed an additional acylation and cycloaddition step. The synthesis proceeded until the target linear triazole-peptoids were obtained. The linear precursors were cleaved from the resin, previously washed with DCM (3 × 1.0 mL), by treatment with three aliquots of a solution of 20% HFIP in

dry DCM (v/v; 3 × 1.0 mL), stirred on a shaker platform at room temperature for 30 min each time. The resin was filtered away and the combined filtrates were concentrated in vacuo. The final products were analyzed by MALDI mass spectrometry and RP-HPLC and used for the cyclization step without further purification.

Solid-phase synthesis of linear precursor 4.14

2-chlorotrityl chloride resin (0.100 g, 0.160 mmol) was washed with DCM (3 × 1.0 mL) and DMF (3 × 1.0 mL) and swollen in dry DCM (1 mL) for 45 min. Then the resin was acylated with azidoacetic acid, (0.026 g, 0.26 mmol) in the presence of DIPEA (139 µL, 0.800 mmol) in dry DCM (1.0 mL). The mixture was stirred on a shaker platform for 60 min at room temperature. The resin was washed with DMF (3 × 1.0 mL), DCM (3 × 1.0 mL) and DMF (3 × 1.0 mL). The cycloaddition reaction was performed by adding copper iodide (0.046 g, 0.240 mmol), *N*-benzylprop-2-ynyl-1-amine (0.046 g, 0.320 mmol), and DIPEA (1.4 mL, 8.00 mmol) in dry THF (1.5 mL) to the resin. The mixture was stirred overnight on the shaker platform at room temperature. Then the resin was washed with THF (5 x 1.0 mL), DMF (3 × 1.0 mL), DCM (3 × 1.0 mL) and DMF (3 × 1.0 mL). Subsequently, bromoacetic acid (0.220 g, 1.60 mmol) and DIC (273 µL, 1.76 mmol) in dry DMF (1.0 mL) was added to the vessel and stirred on a shaker platform for 40 min at room temperature. Then the resin was washed again with DMF (3 × 1.0 mL), DCM (3 × 1.0 mL) and DMF (3 × 1.0 mL) and a solution of benzylamine (171 µL, 1.60 mmol) in dry DMF (1.0 mL) was added to the bromoacetylated resin and stirred on a shaker platform for 40 min at room temperature. The resin was washed with DMF (3 × 1.0 mL), DCM (3 × 1.0 mL) and DMF (3 × 1.0 mL). Afterwards, the oligomer sequence was expanded by acylation with azidoacetic acid, cycloaddition, bromoacetylation and substitution with benzylamine, following the protocol described above. The cleavage from the resin, previously washed with DCM (3 × 1.0 mL), was performed by treatment with three aliquots of a solution of 20% HFIP in dry DCM (v/v; 3 × 1.0 mL). The mixture was stirred on a shaker platform at room temperature for 30 min each time. The resin was filtered away and the combined filtrates were concentrated in vacuo. The final product was analyzed by MALDI mass spectrometry and RP-HPLC and used for the cyclization step without further purification.

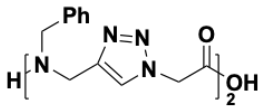

4.12

4.12: light yellow amorphous solid, 0.076 g, 100% yield; Rt 5.8 min; HRMS (MALDI): m/z $[M+H]^+$ Calcd for $C_{24}H_{27}N_8O_3^+$ 475.2201; Found 475.2195;

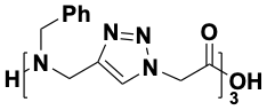

4.13

4.13: light yellow amorphous solid, 0.109 g, 100% yield; Rt 7.6 min; HRMS (MALDI): *m/z* $[M+H]^+$ Calcd for $C_{36}H_{39}N_{12}O_4^+$ 703.3212; Found 703.3284;

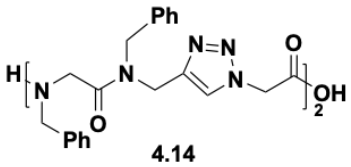

4.14

4.14: light yellow amorphous solid, 0.120 g, 100% yield; Rt 8.2 min; HRMS (MALDI): *m/z* $[M+H]^+$ Calcd for $C_{42}H_{45}N_{10}O_5^+$ 769.3569; Found 769.3555;

4.2.3.3 General procedure for high dilution cyclization. Synthesis of macrocycles 4.9, 4.10 and 4.11

To a stirred solution of HATU (0.243 g, 0.64 mmol) and DIPEA (170 µl, 1.00 mmol) in dry DMF (45 mL) at room temperature, a solution of a linear precursor (0.16 mmol) in dry DMF (8 mL) was added using a syringe pump in 3 h. After 16 h the resulting mixture was concentrated in vacuo, diluted with DCM (40 mL) and washed with 1 M HCl (2 × 20 mL). The aqueous layer was extracted with DCM (80 mL) and the combined organic phases were washed with water (60 mL), dried over $MgSO_4$ and concentrated in vacuo. The crude cyclic peptoids **4.9**, **4.10** and **4.11** were dissolved in hot acetonitrile and precipitated by slowly cooling the solution.

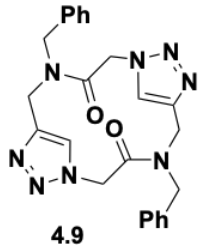

4.9

4.9: white amorphous solid, 0.025 g, 34% yield; Rt 6.8 min; HRMS (MALDI): *m/z* $[M+H]^+$ Calcd for $C_{24}H_{25}N_8O_2^+$ 457.2095; Found 457.2105.

^{1}H NMR (600 MHz, $CDCl_3$) δ: 7.84 (2H, s, C*H*NN), 7.45-7.32 (10H, m, Ar-*H*), 5.56 (2H, d, *J* 13.6 Hz, NNCH*H*CO), 5.29 (2H, d, *J* 14.3 Hz, BnNCH*H*C), 4.80 (2H, d, *J* 16.7 Hz, NCH*H*Ph), 4.75 (2H, d, *J* 13.6 Hz, NNC*H*HCO), 4.11 (2H, d, *J* 16.7 Hz, NC*H*HPh), 3.79 (2H, d, *J* 14.3 Hz, BnNC*H*HC).

^{13}C NMR (150 MHz, $CDCl_3$) δ: 166.0 × 2 (CH_2*C*O), 144.2 × 2 (CH_2*C*CHN), 135.7 × 2 (*C*-Ar), 129.2 × 4 (*C*-Ar), 128.2 × 2 (*C*-Ar), 127.0 × 4 (*C*-Ar), 122.4 × 2 (CH_2C*C*HN), 52.5 × 2 (NN*C*H_2CO), 50.9 × 2 (N*C*H_2Ph), 41.2 × 2 (BnN*C*H_2C).

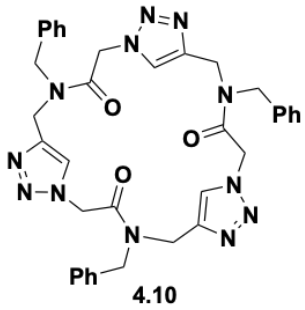

4.10

4.10: white amorphous solid, 0.031 g, 28% yield; Rt 9.3 min; HRMS (MALDI): *m/z* $[M+H]^+$ Calcd for $C_{36}H_{37}N_{12}O_3^+$ 685.3106; Found 685.3094.

^{1}H NMR (600 MHz, DMSO, mixture of rotamers) δ: 8.59-7.74 (3H, m), 7.42-7.29 (15H, m), 5.62-5.47 (6H, m), 4.78-4.47 (12H, m).

^{13}C NMR (150 MHz, DMSO, mixture of rotamers) δ: 166.4, 166.1, 144.0, 143.7, 143.5, 143.4, 143.1, 142.9, 136.8, 136.4, 128.8, 128.5, 127.8, 125.4, 125.0, 124.6, 51.0, 50.8, 50.6, 50.4, 50.3, 48.6, 48.4, 48.2, 42.6, 42.3, 41.9, 41.8, 41.7.

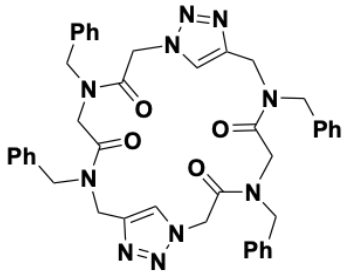

4.11

4.11: white amorphous solid, 0.029 g, 24% yield; Rt 10.1 min; HRMS (MALDI): *m/z* $[M+H]^+$ Calcd for $C_{42}H_{43}N_{10}O_4^+$ 751.3463; Found 751.3491.

^{1}H NMR (600 MHz, $CDCl_3$, mixture of rotamers) δ: 8.66-8.02 (2H, m), 7.43-7.05 (20H, m), 5.40-5.33 (4H, m), 5.00-3.96 (16H, m).

^{13}C NMR (150 MHz, $CDCl_3$, mixture of rotamers) δ: 168.8, 168.7, 167.8, 166.8, 166.5, 165.7, 165.6, 146.8, 144.4, 143.8, 143.7, 143.2, 143.1, 136.5, 136.1, 135.0, 134.9, 129.3, 129.0, 128.8, 128.7, 128.6, 128.4, 128.2, 127.9, 127.8, 127.7, 127.1, 126.9, 126.8, 126.5, 126.4, 126.1, 126.0, 125.7, 125.5, 52.6, 52.4, 52.2, 51.8, 51.3, 51.1, 51.0, 50.6, 50.5, 50.2, 50.0, 49.8, 48.6, 48.4, 48.3, 47.7, 47.5, 47.3, 47.2, 43.5, 43.3, 43.1, 42.9, 42.6, 42.3.

4.2.3.4 Procedure for the Pirkle's alcohol addition to racemic mixture 4.9a/4.9b

To 8.0 mM solution of cyclic triazolopeptoid **4.9a**/**4.9b** in $CDCl_3$ (0.5 mL), 0.5 equivalents of Pirkle's alcohol ((R)-1-(9-anthryl)-2,2,2-trifluoroethanol) were added. After the addition the mixture was mixed for 1 minute and the ^{1}H NMR spectrum was recorded. Further 1, 2, and 3 equivalents of Pirkle's alcohol were added in order to increase the protons resonances splitting (**Figure 4. 22**). NMR spectra were recorded on a Bruker DRX 600 (^{1}H NMR at 600.13 MHz).

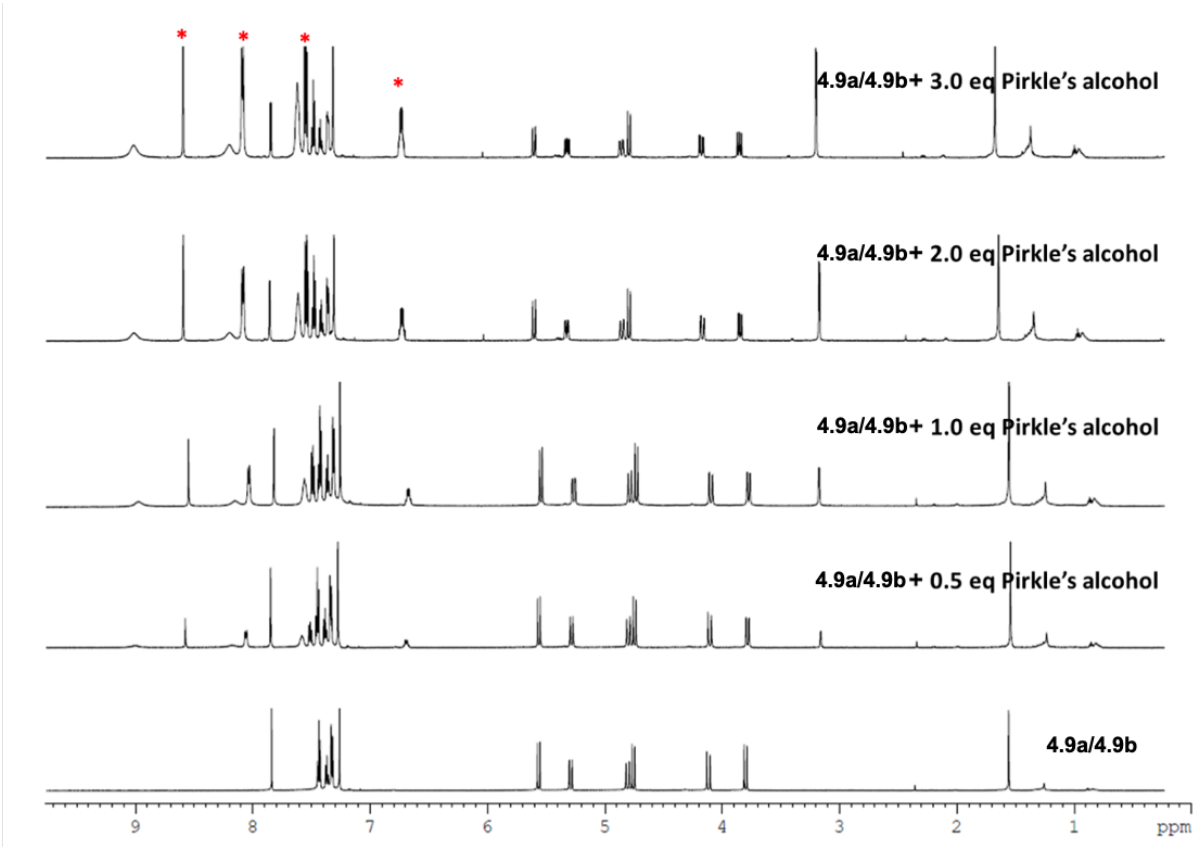

Figure 4. 22. Quantitative step-wise addition of Pirkle‟s alcohol to 4.9a/4.9b. ^{1}H NMR (600 MHz, $CDCl_3$, 298 K, 8.0 mM solution). *Indicates the Pirkle's alcohol resonances.

4.2.3.5 ^{1}H NMR variable temperature experiments for 4.9, 4.10 and 4.11

Cyclic triazolopeptoids **4.9** and **4.11** were dissolved in $C_2D_2Cl_4$ (TCDE, 5.0 mM solution) and **4.10** was dissolved in DMSO (5.0 mM solution). Then ^{1}H NMR spectra were acquired at different temperatures, increasing 10 or 20 K each time. For the compounds **4.9**, **4.10** and **4.11** no coalescence was observed up to 373 K.

4.3. From cyclic triazolopeptoids to new azamacrocycles

4.3.1. Results and discussion

4.3.1.1 Synthesis and characterization of new macrocyclic triazolopeptoids

To further explore and broaden the potential of the previously described new class of macrocyclic triazolopeptoids, and to understand the role of chiral chains on their conformational isomerism, we decided to synthesize new cyclic derivatives comprising *N*-(S)-(1-phenylethyl)glycine (*N*spe) residues: the cyclodimer **4.19** and the cyclotrimer **4.20.** These macrocycles, together with the already described: **4.9**, **4.10**, and **4.11**, were subsequently employed as precursors for the synthesis of new triazole-containing azamacrocycles (**4.21**-**4.25**).

New chiral triazolopeptoids were synthesized by following the procedure reported in **Scheme 4. 6.** To perform the linear triazolopeptoids' synthesis on solid phase, first, we prepared in solution the following building blocks: azido acetic acid **4.5**, *N*-benzylpropargyl amine **4.6** (as previously), and (S)-1-phenylethylpropargyl amine **4.15** by a nucleophilic substitution of propargyl bromide with (S)-1-phenylethyl amine (71% yield).

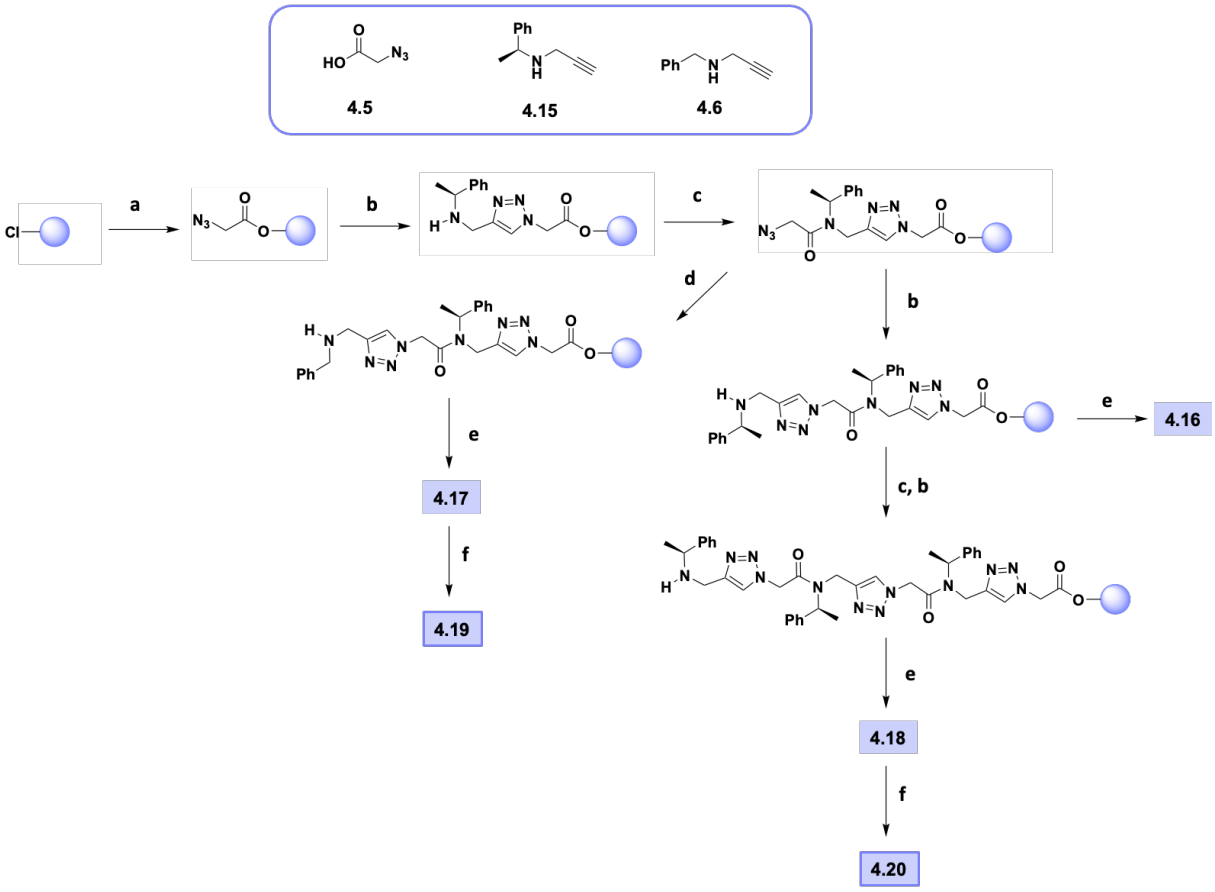

Scheme 4. 6. Synthesis of new chiral triazolopeptoids. (a) **4.5**, DIPEA, DCM dry; (b) **4.15**, CuI, DIPEA, THF dry; (c) **4.5**, DIC, DMF dry; (d) **4.6**, CuI, DIPEA, THF dry; (e) 20% HFIP in DCM dry; (f) HATU, DIPEA, DMF dry

Linear triazolopeptoids, **4.16** and **4.18**, containing two and three extended monomer residues, respectively, were obtained in quantitative yield. However, while trimeric oligomer **4.18** smoothly afforded the macrocyclic derivative **4.20** (37% yield), in the case of **4.16** the ring did not form. The macrocyclization attempts were performed as well at high temperature (50°C) and by microwave assisted cyclization. Unfortunately, in both cases it was impossible to obtain the target macrocyclic compound. In view of this results, we decided to prepare a linear dimeric triazolopeptoid possessing at least one chiral residue. Thus, we synthesized the oligomer **4.17**, the cyclization of which afforded macrocycle **4.19** (49% yield).

^{1}H and ^{13}C NMR spectral analysis of cyclodimer **4.19**, revealed the presence of a mixture of two conformationally stable compounds, with major one accounting for the 95 % (**Figure 4. 23a**). Conformational stability in cyclic peptoids is not always observed due to the presence of tertiary amides in their backbones. As a result, the coexistence of multiple conformations in slow equilibrium on the NMR time scale is frequently reported. In the case

of cyclic dimer **4.9**, described in chapter 4.2.1.2, the all-trans C_2-symmetric conformation was assigned as the most stable one by experimental data, literature evidence and theoretic studies. New cyclic dimer **4.19**, in addition to amide bonds' directionality, observed also in the case of **4.9**, contains another source of asymmetry: a chiral side chain. Consequently, it implies, in principle, the presence of four diastereomorphous conformational isomers with the all-*trans* geometry of amide bonds, **4.19a**-**4.19d** (Figure 4. 23b). **4.19a** and **4.19b** (or **4.19c** and **4.19d**) could be interconverted by contemporaneous inversion of both peptoid bonds and triazoles. On the other hand, **4.19a** and **4.19c** (or **4.19b** and **4.19d**) could be interchanged by inversion of a single amide bond and single triazole ring.

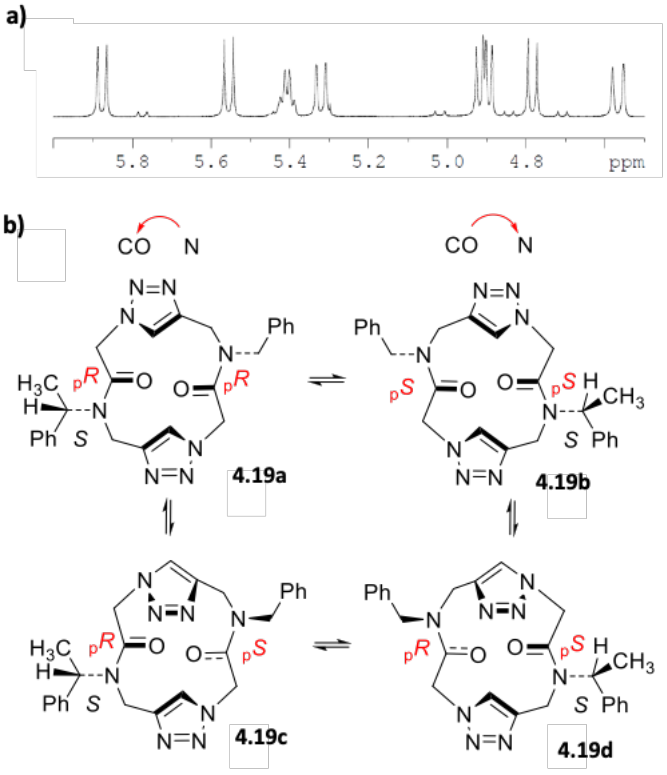

Figure 4. 23. (a) Expansion of ^{1}H NMR spectra of **4.19** (600 MHz, $CDCl_3$); (b) Diastereomorphous conformational isomers of cyclodimer **4.19**.

To attribute the structures to the two diastereoisomers, observed in solution, DFT calculations at the BP86/TZVP level were performed for the all-*trans* potential candidates.[176] Theoretical studies revealed that **4.19a** is the most stable species due to the positioning of the

[176] DFT calculations were performed by prof. C. Costabile, Dpt. of Chemistry and Biology "A. Zambelli", Univ. of Salerno.

side chain's methyl group inside the "open square" backbone (Figure 4. 24a), to avoid unfavorable contacts with the *α*-methylene group.

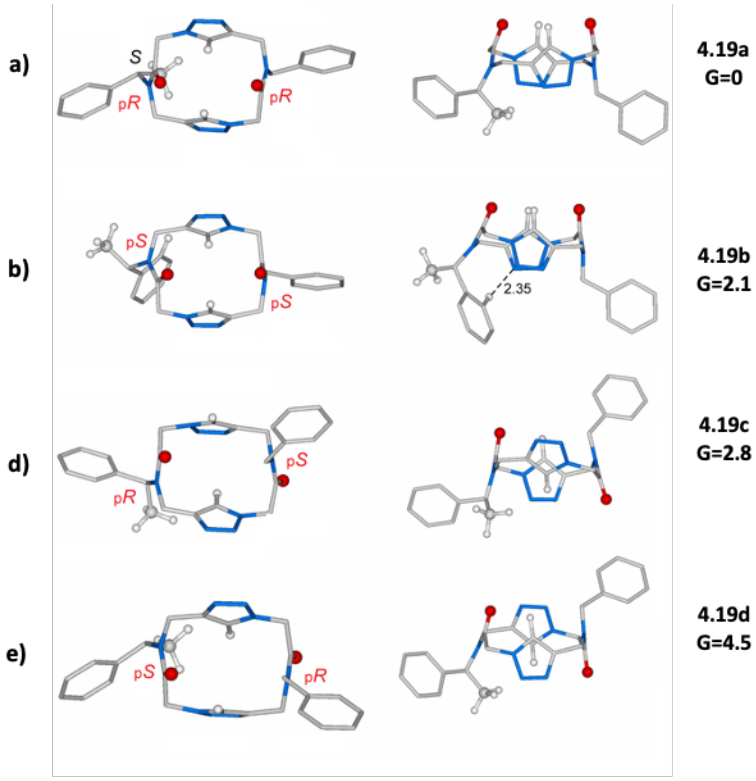

Figure 4. 24. Minimum energy structures of the four potential conformational isomers of **4.19** with the all-*trans* geometry of amide bonds.

This attribution is consistent with the NMR analysis. Specifically, in the ^{1}H NMR spectrum of **4.19**, the chemical shift of methyl group (1.17 ppm) is more shielded, if compared to those observed in cyclic peptoid scaffolds containing the *N*spe side chain on a *trans* amide junction (1.5-1.3 ppm). In contrast, in the case of the spectral analysis of the minor diastereoisomer, the presence of a doublet at 6.83 ppm, for the *ortho*-protons of the aromatic ring, revealed a shielding effect on the phenyl group. This experimental proof is supported by DFT calculations for the following conformer at lower energy, by the short distance observed between the *ortho*-protons and the electron donating nitrogen atom of triazole ring (Figure 4. 24b).

Moreover, the outcome of the theoretical study potentially explains problems encountered with the ring closure in the case of linear triazolopeptoid **4.16**. Specifically, it can be justified by the necessity to accommodate methyl and phenyl groups of another chiral side chain closer to the macrocyclic cavity, in accordance with the minimum energy structure of **4.19a**.

On the other hand, ^{1}H and ^{13}C NMR analysis of cyclotrimer **4.20**, revealed the presence of a mixture of conformers. Unfortunately, even the presence of three side chains was insufficient to induce conformational homogeneity in the macrocycle, in contrast with what was observed for other cyclic peptoids.[177,178] Possibly, it is a result of the larger size of the macrocycle due to the presence of the extended monomer units.

4.3.1.2 From cyclic triazolopeptoids to peraza-macrocycles: synthesis and characterization of new azamacrocycles

Once the macrocyclic triazolopeptoids (**4.9**, **4.10**, **4.11**, **4.19**, **4.20,** Figure 4. 25) have been prepared, we proceeded to test the effectiveness of the reduction reaction on them. To our delight, by following the reduction procedure established for cyclic peptoids[164] (using 5.0 equivalents of 1.0 M solution of a borane tetrahydrofuran complex in THF for each amide group), we were able to obtain a library of new triazole-containing aza-macrocycles (**4.21**-**4.25**, Figure 4. 25), observing a total conversion of all the extended peptoid precursors.

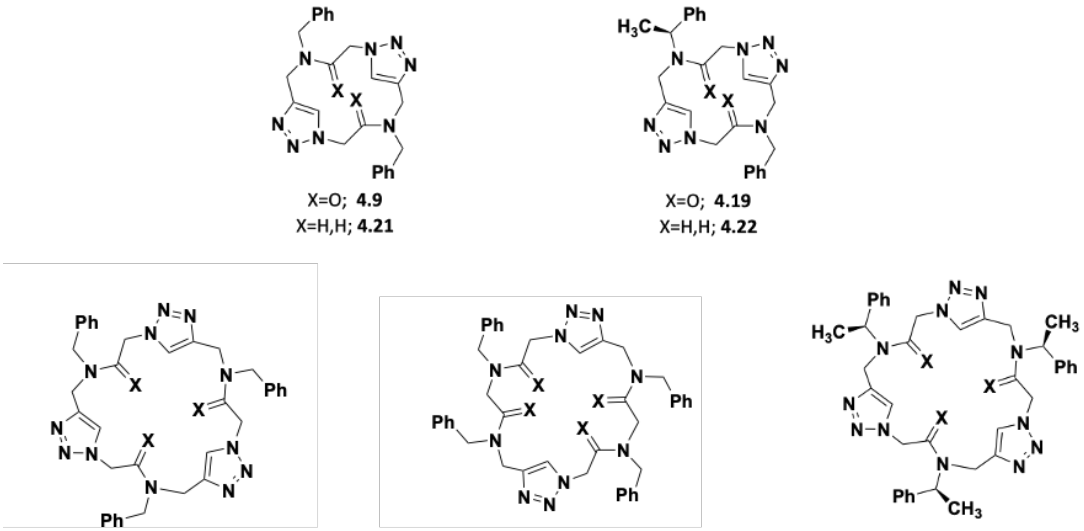

Figure 4. 25. Schematic structures of new azamacrocycles and their precursors.

[177] D'Amato, A.; Pierri, G.; Costabile, C.; Della Sala, G.; Tedesco, C.; Izzo, I.; De Riccardis, F. *Org. Lett*. **2018**, *20*, 640-643.
[178] D'Amato, A.; Pierri, G.; Tedesco, C.; Della Sala, G.; Izzo, I.; Costabile, C.; De Riccardis, F. *J. Org. Chem.* **2019**, 84, 10911-10928.

The crude mixture from reduction of cyclodimer **4.9** afforded, after the purification step, two products, one of which predominantly (69% and 20% from **4.9**). This evidence was attested as well in the reduction of cyclodimer **4.19**: two products respectively in 45% and 5% yields were recovered after purification. The peraza-macrocycle/borane complex ratios for the reduction of both cyclodimers are depicted in **Figure 4. 26**, showing ^{1}H NMR spectral analysis of crude mixtures (reduction of **4.9**, **Figure 4. 26a** and reduction of **4.19**, **Figure 4. 26b**).

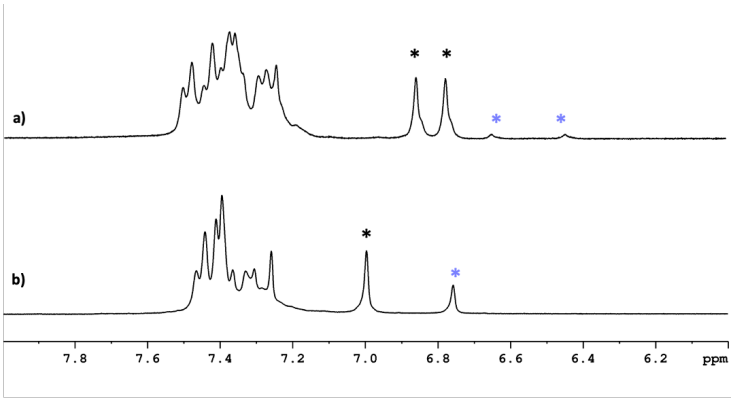

Figure 4. 26. Aromatic region of ^{1}H NMR spectra of crude mixtures evidencing triazole protons' resonances of peraza-macrocycles (labeled with black asterisk) and their borane complexes (violet asterisks); (a) reduction of **4.9**; (b) reduction of **4.19**.

Gratifyingly, we managed to obtain single crystals suitable for X-ray diffraction analysis,[179] by slow evaporation from acetonitrile solutions for three out of four compounds obtained. This allowed us to assign, to the major product from reduction of **4.9**, the structure of its reduced derivative **4.21** (**Figure 4. 27**) and to minor one its borane complex **4.26** (**Figure 4. 28**). Similarly, for reduction of cyclodimer **4.19**, the major product was assigned to be the peraza-macrocycle **4.22** and the minor one its borane complex **4.27** (**Figure 4. 29**).

[179] X-ray analyses were performed by dr. Giovanni Pierri and prof. Consiglia Tedesco, Dpt. of Chemistry and Biology "A. Zambelli", Univ. of Salerno.

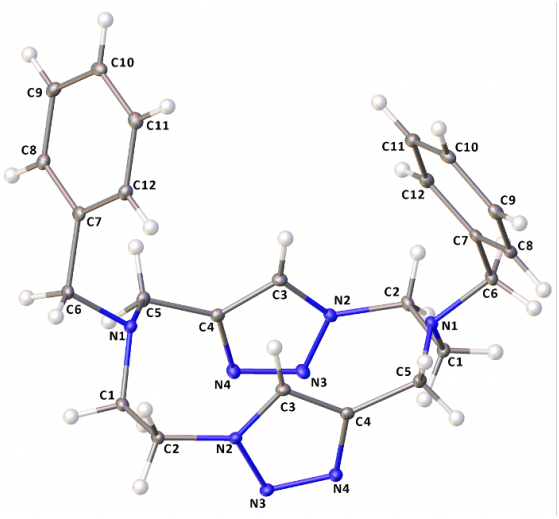

Figure 4. 27. X-ray structure of peraza-macrocycle **4.21**. Atom type: C, light grey; N, blue; and H, white.

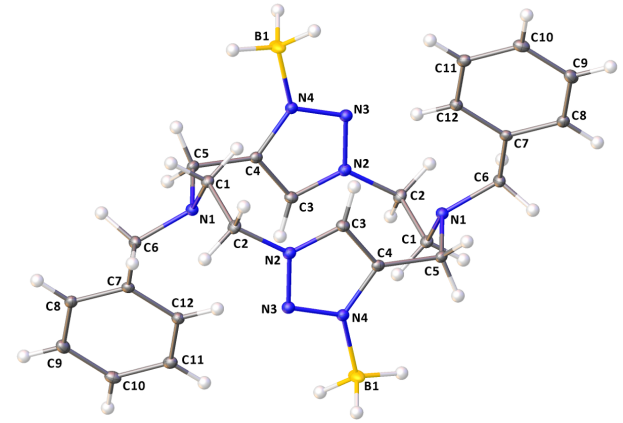

Figure 4. 28. X-ray structure of BH_3-complex of **4.21**: **4.26**. Atom type: C, light grey; N, blue; B, yellow, and H, white.

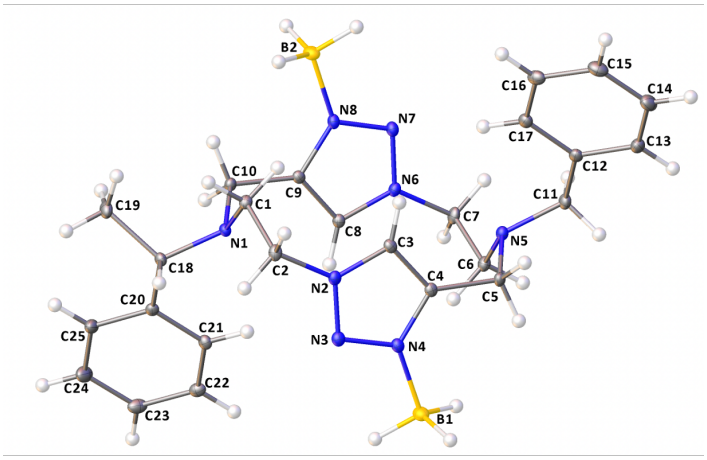

Figure 4. 29. X-ray structure of BH_3-complex of **4.22**: **4.76**. Atom type: C, light grey; N, blue; B, yellow, and H, white.

The analogous reduction reaction was performed as well on the larger macrocycles **4.10**, **4.11** and **4.20**, affording this time exclusively peraza-macrocycles **4.23**, **4.24** and **4.25** in 93%, 38% and 42% yields, respectively. Spectroscopic and spectrometric analysis confirmed the formation of the target macro rings. Moreover, the compound **4.23** was additionally characterized by means of X-ray diffraction analysis (**Figure 4. 30**), as we were able to obtain a single crystal by slow evaporation of its acetonitrile solution.

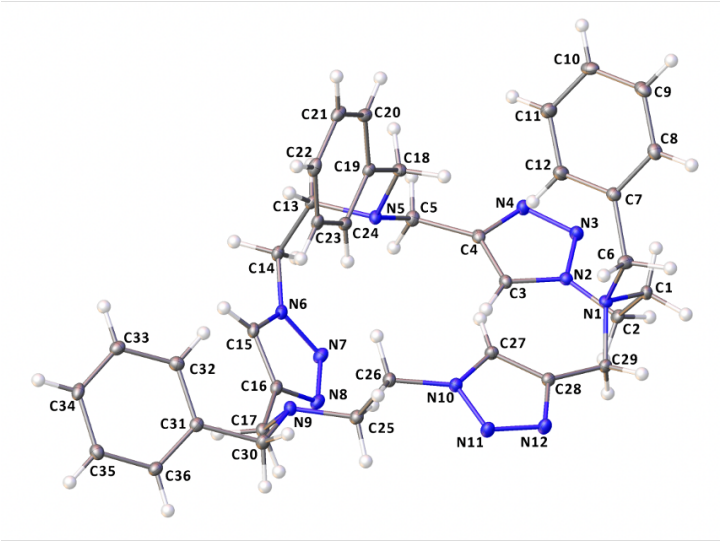

Figure 4. 30. X-ray structure of aza-macrocycle **4.23**. Atom type: C, light grey; N, blue; and H, white.

In order to preliminarily examine the complexation capabilities of the new triazole-containing peraza-macrocycles, we decided to perform qualitative sodium binding studies involving three representative derivatives **4.21**, **4.23** and **4.24**. To our delight, stepwise addition of NaTFPB to the $CDCl_3$ solutions of all three macrocycles induced significant variations of their ^1H NMR spectra, confirming formation of new sodiated species (**Figure 4. 31**, **Figure 4. 32**, **Figure 4. 33**). These qualitative results show the potential as complexing agents of this novel class of azamacrocycles, even if further investigation should be performed.

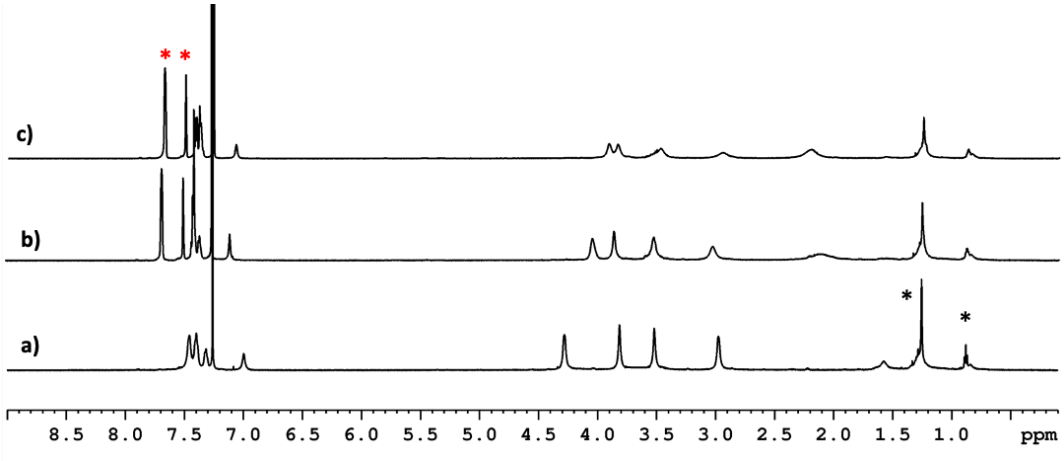

Figure 4. 31. Stepwise addition of NaTFPB to a 8.0 mM solution of **4.21** in $CDCl_3$ (^{1}H NMR, 600 MHz). (a) free host **4.21**; (b) **4.21** and 0.5 eq of NaTFPB; (b) **4.21** and 1.0 eq of NaTFPB. TFPB peaks are labelled with red asterisks. Water/lipid impurities are labelled with black asterisks.

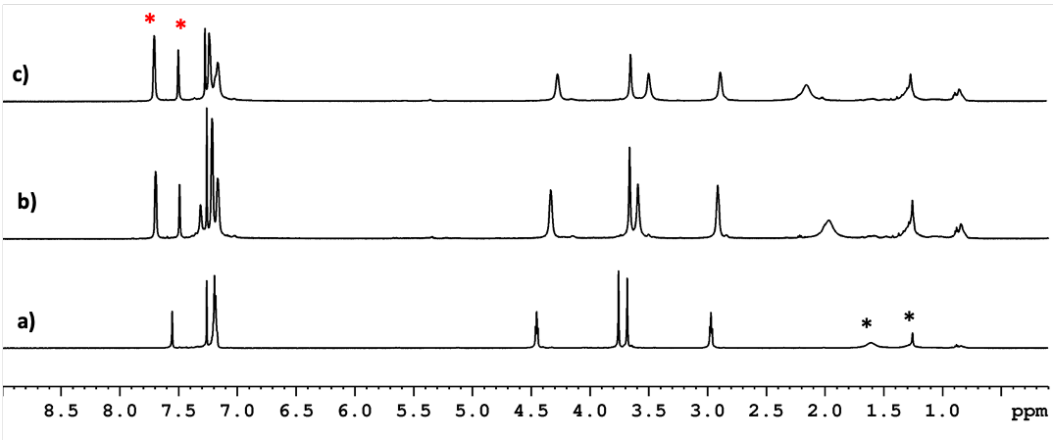

Figure 4. 32. Stepwise addition of NaTFPB to a 8.0 mM solution of **4.23** in $CDCl_3$ (^{1}H NMR, 600 MHz). (a) free host **4.23**; (b) **4.23** and 0.5 eq of NaTFPB; (b) **4.23** and 1.0 eq of NaTFPB. TFPB peaks are labelled with red asterisks. Water/lipid impurities are labelled with black asterisks.

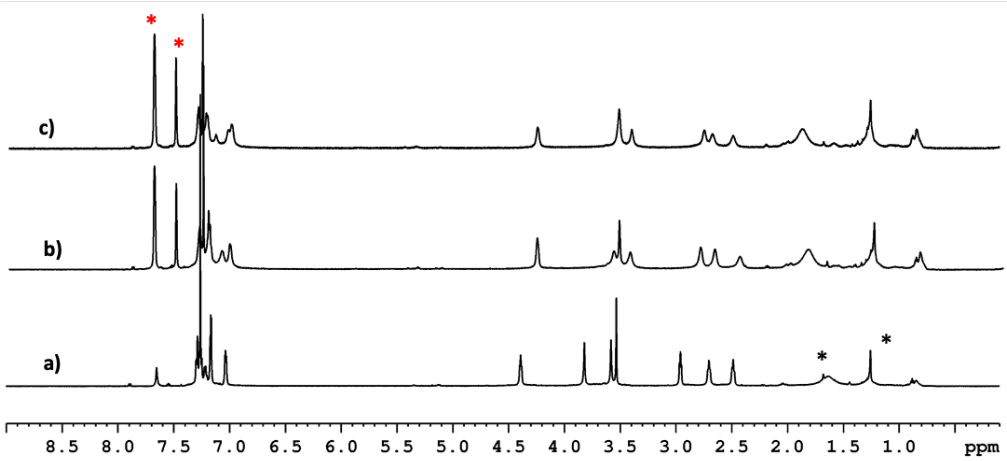

Figure 4. 33. Stepwise addition of NaTFPB to a 8.0 mM solution of **4.24** in $CDCl_3$ (^{1}H NMR, 600 MHz). (a) free host **4.24**; (b) **4.24** and 0.5 eq of NaTFPB; (b) **4.24** and 1.0 eq of NaTFPB. TFPB peaks are labelled with red asterisks. Water/lipid impurities are labelled with black asterisks.

4.3.2. Conclusions

In this work, we synthesized new macrocyclic triazolopeptoids containing *N*-(*S*)-(1-phenylethyl)glycine (*N*spe) residues: the cyclodimer **4.19** and the cyclotrimer **4.20**. Moreover, we prepared a library of new triazole-containing peraza-macrocycles **4.21**, **4.22**, **4.23**, **4.24**, and **4.25** *via* tertiary amide reduction of macrocyclic "extended" peptoids. Additionally, we obtained two stable borane complexes of dimeric peraza-macrocycles **4.21** and **4.22**, the formation of which was attested by X-ray diffraction analysis (compounds **4.26**, and **4.27**, respectively). Crystallographic structures were obtained as well for macrocycles **4.21**, and **4.23**. Furthermore, the preliminary sodium binding studies performed on peraza-macrocycles **4.21**, **4.23**, and **4.24** revealed the promising potential of new triazole-containing macrocycles as hosts.

4.3.3. Experimental section

4.3.3.1 General procedures

Starting materials and reagents, purchased from commercial suppliers, were used without purification unless otherwise mentioned. HPLC analyses were performed on a JASCO LC-NET II/ADC equipped with a JASCO Model PU-2089 Plus Pump and a JASCO MD-2010 Plus UV-vis multiple wavelength detector set at 220 nm. The column used was a C_{18} reversed-phase

analytical column (Waters, Bondapak, 10 µm, 125 Å, 3.9 mm × 300 mm) run with linear gradients of ACN (0.1% TFA) into H_2O (0.1% TFA) over 30 min, at a flow rate of 1.0 mL/min for the analytical runs. High resolution mass spectra (HRMS) were recorded on a Bruker Solarix XR (Bruker Daltonik GmbH, Bremen, Germany) Fourier transform ion cyclotron resonance mass spectrometer ((FTICR analyzer)) equipped with a 7T, using matrix-assisted laser desorption/ionization (MALDI) Yields refer to chromatographically and spectroscopically (^{1}H- and ^{13}C NMR) pure materials. NMR spectra were recorded on a Bruker DRX 600 (^{1}H at 600.13 MHz, ^{13}C at 150.90 MHz). Chemical shifts (δ) are reported in ppm relative to the residual solvent peak ($CHCl_3$, δ = 7.26; ^{13}CDCl3, δ = 77.00) and the multiplicity of each signal is designated by the following abbreviations: s, singlet; d, doublet; t, triplet; m, multiplet; br, broad. 2D NMR experiments such as COSY, HSQC and HMBC were performed for the full assignment of each signal. Coupling constants (*J*) are quoted in Hertz.

DFT calculations were performed by prof. C. Costabile, Dpt. of Chemistry and Biology "A. Zambelli", Univ. of Salerno.

X-ray analyses were performed by dr. Giovanni Pierri and prof. Consiglia Tedesco, Dpt. of Chemistry and Biology "A. Zambelli", Univ. of Salerno.

4.3.3.2 Procedure for synthesis of amine 4.15

A mixture of (S)-1-phenylethylamine (1.37 mL, 10.6 mmol), 3-bromo-1-propyne (1.2021 g, 10.0 mmol), and potassium carbonate (1.728 g, 12.5 mmol) in acetonitrile (20 mL) was stirred at room temperature overnight. The resulting mixture was then filtered through a pad of Celite and the filtrate was concentrated. The residue was purified by chromatography on silica gel (dichloromethane/methanol = 25/1 to 10/1 as the eluent) to obtain (S)-*N*-(1-phenylethyl)-*N*-(prop-2-yn-1-yl)amine **4.15**.

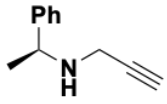

4.15

4.15[180]**:** yellow oil, 1.453 g, 71% yield.

^{1}H NMR NMR (300 MHz, $CDCl_3$) δ: 7.32-7.22 (5H, m), 4.01 (1H, q, *J* 6.6 Hz), 3.35 (1H, dd, *J* 17.1 Hz, *J* 2.4 Hz), 3.15 (1H, dd, *J* 17.1 Hz, *J* 2.3 Hz), 2.20 (1H, t, *J* 2.3 Hz), 1.35 (3H, d, *J* 6.6 Hz).

^{13}C NMR (75 MHz, $CDCl_3$) δ: 144.4, 128.4, 127.1, 126.8, 82.2, 71.2, 56.3, 35.8, 23.9.

4.3.3.3 General procedure for solid phase synthesis. Preparation of linear triazolopeptoids 4.16, 4.17, and 4.18

2-chlorotrityl chloride resin (2,α-dichlorobenzhydryl-polystyrene cross-linked with 1% DVB; 100– 200 mesh; 1.60 mmol g^{-1}, 0.100 g, 0.160 mmol) was washed with DCM (3 × 1 mL) and DMF (3 × 1 mL) and then swollen in dry DCM (1.0 mL) for 45 min. Azidoacetic acid, (handled carefully due to known explosive nature of azides), **4.5**, (0.026 g, 0.26 mmol) and DIPEA (139 µL, 0.80 mmol) in dry DCM (1.0 mL) were added to the resin and the vessel was stirred on a shaker platform for 60 min at room temperature. Then the resin was washed with DMF (3 × 1.0 mL), DCM (3 × 1.0 mL) and then with DMF (3 × 1.0 mL). Subsequent on-resin cycloaddition reaction was accomplished in the presence of copper iodide (0.046 g, 0.24 mmol), (S)-*N*-(1-phenylethyl)-*N*-(prop-2-yn-1-yl)amine, **4.15**, (0.051 g, 0.032 mmol) and DIPEA (1.4 mL, 8.00 mmol) in dry THF (1.5 mL). The resulting mixture was stirred overnight on the shaker platform at room temperature. Then the resin was washed with THF (5 x 1.0 mL), DMF (3 × 1.0 mL), DCM (3 × 1 mL) and with DMF (3 × 1.0 mL). Next, a solution of **4.5** (0.162 g, 1.60 mmol) and DIC (273 µl, 1.76 mmol) in dry DMF (1.0 mL) was added to the resin and stirred on a shaker platform for 40 min at room temperature. Then the resin was washed again with DMF (3 × 1.0 mL), DCM (3 × 1.0 mL) and DMF (3 × 1.0 mL). After, the cycloaddition reaction was repeated following the procedure described above (for the synthesis of **4.16** and **4.18** using amine **4.15**, and in the case of **4.17**, amine **4.6**). The preparation of triazolopeptoid **4.18** needed an additional acylation and cycloaddition step (with amine **4.15**). The synthesis proceeded until the target linear triazole-peptoids were obtained. The linear precursors were cleaved from the resin, previously washed with DCM (3 × 1.0 mL), by treatment with three aliquots of a solution of 20% HFIP in dry DCM (v/v; 3 × 1.0 mL), stirred on a shaker platform at room temperature for 30 min each time. The resin was filtered away and the combined filtrates were

[180] Tayama, E.; Toma, Y. *Tetrahedron* **2015**, *71*, 554-559.

concentrated in vacuo. The final products were analyzed by MALDI mass spectrometry and RP-HPLC and used for the cyclization step without further purification.

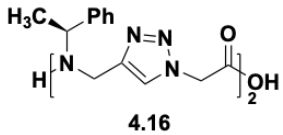

4.16

4.16: light-yellow amorphous solid, 0.080 g, 100% yield; Rt 6.0 min; HRMS (MALDI): *m/z* $[M+H]^+$ Calcd for $C_{26}H_{31}N_8O_3^+$ 503.2514; Found 503.2495.

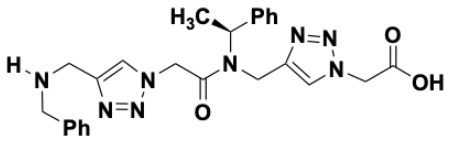

4.17

4.17: light-yellow amorphous solid, 0.078 g, 100% yield; Rt 6.1 min; HRMS (MALDI): *m/z* $[M+H]^+$ Calcd for $C_{25}H_{29}N_8O_3^+$489.2357; Found 489.2473.

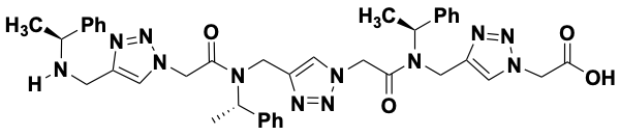

4.18

4.18: light-yellow amorphous solid, 0.119 g, 100% yield; Rt 7.6 min; HRMS (MALDI): *m/z* $[M+H]^+$ Calcd for $C_{39}H_{45}N_{12}O_4^+$ 745.3681; Found 745.3888.

4.3.3.4 General procedure for cyclization in high dilution conditions. Synthesis of macrocyclic triazolopeptoids 4.19 and 4.20

To a stirred solution of HATU (0.243 g, 0.64 mmol) and DIPEA (170 µl, 1.00 mmol) in dry DMF (45 mL) at room temperature, a solution of a linear precursor (0.16 mmol) in dry DMF (8 mL) was added using a syringe pump in 3 h. After 16 h the resulting mixture was concentrated in vacuo, diluted with DCM (40 mL) and washed with 1 M HCl (2 × 20 mL). The aqueous layer was extracted with DCM (80 mL) and the combined organic phases were washed with water (60 mL), dried over $MgSO_4$ and concentrated in vacuo. The crude cyclic peptoids **4.19** and **4.20** were dissolved in hot acetonitrile and precipitated by slowly cooling the solution.

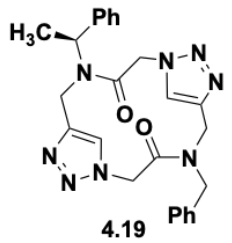

4.19

4.19: white amorphous solid, 0.037 g, 49% yield; Rt 6.6 min; HRMS (MALDI): *m/z* $[M+H]^+$ Calcd for $C_{25}H_{27}N_8O_2^+$471.2251 Found 471.2214.

^{1}H NMR (600 MHz, $CDCl_3$, major conformer) δ: 8.00 (1H, s, C*H*NN), 7.78 (1H, s, C*H*NN), 7.45-7.29 (10H, m, Ar-*H*), 5.87 (1H, d, *J* 13.6 Hz, NNCH*H*CONCH(CH_3)Ph), 5.55 (1H, d, *J* 13.7 Hz, NNCH*H*CONBn), 5.42 (1H, q, *J* 7.0 Hz, C*H*CH_3Ph), 5.31 (1H, d, *J* 14.3 Hz, BnNCH*H*C), 4.91 (1H, d, *J* 14.8 Hz, Ph(CH_3)CHNCH*H*C), 4.89 (1H, d, *J* 13.6 Hz, 1H, d, *J* 13.6 Hz, NNC*H*HCONCH(CH_3)Ph), 4.78 (1H, d, J 13.7 Hz, 1H, d, *J* 13.6 Hz, NNC*H*HCONBn), 4.56 (1H, d, J 16.4 Hz, NCH*H*Ph), 3.94-3.87 (2H, m, NC*H*HPh and Ph(CH_3)CHNC*H*HC), 3.80 (1H, d, *J* 14.3 Hz, BnNC*H*HC), 1.17 (3H, d, *J* 6.8 Hz, CHC*H*$_3$Ph).

^{13}C NMR (150 MHz, $CDCl_3$) δ: 166.2 (CH_2*C*ONCH(CH_3)Ph), 165.9 (CH_2*C*ONBn), 145.9 (Ph(CH_3)CHNCH$_2$*C*CHN), 144.3 (BnNCH$_2$*C*CHN), 139.8 (*C*-Ar), 135.3 (*C*-Ar), 129.1 x 2 (*C*-Ar), 129.0 x 2 (*C*-Ar), 128.2 (*C*-Ar), 128.1 (*C*-Ar), 127.1 x 2 (*C*-Ar), 126.6 x 2 (*C*-Ar), 123.0 (BnNCH$_2$C*C*H), 122.7 (Ph(CH_3)CNCH$_2$C*C*HN), 57.2 (N*C*H(CH_3)Ph), 52.8 (CH_2CON*C*H$_2$Ph), 52.4 (*C*H$_2$CONCH(CH_3)Ph), 50.3 (N*C*H$_2$Ph),41.0 (BnN*C*H$_2$C), 37.7 (Ph(CH_3)CHN*C*H$_2$C), 18.7 (CH*C*H$_3$Ph).

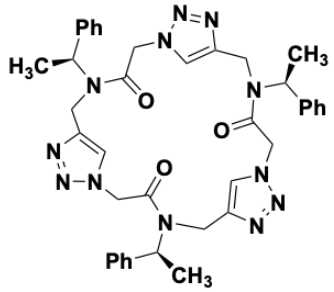

4.20

4.20: white amorphous solid, 0.043 g, 37% yield; Rt 9.1 min; HRMS (MALDI): *m/z* $[M+H]^+$ Calcd for $C_{39}H_{43}N_{12}O_3^+$ 727.3576 Found 727.3534.

^{1}H NMR (600 MHz, $CDCl_3$) δ: 8.54-8.14 (3H, m), 7.82-6.91 (15H, m), 5.57-3.86 (15H, m), 1.28-1.17 (9H, m).

^{13}C NMR (150 MHz, $CDCl_3$) δ: 167.1, 166.6, 166.2, 165.7, 145.2, 144.9, 144.5, 138.8, 139.5, 139.3, 139.1, 138.8, 129.5, 129.3, 128.8, 128.2, 128.1, 128.0, 127.8, 127.7, 127.5, 126.9, 126.7, 126.6, 126.3, 126.3, 126.1, 125.7, 125.5, 125.4, 125.2, 56.6, 56.2, 55.8, 52.6, 51.9, 51.5, 51.1, 40.3, 40.0, 39.6, 39.3, 39.0, 38.6, 38.3, 20.0, 19.8, 19.7, 19.6, 19.3, 19.2, 18.7, 18.4, 18.1.

4.3.3.5 Failed attempts of linear triazolopeptoid's 4.16 cyclization

Cyclization at room temperature

To a stirred solution of HATU (0.243 g, 0.64 mmol) and DIPEA (170 µl, 1.00 mmol) in dry DMF (45 mL) at room temperature, a solution of **4.16** (0.16 mmol) in dry DMF (8 mL) was added using a syringe pump in 3 h. After 16 h the resulting mixture was concentrated in vacuo, diluted with DCM (40 mL) and washed with 1 M HCl (2 × 20 mL). The aqueous layer was extracted with DCM (80 mL) and the combined organic phases were washed with water (60 mL), dried over $MgSO_4$ and concentrated in vacuo.

Cyclization at high temperature

To a stirred solution of HATU (0.243 g, 0.64 mmol) and DIPEA (170 µl, 1.00 mmol) in dry DMF (45 mL) at 50 °C, a solution of **4.16** (0.16 mmol) in dry DMF (8 mL) was added using a syringe pump in 3 h. After 24 h of stirring and 50 °C, the resulting mixture was concentrated in vacuo, diluted with DCM (40 mL) and washed with 1 M HCl (2 × 20 mL). The aqueous layer was extracted with DCM (80 mL) and the combined organic phases were washed with water (60 mL), dried over $MgSO_4$, and concentrated in vacuo.

Microwave assisted cyclization[181]

4.16 was dissolved in dry DMF (10 mL) and to this solution, HATU (0.049 g, 0.13 mmol) and DIPEA (0.035 mL, 0.2 mmol) were added. The vial was inserted in the synthesizer and heated at 75 °C (25 W) for two cycles of 10 min each. Then, the solvent was evaporated, and the residue was diluted with DCM (30 mL) and washed with 1 M HCl (2 × 15 mL). The aqueous layer was extracted with DCM (60 mL) and the combined organic phases were washed with water (45 mL), dried over $MgSO_4$ and concentrated in vacuo.

[181] Cini, E.; Botta, C.B.; Rodriquez, M.; Taddei, M. *Tetrahedron Letters* **2009**, *50*, 7159–7161.

4.3.3.6 General procedure for reduction of cyclic triazolopeptoids. Synthesis of peraza-macrocycles 4.21-4.25 and their borane complexes 4.26-4.27.

To a solution of cyclic triazolopeptoid (0.025 mmol) in dry THF (300 µL), in a reacti-vial, a 1.0 M solution of borane tetrahydrofuran complex in THF (considering 5.0 equivalents for each amide group to-be-reduced) was added dropwise and the mixture was left to stir at 90 °C for for 24 h. Subsequently, the mixture was cooled at 0°C and water (1.0 mL) was slowly added to react with the excess of BH_3, and then the mixture was concentrated under high vacuum. Next, the residue was dissolved in HCl 1N (6 mL) and the mixture was heated to reflux for 3 h. Then, it was cooled to room temperature and KOH pellets were added until pH > 11. The resulting solution was then extracted with DCM (3 x 10 mL). The combined organic layers were dried over $MgSO_4$, and the solvent was removed. The resulting peraza-macrocycles were subjected to spectrometric, spectroscopic, and HPLC analysis after filtration through a short pad of neutral alumina (eluents: 100% dichloromethane to 90:10 dichloromethane:methanol).

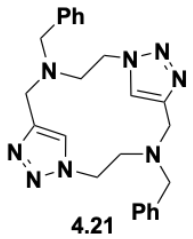

4.21

4.21: white amorphous solid, 0.002 g, 69% yield; Rt 6.5 min; HRMS (MALDI): *m/z* $[M+H]^+$ Calcd for $C_{24}H_{29}N_8^+$ 429.2510; Found 429.2529.

^{1}H NMR (600 MHz, $CDCl_3$) δ: 7.45 (4H, d, *J* 7.3 Hz, Ar-*H*), 7.39 (4H, t, *J* 7.4 Hz, Ar-*H*), 7.31 (2H, t, *J* 7.3 Hz, Ar-*H*), 6.99 (2H, s, C*H*NN), 4.27 (4H, t, *J* 4.6 Hz, NNCH_2CH$_2$), 3.81 (4H, s, NCH_2Ph), 3.51 (4H, s, NCH_2C), 2.98 (4H, t, *J* 4.7 Hz, BnNCH_2CH$_2$).

^{13}C NMR (150 MHz, $CDCl_3$) δ: 146.3 x 2 (CH$_2$*C*CHN), 138.9 x 2 (*C*-Ar), 128.9 x 4 (*C*-Ar), 128.6 x 4 (*C*-Ar), 127.5 x 2 (*C*-Ar), 122.2 x 2 (CH$_2$C*C*HN), 59.5 x 2 (N*C*H$_2$Ph), 55.4 x 2 (BnN*C*H$_2$CH$_2$), 48.8 x 2 (NN*C*H$_2$CH$_2$), 48.7 x 2 (N*C*H$_2$C).

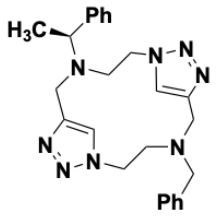

4.22

4.22: white amorphous solid, 0.005 g, 45% yield; Rt 6.9 min; HRMS (MALDI): *m/z* $[M+H]^+$ Calcd for $C_{25}H_{31}N_8^+$ 443.2666; Found 443.2667.

^{1}H NMR (600 MHz, $CDCl_3$) δ: 7.50 (2H, d *J* 7.6 Hz, Ar-*H*), 7.45 (2H, d *J* 7.3 Hz, Ar-*H*), 7.40-7.36 (4H, m, Ar-*H*), 7.30-7.27 (2H, m, Ar-*H*), 6.87 (1H, s, C*H*NN), 6.79 (1H, s, C*H*NN), 4.40-4.34 (2H, m, Ph(CH_3)CHNCH$_2$CH*H*NN, BnNCH$_2$CH*H*NN), 4.20-4.17 (1H, m, Ph(CH_3)CHNCH$_2$C*H*HNN), 4.16-4.10 (2H, m, Ph(CH_3)C*H*N and BnNCH$_2$C*H*HNN), 3.87 (1H, d, *J* 13.3 Hz, NC*H*HPh), 3.73 (1H, d, *J* 13.3 Hz, NCH*H*Ph), 3.56 (1H, d, *J* 13.8 Hz, CC*H*HNCH(CH_3)Ph), 3.50 (1H, d, *J* 13.9 Hz, CCH*H*NBn), 3.48 (1H, d, *J* 13.9 Hz, CC*H*HNBn), 3.35 (1H, d, *J* 13.9 Hz, CCH*H*NCH(CH_3)Ph), 3.17-3.14 (1H, m, Ph(CH_3)CHNCH*H*CH$_2$NN), 3.05-3.00 (2H, m, Ph(CH_3)CHNC*H*HCH$_2$NN and BnNCH*H*CH$_2$NN), 2.96-2.92 (1H, m, BnNC*H*HCH$_2$NN), 1.53 (3H, d, *J* 6.7 Hz, CH_3).

^{13}C NMR (150 MHz, $CDCl_3$) δ: 146.9 (Ph(CH_3)CHNCH$_2$*C*CHN), 146.4 (BnNCH$_2$*C*CHN), 143.0 (*C*-Ar), 138.9 (*C*-Ar), 128.9 x 2 (*C*-Ar), 128.5 x 2 (*C*-Ar), 128.3 x 2 (*C*-Ar), 127.9 x 2 (*C*-Ar), 127.4 (*C*-Ar), 127.1 (*C*-Ar), 122.1 (Ph(CH_3)CNCH$_2$C*C*HN), 121.8 (BnNCH$_2$C*C*H), 59.5 (N*C*H$_2$Ph), 58.4 (N*C*H(CH_3)Ph), 53.3 (BnN*C*H$_2$CH$_2$NN), 49.9 (Ph(CH_3)CHN*C*H$_2$CH$_2$NN), 49.3 (Ph(CH_3)CHNCH$_2$*C*H$_2$-NN), 48.9 (BnNCH$_2$*C*H$_2$NN), 48.6 (BnN*C*H$_2$C), 44.6 (Ph(CH_3)CHN*C*H$_2$C), 13.5 (*C*H$_3$).

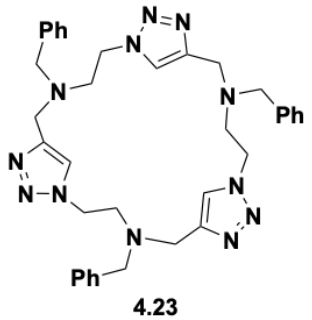

4.23

4.23: white amorphous solid, 0.015 g, 93% yield; Rt 7.1 min; HRMS (MALDI): *m/z* $[M+H]^+$ Calcd for $C_{36}H_{43}N_{12}^+$ 643.3728; Found 643.3700.

^{1}H NMR (600 MHz, $CDCl_3$) δ: 7.56 (3H, s, C*H*NN), 7.23-7.15 (15H, m, Ar-*H*), 4.45 (6H, t, *J* 5.9 Hz, NNC*H*$_2$CH$_2$), 3.75 (6H, s, NC*H*$_2$C), 3.68 (6H, s, NC*H*$_2$Ph), 2.96 (6H, t, *J* 5.9 Hz, BnNC*H*$_2$CH$_2$).

^{13}C NMR (150 MHz, $CDCl_3$) δ: 144.7 x 3 (CH$_2$*C*CHN), 138.1 x 3 (*C*-Ar), 128.7 x 6 (*C*-Ar), 128.4 x 6 (*C*-Ar), 127.3 x 3 (*C*-Ar), 123.5 x 3 (CH$_2$C*C*HN), 59.0 x 3 (NCH$_2$Ph), 53.0 x 3 (BnNCH$_2$CH$_2$), 48.9 x 3 (NCH$_2$C), 48.3 x 3 (NNCH$_2$CH$_2$).

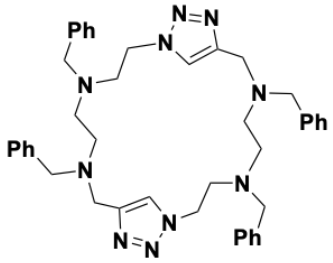

4.24

4.24: white amorphous solid, 0.007 g, 38% yield; Rt 9.4 min; HRMS (MALDI): *m/z* $[M+H]^+$ Calcd for $C_{42}H_{51}N_{10}^+$ 695.4293; Found 695.4271.

^{1}H NMR (600 MHz, $CDCl_3$) δ: 7.65 (2H, s, C*H*NN), 7.29-7.16 (16H, m, Ar-*H*), 7.04-7.02 (4H, m, Ar-*H*), 4.39 (4H, t, *J* 5.6 Hz, NNC*H*$_2$CH$_2$), 3.82 (4H, s, NC*H*$_2$C), 3.58 (4H, s, NC*H*$_2$Ph), 3.53 (4H, s, NC*H*$_2$Ph), 2.95 (4H, t, *J* 5.6 Hz, NNCH$_2$C*H*$_2$), 2.70 (4H, t, *J* 6.4 Hz, CHCH$_2$NBnC*H*$_2$CH$_2$), 2.48 (4H, t, *J* 6.8 Hz, CHCH$_2$NBnCH$_2$C*H*$_2$).

^{13}C NMR (150 MHz, $CDCl_3$) δ: 143.5 x 2 (CH$_2$*C*CHN), 138.9 x 2 (*C*-Ar), 138.6 x 2 (*C*-Ar), 129.0 x 4 (*C*-Ar), 128.6 x 4 (*C*-Ar), 128.3 x 8 (*C*-Ar), 127.1 x 2 (*C*-Ar), 127.0 x 2 (*C*-Ar), 124.1 x 2 (*C*-Ar), 59.5 x 2 (NCH$_2$Ph), 58.7 x 2 (NCH$_2$Ph), 54.2 x 2 (NNCH$_2$*C*H$_2$), 51.3 x 4 (HCH$_2$NBn*C*H$_2$CH$_2$ and HCH$_2$NBnCH$_2$*C*H$_2$), 48.4 x 2 (NCH$_2$C), 48.3 x 2 (NNCH$_2$CH$_2$).

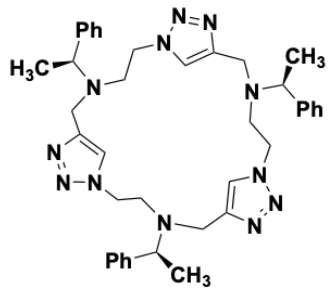

4.25

4.25: white amorphous solid, 0.007 g, 42% yield; Rt 8.2 min; HRMS (MALDI): *m/z* $[M+H]^+$ Calcd for $C_{39}H_{49}N_{12}^+$ 685.4198 Found 685.4207.

^{1}H NMR NMR (300 MHz, $CDCl_3$) δ: 7.65 (3H, br s), 7.34-7.25 (15H, m), 4.46-2.6 (21H, m), 1.39-1.19 (9H, m).

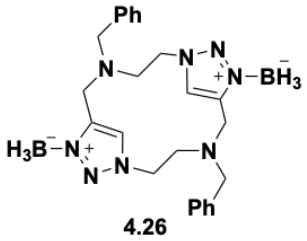

4.26

4.26: white amorphous solid, 20% yield; characterized by X-ray diffraction analysis.

^{1}H NMR (300 MHz, $CDCl_3$) δ: 7.42-7.41 (10H, m), 6.77 (2H, s), 4.36 (4H, t, *J* 4.9 Hz), 3.81 (4H, s), 3.76 (4H, s), 3.16 (4H, t, *J* 4.9 Hz).

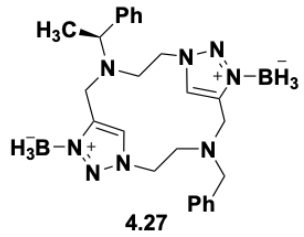

4.27

4.27: white amorphous solid, 5% yield; characterized by X-ray diffraction analysis.

^{1}H NMR (300 MHz, $CDCl_3$) δ: 7.45-7.30 (10H, m), 6.66 (1H, s), 6.45 (1H, s), 5.00-4.97 (1H, m), 4.93-4.91 (1H, m), 4.74-4.67 (2H, m), 4.52-4.22 (2H, m), 4.28-4.24 (1H, m), 4.20-4.13 (1H, m), 3.94-3.84 (2H, m), 3.69-3.60 (2H, m), 3.40-3.34 (1H, m), 3.22-3.18 (1H, m), 3.14-3.11 (1H, m), 1.25 (3H, overlapping with lipid signal).

4.4. Cyclopeptoid derivatives with polar side chains *via* CuAAC

4.4.1. Results and discussion

To obtain cyclotetra- and cyclohexapeptoid systems functionalized with polar side chains, subsequent strategy has been planned:

- Synthesis of linear peptoids
- Head-to-tail macrocyclization of linear precursors
- Solution synthesis of azides
- CuAAC-mediated functionalization of cyclic peptoids.

4.4.1.1 Synthesis of macrocyclic peptoid scaffolds 4.28-4.30

Linear *N*-propargylated oligoamides of different chain's length (**4.28**, **4.29**, and **4.30**) were obtained in quantitative yields, by following the standard "sub-monomeric" protocols for the peptoid solid phase synthesis. Oligomer **4.33** (precursor of the cyclic product **4.30**) was designed to provide target macrocycles with intermediate polarity. The HATU-mediated cyclization of linear peptoids and subsequent precipitation from hot acetonitrile solution afforded macrocycles (**4.28**, **4.29**,[156] **4.30**, **Figure 4. 34**) with acceptable yields (19%, 31%, 33%, respectively). Cyclic peptoids were then characterized by NMR spectroscopy (^{1}H NMR and ^{13}C NMR), HR-MS and HPLC analysis.

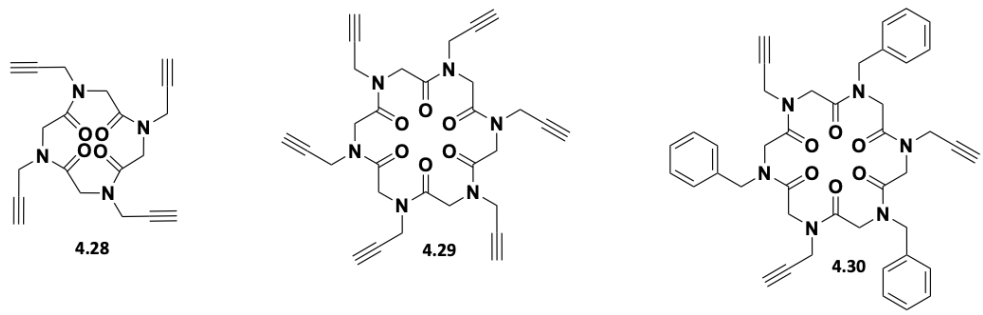

Figure 4. 34. Schematic structures of cyclopeptoidic platforms containing *N*-propargyl side chains.

4.4.1.2 Preparation of azides

Synthesis of azides (**Figure 4. 35**), as a source of polar functionalities, to-be-introduced into the side chains *via* CuAAC-mediated conjugation with *N*-propargylated cyclopeptoids, was carried out in solution through classical transformations. The azides **4.34**,[182] **4.35**,[183] **4.36**,[184] and **4.39,**[185] were obtained from corresponding bromides, by nucleophilic substitution reaction with sodium azide (**Scheme 4. 7**).

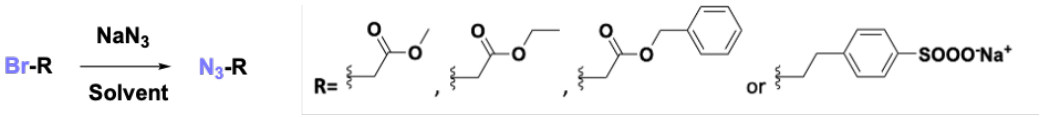

Scheme 4. 7. General scheme for azides' **4.34**, **4.35**, **4.36**, and **4.39** synthesis.

Azides **4.37** and **4.38** were prepared from glycerol by following a multi-step biocatalytic approach[186] (**Scheme 4. 8**).

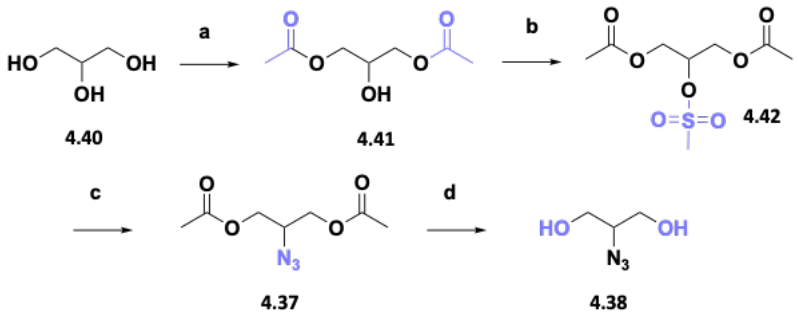

Scheme 4. 8. Synthesis of azides **4.37** and **4.38**. (a) Novozym 435, THF, vinyl acetate, 1.5 h, 25 °C; (b) MsCl, Triethylamine, DCM, 0-25 °C; (c) NaN_3, DMF, 12 h, 90 °C; (d) K_2CO_3, C_2H_5OH, 12 h, 25 °C.

In particular, the first step involves regioselective acetylation of the primary hydroxyl groups of glycerol, **4.40**, by a chemoenzymatic approach using Novozym-435 and vinyl acetate as the acyl donor. Novozym-435 is a Candida antarctica lipase (CALB) immobilized on a macroporous

[182] Baykal. A.; Plietker, B. *Eur. J. Org. Chem*. **2019**, 1145-1147.
[183] O'Brien, A.G.; Lévesque, F.; Seeberger, P.H. *Chem. Commun*. **2011,** *47*, 2688-2690.
[184] Pokorski, J.K.; Miller Jenkins, L.M.; Feng, H.; Durell, S.R.; Bai, Y.; Appella, D. *Org. Lett*. **2007**, *9*, 2381–2383.
[185] Roeder, R.D.; Rungta, P.; Tsyalkovskyy, V.; Banderaa, Y.; Foulger, S.H. *Soft Matter* **2012**, *8*, 5493-5500.
[186] Gupta, S.; Schade, B.; Kumar, S.; Böttcher, C.; Sharma, S.K.; Haag, R. *Small*, **2013**, *9,* 894-904.

acrylic polymer resin.[187] The enzyme shows a high degree of specificity of the substrate, with respect to both regio- and enantioselectivity. CALB lipase has been widely used in the resolution of racemic alcohols, amines, and acids and in the preparation of optically active compounds from meso substrates. The resulting optically pure products are very difficult to obtain by alternative routes and thus can be of great synthetic value. Moreover, CALB has been used also as a regioselective catalyst in the selective acylation of various carbohydrates. Vinyl acetate is a classic acyl donor of lipases. Once the acyl group is released, it forms an enol, which isomerizes immediately to acetaldehyde making the transesterification stage irreversible.

The subsequent mesylation of the secondary hydroxyl group of the acetylated compound **4.41** was performed to favor substitution with azide in the next step, furnishing another target azide **4.37**. Additionally, deacetylation of **4.37** in the presence of potassium carbonate in ethanol, led to the last designed azide **4.38**. Flash chromatography purification of compounds **4.37** and **4.38** (dichloromethane/methanol eluent mixture) afforded pure products in yields of 27% and 15%, respectively.

Azide structure	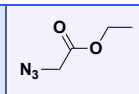	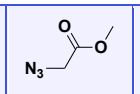	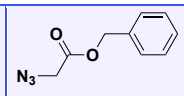	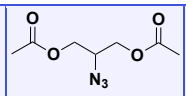	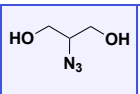	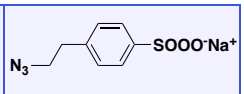
Azide number	**4.34**	**4.35**	**4.36**	**4.37**	**4.38**	**4.39**

Figure 4. 35. Structures of investigated azides.

4.4.1.3 Cycloaddition trials: Synthesis of polar cyclopeptoids 4.40-4.51

Once the building blocks (cyclic peptoids **4.28**-**4.30,** and azides **4.34**-**4.39**) have been prepared, we proceeded with cycloaddition reactions. We decided to begin our investigations with the structurally simplest models. In order to obtain macrocycles **4.43** and **4.44** (**Figure 4. 36**) functionalized with free carboxyl groups, we planned to perform the CuAAC reaction between

[187] Ortiz, C.; Ferreira, M.L.; Barbosa, O.; Dos Santos, J.C.S.; Rodrigues, R.C.; Berenguer-Murcia, A.; Briand, L.E.; Fernandez-Lafuente, R. *Catal. Sci. Technol*. **2019**, *9*, 2380-2420.

N-propargylated cyclopeptoids and the appropriate azide in the ethyl ester form, **4.34**, followed by a global hydrolysis of final macrocyclic products.

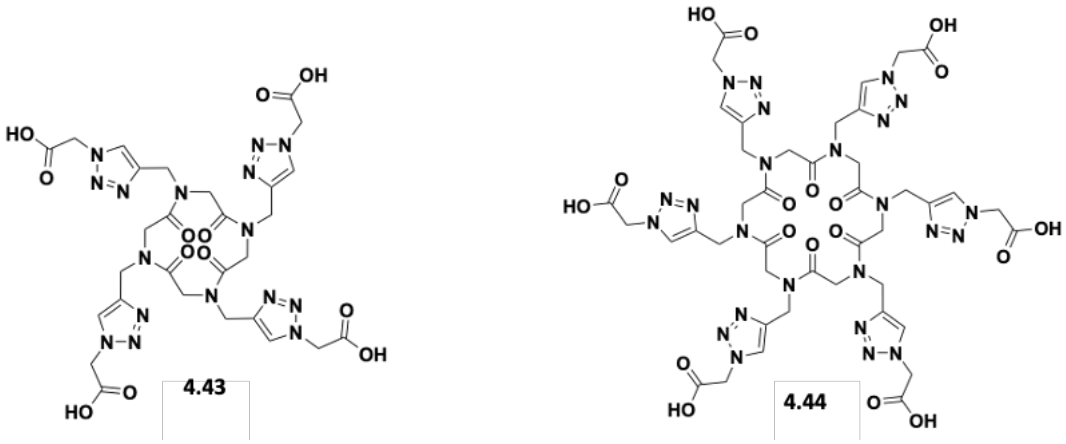

Figure 4. 36. Schematic structures of target macrocycles **4.43** and **4.44**.

The first cycloaddition reaction between **4.28** and **4.34** was performed in the presence of copper sulfate pentahydrate reduced *in situ* by sodium ascorbate in a solvent mixture composed of water and *tert*-butanol in a 2:1 ratio (**Scheme 4. 9**).

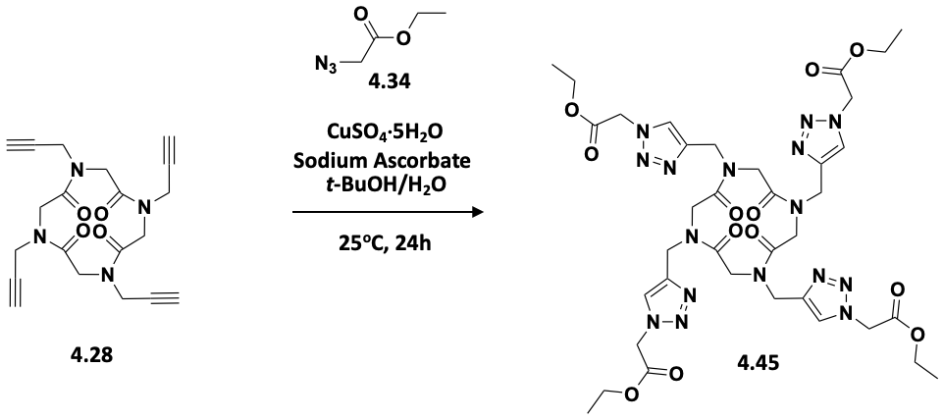

Scheme 4. 9. Synthetic scheme towards cycloaddition product **4.45**.

Compound **4.45**, purified by precipitation from hot acetonitrile solution, was obtained in 43% yield. A clear evidence of target product formation was furnished by NMR analysis. By comparing the ^{1}H NMR spectra of cyclopeptoid precursor **4.28** and the first cycloaddition product **4.45**, a disappearance of propargyl protons' resonances can be observed, with the simultaneous emergence of triazole signals in the aromatic region (**Figure 4. 37**).

Moreover, the presence of two distinct resonances for triazole protons suggests formation of a conformationally stable macrocycle with a *ctct* geometry (in accordance with the known nature of cyclopeptoid tetramers).[168]

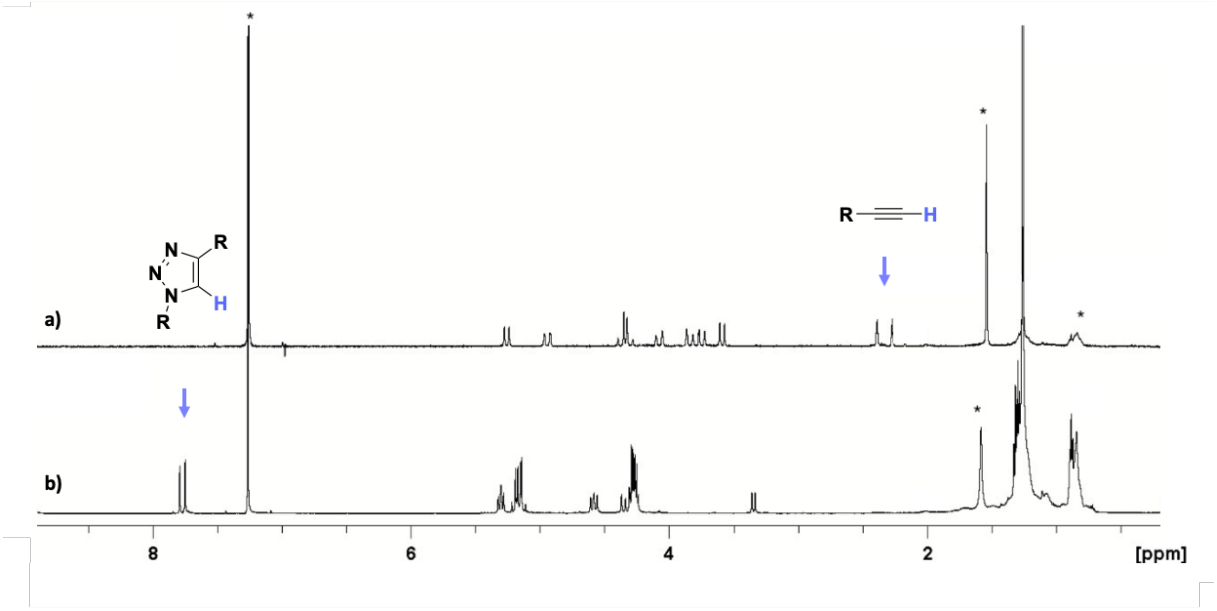

Figure 4. 37. Comparison of ^{1}H NMR spectra of **4.28** (a) and **4.45** (b); 400 MHz, $CDCl_3$.

Analogously, the cycloaddition reaction on cyclohexameric compound **4.29** was carried out using azide **4.34** (**Scheme 4. 10**). Compound **4.46** was purified by dissolution in dichloromethane and precipitation by dropwise addition of *n*-pentane to afford a white solid with a yield of 42%.

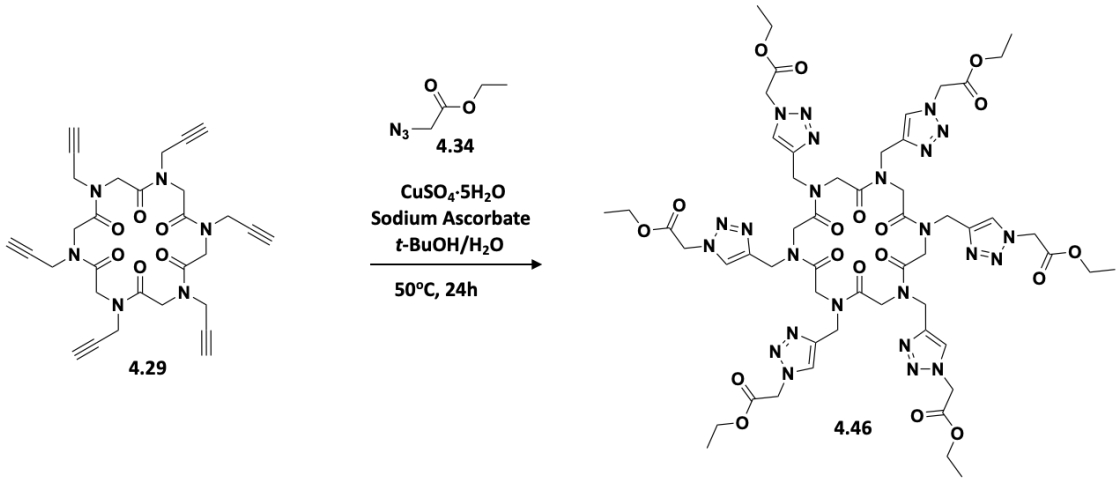

Scheme 4. 10. Synthetic scheme towards cycloaddition product **4.46**.

The next step consisted in the hydrolysis of the ester functions to afford the target cyclopeptoids **4.43** and **4.44**, containing free carboxyl groups. To this end, we attempted to perform hydrolysis reaction in the presence of LiOH in THF/H_2O mixture.[188] Unfortunately, in both cases we were unable to isolate and identify the products by means of spectroscopic and spectrometric methods.

In view of these results, we decided to prepare the precursor azide in the form of a methyl ester, **4.36**, with the expectation that this time we would manage to obtain the final products by means of a last-step hydrolysis. To verify this assumption, we prepared a methyl ester-containing tetrameric derivative **4.47** *via* CuAAC with good yield (65%), and we proceeded with hydrolysis attempts by varying the base equivalents, reaction time and temperature, but unfortunately again it was not possible to isolate compound **4.43** (Scheme 4. 11).

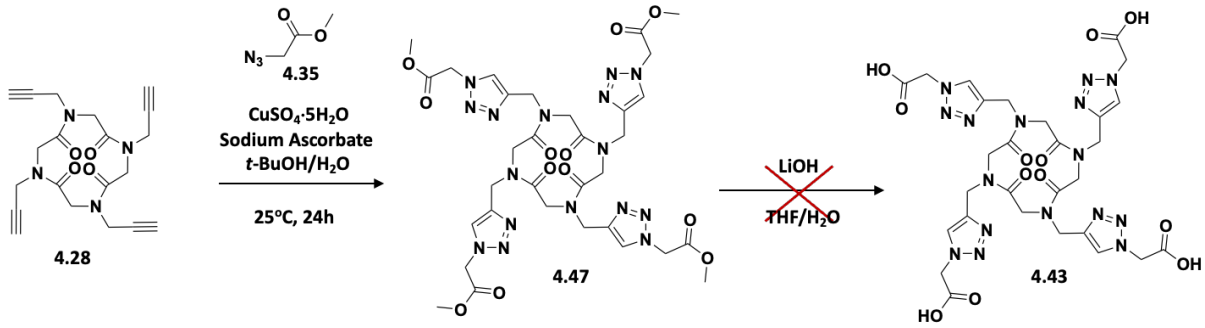

Scheme 4. 11. Synthetic scheme towards cycloaddition product **4.47** with subsequent hydrolysis attempt.

To overcome difficulties relative to hydrolysis efficiency and isolation of final products we decided to modify the initial strategy and move our focus toward protection of carboxyl functionalities *via* benzyl esters. The implementation of this protecting group is advantageous as it can be easily removed under hydrogenolysis conditions, using Pd/C as a catalyst and it does not require challenging purification step. The azide **4.37** required for Huisgen's 1,3-dipolar cycloaddition leading to compounds **4.48** and **4.49** was obtained by nucleophilic substitution of the corresponding bromide according to the methodology already reported in the literature.[184] The azide **4.37** was subjected to the CuAAC reaction with *N*-proparyglated

[188] Lee, J.; Ha, M.W.; Kim, T.S.; Kim, M.J.; Ku, J.M.; Jew, S.S.; Park, H.G.; Jeong, B.S. *Tetrahedron* **2009**, *65*, 43, 8839-8843.

cyclopeptoid **4.28** leading to formation of corresponding macrocyclic adduct **4.48** (Scheme 4. 12). Compound **4.48** was isolated in good yield (67%) by a chromatographic purification. Analogous reaction performed on cyclic hexamer **4.29** led to formation of the corresponding cycloaddition product **4.49** (Scheme 4. 13), however with lower yield (19%). Once both macrocycles had been prepared, we proceeded with hydrogenolysis reaction using Pd/C as catalyst and DMF as the most suitable solvent. In the case of cyclic tetrapeptoid derivative **4.48**, we succeeded to obtain deprotected product **4.43** in quantitative yield. However, in the case of the larger macrocycle **4.46**, the formation of product **4.44** could only be assessed by means of mass spectrometry (*m/z*=1177.3524, $[M+H]^+$). Its ^1H NMR analysis resulted in a highly complex spectrum, and it was not possible to clearly determine the outcome of the reaction. However, the successful formation of product **4.44** showed a more promising potential of this methodology. Nevertheless, further studies will be needed to optimize the reaction conditions to give access to a wider variety of structures.

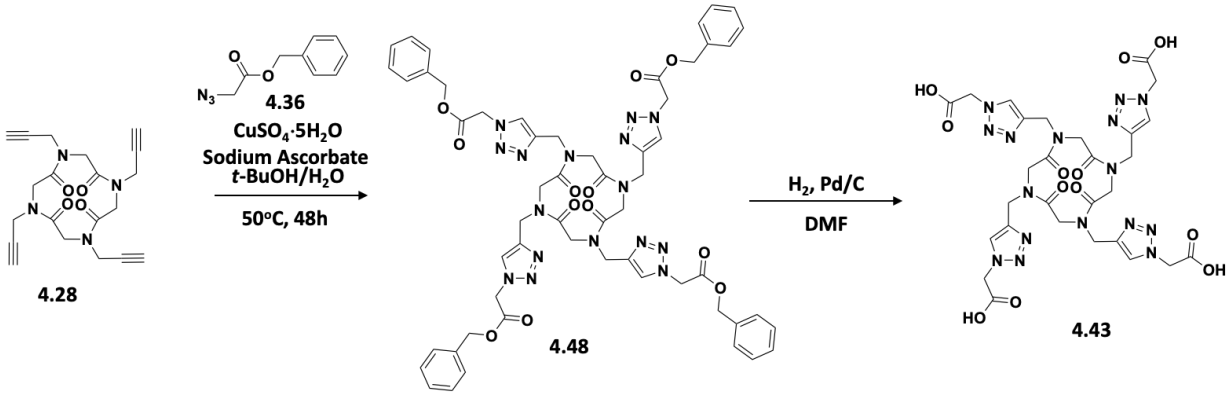

Scheme 4. 12. Synthetic scheme towards cycloaddition product **4.48** with subsequent hydrogenolysis leading to **4.43**.

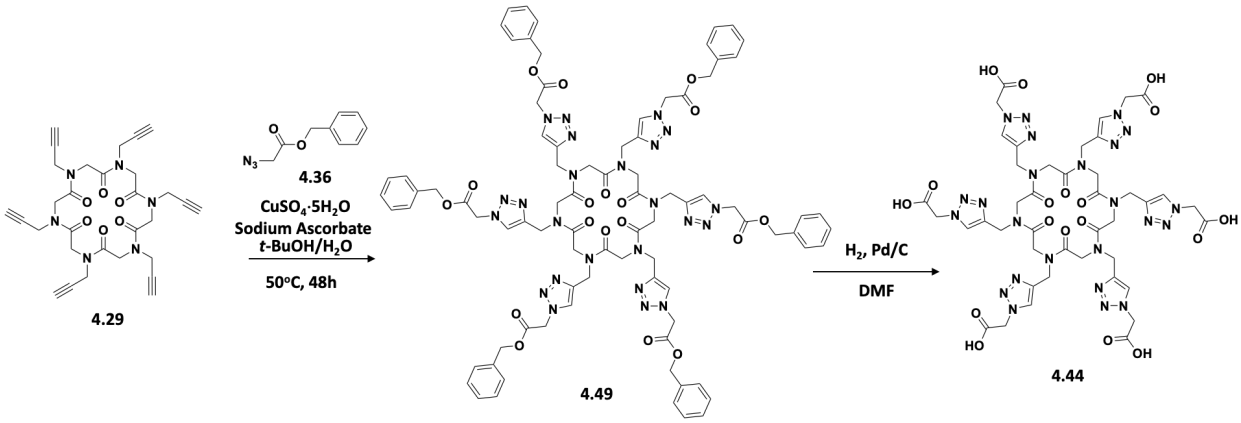

Scheme 4. 13. Synthetic scheme towards cycloaddition product **4.49** with subsequent hydrogenolysis leading to **4.43**.

The synthetic procedures described so far were applied as well for more structurally complex azides (**4.37** and **4.38**). In particular, we first examined the cycloaddition reaction between azide **4.37** and cyclopeptoid **4.28** to obtain compound **4.50** (Scheme 4. 14). However, a modification of some parameters was needed to obtain the target product. Specifically, we replaced *tert*-butanol with DMF, and we increased both the temperature and reaction time (70 °C, 48h). The pure product **4.50** was obtained after a chromatographic purification with yield of 17%. The same synthetic procedure was implemented with success to obtain a larger macrocyclic derivative **4.51** (Scheme 4. 15). The cyclic hexamer **4.51** was obtained with 61% yield by precipitation from hot acetonitrile solution.

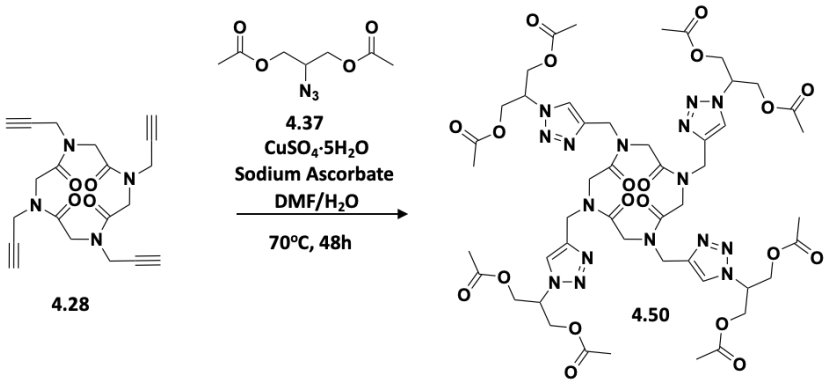

Scheme 4. 14. Synthetic scheme towards cycloaddition product **4.50**.

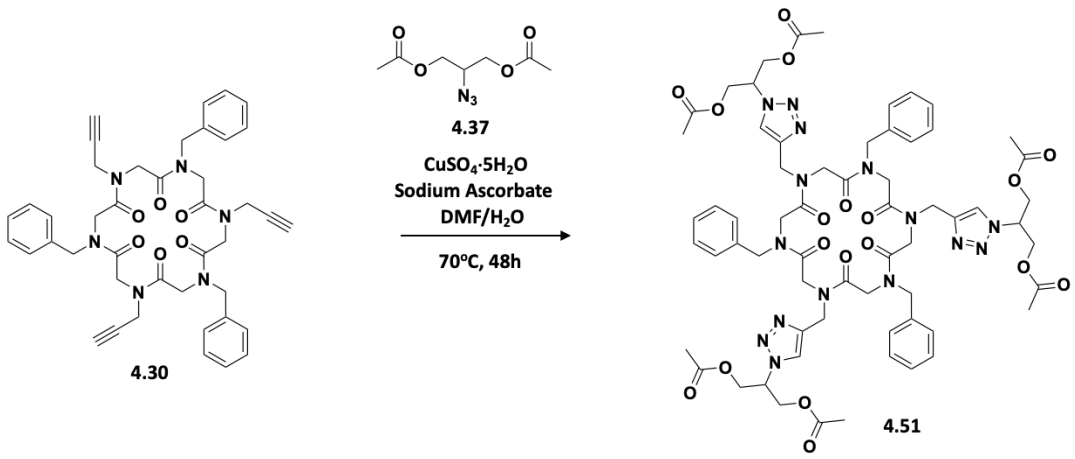

Scheme 4. 15. Synthetic scheme towards cycloaddition product **4.51**.

To obtain cyclopeptoids functionalized with hydroxyl groups, initially, we have planned to perform a "click" reaction employing azide **4.38** (deacetylated analogue of **4.37**). However, attempts of cycloaddition in the presence of **4.38** did not furnish desired macrocyclic products.

Regarding these results, we opted for an alternative way. Particularly, we tried to perform deacetylation directly on the cycloaddition product **4.50** in the presence of potassium carbonate in ethanol (**Scheme 4. 16**). To our delight it was possible to obtain the desired peptoid **4.52** in quantitative yield. This outcome demonstrated that the alternative strategy, in principle, could be applicable as well to other cyclopeptoids.

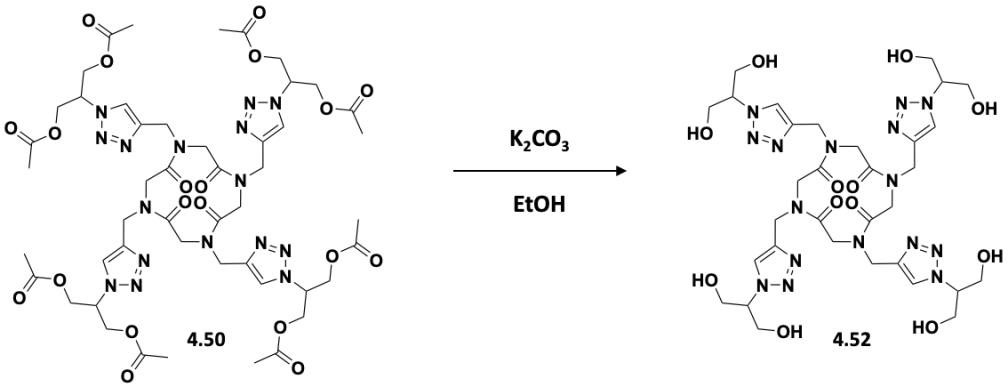

Scheme 4. 16. Synthesis of **4.52** from **4.50**.

The cycloaddition reaction involving benzensulfone motif turned out to be more challenging. In order to obtain a cyclic tetrapeptide functionalized with this polar group, it was necessary to carry out a number of trials and optimize parameters such as temperature, reaction time, equivalents of azide per propargyl group and to find the optimal solvents mixture (**Table 4. 3**).

Azide (eq per propargyl unit)	Sodium ascorbate (eq per propargyl unit)	$CuSO_4 \cdot 5H_2O$ (eq per propargyl unit)	Reaction time [h]	Temperature [°C]	Solvents	Yield
3 eq x 4	2.8 eq x 4	0.7 eq x 4	48 h	50 °C	*t*-BuOH/H_2O (2:1)	-
3 eq x 4	2.8 eq x 4	0.7 eq x 4	48 h	50 °C	DMF/H_2O (2:1)	-
3 eq x 4	2.8 eq x 4	0.7 eq x 4	72 h	70 °C	DMF/H_2O (2:1)	-
2 eq x 4	1 eq x 4	0.7 eq x 4	48 h	70 °C	DMF/H_2O (2:1)	95%
1.2 eq x 4	1 eq x 4	0.7 eq x 4	48 h	70 °C	DMF/H_2O (2:1)	94%

Table 4. 3. Conditions' optimization: synthesis of **4.53**.

The first attempt, replicating the reaction conditions of earlier cycloadditions, did not bring the expected result: we isolated only the cyclic precursor and an excess of azide. To improve the solubility of both substrates, we decided to replace *tert*-butanol with DMF, which allowed us to observe the product formation *via* ^{1}H NMR analysis, however, in the presence of

unreacted precursor **4.28**. During our studies, we also noticed that increasing the reaction time did not bring a positive effect. In another attempt, in turn, we noted that temperature is a key factor for this reaction. We managed to obtain the product in a reaction performed at 70 °C. Moreover, it was also possible to reduce the equivalents of the azide from 3 to 1.2 per propargyl group, which greatly facilitated the final purification. This allowed us to obtain the target macrocycle with 94% yield by precipitation from hot methanol solution. ^{1}H NMR analysis revealed a formation of a single conformationally stable species, in agreement with the nature of cyclic tetrapeptides.

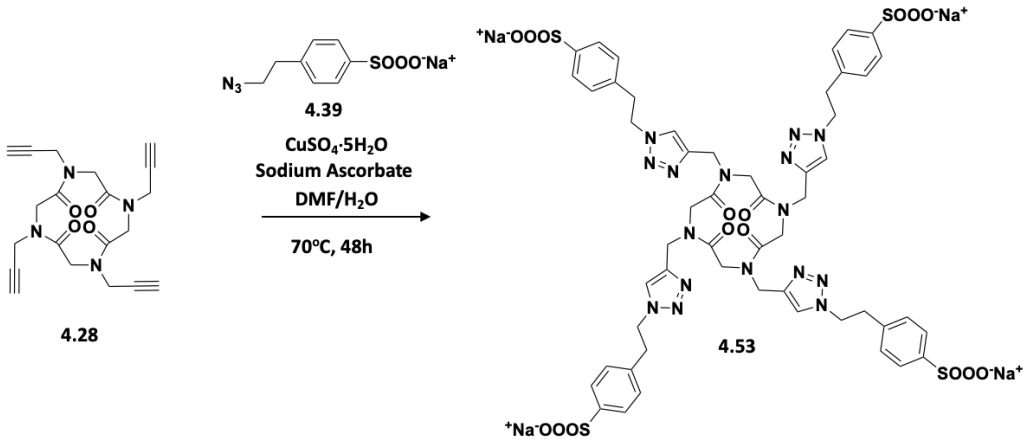

Scheme 4. 17. Synthetic scheme towards cycloaddition product **4.53**.

Motivated by this long-awaited result, we tried to extend this procedure for a larger cyclopeptoid **4.29**. An analogous attempt for a cyclic hexamer (Scheme 4. 18) led to the formation of the product **4.54** (as confirmed by HR-MS analysis, *m/z*=2041.3458, $[M\text{-}Na]^{-}$), but unfortunately, we were unable to isolate the pure target compound. Therefore, further optimizations are needed in this case.

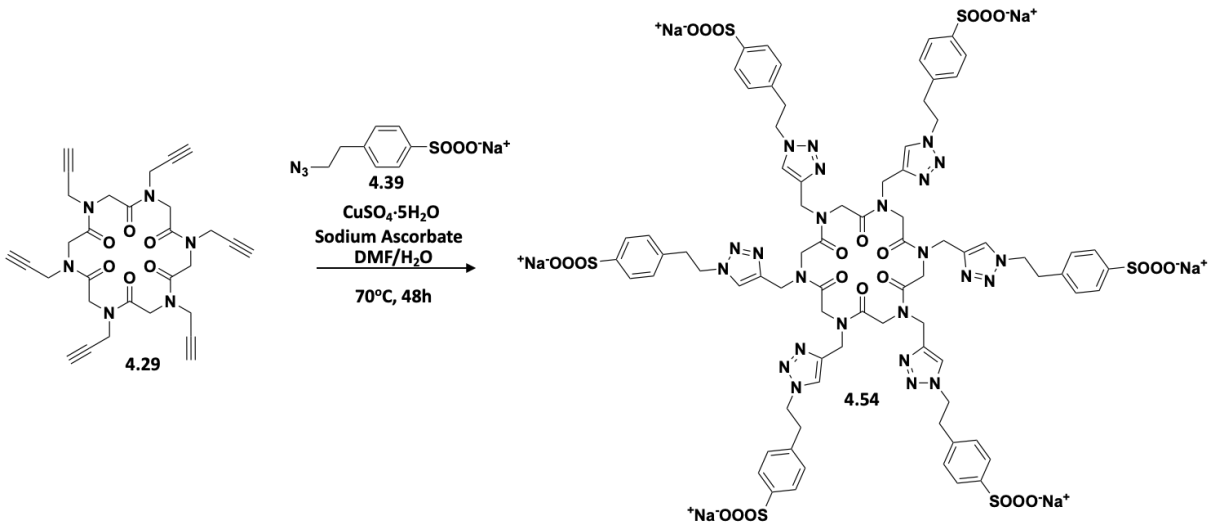

Scheme 4. 18. Synthetic scheme towards cycloaddition product **4.54**.

4.4.2. Conclusions

In this work, we synthesized new cyclopeptoids containing triazole residues functionalized with polar (i.e., carboxyl, alcohol and benzensulfone) groups. The synthetic methodology proved to be efficient and easily applicable. In particular, solid-phase oligomerization followed by head-to-tail macrocyclizations afforded cyclopeptoids **4.28**-**4.30**. These macrocycles were used as platforms for subsequent derivatization with polar groups *via* CuAAC reaction (employing a series of suitably designed azides **4.34**-**4.39**). By following this methodology, we obtained a library of macrocyclic peptoids decorated with polar side chains (**4.43**-**4.54**).

However, it should be noted that more polar compounds **4.43**, **4.44**, **4.52**, **4.53** and **4.54** were found to be challenging to obtain and purify and required a series of trials and optimizations (some additional synthetic improvements are still needed in case of **4.44** and **4.54**). Nevertheless, the new derivatives are attractive molecules with potential complexation abilities owing to both the peptoid skeleton and the triazole residue with its polar substituents. Moreover, the novel triazole-containing macro rings could be subsequently transformed into the corresponding peraza-macrocycles, following the reduction procedure applied previously for cyclic peptoids and triazolopeptoids, leading to new hosts possessing multiple coordinating elements (aza core, triazole rings, polar side chains).

4.4.3. Experimental section

4.4.3.1 General methods

Starting materials and solvents were purchased from Sigma-Aldrich, TCI Chemicals, and Fluorochem and were used without further purification. For reactions conducted in an inert atmosphere (nitrogen), the necessary glassware was previously kept in an oven at temperatures above 100°C, and anhydrous solvents were used. All reactions in solution were followed by thin-layer chromatography (TLC), on Macherey-Nagel silica gel plates (0.25 mm), and the spots were detected with a UV/Vis lamp at a wavelength of 254 nm, either with a potassium permanganate solution or with iodine vapor. The obtained products were purified by flash chromatography on Merck silica gel column (60 Mesh, particle size 0.040-0.063 mm) or by chromatography on Polygoprep 60-50 C18 Macherey-Nagel silica (carbon content 12%, pore size 60 Å, particle size 40-63 µm). Polypropylene reactors provided by Varian were used for reactions performed on solid phase and for purification on reverse phase column to avoid sodium complexation by cyclopeptoids. Qualitative analyses on the obtained products were carried out by HPLC with a C18 reversed-phase analytical column (Waters, Bondapak, 10 µm, 125 Å, 3.9 x 300 mm), using a mixture of 5% acetonitrile in water (+ 0.1% TFA) to 100% acetonitrile (+ 0.1% TFA) as eluent, with linear gradient in 30 min and flow rate 1mL/min. The instrument used is Jasco series BS 997- 01 liquid chromatography, equipped with a Jasco PU-2089 Plus quaternary pump, a rheodyne 7725i injector, and a Jasco MD-2010 Plus detector, variable wavelength and at a wavelength programmed to 220 nm. Proton and ^{13}C NMR spectra were recorded by dissolving the products in deuterated chloroform ($CDCl_3$), deuterated methanol (MeOD), deuterated water (D_2O) and deuterated dimethyl sulfoxide (DMSO-d_6) using Bruker DRX-600 spectrometers (1H at 600. 13 MHz, 13C at 150.90 MHz), Bruker DRX-400 (1H at 400.13 MHz, 13C at 100.03 MHz) and Bruker DRX 300 (1H at 300.1 MHz). The signals were calibrated at 7.26 ppm (1H NMR) and 77.0 ppm (13C NMR) for deuterated chloroform, 3.34 ppm (^{1}H-NMR) and 49.0 ppm (^{13}C NMR) for deuterated methanol, 4.79 (^{1}H NMR) for deuterated water, and 2.54 for deuterated dimethyl sulfoxide (^{1}H NMR). Chemical shifts are reported in ppm, coupling constants *J* in Hertz, and multiplicities as follows: s (singlet), d (doublet), dd (double doublet), t (triplet), m (multiplet), and br (broad) if the signal is broadened. Assignments were made using two-dimensional COSY, HSQC and HMBC spectra.

Mass spectra of the obtained products were recorded using a high-resolution Fourier transform cyclotron ion resonance mass spectrometer using MALDI ionization.

4.4.3.2 Procedures for azides' synthesis

Synthesis of azide 4.34[182]

NaN_3 (4.07 mmol, 0.265 g) was added to the solution of the corresponding bromide (2.71 mmol, 0.453 g) in water/acetone mixture (1.08/4.32 mL). The reacting mixture was left stirring overnight at room temperature. The next day, 5.0 mL of dichloromethane was added, and the aqueous phase was extracted 3 times with 5.0 mL of dichloromethane. Then the organic phase was anhydrified with Na_2SO_4 and the solvent was removed, to obtain azide **4.34** in 63% yield.

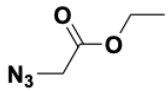

4.34

4.34: colorless oil, 0.331, 63% yield.

^{1}H NMR ($CDCl_3$, 300 MHz) δ: 4.26 (2H, q, *J* 7.1 Hz), 3.86 (2H, s), 1.31 (3H, t, *J* 7.2 Hz).

Synthesis of azide 4.35[183]

To a solution of methyl 2-bromoacetate (10.6 mmol, 1.61 g) in methanol (0.8 mL), was added a solution of sodium azide (12.7 mmol, 0.825 g) in water (0.6 mL). The resulting suspension was stirred at rt for 20 min at rt and then heated to 80 °C and left to stir for 2 h. After cooling to rt, the reaction mixture was concentrated under reduced pressure to remove methanol. The residue was poured into water (10 mL) and extracted with diethyl ether (3 x 20 mL). The combined organic extracts were dried (Na_2SO_4) and carefully concentrated under reduced pressure.

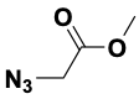

4.35

4.35: colorless oil, 1.098 g, 90% yield.

^{1}H NMR ($CDCl_3$, 400 MHz) δ: 3.89 (2H, s), 3.80 (3H, s).

Synthesis of azide 4.36[184]

To a solution of benzylbromoacetate (6.31 mmol, 1.00 mL) in anhydrous DMF (12.6 mL), sodium azide (25.2 mmol, 1.64 g) was added, and the resulting mixture was left stirring at room temperature overnight. The next day, DMF was removed, and the resulting crude mixture was dissolved in ethyl acetate (30 mL) and washed with saturated aqueous solution of NaCl (5 x 15 mL). The organic phase was then anhydrified with Na_2SO_4 and the solvent was removed leading to the product **4.36** in quantitative yield.

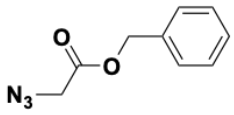

4.36

4.36: colorless oil, 1.206 g, 100% yield.

^{1}H-NMR ($CDCl_3$, 300 MHz) δ: 7.39 (5H, m), 5.25 (2H, s), 3.92 (2H, s).

Synthesis of azide 4.37[186]

To the solution of glycerol (33.2 mmol, 3.06 g) and vinyl acetate (83.0 mmol, 7.68 mL) in anhydrous THF was added Novozyme-435 lipase (10 wt% of the two reagents), and the reaction was left stirring at 25 °C overnight. After that time, the enzyme was removed by filtration and the solvent was removed to obtain the diacetylated compound in the form of a colorless oil. To the solution of the latter in dichloromethane (176.0 mL) was added methanesulfonyl chloride (133 mmol, 10.2 mL) and triethylamine (133 mmol, 18.5 mL) in an at 0 °C, and the mixture was left stirring at 25 °C overnight. The progress of the reaction was checked by TLC, and once it was finished, washes with distilled H_2O (3 x 50.0 mL) were performed to remove excess of triethylamine. After anhydrification with Na_2SO_4 and removal of the solvent, the crude was dissolved in anhydrous DMF (189.0 mL), and NaN_3 (166 mmol, 10.7 g) was added to the resulting solution. The reaction mixture was left stirring overnight at 90°C in an N_2 atmosphere. Purification of compound **4.37** was performed by column chromatography using a dichloromethane/methanol eluent mixture to obtain a yield of 27%.

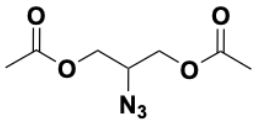

4.37

4.37: light-yellow oil, 1.803, 27% yield (over three steps).

^{1}H NMR (400 MHz, $CDCl_3$) δ: 4.26 (2H, dd, *J* 12.0, 4.8 Hz, CH*H*CHCH*H*), 4.12 (2H, dd, *J* 12.0, 6.8 Hz, C*H*HCHC*H*H), 3.89-3.83 (1H, m, CH_2CHCH_2), 2.07 (6H, s, $COCH_3$).

Synthesis of azide 4.38[186]

To the solution of **4.37** (8.96 mmol, 1.80 g) in ethanol (63.0 mL) was added potassium carbonate (38.5 mmol, 5.33 g) and the resulting mixture was left stirring at 25°C overnight. Then, a gravity filtration was performed to remove excess potassium carbonate and the solvent was removed. Purification of compound **4.38** was performed on silica gel, using a dichloromethane/methanol eluent mixture to obtain the target azide with a yield of 15%.

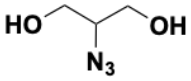

4.38

4:38: light-yellow oil, 0.5832, 15% yield (over four steps).

^{1}H NMR (400 MHz, MeOD, δ): 3.68 (2H, dd, *J* 12.0, 4.0 Hz, CH*H*CHCH*H*), 3.56 (2H, dd, *J* 12.0, 8.0 Hz, C*H*HCHC*H*H), 3.50-3.47 (1H, m, CH_2CHCH_2).

Synthesis of azide 4.39[185]

Inside an ACE tube, sodium 4-(2-bromoethyl) benzensulfonate (10.4 mmol, 3.00 g), sodium azide (11.5 mmol, 0.747 g) and 15 mL of DMF were introduced. The resulting mixture was left to stir at 80 °C. After that time, the reaction mixture was transferred to a flask and 15 mL of DCM were and the formation of a white precipitate was observed. Then, solvent was removed by vacuum filtration, and several washes with DCM were performed on the recovered white solid. Spectroscopic analysis confirmed isolation of pure compound **4.39**.

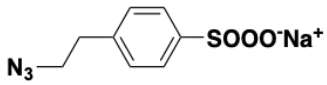

4.39

4.39: white amorphous solid, 2.322 g, 89% yield.

^{1}H NMR: (400 MHz, DMSO) δ: 7.58 (2H, d, *J* 7.8 Hz, Ar-*H*), 7.23 (2H, d, *J* 7.8 Hz, Ar-*H*), 3.54 (2H, t, *J* 6.7 Hz, NCH_2CH_2), 2.83 (2H, t, J 6.6 Hz, NCH_2CH_2).

4.4.3.3 Procedure for solid-phase oligomerization. Synthesis of 4.31-4.33.

Linear peptoid oligomers **4.31**-**4.33** were synthesized following the "sub-monomer" solid-phase approach. 2-Chlorotrityl chloride resin (α-dichlorobenzhydryl-polystyrene cross-linked with 1% DVB; 100–200 mesh; 1.60 mmol g^{-1}, 0.50 g, 0.8 mmol) was swelled in dry CH_2Cl_2 (5 mL) for 45 min and then washed with DCM (3 x 5 mL), DMF (3 x 5 mL) and DCM again (3 x 5 mL).For loading, a solution of bromoacetic acid (1.6 equiv, 1.30 mmol, 0.179 g) dissolved in 5 mL of dry DCM was prepared. DIPEA (5.0 equiv, 4.05 mmol, 0.70 mL) was added to this solution, and the mixture was left stirring for one hour. Subsequently, washes with DMF (3 x 5 mL), DCM (3 x 5 mL) and DMF (3 x 5 mL) were performed (this cycle of lavages was performed each time prior to the addition of the new sub-monomer). To construct the first monomer, a primary amine solution in 5 mL of DMF dry (propargylamine for peptoids **4.31** and **4.32** and benzylamine for peptoid **4.33**) (10.0 equiv, 8.10 mmol) was then added to the resin and the reaction mixture was left to stir for 30 min. The previously described washes were carried out again, and a solution of bromoacetic acid (10.0 equiv, 8.10 mmol, 1.12 g), DIC (11.0 equiv, 8.91 mmol, 1.38 mL) in 5 mL of dry DMF was added, and the solution was left to stir for 40 minutes (the coupling reactions' efficiency was verified by chloranil test). Then the previously indicated washes were repeated in the reactor and once again the primary amine solution (propargylamine for **4.31**-**4.33**) (10.0 equiv, 8.10 mmol) was added to obtain the second resin-bound monomer. The addition of the two sub-monomers (the bromoacetic acid and the primary amine) described in these last two steps was repeated iteratively (for the synthesis of compound **4.33**, benzylamine and propargylamine are added alternately) until the oligomer of the desired length was obtained. Cleavage from the resin was accomplished in the presence

of 20% solution of HFIP in dry DCM (3 x 5 mL). After each addition the reaction mixture was left to stir for 30 min, then the resin was filtered away and the combined filtrates were concentrated in vacuo. Oligomers **4.31**-**4.33** were analyzed by HR-MS and RP-HPLC. The HPLC run was carried out by dissolving the sample in an ACN (+ 0.1% TFA)/ H_2O (+ 0.1% TFA) mixture in a 1:1 ratio (conditions: 5 → 100% A in 30 min (A, 0.1% TFA in acetonitrile, B, 0.1% TFA in water); flow: 1.0 mL min^{-1}, 220 nm). The linear oligomers were subjected to the cyclization reaction without further purification.

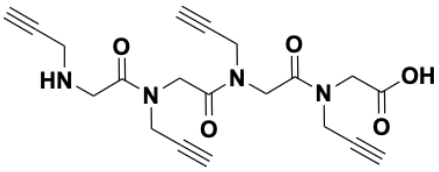

4.31

4.31: white amorphous solid, 0.318 g, 100% yield; Rt 3.7 min; HRMS (MALDI): *m/z* $[M+H]^+$ calcd for $C_{20}H_{23}N_4O_5^+$ 399.1663; found 399.1672.

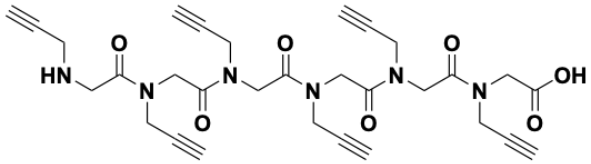

4.32

4.32: white amorphous solid, 0.470 g, 100% yield; Rt 7.0 min; HRMS (MALDI): *m/z* $[M+H]^+$ calcd for $C_{30}H_{33}N_6O_7^+$ 589.2405; found 589.2418.

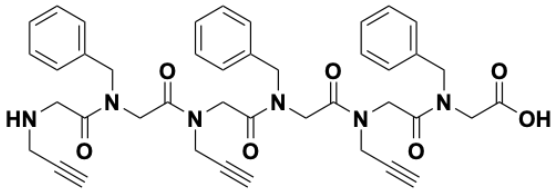

4.33

4.33: white amorphous solid, 0.598 g, 100% yield; Rt 6.7 min; HRMS (MALDI): *m/z* $[M+K]^+$ calcd for $C_{42}H_{44}KN_6O_7^+$ 783.2903; found 783.2895.

4.4.3.4 General procedure for the head-to-tail cyclization reaction. Synthesis of cyclic peptoids 4.28-2.30.

To a stirred solution of HATU (4.0 eq, 0.324 mmol) and DIPEA (6.2 eq, 5.02 mmol) in dry DMF (290 mL) at room temperature, a solution of linear precursors **4.31**-**4.33** (0.8 mmol) in dry DMF (9 mL) was added using a syringe pump in 3 h. After 18 h, the resulting mixture was concentrated in vacuo, diluted with DCM (200 mL) and washed with 1 M HCl (2 × 100 mL). The aqueous layer was extracted with DCM (400 mL) and the combined organic phases were washed with water (300 mL), dried over $MgSO_4$ and concentrated in vacuo. The crude cyclic peptoids **4.28**-**4.30** were purified by precipitation from hot acetonitrile solutions and then analyzed by HR-MS, RP-HPLC (by dissolving the sample in an ACN (+ 0.1% TFA)/ H_2O (+ 0.1% TFA) mixture in a 1:1 ratio (conditions: 5 → 100% A in 30 min (A, 0.1% TFA in acetonitrile, B, 0.1% TFA in water); flow: 1.0 mL min^{-1}, 220 nm) and by NMR spectroscopy.

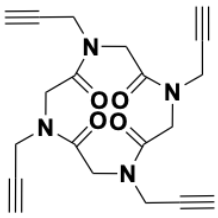

4.28

4.28: white amorphous solid, 0.058 g, 19% yield; Rt 4.1 min; HRMS (MALDI): *m/z* $[M+H]^+$ calcd for $C_{20}H_{21}N_4O_4^+$ 381.1557; found 381.1485.

^{1}H NMR: ($CDCl_3$, 600 MHz) δ: 5.25 (2H, d, *J* 14.8 Hz, $COCH_2N$), 4.94 (2H, dd, *J* 17.6 Hz, *J* 2.40 Hz, NCH_2CCH), 4.37 (2H, d, *J* 18.1 Hz, $COCH_2N$), 4.31 (2H, d, *J* 18.1 Hz, $COCH_2N$), 4.07 (2H, dd, *J* 17.1 Hz, *J* 1.28 Hz, NCH_2CCH), 3.83 (2H, dd, *J* 19.1 Hz *J* 2.44 Hz, NCH_2CCH), 3.74 (2H, dd, *J* 17.6 Hz, *J* 2.40 Hz, NCH_2CCH), 3.59 (2H, d, *J* 14.8 Hz, $COCH_2N$), 2.39 (2H, t, *J* 2.40 Hz, NCH_2CCH), 2.27 (2H, t, *J* 2.44 Hz, NCH_2CCH).

^{13}C NMR: (DMSO, 150 MHz) δ: 169.3 ($COCH_2N$), 168.1 ($COCH_2N$), 79.9 (NCH_2CCH), 78.6 (NCH_2CCH), 77.2 (NCH_2CCH), 76.0 (NCH_2CCH), 48.6 ($COCH_2N$), 48.4 ($COCH_2N$), 37.4 (NCH_2CCH), 36.1 (NCH_2CCH).

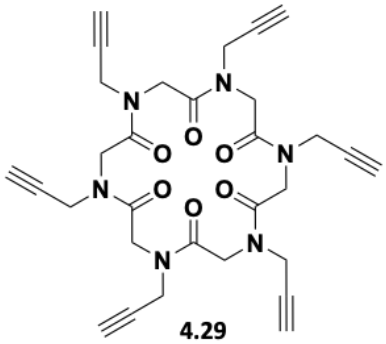

4.29

4.29: white amorphous solid, 0.141 g, 31% yield; Rt 8.6 min; HRMS (MALDI): *m/z* $[M+Na]^+$ calcd for $C_{30}H_{30}N_6NaO_6^+$ 593.2119; found 593.2195.

^{1}H NMR: (DMSO, 400 MHz, mixture of conformers) δ: 5.60-2.90 (30H, m, COC*H*$_2$N, NC*H*$_2$CCH, NCH$_2$CC*H*).

^{13}C NMR: (DMSO, 100 MHz, mixture of conformers) δ: 170.7, 169.8, 169.5, 169.3, 169.2, 169.0, 168.9, 168.8, 168.6, 168.4, 168.2, 167.9, 167.8, 167.7, 167.1, 79.5, 79.4, 79.3, 79.1, 79.0, 78.8, 78.7, 78.5, 78.4, 78.3, 78.2, 78.0, 77.9, 76.3, 76.2, 76.1, 75.9, 75.7, 75.6, 75.4, 75.2, 75.1, 74.7, 74.5, 49.4, 49.3, 49.0, 48.4, 48.3, 47.9, 47.7, 47.6, 47.4, 47.3, 47.0, 46.8, 46.7, 37.2, 36.8, 36.6, 36.4, 36.2, 36.0, 35.7, 35.3, 35.1, 34.7, 34.5, 34.4.

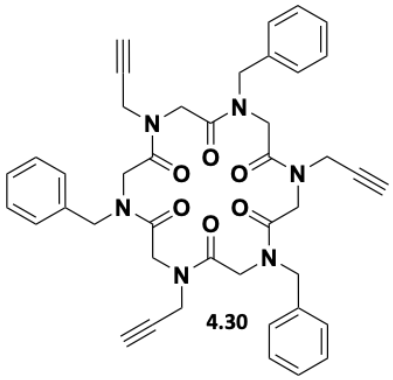

4.30

4.30: white amorphous solid, 0.192 g, 33% yield; Rt 9.7 min; HRMS (MALDI): *m/z* $[M+Na]^+$ calcd for $C_{42}H_{42}N_6NaO_6^+$ 749.3058 found 749.3117.

^{1}H NMR ($CDCl_3$, 400 MHz, mixture of conformers) δ: 7.52-7.98 (15H, m), 5.51- 3.31 (24H, m), 2.42-2.00 (3H, m).

^{13}C NMR ($CDCl_3$, 100 MHz, mixture of conformers) δ: 171.3, 170.6, 169.8, 169.3, 168.9, 168.5, 168.3, 167.9, 167.6, 167.0, 136.6, 136.3, 135.8, 135.2, 134.9, 129.2, 128.8, 128.5, 128.2, 127.9, 127.8, 127.4, 127.2, 127.0, 126.8, 126.6, 126.4, 125.5, 78.4, 78.0, 74.2, 73.8, 73.4, 72.8, 53.0, 52.2, 51.5, 51.2, 51.1, 50.5, 50.2, 49.8, 49.6, 49.1, 49.0 48.5, 48.2, 48.0, 47.6, 47.0, 43.8, 39.1, 38.0, 36.9, 36.3, 36.1, 35.5, 34.4.

4.4.3.5 Procedures for CuAAC-mediated functionalization of cyclopeptoids

Synthesis of macrocycle 4.45

To a solution of cyclopeptoid **4.28** (0.026 mmol, 0.010 g) and azide **4.34** (0.158 mmol, 0.020 g) in H_2O/*t*-BuOH (19.3/9.7 mL) $CuSO_4 \cdot 5H_2O$ (0.463 mmol, 0.116 g) and sodium ascorbate (0.705 mmol, 0.140 g) were added. The reaction mixture was left stirring overnight at 50°C, and the next day it was concentrated in vacuo. Then the crude product was dissolved in 10.0 mL of distilled H_2O and extracted 3 times with 20.0 mL of dichloromethane. The organic phases were anhydrified with Na_2SO_4 and then the solvent was removed.

The pure product was obtained as a white solid by the precipitation from hot acetonitrile solution.

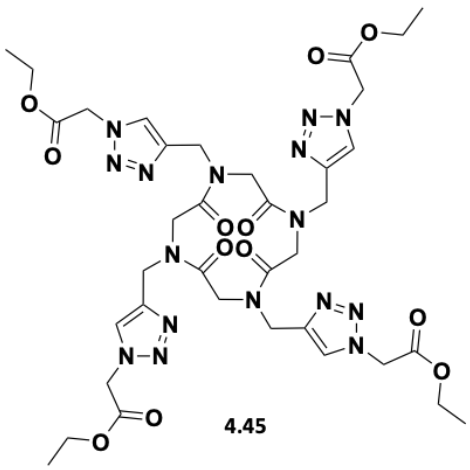

4.45

4.45: white amorphous solid, 0.010 g, 43% yield; Rt 8.2 min; HRMS (MALDI): *m/z* $[M+H]^+$ calcd for $C_{36}H_{49}N_{16}O_{12}^+$ 897.3710 found 897.3791.

^{1}H NMR ($CDCl_3$, 600 MHz) δ: 7.79 (2H, s, CCHN), 7.75 (2H, s, CCHN), 5.31 (2H, d, *J* 14.8 Hz, $COCH_2N$), 5.29 (2H, d, *J* 16Hz, NCH_2CN), 5.22-5.14 (8H, m, NCH_2COO), 4.59 (2H, d, *J* 16Hz,

NCH_2CN), 4.57 (2H, d, *J* 14Hz, $COCH_2N$), 4.35 (2H, d, *J* 18.1 Hz, $COCH_2N$), 4.31-4.24 (12 H, m, NCH_2CN, NCH_2CN, $COOCH_2CH_3$), 3.35 (2H, d, *J* 14.8 Hz, $COCH_2N$), 1.29 (12H, m, $COOCH_2CH_3$). ^{13}C NMR ($CDCl_3$, 150 MHz) δ: 169.5, 167.8, 166.3, 166.2, 143.5, 142.0, 125.1, 124.7, 62.6, 62.5, 51.0, 49.1, 47.9, 42.9, 41.1, 14.2.

Synthesis of macrocycle 4.46

To a solution of cyclopeptoid **4.29** (0.035 mmol, 0.020 g) and azide **3.34** (0.315 mmol, 0.041 g) in H_2O/*t*-BuOH (3. 3/1.7 mL), $CuSO_4{\cdot}5H_2O$ (0.147 mmol, 0.037 g) and sodium ascorbate (0.211 mmol, 0.042 g) were added. The reaction mixture was left stirring at 50°C overnight. The next day, the solvents were removed, and after the addition of 20.0 mL of distilled H_2O, the resulting solution was extracted with 40.0 mL of dichloromethane three times. Then the organic phase was anhydrified with Na_2SO_4 and the solvent was removed.

Purification of compound **4.46** was achieved by dissolving the crude mixture in dichloromethane and then adding pentane drop by drop until a white precipitate has been obtained.

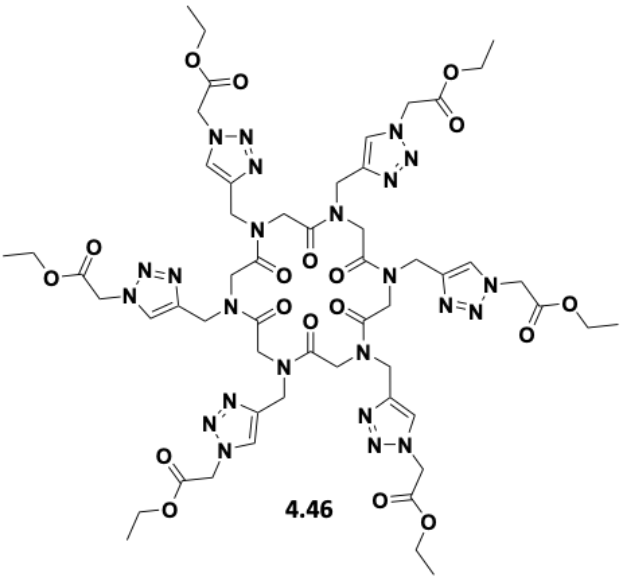

4.46

4.46: white amorphous solid, 0.011 g, 23% yield; Rt 9.5 min; HRMS (MALDI): *m/z* $[M+Na]^+$ calcd for $C_{54}H_{72}N_{24}NaO_{18}^+$ 1367.5349 found 1367.5466.

^1H NMR ($CDCl_3$, 400 MHz, mixture of conformers, δ): 8.02-7.64 (6H, m), 5.29- 3.98 (48H, m), 2.00-1.00 (18H, m).

Synthesis of macrocycle 4.47

To a solution of cyclopeptoid **4.28** (0.026 mmol, 0.010 g) and azide **3.35** (0.337 mmol, 0.039 g) in H_2O/*t*-BuOH (3.3/1.7 mL), $CuSO_4 \cdot 5H_2O$ (0.074 mmol, 0.018 g) and sodium ascorbate (0.105 mmol, 0.0208 g) were added. The solution was left to stir overnight at 50°C. Subsequently, the solvents were removed, distilled H_2O (10.0 mL) was added, and an extraction was performed with 3 x 20.0 mL dichloromethane. The organic phase was anhydrified with Na_2SO_4 and the solvent was removed. The pure product was obtained by precipitation from hot acetonitrile solution as a white solid.

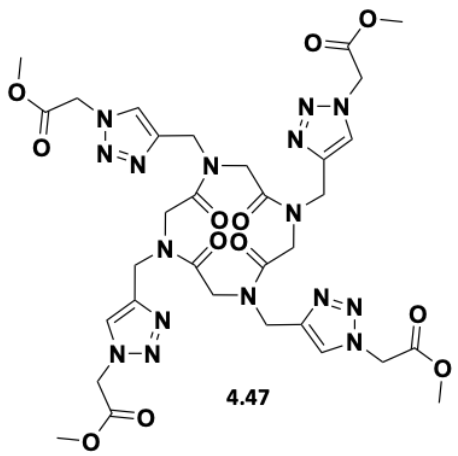

4.47: white amorphous solid, 0.014 g, 65% yield; HRMS (MALDI): *m/z* $[M+H]^+$ calcd for $C_{32}H_{41}N_{16}O_{12}^+$ 841.3084 found 841.3072.

^{1}H NMR (DMSO-d_6, 300 MHZ) δ: 8.12 (2H, s, CCHN), 8.03 (2H, s, CCHN), 5.43-5.39 (10H, m NCH_2COO e NCH_2CN), 5.14 (2H, d, *J* 14.8 Hz, $COCH_2N$), 4.73-4.66 (4H, m, $COCH_2N$ e NCH_2CN), 4.10-3.99 (6H, m, $COCH_2N$, NCH_2CN) e NCH_2CN), 3.73 (6H, s, $COOCH_3$), 3.71(6H, s, $COOCH_3$), 3.16 (2H, d, *J* 14.8 Hz, $COCH_2N$).

Synthesis of macrocycle 4.48

To a solution of cyclopeptoid **4.28** (0.053 mmol, 0.020 g) and azide **4.36** (0.624 mmol, 0.119 g), H_2O/*t*-BuOH (3. 3/1.7 mL), $CuSO_4 \cdot 5H_2O$ (0.145 mmol, 0.036 g) and sodium ascorbate (0.208 mmol, 0.041 g). The solution was left to stir for two days at 50°C. After that time, the solvents were removed, 10.0 mL of distilled H_2O was added, and an extraction was performed with 3 x 20.0 mL of dichloromethane. The organic phase was anhydrified with Na_2SO_4 and the

solvent was removed. The reaction crude was purified by column chromatography using an eluent mixture consisting of dichloromethane and methanol. Compound **4.48** was obtained as a white solid.

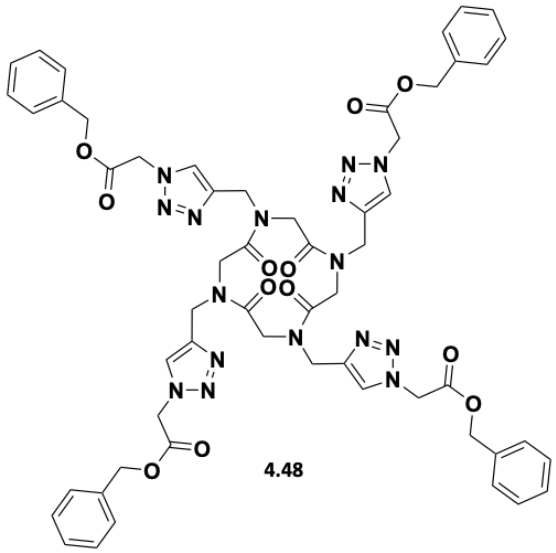

4.48: white amorphous solid, 0.041 g, 67% yield; Rt 11.8 min; HRMS (MALDI): *m/z* $[M+Na]^+$ calcd for $C_{56}H_{56}N_{16}NaO_{12}^+$ 1167.4156 found 1167.4056.

^{1}H NMR ($CDCl_3$, 600 MHz, δ): 7.77 (2H, s, CCHN), 7.75 (2H, s, CCHN), 7.37- 7.32 (20H, m, Ph-H), 5.27-5.17 (20H, m, NCH_2COO, $PhCH_2O$, $COCH_2N$, NCH_2CN), 4.56-4.51 (4H, m, $COCH_2N$, NCH_2CN), 4.31-4.25 6H, m, $COCH_2N$, NCH_2CN) e NCH_2CN), 3.29 (2H, d, *J* 14.8 Hz, $COCH_2N$).

^{13}C NMR ($CDCl_3$, 150 MHz, δ): 169.3, 167.7, 166.1, 166.0, 143.5, 142.0, 134.6, 134.5, 128.9, 128.8, 128.6, 128.5, 125.0, 124.6, 68.1, 68.0, 50.9, 48.9, 47.7, 42.7, 40.9.

Synthesis of macrocycle 4.49

To the solution of cyclopeptoid **4.26** (0.035 mmol, 0.020 g) and azide **4.36** (0.630 mmol, 0.120 g), H_2O/*t*-BuOH (3.3/1.7 mL), $CuSO_4{\cdot}5H_2O$ (0.147 mmol, 0.037 g) and sodium ascorbate (0.210 mmol, 0.042 g) were added. The solution was left stirring for two days at 50°C, then the solvents were removed on rotavapor, after 10.0 mL of distilled H_2O was added and the aqueous phase was extracted with dichloromethane (3 x 20.0 mL). The organic phase was then anhydrified with Na_2SO_4 and the solvent was removed. Cyclopeptoid **4.49** was purified on reverse silica gel (C_{18}); conditions: 10% – 100% A (A: 0.1% TFA in acetonitrile; B: 0.1% TFA in water).

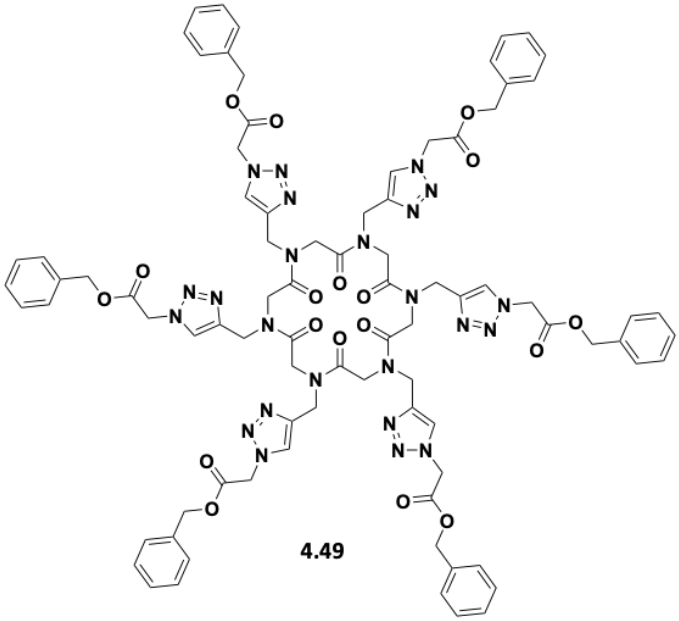

4.49

4.49: white amorphous solid, 0.011 g, 19% yield; Rt 13.7 min; HRMS (MALDI): *m/z* $[M+Na]^+$ calcd for $C_{84}H_{84}N_{24}NaO_{18}^+$ 1739,6288 found 1717.6267.

^1H NMR ($CDCl_3$, 600 MHz mixture of conformers, δ): 8.09-7.52 (6H, m), 7.46- 6.87 (30H, m), 5.33-3.44 (48H, m).

^{13}C NMR ($CDCl_3$, 150 MHz, mixture of conformers, δ): 169.7, 169.4, 169.13, 168.8, 168.5, 168.0, 167.02, 166.5, 164.5, 143.9, 143.5, 143.0, 142.9, 142.5, 140.7, 134.6, 128.7, 128.4, 125.9, 125.3, 125.0, 124.7, 67.9, 50.8, 49.9, 49.3, 49.1, 48.4, 48.1, 44.8, 44.1, 43.5, 42.8, 42.3, 41.0.

Synthesis of macrocycle 4.43

Hydrolysis trials

To the solution of cyclopeptoid **4.45** (0.019 mmol, 0.017 g) in THF/water mixture (0.50/0.50 mL), LiOH (4 x 1.5 equiv, 0.116 mmol, 0.005 g) was added, and the reaction mixture was left to stir for 90 min. After that time, 1.0 mL of a 0.5 M HCl solution and 5.0 mL of ethyl acetate were added to the mixture. The organic phase was separated, and the aqueous phase was extracted 6 times with 5.0 mL of ethyl acetate. The organic phases were then anhydrified with $MgSO_4$ and the solvent was removed. The ^1H NMR and HR-MS analysis did not reveal any trace of product **4.43**. An analogous trial has been performed on methyl ester derivative **4.47** (also prolonging the reaction time, up to 72 h, and increasing the temperature, up to 50 ^oC) but

once again the target molecule was not obtained as verified by spectrometric and spectroscopic analyses.

Hydrogenolysis

In a flask containing cyclopeptoid **4.48** (0.009 mmol, 0.010 g), Pd/C (0.005 g) and DMF (10.0 mL) were added. After performing a series of three vacuum-hydrogen cycles, the mixture was left stirring in H_2 atmosphere overnight. The next day it was filtered over celite and washed with methanol to obtain a white solid, once the solvents have been removed.

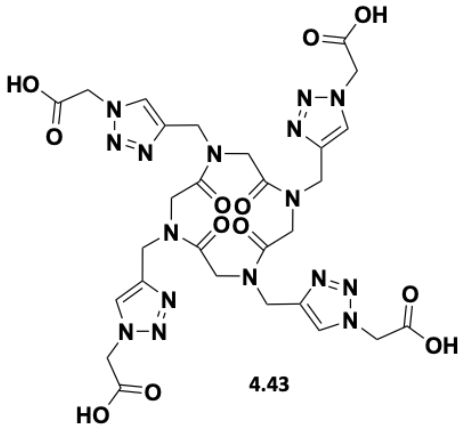

4.43

4.43: white amorphous solid, 0.007 g, 100% yield; Rt 4.6 min; HRMS (MALDI): *m/z* $[M+H]^+$ calcd $C_{28}H_{33}N_{16}O_{12}^+$ 785.2458 found 785.2404.

^{1}H NMR (D_2O, 600 MHz) δ: 8.04 (2H, s, CCHN), 8.01 (2H, s, CCHN), 5.47 (2H, d, *J* 15.0 Hz, $COCH_2N$), 5.19 (2H, d, *J* 14.9 Hz, NCH_2CN), 5.16-5.14 (8H, m, NCH_2CO_2H), 4.34-4.27 (4H, m, $COCH_2N$ e NCH_2CN, overlapping with H_2O), 4.38 (2H, d, *J* 14.9 Hz, NCH_2CN), 4.30-4.27 (4H, m, $COCH_2N$ e NCH_2CN), 3.47 (2H, d, *J* 15.0 Hz, $COCH_2N$).

Synthesis of macrocycle 4.44

Hydrolysis trial

To the solution of cyclopeptoid **4.46** (0.013 mmol, 0.018 g) n THF/water mixture (0.34/0.34 mL) LiOH (6 x 1.5 equiv, 0.117 mmol, 0.005 g) was added, and the reaction mixture was left to stir for 90 min. After that time, 1.0 mL of a 0.5 M HCl solution and 5.0 mL of ethyl acetate were added to the mixture. The organic phase was separated, and the aqueous phase was extracted 6 times with 5.0 mL of ethyl acetate. The organic phases were then anhydrified with $MgSO_4$

and the solvent was removed, and by means of an ^{1}H NMR check, the absence of product **4.44** was attested. It was then decided to follow an alternative procedure involving hydrogenolysis of cyclopeptoid **4.49**.

Hydrogenolysis

Pd/C (0.006 g) and DMF (3.00 mL) were added to a flask containing cyclopeptoid **4.49** (0.007 mmol, 0.012 g). After performing a series of three vacuum-hydrogen cycles, the mixture was left stirring in H_2 atmosphere overnight. The next day it was filtered over celite and washed with methanol to obtain a white solid. NMR analysis revealed a complex spectrum, showing a mixture of products, among which a resonance pattern belonging to the hexacyclic precursor was noted. HR-MS analysis, however, confirmed the formation of the target macrocycle **4.44**.

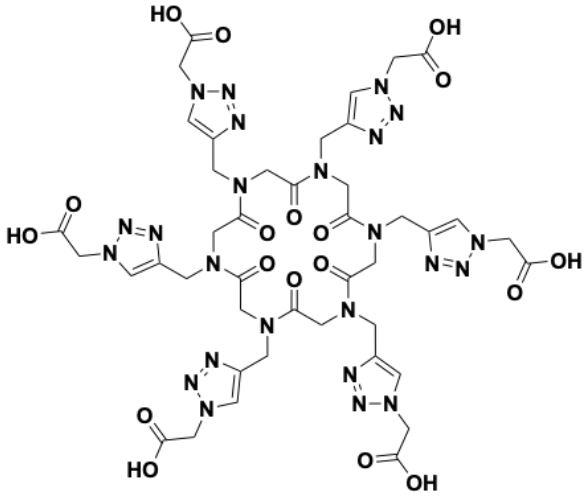

4.44

4.44: HRMS (MALDI): *m/z* $[M+H]^+$ calcd for $C_{42}H_{49}N_{24}O_{18}^{+}$ 1177.3651 found 1177.3524.

Synthesis of macrocycle 4.50

To the cyclopeptoid **4.28** (0.053 mmol, 0.020 g) and azide **4.37** (0.252 mmol, 0.050 g) solution in DMF/H2O (3.3/1.7 mL) $CuSO_4 \cdot 5H_2O$ (0.145 mmol, 0.036 g) and sodium ascorbate (0.208 mmol, 0.041 g) were added. The solution was left stirring for two days at 70°C. Then the solvents were removed, 10.0 mL of distilled H_2O was added, and then extraction was performed with 3 x 20.0 mL of dichloromethane. The organic phase was anhydrified with Na_2SO_4 and the solvent was removed. Washings with toluene and chloroform were performed

to remove residual DMF. Purification of compound **4.50** was performed by flash chromatography using an eluent mixture consisting of dichloromethane and methanol.

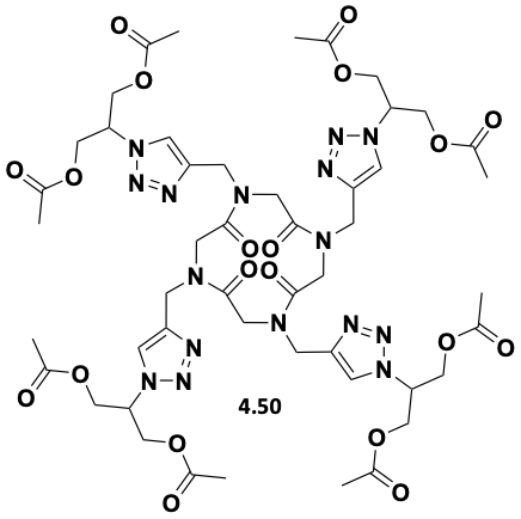

4.50 white amorphous solid, 0.011 g, 17% yield; Rt 8.0 min; HRMS (MALDI): *m/z* $[M+Na]^+$ calcd $C_{48}H_{64}N_{16}NaO_{20}^+$ 1207.4375 found 1207.4418.

^{1}H NMR ($CDCl_3$, 600 MHz) δ: 7.81 (2H, s, CCHN), 7.74 (2H, s, CCHN), 5.31 (2H, d, *J* 14.7 Hz, NCH_2CN), 5.29 (2H, d, *J* 14.8, $COCH_2N$), 5.07 (4H, m, $CHCH_2OCO$), 4.61-4.49 (22H, m, $CHCH_2OCO$, NCH_2CN, $COCH_2N$), 4.26 (2H, d, *J* 16.2 Hz, NCH_2CN), 4.21 (2H, d, *J* 14.7 Hz, NCH_2CN), 3.29 (2H, d, *J* 14.8, $COCH_2N$), 2.07 (12H, s, $OCOCH_3$), 2.05 (12H, s, $OCOCH_3$).

^{13}C NMR ($CDCl_3$, 150 MHz) δ: 170.2 x 4 (CH_3COO), 169.3 x 2 (NCH_2CO), 167.7 2 x 2 (NCH_2CO), 143.1 x 2 (CH_2CCHN), 141.5 x 2 (CH_2CCHN), 123.1 x 4 (CH_2CCHN), 62.4 x 8 ($CHCH_2OCO$), 58.8 x 2 ($CHCH_2OCO$), 58.5 x 2 ($CHCH_2OCO$), 48.9 x 2 ($COCH_2N$), 47.6 x 2 ($COCH_2N$), 42.5 x 2 (NCH_2CN), 40.9 x 2 (NCH_2CN), 20.6 x 8 ($OCOCH_3$).

Synthesis of macrocycle 4.51

To the cyclopeptoid **4.30** (0.028 mmol, 0.020 g) and azide **4.37** (0.099 mmol, 0.020 g) solution in DMF/H2O (3.3/1.7 mL) $CuSO_4 \cdot 5H_2O$ (0.058 mmol, 0.014 g) and sodium ascorbate (0.083 mmol, 0.016 g) were added. The solution was left stirring for two days at 70°C. The solvents were removed, 10.0 mL of distilled water was added, and an extraction was performed with 3 x 20.0 mL of dichloromethane. The organic phase was anhydrified with Na_2SO_4 and the solvent was removed. Washings with toluene and chloroform were performed on the

obtained crude to remove residual DMF. Compound **4.51** was then precipitated from hot ethyl acetate solution.

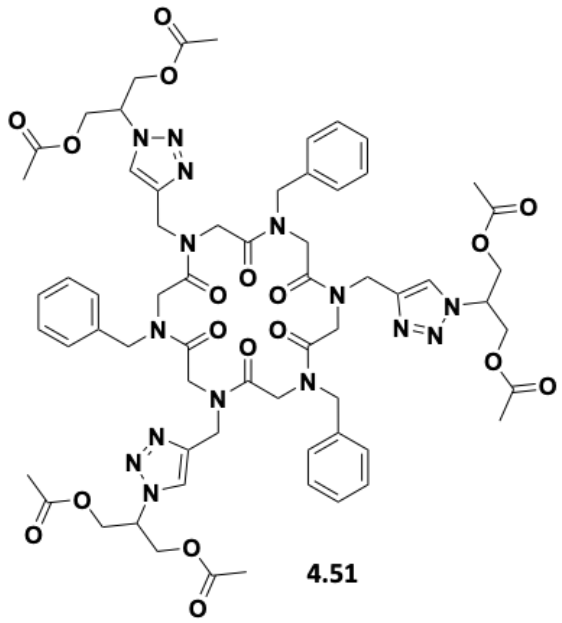

4.51

4.51: white amorphous solid, 0.027 g, 61% yield; Rt 9.9 min; HRMS (MALDI): *m/z* $[M+Na]^+$ calcd $C_{63}H_{75}N_{15}NaO_{18}^+$ 1352.5307 found 1352.5294.

^{1}H NMR ($CDCl_3$, 400 MHz, mixture of conformers) δ: 7.89-7.58 (3H, m), 7.29- 7.03 (15H, m), 5.29-3.89 (36H, m), 2.11-1.97 (18H, m).

^{13}C NMR ($CDCl_3$, 100 MHz) δ: 170.4, 129.3, 128.9, 128.3, 127.8, 125.4, 62.6, 58.8, 48.8, 29.8.

Synthesis of macrocycle 4.52

Solution of potassium carbonate (0.155 mmol, 0.022 g) in ethanol (1.00 mL) was added to a flask containing cyclopeptoid **4.50** (0.009 mmol, 0.011 g). The resulting mixture was left stirring overnight at 25°C. After 24 h, the solution was gravity-filtered to remove excess of potassium carbonate, and the solvent was removed.

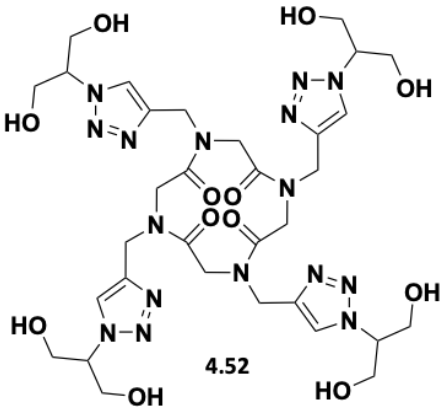

4.52: white amorphous solid, 0.008 g, 100% yield; Rt 3.4 min; HRMS (MALDI): *m/z* $[M+K]^+$ calcd $C_{32}H_{47}KN_{16}O_{12}^+$ 886.3191 found 888.3278.

^{1}H NMR (MeOD, 600 MHz) δ: 8.13 (2H, s, CCHN), 8.08 (2H, s, CCHN), 5.26 (2H, d, *J* 15.4), 4.90 (2H, m overlapping with H_2O), 4.76-4.70 (6H, m), 4.29 (2H, d, *J* 15.4), 4.24 (2H, d, *J* 16.8 Hz), 4.03-3.98 (16 H, m), 3.34 (2H, overlapping with MeOH).

^{13}C NMR (MeOD, 150 MHz) δ: 172.7 (×2), 170.3 (×2), 144.8 (×2), 143.6 (×2), 125.9 (×4), 67.8 (×2), 67.6 (×2), 63.1 (×8), 50.7 (×4, overlapping with MeOH), 44.7 (×2), 42.78 (×2).

Synthesis of macrocycle 4.53

To a solution of cyclopeptoid **4.28** (0.026 mmol, 0.010 g) and azide **4.39** (0.1262 mmol, 0.032 g) in DMF/*t*-BuOH (3.3/1.7 mL), $CuSO_4 \cdot 5H_2O$ (0.074 mmol, 0.018 g) and sodium ascorbate (0.105 mmol, 0.021 g) were added. The solution was left to stir overnight at 70°C. Subsequently, the solvents were removed, distilled H_2O (10.0 mL) was added, and an extraction was performed with 3 x 20.0 mL dichloromethane. The aqueous phase, containing product (as attested by an ^{1}H NMR check), was dried and treated with hot methanol to induce precipitation of the target macrocycle **4.53** as a white amorphous solid with 94% yield.

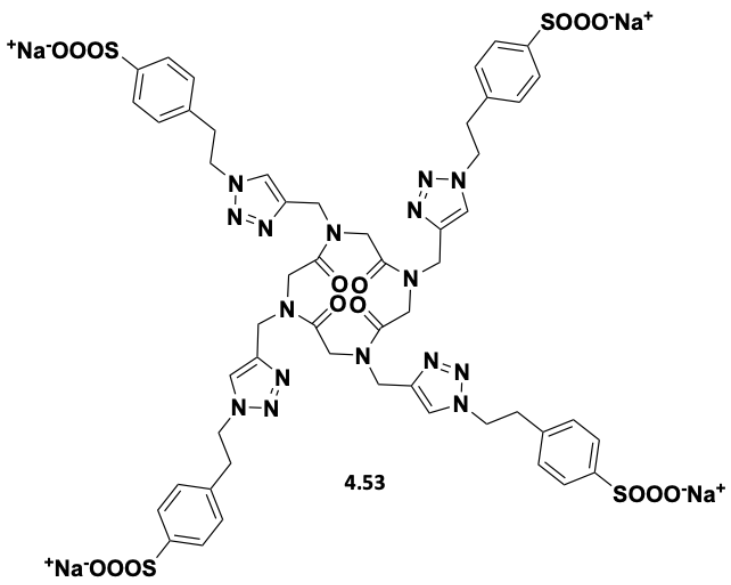

4.53: white amorphous solid, 0.034 g, 94% yield; Rt 3.4 min; HRMS (negative-mode MALDI): *m/z* [M-Na]$^-$ calcd $C_{52}H_{52}N_{16}Na_3O_{16}S_4^-$ 1353.2329 found 1353.2412.

^{1}H NMR: (600 MHz, DMSO) δ: 8.13 (2H, s), 8.05 (2H, s), 7.51-7.49 (8H, m), 7.18-7.16 (8H, m), 5.32 (2H, d, *J* 14. 3 Hz), 5.06 (2H, d, *J* 14.8 Hz), 4.65-4.55 (12H, m), 4.05 (4H, m), 3.97 (2H, d, *J* 16.4 Hz), 3.18-3.09 (10H, m).

^{13}C NMR: (150 MHz, DMSO) δ: 169.0, 167.4, 146.7, 142.8, 141.5, 138.5, 137.8, 127.9, 125.6, 123.7, 50.4, 50.3, 48.2, 47.3, 42.4, 39.7 (overlapped with solvent signal), 35.3.

Synthesis of macrocycle 4.54

To a solution of cyclopeptoid **4.29** (0.017 mmol, 0.010 g) and azide **4.39** (0.126 mmol, 0.032 g) in DMF/*t*-BuOH (3.3/1.7 mL), $CuSO_4 \cdot 5H_2O$ (0.074 mmol, 0.018 g) and sodium ascorbate (0.105 mmol, 0.021 g) were added. The solution was left to stir overnight at 70°C. Subsequently, the solvents were removed, distilled H_2O (10.0 mL) was added, and an extraction was performed with 3 x 20.0 mL dichloromethane. The dried aqueous phase was subjected to ^{1}H NMR and HR-MS analysis revealing the product formation. However, it was not possible to isolate the pure compound **4.54**.

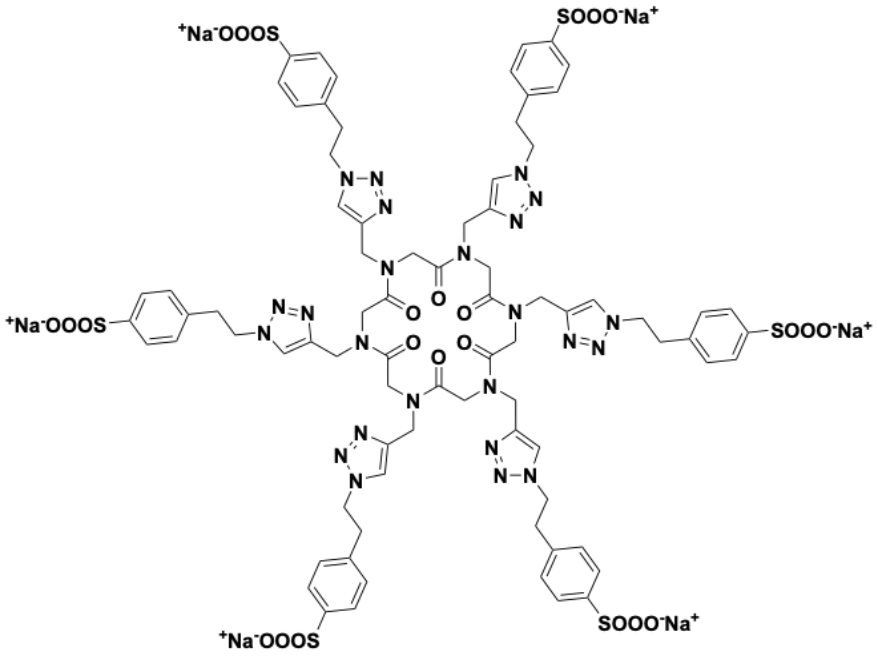

4.54

4.54: HRMS (negative-mode MALDI): *m/z* $[M\text{-}Na]^-$ calcd for $C_{78}H_{78}N_{24}Na_5O_{24}S_6^-$ 2041.3439. found 2041.3458.

Acknowledgements

I would like to thank my supervisor, **Professor Irene Izzo**, for opening the door to this enriching adventure to me. I am thankful for the patient guidance, constant availability, all the valuable advice, kindness, support, and for everything I could learn during these three years.

I would like to also thank **Professor Francesco De Riccardis** and **Professor Giorgio Della Sala** for their availability, kindness, all the help and support.

Special thanks to **Rosaria**, **Assunta**, **Giovanni**, **Ibrahim** and **Maria**. Thank you for everything you have done for me. I am lucky to have met such wonderful people and to have had the opportunity to work and share this unique adventure with you.

Thanks to **Andreana**, **Antoine**, **Antonello**, **Carmela**, **Eleonora**, **Giuseppe**, **Mario**, and **Michelangelo** - our adventures in the lab will remain forever in my heart.

Finally, I would like to thank my wonderful parents, **Damian** and **Małgorzata**, and my best brother **Adam**. Without you, nothing would have been possible.